

Air Force Institute of Technology

AFIT Scholar

Theses and Dissertations

Student Graduate Works

6-10-2008

A Secure and Efficient Communications Architecture for Global Information Grid Users via Cooperating Space Assets

Victor P. Hubenko

Follow this and additional works at: <https://scholar.afit.edu/etd>



Part of the [Systems and Communications Commons](#), and the [Systems Architecture Commons](#)

Recommended Citation

Hubenko, Victor P., "A Secure and Efficient Communications Architecture for Global Information Grid Users via Cooperating Space Assets" (2008). *Theses and Dissertations*. 2629.
<https://scholar.afit.edu/etd/2629>

This Dissertation is brought to you for free and open access by the Student Graduate Works at AFIT Scholar. It has been accepted for inclusion in Theses and Dissertations by an authorized administrator of AFIT Scholar. For more information, please contact richard.mansfield@afit.edu.



**A SECURE AND EFFICIENT COMMUNICATIONS ARCHITECTURE FOR
GLOBAL INFORMATION GRID USERS VIA COOPERATING SPACE ASSETS**

DISSERTATION

Victor P. Hubenko, Jr., Major, USAF

AFIT/DCE/ENG/08-02

**DEPARTMENT OF THE AIR FORCE
AIR UNIVERSITY**

AIR FORCE INSTITUTE OF TECHNOLOGY

Wright-Patterson Air Force Base, Ohio

APPROVED FOR PUBLIC RELEASE; DISTRIBUTION UNLIMITED

The views expressed in this dissertation are those of the author and do not reflect the official policy or position of the United States Air Force, Department of Defense, or the U.S. Government.

AFIT/DCE/ENG/08-02

**A SECURE AND EFFICIENT COMMUNICATIONS ARCHITECTURE FOR
GLOBAL INFORMATION GRID USERS VIA COOPERATING SPACE ASSETS**

DISSERTATION

Presented to the Faculty

Graduate School of Engineering and Management

Air Force Institute of Technology

Air University

Air Education and Training Command

In Partial Fulfillment of the Requirements for the

Degree of Doctor of Philosophy

Victor P. Hubenko, Jr., BS EE, MS EE

Major, USAF

June 2008

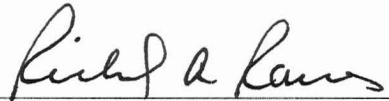
APPROVED FOR PUBLIC RELEASE; DISTRIBUTION UNLIMITED

**A SECURE AND EFFICIENT COMMUNICATIONS ARCHITECTURE FOR
GLOBAL INFORMATION GRID USERS VIA COOPERATING SPACE ASSETS**

Victor P. Hubenko, Jr., BS EE, MS EE

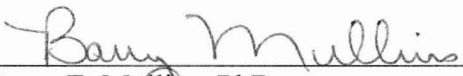
Major, USAF

Approved:



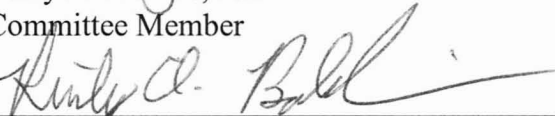
Richard A. Raines, PhD
Committee Chairman

6 Jun 08
Date



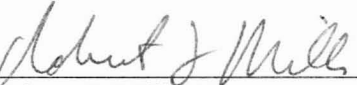
Barry E. Mullins, PhD
Committee Member

2 Jun 08
Date




Rusty O. Baldwin, PhD
Committee Member

6 Jun 08
Date



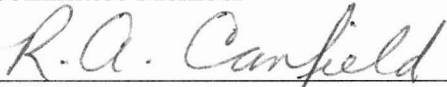
Robert F. Mills, PhD
Committee Member

4 Jun 08
Date



Michael A. Grimala, PhD
Committee Member

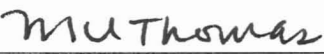
04 Jun 08
Date



Robert A. Canfield, PhD
Dean's Representative

4 Jun 08
Date

Accepted:



Marlin U. Thomas, PhD
Dean

10 Jun 08
Date

A SECURE AND EFFICIENT COMMUNICATIONS ARCHITECTURE FOR
GLOBAL INFORMATION GRID USERS VIA COOPERATING SPACE ASSETS

by

Victor P. Hubenko, Jr., BS EE, MS EE
Major, USAF

Dr. Richard A. Raines, Advisor

Abstract

With the Information Age fully in place and still experiencing rapid development, users expect to have global, seamless, ubiquitous, secure, and efficient communications that provide access to real-time applications and collaboration. The United States Department of Defense's (DoD) Network-Centric Enterprise Services initiative, along with the notion of pushing the "power to the edge," will provide end-users with maximum situational awareness, a comprehensive view of the battlespace, all within a secure networking environment.

This research develops a novel security framework architecture to provide efficient and scalable secure multicasting in the low earth orbit satellite network environment. This security framework architecture combines several key aspects of other secure group communications architectures in a way that increases efficiency and scalability, while maintaining the overall system security level. This security architecture in a deployed environment with heterogeneous communications users will reduce re-keying. Less frequent re-keying means more resources are available for user data rather

than security overhead. This translates to greater performance for the end user; it will seem as if they have a “larger pipe” for their network links.

This research develops and analyzes multiple mobile communication environment scenarios to demonstrate the superior re-keying offered by the novel “Hubenko Security Framework Architecture” compared to traditional and clustered multicast security architectures. For example, in the scenario containing a heterogeneous mix of user types (Stationary, Ground, Sea, and Air), the Hubenko Architecture achieves a minimum ten-fold reduction in total keys distributed compared to other known architectures. For another scenario, the Hubenko Architecture operates at 6% capacity while other architectures consumed 98% of capacity. With 80% user mobility for 40% Air users, re-keying in other architectures increased 900%, whereas the Hubenko Architecture only increased 65%. By reducing overall system re-keying, the Hubenko Architecture increases system efficiency and scalability.

This new architecture is extensible to numerous secure group communications environments beyond the low earth orbit satellite network environment, including unmanned aerial vehicle swarms, wireless sensor networks, and mobile ad hoc networks. At the time of publication, the Hubenko Architecture was the basis for several current Master’s level research efforts in the aforementioned areas.

Acknowledgments

Just as they are first in my life, my wife and children are first to be thanked. Thank you for enduring the many nights and weekends that we shared together, yet apart, as I worked towards graduation. I can never express enough how much gratitude I have for my wife continually resetting and putting her career on hold so I could advance in mine. She is the reason I was able to focus on this degree, and is the pillar of my success. I also thank my parents for giving me the best opportunities for success as they could.

I thank Dr. Richard Raines, my advisor, for allowing me to spread my wings, yet keeping me on the path to graduation. I also thank my committee (Drs. Raines, Mullins, Baldwin, Mills, and Grimala) for the numerous document reviews, feedback, and support of my research, publications, and dissertation.

Academics aside, I thank Ms. Stacey Johnston, the unsung hero of the Center for Cyber Research for always selflessly taking care of the CCR students (and staff!), making our lives at AFIT that much less stressful.

Thanks to my AFIT Dining Out 2006 Committee for helping reestablish the grandeur of AFIT spirit and camaraderie as we “Experienced the Excellence,” achieving miracles and a sold-out event in seven weeks time. Also, my fellow staff of the 2005-2006 AFIT Student Association are owed many thanks for the long hours put in to make the lives of our fellow AFIT students more enjoyable, from Doolittle’s and beyond!

Speaking of camaraderie and friends, thanks to Major Chris Augeri for teaching me that MatLab can run inside of Word inside of Excel and for all that help with getting my MatLab code (and any software app) to work properly. Thanks to Major Kevin

Cousin and family for always volunteering to help us out. Thanks to Major Ken Edge and Captain Mark Kleeman for keeping things interesting in the PhD Penthouse. A special thanks to Major George Dalton for always looking out for me, for being a great friend, and sharing his 24 years of leadership experience with me so I can grow into a better leader.

My journey down the road to AFIT started with Mr. John Cunningham, who personally nominated me for an Advanced Academic Degree slot and then made sure I had the best shot possible for being selected. Finally, I owe a debt of gratitude to the “C-Cubed Aerospace Mafia” (John Overton, Chris Pate, Mike Wenkel) for making me look good while I reigned as Mayor of C-Cubeville at NPOESS. They shared three lifetimes of experiences, wisdom, and lessons that I carry with me today. They gave me the opportunity and support to stand out as a shining star and get noticed.

It takes the support of many people to achieve success. I thank all those people, named and unnamed, now and in the past, for their help in getting me this far in life. I am fortunate to have such a caring assemblage of people touch my life.

Table of Contents

	Page
Abstract.....	iv
Acknowledgments.....	vi
Table of Contents.....	viii
List of Figures.....	xii
List of Tables	xv
List of Acronyms	xvii
I. Introduction	1
1.1 Background	1
1.2 Problem Statement	3
1.3 Research Goal	3
1.4 Research Contributions	4
1.4.1 Coherent, Secure, and Efficient Architecture for LEOSat Environment ..	4
1.4.2 Extension of Hubenko Architecture to Other Highly Mobile Environments.....	6
1.5 Assumptions/Limitations	6
1.6 Dissertation Organization.....	7
II. Literature Review	8
2.1 Chapter Overview	8
2.2 Communication Satellite Systems	8
2.2.1 Global Information Grid.....	11
2.2.2 Highlights of the IRIDIUM [®] LEO Satellite System	20
2.2.3 Other Satellite Communications Systems	22
2.2.4 Inter-Satellite Links and On-orbit Routing.....	23
2.3 Multicasting Technologies	25

2.3.1	Multicast Overview	25
2.3.2	Link State and Distance Vector Routing Algorithms Overview	26
2.3.3	Dense and Sparse Types of Multicast	30
2.3.4	Some Options for Multicast Networks	31
2.3.5	Group Management Protocols.....	33
2.3.6	Multicast Satellite Networks: Architectures and Multicast Protocols.....	34
2.3.7	Issues Surrounding Multicast Communications.....	36
2.4	Multicasting Security	38
2.4.1	General Security Services.....	39
2.4.2	Issues Surrounding Multicast Security	41
2.4.3	Scalable, Secure Multicast Systems and Architectures.....	46
2.4.4	Deficiencies of Known Scalable, Secure Multicast Systems and Architectures.....	53
2.5	Summary	54
III.	Methodology	55
3.1	Chapter Overview	55
3.2	Hubenko LEOSat Security Framework Architecture Motivation.....	55
3.3	LEOSat Network Environment Validation	57
3.4	Continued Viability of PIM-DM.....	62
3.5	Hubenko Security Framework Architecture Development.....	64
3.5.1	Baseline Security Architecture for the LEO Satellite Environment.....	65
3.5.2	Clusterized Security Architecture.....	68
3.5.3	Hubenko Security Framework Architecture.....	73
3.5.4	Demonstrate Improved System Security Performance.....	79
3.6	Simulation Environment and Architecture Models.....	80

3.6.1	Simulation Environment.....	80
3.6.2	Architecture Models	87
3.6.3	Confidence Interval	95
3.7	Simulation Equipment.....	96
3.8	Metrics for Security Performance Evaluation and Analysis	97
3.9	Time Scaling for Modeling Expediency	98
3.10	Model Verification	98
3.11	Model Validation	105
3.12	Summary	111
IV.	Performance Results and Analysis	112
4.1	Chapter Overview	112
4.2	Model Scenarios.....	112
4.2.1	Highly Mobile User Environment (Four Different RoM).....	112
4.2.2	Short versus Long Duration.....	120
4.2.3	Increasing Aircraft over Stationary Users	130
4.2.4	Varied Air Content Rate of Mobility.....	137
4.3	Performance Conclusions	141
4.3.1	Re-Keying Performance Results	141
4.3.2	Hubenko Saturation	146
4.3.3	RoM Sensitivity	146
4.4	Analysis of Variance	150
4.5	Summary	154
V.	Conclusion	156
5.1	Summary of Research	156

5.2	Research Contributions	157
5.3	Publications	158
5.4	Recommendations for Future Research	158
5.4.1	Adapt Hubenko Security Framework Architecture to Other Environments.....	158
5.4.2	Incorporate Features from the Integrated Architecture Concept.....	158
5.4.3	Re-establish Original LEOSat Baseline with Hubenko Architecture....	160
VI.	Appendix.....	162
6.1	Short versus Long Duration Scenario 1 (Section 4.2.2).....	163
6.2	Short versus Long Duration Scenario 2 (Section 4.2.2).....	167
6.3	Increasing Aircraft Over Stationary Users Scenario 2 (Section 4.2.3)	171
6.4	Analysis of Variance Data	175
6.5	MatLab Code from Increasing Aircraft Over Stationary Users Scenario 2 (Section 4.2.3).....	175
VII.	Bibliography	196
VIII.	Vita.....	206

List of Figures

	Page
Figure 1 - Relative Re-keying Performance	5
Figure 2 - Global Information Grid Layers [SMC06a].....	12
Figure 3 - The Gothic Architecture [JuA02].....	47
Figure 4 - Example of a Secure Distribution Tree [Mit97]	50
Figure 5 - GSA Multicast Forwarding Performance [Mit97]	51
Figure 6 - Baseline LEOsat Security Architecture	66
Figure 7 - Initialize Baseline Architecture Example.....	67
Figure 8 - Baseline Example - Two	67
Figure 9 - Baseline Example - Three	67
Figure 10 - Baseline Example - Four	67
Figure 11 - Baseline Example - Finish	68
Figure 12 - Clusterized Security Architecture	70
Figure 13 - Initialize Cluster Example.....	71
Figure 14 - Cluster Example - Two	71
Figure 15 - Cluster Example - Three	72
Figure 16 - Cluster Example - Four	72
Figure 17 - Cluster Example - Finish.....	72
Figure 18 - Hubenko Architecture Flow Chart.....	75
Figure 19 - Hubenko Security Framework Architecture	76
Figure 20 - Initialize Hubenko Architecture	78
Figure 21 - Hubenko Example - Two	78
Figure 22 - Hubenko Example - Three	78

Figure 23 - Hubenko Example - Four	78
Figure 24 - Flow Diagram for MatLab Simulation Code	91
Figure 25 - User Satellite Assignments	100
Figure 26 - User Cluster Assignments	100
Figure 27 - User Mobility Assignments.....	100
Figure 28 - User Mobility Verification.....	100
Figure 29 - User Join Time Assignments	100
Figure 30 - User Duration Assignments	100
Figure 31 - User Activity Verification.....	101
Figure 32 - Cluster Trigger Verification.....	102
Figure 33 - Average Per-User Re-keying	103
Figure 34 - Total System Keys	103
Figure 35 - Group Key Management Overhead - Actual Trace [JuA02]	106
Figure 36 - Group Key Management Overhead - Simulated Trace [JuA02].....	106
Figure 37 - Average Keys Distributed in a Highly Mobile Environment.....	108
Figure 38 - Spatial Clustering- Varying the Number of Hosts Leaving [BaB02]	109
Figure 39 - Hubenko Model - Varying the Number of Hosts Leaving.....	109
Figure 40 - Rates of Mobility for Highly Mobile Scenario	113
Figure 41 - Average Times Each User is Re-Keyed (from 10 to 2000 Users, 2000 Time Steps, Highly Mobile User Environment Scenario).....	116
Figure 42 - Total Keys Distributed in Each Architecture (from 10 to 2000 Users, 2000 Time Steps, Highly Mobile User Environment Scenario)	119
Figure 43 - Total Keys Distributed - 1% Mobility (from 10 to 1000 Users, 1000 Time Steps, Short versus Long Duration Scenario 1)	123
Figure 44 - Average Per-User Re-Key - 50% Mobility (from 10 to 1000 Users, 1000 Time Steps, Short versus Long Duration Scenario 1).....	125

Figure 45 - Average Per-User Re-Key - 50% Mobility (from 10 to 10,000 Users, 10,000 Time Steps, Short versus Long Duration Scenario 2).....	127
Figure 46 - Total Keys Distributed - All Users (from 10 to 10,000 Users, 10,000 Time Steps, Short versus Long Duration Scenario 2)	128
Figure 47 - Total Keys Distributed - Control Group (from 10 to 10,000 Users, 10,000 Time Steps, Short versus Long Duration Scenario 2).....	129
Figure 48 - Average Per-User Re-Key - All Users (from 10 to 1000 Users, 1000 Time Steps, Increasing Aircraft Scenario 1)	132
Figure 49 - Average Per-User Re-Key - Control Group (from 10 to 1000 Users, 1000 Time Steps, Increasing Aircraft Scenario 1).....	132
Figure 50 - Total Keys Distributed - All Users (from 10 to 1000 Users, 1000 Time Steps, Increasing Aircraft Scenario 1)	133
Figure 51 - Total Keys Distributed - Control Group (from 10 to 1000 Users, 1000 Time Steps, Increasing Aircraft Scenario 1)	134
Figure 52 - Total Keys Distributed - All Users (from 10 to 10,000 Users, 10,000 Time Steps, Increasing Aircraft Scenario 2)	136
Figure 53 - Average Per-User Re-Key - All Users (from 10 to 10,000 Users, 10,000 Time Steps, Increasing Aircraft Scenario 2)	137
Figure 54 - Per-User Average Re-Key Results - All Users (from 10 to 2000 Users, 2000 Time Steps, Varied Air Content Scenario)	139
Figure 55 - Varied Air Content RoM Scenario Revisited (from 10 to 2000 Users, 2000 Time Steps)	149
Figure 56 - Integrated Architecture Services Added	160

List of Tables

	Page
Table 1 - Data-to-Overhead Comparison.....	58
Table 2 - Received-to-Sent Comparison.....	59
Table 3 - End-to-End Delay Comparison	60
Table 4 - System, Scenario, and Iteration Level Parameters and Factors.....	83
Table 5 - Highly Mobile User Environment Parameters	114
Table 6 - First Short vs. Long Duration Scenario Parameters	122
Table 7 - Second Short vs. Long Duration Scenario Parameters.....	124
Table 8 - Increasing Aircraft Parameters - Scenario 1	131
Table 9 - Increasing Aircraft Parameters - Scenario 2.....	135
Table 10 - Rates of Mobility (Varied Air Content)	138
Table 11 - Varied Air Content RoM Parameters	138
Table 12 - Per-User Average Re-Keying Summary	141
Table 13 - Total Keys Distributed Summary	144
Table 14 - Mobility Content for Varied Air Content Scenario.....	148
Table 15 - ANOVA with Duration = 0.2	152
Table 16 - ANOVA with Duration = 0.5	153
Table 17 - ANOVA with Duration = 0.8	154
Table 18 - Total Keys Distributed (All Users, Short vs. Long Duration Scenario 1).....	163
Table 19 - Total Keys Distributed (Control Group Users, Short vs. Long Duration Scenario 1)	164
Table 20 - Average Per-User Re-Key (All Users, Short vs. Long Duration Scenario 1)	165
Table 21 - Average Per-User Re-Key (Control Group Users, Short vs. Long Duration Scenario 1)	166

Table 22 - Total Keys Distributed (All Users, Short vs. Long Duration Scenario 2).....	167
Table 23 - Total Keys Distributed (Control Group Users, Short vs. Long Duration Scenario 2)	168
Table 24 - Average Per-User Re-Key (All Users, Short vs. Long Duration Scenario 2)	169
Table 25 - Average Per-User Re-Key (Control Group Users, Short vs. Long Duration Scenario 2)	170
Table 26 - Total Keys Distributed (All Users, Increasing Aircraft Over Stationary Users Scenario 2)	171
Table 27 - Total Keys Distributed (Control Group Users, Increasing Aircraft Over Stationary Users Scenario 2).....	172
Table 28 - Average Per-User Re-Key (All Users, Increasing Aircraft Over Stationary Users Scenario 2)	173
Table 29 - Average Per-User Re-Key (Control Group Users, Increasing Aircraft Over Stationary Users Scenario 2).....	174
Table 30 - Data in Raw Format for use in ANOVA.....	175

List of Acronyms

ACS	Access Control Server	DtO	Data-to-Overhead ratio
AEHF	Advanced Extremely High Frequency	DV	Distance Vector
AFIT	Air Force Institute of Technology	DVBMT	Delay-Variation-Bounded Multicast Tree
AJ	Anti-Jam	DVB-S	Digital Video Broadcast – Satellite
ANOVA	Analysis of Variance	DVMRP	Distance Vector Multicast Routing Protocol
AOR	Area of Responsibility	DWDM	Dense Wave Division Multiplexing
AS	Anti-Scintillation	EHF	Extremely High Frequency
AWACS	Airborne Warning and Control System	EIGRP	Enhanced IGRP
BACN	Battlefield Airborne Communications Node	EPS	Enhanced Polar System
BGMP	Border Gateway Multicast Protocol	EtE	End to End
BGP	Border Gateway Protocol	FAB-T	Family of Advanced Beyond Line-of-sight Terminals
CBT	Core Based Trees	FAI	International Aeronautical Federation
CIO	Chief Information Officer	GAC	Group Access Control
COV	Coefficient of Variance	GACA	Group Access Control Awareness
CRT	Chinese Remainder Theorem	GACA-GKM	Group Access Control Aware-Group Key Management
CWDM	Coarse Wave Division Multiplexing	GBS	Global Broadcast Service Satellite System
DBST	Delay-Bounded Steiner Tree	GEO	Geostationary earth orbit
DES	Discrete Event Simulation	GEO	Geosynchronous earth orbit
DiRK	Distributed Registration and Key Distribution	GIG	Global Information Grid
DISN	Defense Information Systems Network	GIG-BE	Global Information Grid – Bandwidth Expansion
DoD	Department of Defense	GKM	Group Key Management
DoS	Denial of Service		
DSCS	Defense Satellite Communications Systems		

GMAS	Group Member Authorization System	KEK	Key-Encryption-Keys
GMNF-DVMRP	Group Membership Near First DVMRP	LEO	Low earth orbit
GPMS	Group Policy Management System	LEOsat	LEO Satellite-based networks
GPS	Navistar Global Positioning System	LKH	Logical Key Hierarchy
GSA	Group Security Agents	LPI/D	Low Probability of Intercept/Detection
GSC	Group Security Controller	LS	Link State
GSI	Group Security Intermediaries	MAC	Message Authentication Codes
HEO	Highly elliptical orbit	MANET	Mobile ad hoc network
HSRP	Hierarchical Satellite Routing Protocol	MAODV	Multicast extension to Ad hoc On demand Distance Vector routing protocol
ICO	Intermediate Circular Orbit	MBone	Multicast Backbone
IEEE	The Institute for Electrical and Electronics Engineers	MEF	Marine Expeditionary Force
IETF	Internet Engineering Task Force	MEO	Medium earth orbit
IGMP	Internet Group Management Protocol	Milstar	Military Strategic and Tactical Relay Satellite
IGRP	Interior Gateway Routing Protocol	MLD	Multicast Listener discovery
IOS	Cisco's Internetwork Operating System	MOSPF	Multicast Open Shortest Path First
IP	Internet Protocol	MUOS	Mobile User Objective System
IS-IS	Intermediate System to Intermediate System	NCW	Network Centric Warfare
ISL	Inter-Satellite Links	NLSP	Novell's NetWare Link State Protocol
ISP	Internet Service Provider	NMT	Navy Multiband Terminals
ISR	Intelligence, Surveillance, Reconnaissance	NPOESS	National Polar-orbiting Operational Environmental Satellite System
J-STARS	Joint Surveillance and Target Attack Radar System	ODMRP	On-demand Distance Multicast Routing Protocol
JTRS	Joint Tactical Radio System	OPNET	OPNET, Inc.
		OSPF	Open Shortest Path First

P2P	Point-to-point	UHF	Ultra High Frequency
PIM-Bidir	Bi-directional PIM	VoIP	Voice over IP
PIM-DM	Protocol Independent Multicast – Dense Mode	VPN	Virtual Private Network
PIM-SM	Protocol Independent Multicast – Sparse Mode	WGS	Wideband Gapfiller Satellite
PKI	Public-Key Infrastructure	WSN	Wireless Sensor Network
QoS	Quality of Service		
RF	Radio Frequency		
RFC	Request For Comments		
RIP	Routing Information Protocol		
RoM	Rate of Mobility		
RtS	Received-to-Sent ratio		
RTT	Round Trip Time		
SCAMP	Single Channel Anti-Jam Man Portable		
SGRP	Satellite Grouping and Routing Protocol		
SMART-T	Secure Mobile Anti-Jam Reliable Tactical-Terminal		
SOS	Satellite Over Satellite Network		
STK	Satellite Tool Kit		
S-UMTS	Satellite-Universal Mobile Telecommunications System		
TCA	Transformational Communications Architecture		
TCP	Transmission Control Protocol		
TSAT	Transformational Satellite System		
UAV	Unmanned Aerial Vehicle		
UFO	UHF Follow-On Satellite System		

A SECURE AND EFFICIENT COMMUNICATIONS ARCHITECTURE FOR GLOBAL INFORMATION GRID USERS VIA COOPERATING SPACE ASSETS

I. Introduction

1.1 Background

The Information Age is in a stage of rapid growth. As soon as new technologies are introduced, users expect even more capability, more speed, and greater flexibility. Rarely does any new technology exist as a stand-alone entity. Rather, society advances together, through sharing of knowledge, techniques, and technology. At the heart of this information sharing society is a communications network that always seems to be one step behind the needs of its users. Physical communications technologies, whether in the form of terrestrial or satellite systems, are also rapidly advancing in capacity and capabilities to meet the needs of bandwidth-hungry users. From the users' perspective, however, it seems "more" is never enough.

One way of addressing the problem of insufficient communications capacity is to focus on the actual data generation and usage of communications. At the dawn of the Information Age, the relatively small numbers of users were able to communicate in a point-to-point (P2P) fashion between local areas. Today, users need more capabilities than P2P systems can provide. Users expect to communicate in a one-to-many and even many-to-many fashion.

The United States Department of Defense (DoD) recognizes the need to change the data-sharing paradigm from a "stove-piped" point-to-point fashion to more of a group data sharing environment:

“Across the DoD, broad leadership goals are transforming the way information is managed to accelerate decision-making, improve joint warfighting, and create intelligence advantages...

Net-centricity compels a shift to a “many-to-many” exchange of data, enabling many users and applications to leverage the same data—extending beyond the previous focus on standardized, predefined, point-to-point interfaces.” [Ste03]

-John P. Stenbit, Former DoD Chief Information Officer

The enabling infrastructure that will deliver this “network-centric” environment for the DoD is the Global Information Grid (GIG). The GIG is “The globally interconnected, end-to-end set of information capabilities, associated processes, and personnel for collecting, processing, storing, disseminating, and managing information on demand to war-fighters, policy makers, and support personnel. The GIG includes all owned and leased communications and computing systems and services, software (including applications), data, security services and other associated services necessary to achieve Information Superiority.” [DoD02]. As noted in [AIH03], the GIG enables the aforementioned change in mindset, termed “power to the edge,” that delivers vast computing power to all DoD entities, regardless of their physical location, so long as they are “net-ready, meaning connected to the GIG.”

Satellites are an indispensable component of the GIG’s approach to connecting every warfighter with the information they need to make rapid, well-informed decisions. As is the case in all communications systems, secure, efficient, and effective methods for transferring information are essential. Multicasting in a satellite environment can provide the necessary performance and security while improving the efficient use of critical bandwidth.

1.2 Problem Statement

Throughout the GIG, as well as the Internet in general, communications predominantly flow in a point-to-point fashion, which is inefficient when large groups of users are accessing or sharing the same information. Additionally, secure group communications architectures face several issues, including limited scalability for very large groups of users, and excessive time and processing overhead to achieve a secure system. A secure group communications environment that must accommodate highly mobile users exacerbates these issues. Finally, users in the field, whether they are terrestrial or airborne, typically need bulky equipment to access limited, low-rate connectivity. Those users should not have to worry about excessive security overhead further hindering their communications as well. Proposals in the research literature address some of the issues. However, a solution that meets both the security and scalability needs of highly mobile users has yet to be proposed.

1.3 Research Goal

This research develops a novel security architecture, dubbed the “Hubenko Security Framework Architecture,” (Hubenko Architecture for short) to secure group communications (namely, multicast) in the low earth orbit satellite network environment more efficiently than currently proposed architectures. To achieve this goal, the Hubenko Architecture combines key aspects of different secure group communications architectures in a way that increases efficiency and scalability.

Implementing the Hubenko Architecture in a deployed environment with heterogeneous communications users will reduce the frequency of re-keying. Less

frequent re-keying equates to more resources available for data throughput versus security overhead. This translates to performance to the end user; it will seem as if they have a “larger pipe” for their network links.

1.4 Research Contributions

1.4.1 Coherent, Secure, and Efficient Architecture for LEOSat Environment

The primary objective of this research is to develop a coherent security framework architecture that improves the scalability of secure group communications for highly mobile users. This framework architecture is then applied to the LEO satellite network environment.

This research results in a scalable system security architecture capable of handling large groups of users (e.g., ten thousand or more) without loss of efficiency or significantly affecting data throughput. The architecture allows the system to handle at least an order of magnitude more highly mobile users while providing superior re-keying performance over the traditional and clustered architectures.

Multiple mobile communication environment scenarios are developed and analyzed to demonstrate the superior re-keying advantage offered by the Hubenko Architecture over traditional and clustered multicast security architectures. The first scenario compares the performance for different levels of user mobility. The second scenario compares the performance for different levels of user persistence in a multicast group. The third scenario compares the performance for increasing the number of aircraft flying over stationary users. The final scenario compares the performance of varied numbers of aircraft in a heterogeneous user environment. A sampling of the results

includes the following. In the scenario containing a heterogeneous mix of user types (Stationary, Ground, Sea, and Air), the Hubenko Architecture achieved a minimum ten-fold reduction in total keys distributed compared to the Cluster and Baseline architectures. In the “Increasing Aircraft over Stationary Users” scenario, the Hubenko Architecture operated at 6% capacity while the Cluster and Baseline architectures operated at 98% capacity. In the 80% overall mobility experiment with 40% Air users, the Cluster and Baseline architecture re-keying increased 900% over the Stationary case, whereas the Hubenko Architecture only increased 65%. A relative performance example for each of the scenarios is plotted in Figure 1 for illustrative purposes. The amount of re-keying was independently normalized for each scenario (i.e., the amount of re-keying in scenario one does not directly correlate to the amount of re-keying in scenario two). In each scenario, the Hubenko Architecture required less re-keying than the Cluster Architecture, as illustrated in the figure by the lower amount of relative re-keying.

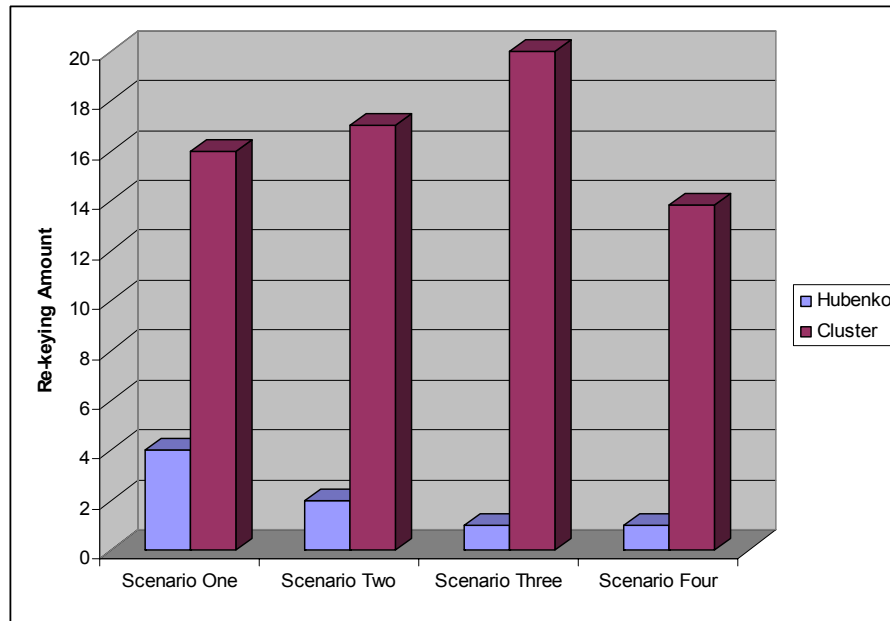


Figure 1 - Relative Re-keying Performance

1.4.2 Extension of Hubenko Architecture to Other Highly Mobile Environments

The unique topological and environmental challenges of the LEO satellite network originally motivated the development of the Hubenko Architecture. Once the benefits of the research materialized, it became obvious that the topology could be collapsed to a single terrestrial plane (versus a hybrid satellite-terrestrial topology), and the architecture could be extended to accommodate a variety of environments.

The Hubenko Architecture can easily adapt to multicast protocols and security architectures in numerous operational and deployed environments. Other research in the design stages is adapting the Hubenko Architecture for use in secure multicast communications of unmanned aerial vehicle (UAV) swarms. Additionally, the architecture could be used in mobile ad hoc networks (MANET), wireless sensor networks (WSN), and other heterogeneous mobile communications environments.

1.5 Assumptions/Limitations

The Hubenko Architecture's advantage is limited in environments where the communicating users are predominantly stationary, or where the users' movements are localized within a single area (i.e., a single cluster). In these environments, the Hubenko Architecture has the same performance as the clustered environment, but has extra overhead from an access control awareness feature implementation. Therefore, in a homogenous wireless sensor network where the sensors are immobile and extremely limited in battery and processing power, an implementation of the Hubenko Architecture for this environment would be detrimental. The overhead would unnecessarily decrease battery life through increased computational and communications cycles required to

support the access control awareness functions, which provide no benefit in this case. However, in a heterogeneous environment where the wireless sensor network is part of a larger network with mobile communications units passing through, and communicating with, the wireless sensor network, the reduced re-keying will greatly improve scalability and efficiency, and therefore battery life.

1.6 Dissertation Organization

This document is divided into five chapters. Chapter II reviews relevant literature for satellite systems, multicasting technologies, and multicasting security. Chapter III discusses the development and the details of the Hubenko Security Framework Architecture, along with the motivation for pursuing this architecture. This chapter also discusses the simulations and models that support the performance claims. Chapter IV presents the results and analysis of the numerous simulations performed during the course of this research. Chapter V concludes the document with a brief summary of the research, highlights of the contributions this research provides to the network communications community, and recommendations for future research.

II. Literature Review

2.1 Chapter Overview

This chapter presents a literature review covering three broad areas related to: 1) communication satellite systems, 2) multicasting technologies, and 3) multicasting security. The first area of research includes: low earth orbit, medium earth orbit, and geosynchronous earth orbit (and hybrids thereof) communication satellite systems and architectures; and the modeling, simulation, and analysis of such systems. The second area covers multicasting protocols and algorithms suitable for adaptation to satellite network environments, along with relevant modeling, simulation, and analysis of the protocols and algorithms. Finally, the third area of review pertains to multicasting security.

2.2 Communication Satellite Systems

Before discussing communication satellite systems, a brief overview of the four main satellite orbits is presented including: the low earth orbit (LEO), the medium earth orbit (MEO), the highly elliptical orbit (HEO), and the geosynchronous earth orbit (GEO).

The first orbit, the low earth orbit, places the satellite at an altitude between 200 to about 2,000 kilometers above the surface of the earth. Depending on the angle of the orbit with respect to the equator, the orbit can be classified as either prograde (0 to 90 degrees, “with” the rotation of the earth) or retrograde (90 to 180 degrees, “against” the rotation of the earth). LEO satellites that pass over the polar regions of earth are often referred to as “polar-orbiting.” Since LEO satellites orbit relatively closely to the earth,

radio frequency propagation round trip times (one link up, and one link down) are about 1.33 to 13.33 milliseconds, depending on the orbit altitude.

The medium earth orbit is also known as the intermediate circular orbit (ICO). MEOs are typically circular at an altitude of around 10,000 kilometers. This orbital height places the satellites between the two Van Allen radiation belts and therefore leads to longer satellite life as compared to an elliptical orbit where satellites pass through the radiation belts. Due to their altitude, MEOs provide coverage to the same ground location for several hours, and have a radio frequency propagation round trip time of about 67 milliseconds. One of the best-known examples of a MEO satellite system is the United States Navistar Global Positioning System (GPS).

A highly elliptical orbit's altitude varies, bringing a satellite relatively close to the earth at its perigee, and relatively far from the earth at its apogee. The HEO typically serves a very specialized purpose, as with the Molnya satellite system (which gave the name to its specific orbit). The Molnya system has an orbit that varies from an altitude of about 1,000 kilometers to about 40,000 kilometers, and is highly inclined, thus providing long periods of coverage to the northern latitudes of Russia.

Finally, the geosynchronous earth orbit places a satellite in a near-stationary position above the earth's surface. However, this is a common point of confusion, since a geosynchronous satellite technically only requires a rotation in the direction of the earth, and need not appear stationary from the ground. The Geostationary orbit, at an altitude of approximately 35,768 kilometers above the surface of the earth, is a subcategory of geosynchronous orbits, and is generally used when GEO satellites are referenced. Based

on this altitude, the radio frequency propagation round trip time for a GEO satellite is approximately 238.45 milliseconds. A comprehensive discussion of these orbits can be found in [Rod01, Sae03].

Existing long haul satellite communications systems primarily use geostationary earth orbit (GEO) satellites. GEO satellite systems allow full earth coverage below ~78 degrees latitude with as few as three satellites. Drawbacks to using these systems include the long propagation delay and the large propagation loss. The transmission power required to overcome the propagation loss of a 35,768 kilometers path makes GEO user handheld terminals impractical compared to LEO user handheld terminals. Therefore, the primary advantages associated with LEO satellites are a lower transmission power, a lower propagation delay, and polar coverage.

One aspect of defining a communications satellite system is its orbit. From a data handling perspective, communications satellite systems typically process data in two ways: “bent-pipe” or “store-and-forward.” When communication satellites operate in a bent-pipe fashion, they receive a signal from a terrestrial user and then echo the same signal back to the earth for further processing by some other entity. A store-and-forward satellite makes processing decisions on where to send a received signal, either back to the same geographical location, or to some other location on another transmitter [BeF99]. This includes being able to route signals to other satellites in a crosslink manner, where supported.

In addition to categorizing satellite systems based on their orbits and data handling characteristics, communication satellite systems can be divided according to the

different types of communications services they provide: narrowband, wideband, and protected communications services. To illustrate this, consider the Global Information Grid (GIG) and its subsystems as an example of a communications architecture that incorporates each of these services in its “layers.”

2.2.1 Global Information Grid

The DoD defines the GIG as a “globally interconnected, end-to-end set of information capabilities, associated processes, and personnel for collecting, processing, storing, disseminating, and managing information” [GAO04]. Furthermore, the GIG incorporates almost all of DoD’s information systems, services, applications, and data into a single seamless, reliable, and secure Internet-like network. The GIG promotes interoperability by using standards-based technologies across all platforms. The GIG will integrate most, if not all, of DoD’s weapon systems, command, control, and communications systems, as well as business systems. When complete, the GIG will have a new core network consisting of both a Satellite Layer and a Surface Layer. There is also an Aerospace Layer populated with mobile users and weapons systems. Finally, there is a “Near-Space Layer” between the altitudes of air flight and space, which may eventually make its way into the final architecture.

2.2.1.1 The GIG Satellite Layer

As depicted in Figure 2, the majority of the GIG’s communication assets in the Satellite Layer, either operational or in development, are geosynchronous earth orbit (GEO) satellites. The different systems provide the military with narrowband, wideband, and protected communications capabilities. In general, the narrowband capabilities

support highly mobile users needing low rate data or voice connectivity. Wideband capabilities are geared towards users that need much higher data rate connectivity and have sufficient power and available area to support the larger infrastructure required. The protected capabilities ensure users are able to communicate through various electronic warfare attacks, survive nuclear radiation environments, and have a lower probability of detection and interception.

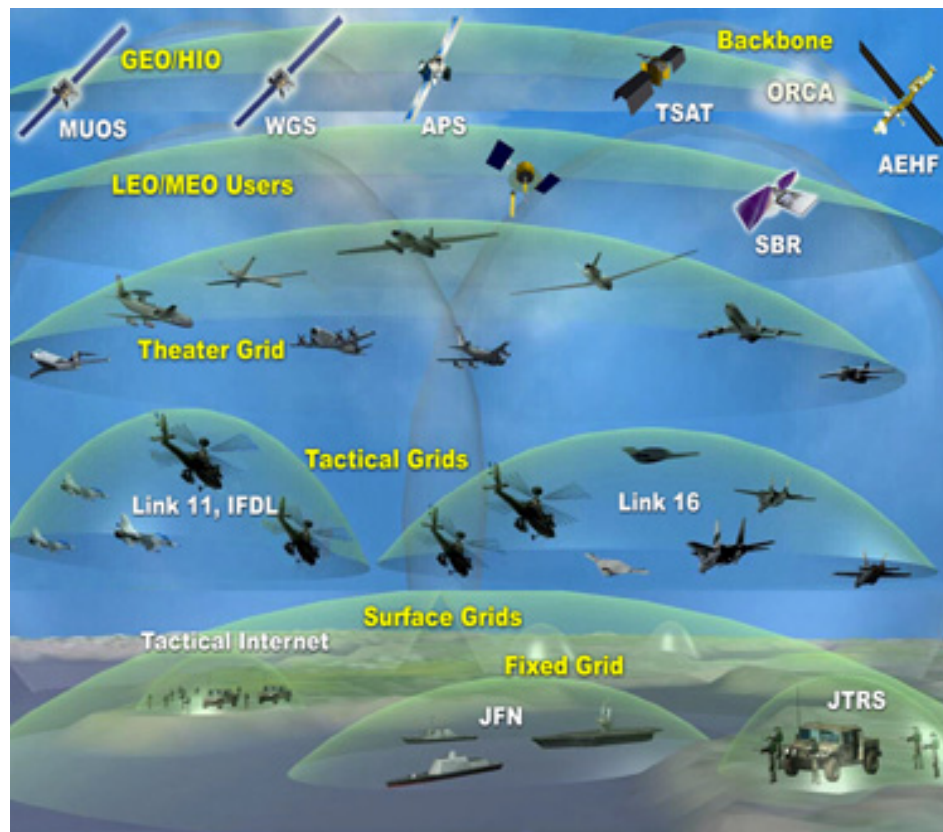


Figure 2 - Global Information Grid Layers [SMC06a]

2.2.1.1.1 Narrowband Satellite Systems

The needs of the highly mobile warfighter are currently supported by the Ultra High Frequency (UHF) Follow-On (UFO) satellite system, soon to be replaced by the Next Generation Mobile User Objective System (MUOS) [SPA06]. Tactical field

equipment has to be small, light, and rugged to survive the harsh environments faced by the typical warfighter. To support increased mobility, tactical terminals typically have much smaller antennas and less processing power than users that are stationary. Because of these constraints, low rate voice or data communications are the usual services provided to the warfighter on the move. Utilizing the UHF spectrum allows signals to penetrate buildings, harsh weather, and thick vegetation. In addition, UHF frequencies are well-suited for use in low-power, inexpensive, lightweight, rugged communication systems [SMC06b].

2.2.1.1.2 Wideband Satellite Systems

Tactical forces in the field rely upon wideband satellite systems to reach back to the surface portions of the GIG. The Defense Satellite Communications Systems Phase III (DSCS III) wideband satellites use a portion of the X-band frequency to provide secure voice and high data rate communications for the military's typical long-haul, high-capacity communications needs when a high speed, high capacity terrestrial network is not available [SMC06b].

In the near future, the Wideband Gapfiller Satellite (WGS) system will replace DSCS as the next generation of high capacity communications connectivity. Notionally, there will be three to five WGS's on orbit, depending on the development pace of the Transformational Satellite System (TSAT). WGS will augment and then replace the DSCS support in X-band, as well as augment and replace the one-way Ka-band broadcast of the Global Broadcast Service Satellite System (GBS). WGS will also provide a new two-way Ka-band communication capability for the warfighter.

As the name implies, the Global Broadcast Service provides a high speed, high volume “broadcast-from-the-sky” service for the military. The GBS will augment, as well as interface with, other communication services to provide a medium for continuous information flow to users. The GBS platforms are hosted on three of the UFO satellites, and will fly on three WGS’s. Additionally, future requirements for the broadcast service will be met by hosting GBS packages on TSAT platforms [SMC06b].

TSAT rounds out the capabilities of all the previous DoD wideband communication satellite systems and is the ultimate enabler of the Transformational Communications Architecture (TCA). TSAT will provide another source of high data rate satellite communications along with services modeled after the Internet. Notionally, five operational satellites will be connected in a ring through laser crosslinks, and will provide laser and radio frequency (RF) connections to the Surface layer. TSAT will extend routing capabilities of the previous wideband satellite systems and be able to route packets in space rather than provide bent-pipe, point-to-point connections between ground users. The satellite crosslinking reduces the need for packets to make multiple ground/satellite hops to reach distant users. This reduces end-to-end latency, and allows for near-real time communications speeds [DTI05].

2.2.1.1.3 Protected Satellite Systems

Protected communications are serviced by a global extremely high frequency (EHF) system, composed of the Military Strategic and Tactical Relay Satellite (Milstar) system, the Advanced Extremely High Frequency System and Enhanced Polar System. Protected communications offer Low Probability of Intercept/Detection (LPI/D), Anti-

Jam (AJ), and Anti-Scintillation (AS) protection, as well as being encrypted. The main methods of protecting the communication links originate from operating in the Ka-band as well as using advanced communications techniques, such as frequency hopping and active phased array antennas. This combination offers resilience against electronic warfare and reduces the probability of physical attacks.

The first in the series of satellite systems to provide protected communications for the DoD is the Military Strategic and Tactical Relay Satellite (Milstar). Launched in 1994, Milstar provides connectivity to ships, submarines, aircraft, and other terrestrial users through five geosynchronous satellites. Since the satellites are crosslinked and can process traffic rather than simply transpond signals between two ground users, Milstar satellites establish circuits between themselves and the ground, based on dynamic user needs [SMC06b].

In the next few years, the Advanced Extremely High Frequency (AEHF) System will launch three geosynchronous satellites, continuing and enhancing the protected services offered by Milstar. The AEHF enhancements over Milstar include a 100-times capacity increase, as well as enhanced anti-jam and LPI/D capabilities, and advanced encryption systems. Once a single TSAT is operational, DoD will have achieved continuous 24-hour communications coverage between the latitudes of +/- 65 degrees with the three AEHF satellites and one TSAT.

To augment the current northern polar coverage gap in Milstar services, the Interim Polar EHF system places protected communications packages on three classified spacecraft that occupy highly elliptical orbits. This system provides protected

communications services similar to Milstar, but in the northern polar region. When AEHF comes online, the Enhanced Polar System (EPS) will provide protected communications that are comparable to AEHF, but will be on a classified spacecraft, just like the Interim Polar EHF system. However, unlike Interim Polar, EPS will have crosslink capabilities, enabling cross connections to not only other EPS packages, but to AEHF and TSAT as well [SMC06b].

There has been a steady progression of capabilities in each of the different types of satellite communications systems, as well as a move towards a highly cooperative Satellite layer to maximize communications support to the warfighter. Each piece of the Satellite layer contributes directly to achieving the concept of Network Centric communications for the DoD user.

Operating in the realm of the Satellite layer is well understood by the DoD, with mature technologies deployed and well-developed operational concepts in place. To follow the intent of the Transformational mantra means taking a fresh look at how best to utilize available resources for providing information to the warfighter. Using lessons learned in the Satellite layer and applying them to the Near-Space layer may greatly enhance the DoD's capabilities for a fraction of the cost.

2.2.1.2 The GIG Near-Space Layer

Near space begins at an altitude of 22.86 kilometers and ends at the beginning of space or at 100.58 kilometers according to the International Aeronautical Federation (FAI) [Tom05]. Near-Space is the region between the traditional realms of satellites and air-breathing assets such as unmanned aerial vehicles (UAVs) and typical airplanes.

Though not formally incorporated as a layer in the GIG, research into exploiting the Near-Space layer is gaining support within the DoD. When the Near-Space technologies mature, this layer will most likely find a home in the GIG. Examples of “nearcraft” platforms for carrying sensors or communications packages include balloons, gliders, special motorized nearcraft, all of which are currently under development.

There are several key advantages to operating in the Near-Space layer over the Satellite layer [Tom05]. The first advantage is significantly reduced developmental and operational cost, since the assets do not have to be space hardened and space qualified. Another advantage is the reduced component sizes of sensors and communications equipment needed to achieve performance levels similar to like systems in the Satellite layer since sensors are significantly closer than those placed on satellites. On the other hand, if the same satellite sensors or communications packages are used on platforms in the Near-Space layer, large increases (10-20 fold) in image resolution, sensitivity, and accuracy can be achieved. In addition to the cost and component advantages, Near-Space atmospheric conditions allow sensors and communications equipment to operate with less interference and/or distortion. For example, “nearcraft” operate at altitudes low enough to avoid most space weather effects. In addition, they are below the wave-refracting or blocking ionosphere, which allows better sensor performance, and yet are high enough to avoid most atmospheric weather effects, like high winds or rain. With the development of Near-Space vehicles comes the potential to achieve true continuous, persistent Intelligence, Surveillance, and Reconnaissance (ISR) or communications coverage of

specific tactical areas. While Near-Space offers unique opportunities, the Aerospace layer contains many of the contemporary platforms needed for military operations.

2.2.1.3 The GIG Aerospace Layer

The conventional Aerospace layer is by far the most familiar layer above the Surface layer. New technologies and applications are continuously developed to enhance and improve capabilities. This layer is dominated by aircraft such as helicopters, fighters, tankers, and cargo jets. However, the impact of the unmanned aerial vehicles is being felt due to increased operational capabilities.

Familiar equipment using the Aerospace layer includes the Airborne Warning and Control System (AWACS) and the Joint Surveillance and Target Attack Radar System (JSTARS). These assets are used for long-range surveillance and target acquisition, as well as command and control functions for both ground and aerospace assets. The employment of the Aerospace layer goes beyond conventional ISR collection and delivery of munitions and supplies. This layer is emerging to take on new roles in the communications arena with the development of the Battlefield Airborne Communications Node (BACN). The BACN will provide communications connections to both legacy radio systems as well as advanced Internet Protocol (IP) communications (data as well as voice).

2.2.1.4 The GIG Surface Layer

Bridging the Aerospace layer and the Surface layer is a new communication system called Joint Tactical Radio System (JTRS) [GAO04]. This software radio system will bridge interoperability gaps between current user terminals and new IP terminals for

mobile users on the ground, at sea, or in the air, as well as connect those same users to the permanent terrestrial network. In instances when a JTRS is not available, users can directly access the Satellite layer systems for their communications needs. Examples of user terminals supported by AEHF include Secure Mobile Anti-Jam Reliable Tactical-Terminal (SMART-T), Single Channel Anti-Jam Man Portable (SCAMP), Family of Advanced Beyond Line-of-sight Terminals (FAB-T), and Navy Multiband Terminals (NMT).

As part of the core backbone, the terrestrial networks of the GIG are also being enhanced to provide maximum information sharing between entities. The Defense Information Systems Network (DISN) was recently upgraded through an effort known as “Global Information Grid-Bandwidth Expansion,” or GIG-BE [GAO04]. GIG-BE provides fiber optic connectivity to several key military installations, as well as upgraded the network capacity to about 90 DoD installations.

2.2.1.5 The GIG’s “Missing” Layer

The Satellite layer is typically associated with GEO satellites. Because of the steadily increasing usage of the GEO belt (to near saturation), new approaches for using orbital assets are needed. Non-GEO orbits were proposed in the early 1990s and fielded in the late 1990s. Particular emphasis was placed on fielding low earth orbit (LEO) systems of cooperating assets. The LEO belt can be considered the GIG’s “Missing” layer.

LEOs typically reside 200 to 2,000 kilometers above the earth’s surface. Because of this orbit, communications between a terrestrial observer and a LEO satellite may last

for only 8 to 20 minutes, but with up to 45 times less latency compared to a GEO satellite. Because of the short viewing time, multiple satellites must be placed into multiple orbital planes to provide extended viewing coverage. Perhaps two of the best-known LEO satellite systems are IRIDIUM[®] and GlobalStar[®]. IRIDIUM[®] uses 66 satellites and has store-and-forward capabilities, while GlobalStar[®] uses 40 satellites and operates as a bent-pipe.

2.2.2 Highlights of the IRIDIUM[®] LEO Satellite System

The Air Force Institute of Technology's (AFIT) initial venture into the realm of low earth orbit (LEO) satellite network architectures began with an investigation on the packet delays, convergence speeds, and protocol overhead of the Extended Bellman-Ford and Darting unicast routing protocols adapted to a satellite network and modeled and simulated on the IRIDIUM[®] and GlobalStar[®] satellite systems [RaJ97]. Following this effort, a higher fidelity model of the IRIDIUM[®] LEO satellite network was developed [FoR98, PrR99].

The information in this section was derived from [FoR98, Hub97, PrR99, RaJ97, Sae03]. The IRIDIUM[®] system is a worldwide LEO satellite communications system designed to support voice, data, facsimile, and paging. The IRIDIUM[®] satellite constellation has six orbital planes with eleven satellites in each plane. The satellites are in a circular orbit at an altitude of approximately 780 kilometers and an inclination of 86.4 degrees. Orbital planes one and six are counter-rotating and separated by approximately 22 degrees. The remaining orbital planes are co-rotating and are separated by approximately 31.6 degrees.

The velocity of a LEO satellite relative to earth is 26,804-kilometers/hour and results in an orbital period of 100.13 minutes. The minimum inclination angle for a user to see a given satellite is 8.2 degrees. At a fixed location on earth, the average in-view time for a satellite is approximately nine minutes and either one or two satellites are visible at a time.

A link is established from an earth station to the satellite with the strongest signal. There are 48 spot beams per satellite, with 80 circuits per spot beam. Each spot beam is approximately 30 miles in diameter, depending on the satellite's current position. Since the satellites are moving much faster than the mobile users, the mobile users are considered stationary with respect to the velocity of the satellites, as even a mobile user in an airplane is traveling much slower than a satellite. As the satellites pass overhead, the link from user to satellite is handed off from a satellite leaving the users area to one entering the user's area, much like a cellular phone user hands off between cellular phone towers when passing from one cell to the next.

Each IRIDIUM[®] satellite maintains up to four inter-satellite links (ISL). Intra-plane links (crosslinks to satellites in the same orbital plane) are maintained permanently, while inter-plane links (crosslinks to satellites in different orbital planes) are dynamically established and terminated to avoid excessive overlap near the polar regions. Satellites along the counter-rotating seams do not establish ISLs between each other due to the rapid angular change.

2.2.3 Other Satellite Communications Systems

The GIG is an excellent example of multiple systems cooperating to deliver services to customers. The satellite systems within the GIG, however, are but a small subset of the total number of worldwide communications satellite systems planned, in the development stages, or are currently in operation. The late 1990s saw a flurry of activity from numerous entities to meet the needs projected for satellite users. As a result, much research and development money went into the area of satellite communications. For example, 17 companies filed for EHF spectrum to operate their proposed satellite systems [FrH99]. Still others proposed and investigated systems ranging from LEO systems to MEO to GEO, and even hybrid systems [BhH02, CaL99, GhS99, JaK99, Yam97]. This created extensive development of non-geostationary orbital analysis as well as much-needed research in intra- and inter-satellite routing techniques, satellite network architectures, business models, and user terminal technologies [Ake02, Bar04, WuS05]. The first known research efforts regarding LEO constellations date back to the early 1970s [RaD99, Wal70, Wal71].

Despite the extensive research and investment, the majority of the 1990s-proposed satellite systems never launched, while a few systems, like ICO[®], were successfully placed into orbit, yet did not succeed commercially. Fortunately, most of the research efforts were not in vain. One technology that is still being developed, and fielded is the Digital Video Broadcast – Satellite (DVB-S) [BeH05, BeQ05, CaD04, ChK04, ChT03, CoB05, CoM00, CrH05, MoR04, Rei06, RiV04, SkL04, SkV05, SuJ04].

However, this technology is not applicable to the focus of this research due to its one-way, broadcast-type technology.

Another technology that is gaining interest (at least from a research perspective) is the Universal Mobile Telecommunications System (UMTS) [BaL03, KaH04, LoL04, NaK04, SuE02]. The main focus of this effort is the deployment of an extensive downlink capability from the LEO and GEO satellites (Satellite-Universal Mobile Telecommunications System, or S-UMTS), with relatively little satellite uplink capability except for remote users. The UMTS uplink will most often be handled by the Terrestrial-Universal Mobile Telecommunications System (T-UMTS) portion of the network. As such, the UMTS system does not fall within the scope and intent of this research.

2.2.4 Inter-Satellite Links and On-orbit Routing

From a communications network standpoint, the most critical research areas derived from the systems developed in the 1990's is that of the inter-satellite links (ISLs) which enable on-orbit routing capabilities. Numerous constellations and architectures have been analyzed, validating the proposed use of LEO satellite constellations instead of GEO satellites in communications networks [FoR98, MoS02, PrR99, RaD99], as well as comparing different constellations to minimize the impacts of the non-communicating counter-rotating seams of the near-polar star pattern constellations [WeF01]. Other issues related to satellite networking are caused by the high mobility of the satellites, and their constant, rapidly changing topology. Fortunately, satellites maintain regular, highly predictable, periodic orbits which allow convenient adaptations of terrestrial routing algorithms and protocols to a satellite network [HuR06a, RaD99, RaJ97, ThR02,

WoC01]. In addition to adapting the routing protocol, there are other methods of using a terrestrial protocol in a satellite environment. For example, dividing the network between terrestrial and orbit assets using tunneling, network address translation, or an exterior gateway protocol prevents the propagation of too many IP routing table updates from the satellite portion of the network from entering the terrestrial network [WoC01].

Extensive research has investigated the effects of transmission control protocol (TCP) and routing strategies in satellite constellations. Some focus on improving the GEO communications systems with their long latencies rather than improvements for LEO systems, but benefits derived for GEO systems can be adapted to make improvements in LEO systems [AkJ04, AkM01a, AkM01b, AkX02, BhB01, GoJ01, JiA02, KaT04, Kot05, MaP03, Mar01, MiS01, TsO05, WoP01, ZhB02].

Since existing long-haul satellite communications systems primarily use GEO satellites at altitudes of approximately 35,768 kilometers, GEO satellite systems provide full earth coverage below ~ 78 degrees latitude with as few as three satellites. However, the one-way (ground to satellite or satellite to ground) signal propagation delay is approximately 119.23 milliseconds as compared to approximately 0.67 to 6.67 milliseconds for a LEO. While the GEO systems in the GIG use crosslinks to route traffic from one part of the world to another with end-to-end latencies of at least 238.45 milliseconds, LEO communications systems can achieve average end-to-end latencies of less than 100 milliseconds for intercontinental communications using satellite crosslinks [HuR06a]. Thus, LEO communication satellite systems with lower transmission power

requirements, shorter propagation delays, and global coverage are worth including in the overall GIG architecture.

If low-latency voice and video communications are important requirements for tactical users in the field, the LEO communications system are the better choice. If seconds matter in Network Centric military communications, an extra 138 milliseconds latency could mean the difference between meeting or missing an objective. However, realizing these communication capabilities will require efficient transmission strategies.

2.3 Multicasting Technologies

Most Internet communication uses a one-to-one (unicast) approach for source-destination communications. Unicast requires a node to send an individual message to every recipient. This approach works well until a single message needs to be sent to multiple nodes. In this case, separate copies of the message must be sent. This approach is obviously inefficient as it wastes bandwidth and resources. It would be especially inefficient in a multi-layered, long-haul communications environment such as the GIG. An approach that improves efficiency and alleviates possibly significant traffic on long-haul links is multicast routing to groups of users that are receiving the same data. This concept was first proposed by Stephen Deering [DeC90, Dee91].

2.3.1 Multicast Overview

Multicast routing fits in between unicast routing and broadcast routing. Broadcast routing sends one message to each node in the entire broadcast domain (similar to a bent-pipe satellite operation). While this is a very effective method of ensuring all users on the network receive an important message, it is quite wasteful, especially if the message

is actually intended for a small subset of the available users. Multicast routing, as compared to unicast routing, sends a single message per link instead of sending a copy for each node accessing the information on the link. This single copy is reproduced across multiple links as close to the individual receiving nodes as possible. In this way, multicasting enables a large amount of information to be efficiently distributed between a large group of interested users. Satellites, because of their large coverage areas, are an ideal means of implementing multicast.

There are several dozen different multicasting protocols proposed in the literature, some of which warrant further investigation. When selecting a multicasting protocol, desirable properties are: low cost; low end-to-end delay; scalability; ability to support dynamic group membership; survivable in terms of network, link, or node outages; and some level of fairness to all members [SaM00]. In addition to these properties, it is also important to ensure a high level of efficiency (maximum data transmitted for the least overhead) and a high level of effectiveness (maximum received-to-sent ratio), indicating few lost packets throughout the system [HuR06a, ThR02]. A final consideration is the viability of the protocol either in the commercial world or as a developing or established standard. Before exploring the various multicasting protocols, two major types of unicast routing protocols in use today are examined.

2.3.2 Link State and Distance Vector Routing Algorithms Overview

When a host sends a packet to a user on another host, the packet is sent down the protocol stack to the physical network, where it is carried to its intended destination. Several key tasks must be performed to ensure this happens correctly. One such task is

obtaining the destination's address. The other is to direct the packet towards that address. Assuming the address is already known (by some unspecified means), network routers communicate among themselves to determine the best path to the destination node. The two most prevalent routing algorithm categories used throughout the Internet are Link State and Distance Vector. Both algorithms provide a means to route packets towards intended destinations using Dijkstra's algorithm [Dij59] to determine the shortest paths. Both algorithms use routing tables stored in the routers, and they both share at least some of their routing tables with other routers in the network. Distance Vector algorithms are well-suited for small, simple networks, and Link State algorithms are better at handling larger, more complex networks.

Link State-based algorithms include Open Shortest Path First (OSPF), Intermediate System to Intermediate System (IS-IS), Border Gateway Protocol (BGP), and Novell's NLSP (NetWare Link State Protocol). The best known Distance Vector algorithm is the Bellman-Ford algorithm, which is used in many routing protocols such as Routing Information Protocol (RIP v1 and v2), Interior Gateway Routing Protocol (IGRP), Internet BGP, Novell IPX, and the original ARPAnet. Enhanced IGRP (EIGRP) is a well-known Cisco proprietary routing protocol that integrates the capabilities of link-state protocols into distance vector protocols.

One of the most obvious differences between the Link State (LS) and Distance Vector (DV) routing algorithms is the way information is shared between routers in the respective networks. Each LS router periodically floods the entire network with the state of its own local connections. From this flooding, each LS router calculates routes for the

entire network because it has knowledge of all connectivity and link costs. In this respect, LS algorithms have a “global view” of the network, i.e., the routers exchange information to make informed decisions on the best routes for the entire network. Ideally, all routers would have identical routing tables.

Distance Vector routing algorithms share much more information (possibly their entire routing tables instead of only their local connections) than LS algorithms, but the routers only share this information with their neighbors. While LS algorithms share the information with a regular period, DV algorithms send the information only when there are changes. Once the network reaches a steady state, the routers will no longer share data if there are no more changes. To build a complete routing table, DV routers iteratively build the tables as they receive information. Router tables store which router is the next hop in the route and what the trip cost will be. Unlike the LS algorithm, the DV routing tables do not have complete route information for every link in the route.

Assuming there are n nodes and L links in the network, the worst case computational complexity of a LS network is $O(n^2)$, with approximately $O(nL)$ messages sent to achieve full network convergence. DV networks converge at varying rates, depending on the topology of the network. When a link cost is reduced, that information flows quickly throughout the network. On the other hand, when a cost is increased, the information travels much slower through the network, and a phenomenon known as the “count to infinity problem” could arise. Count to infinity occurs when two nodes iteratively increase their cost information based on their direct neighbor, resulting in an inaccurately increasing cost. This is similar to what occurs if a clockmaker adjusts his

clocks based on the town clock tower, and the keeper of the clock tower sets his time based on the clockmaker's clocks.

DV algorithms converge slower than LS algorithms, and are likely to have routing loops while converging. LS algorithms, because they converge more quickly, are somewhat less prone to routing loops than distance vector algorithms. DVs typically do not experience route oscillation, whereas LS algorithms are likely to oscillate on occasion because they respond so quickly to routing changes.

Link-state algorithms require more CPU power and memory than distance vector algorithms. LS algorithms, therefore, can be more expensive to implement and support. LS protocols are generally more scalable than distance vector protocols.

LS networks are continually refreshed with the latest information, so failure notification spreads quickly throughout a large network, whereas a failure in a large DV network may take a relatively long time to propagate to all routers. Again, this comes at the cost of more message traffic overhead from the frequent flooding of connectivity data. Since LS algorithms only flood their own connection information, this reduces the effect of errors propagating throughout the network. Should a link state router fail, or have its routing table corrupted and send out incorrect link information, only the local area and traffic destined for that specific location is jeopardized. In the case of DV algorithms, a corrupted link status would propagate throughout the whole network since routers depend on data from each other to gather the network connectivity beyond their neighborhood. Incorrect information passed from one router to the next will eventually make its way throughout the network.

The Link State and Distance Vector routing algorithms are not only used in unicast routing; the design concepts are used in multicasting protocols as well. For example, Multicast Open Shortest Path First (MOSPF) [Moy94] is a link-state algorithm, while Distance Vector Multicast Routing Protocol (DVMRP) [FiD01, Pus04, ThR02], On-demand Distance Multicast Routing Protocol (ODMRP) [YiS03], and Multicast extension to Ad hoc On demand Distance Vector routing protocol (MAODV) [RoP00] are distance vector algorithms. Since Protocol Independent Multicast – Dense Mode (PIM-DM) [AdN05, DeE96, HuR06a, Sae03] and Protocol Independent Multicast – Sparse Mode (PIM-SM) [FeH06] are “protocol independent” as their names indicate, they inherit the underlying routing tables and are neither link-state nor distance vector algorithms. Aside from the LS or DV categorization, multicasting protocols can be classified as Dense or Sparse.

2.3.3 Dense and Sparse Types of Multicast

Multicast protocols support two modes of operation: dense mode and sparse mode. Dense Mode protocols perform best when the topology is densely populated with group members. Routers assume there are group members downstream, and continue to forward packets unless a prune message (indicating no members exist or remain in the group) is received. Dense Mode protocols, also known as broadcast-and-prune protocols, are typically source-based, meaning the root of the multicast tree starts at the source. Examples of Dense Mode protocols include DVMRP, Group Membership Near First DVMRP (GMNF-DVMRP) [LaD98], and Protocol Independent Multicast – Dense Mode (PIM-DM). ODMRP is a mesh-type protocol that provides maximum connectivity and

robustness for highly mobile networks. While not specifically classified as a dense protocol, the broadcasting characteristic of ODMRP safely places it in this category.

Sparse Mode protocols work more efficiently with a small, widely distributed group membership. Members are expected to explicitly join groups by way of a core router that is typically located in a central portion of the network. Source members communicate with the core router as a “meeting place,” and build the multicast tree from there. Examples include Protocol Independent Multicast – Sparse Mode (PIM-SM), and Core Based Trees (CBT) [Bal97]. MAODV is a hybrid of dense and sparse modes. An MAODV user broadcasts to find the multicast trees, and joins the nearest tree discovered. MAODV multicast groups also establish group leaders to initiate and maintain group sequence numbers.

2.3.4 Some Options for Multicast Networks

To support the aforementioned multicast protocols, a network must have multicast-aware routers in the network. The obvious way to achieve this is to deploy an entire network of routers that are multicast-aware. However, that may be impractical for numerous reasons, such as fiscal limitations or not having control of the entire network. A solution for the first requirement is to deploy virtual private networks (VPNs) across the Internet, and even departmentalized VPNs within a corporate network [KaK01]. In March 1992, the Multicast Backbone (MBone) network became the first operational multicasting network, using IP-encapsulated tunnels to multicast (via DVMRP) video conferencing between 20 geographically separated sites through the Internet [Alm00]. Aside from tunneling across domains to connect multicast domains, a host can contact a

“multicast reflector” or participate in an “overlay multicast” group [ElR03]. If a host only has access to unicast capabilities, that host can contact another host on the edge of its unicast domain and the desired multicast domain. The reflector host acts as a proxy for the first host. This concept is similar to tunneling, except the tunnels are not permanent as they are in MBone. In the overlay case, the end systems take control of the multicasting functionalities such as group membership and packet handling. Directed virtual graphs connect each of the participating nodes, thus masking the actual physical connection information. To achieve this, the overlay multicast group needs complete control of the network. This contrasts with traditional multicasting where the core routers handle the routing, replication, membership; manage the physical connections; and retain control of the network across the various domains [ElR03].

The new 802.1a(x) standards groups are carrier-grade Ethernet adaptations to allow Internet Service Providers the ability to offer widespread Layer 3 multicast and broadcast services to their customers across a shared medium [ElA05]. This differs from Layer 3 multicast and broadcast technologies that ultimately rely on point-to-point connections between users and not a shared medium. While some of the ideas for enhancing efficiency in the shared multicast arena have some benefit to the proposed research topic, the standards groups are only in their first drafts, and are mostly forward-looking. The scope of the 802.1a(x) research does not specifically include multicasting on shared access medium such as Ethernet or ad hoc sensor networks, although the findings may support adaptation to these technologies.

Besides being able to connect to other multicast routers, the various multicast groups must be managed. Currently, two Internet standards address this requirement, and they are discussed in the next section.

2.3.5 Group Management Protocols

Internet Group Management Protocol (IGMP) [CaD02, Fen02] and Multicast Listener Discovery (MLD) [DeF99, Hab03, ViC04] are protocols that assist the multicasting protocol users in managing groups. IGMP was developed primarily for use in IPv4 multicast systems, while MLD was developed for IPv6 multicast systems. Since the two are closely related, several other standards documents address their common functionalities [FeH04, HaM03, HoC04].

IGMP is an asymmetric protocol that handles group members and multicast routers separately within the same specification [CaD02]. IPv4 systems use IGMP to share local IP multicast group membership information with their neighbor multicast routers along with other IP multicast management functions. Joins, Leaves, Queries and Reports are all provided by IGMP [CaD02, Fen02, Sae03].

IPv6 routers use MLD to maintain a list of multicast listeners attached to its local interfaces, as well as communicate with neighboring multicast routers to share those multicast addresses of interest to each other [ViC04]. Much like IGMP, MLD is also an asymmetric protocol, specifying separate behaviors for multicast address listeners and multicast routers.

Having covered the basics of multicasting, the next section discusses multicasting systems that have either been proposed or implemented in a satellite network environment.

2.3.6 Multicast Satellite Networks: Architectures and Multicast Protocols

There are several communications satellite architectures with varying constellation designs across the LEO, MEO, and GEO realms. The first relevant satellite architecture has a LEO and a MEO layer of satellites [LeK00, LeL00]. LEO-only architectures with numerous satellites (72, 288, and 1,152) in the constellation suffered significant delays due to large numbers of hops when traversing the LEO network. To preclude this, the MEO layer is added as well as the Hierarchical Satellite Routing Protocol (HSRP). This protocol minimizes hop counts for long distance routes by sending traffic from the LEO layer up to the MEO layer that has a smaller node count, and then back to the LEO layer down instead of traversing through the extensive LEO layer with its large node count. HSRP simulation results show a 75 milliseconds delay and are on par with those found in [HuR06a].

The fundamental shortcomings of typical connectionless routing schemes in satellite networks are due to path metric calculations that do not properly account for the total delay [ChE02]. The Satellite Grouping and Routing Protocol (SGRP) evaluates the overall path delays, to include processing, transmission, and propagation in a LEO/MEO satellite architecture. The MEO's main function is to perform the route and delay calculations for the LEOs, thereby offsetting significant amounts of processing and power utilization on the LEOs. MEOs can also perform routing if necessary. Metrics have been

reported on Path Optimality, Link Congestion, and Satellite Failures, but the end-to-end performance of this new protocol has not been evaluated [ChE02].

The “Multi-Layered Satellite Routing” Algorithm, or MLSR, assumes a satellite network with LEO, MEO, and GEO satellite layers [Ake02]. The bulk of the routing is handled by the LEO layer, while the GEO layer is used primarily for handling the routing protocol calculations. The GEO routers use route aggregation from one layer to the next, and make routing decisions based on link delays and the status of the total topology. The GEO layer does not route data traffic. Simulation studies in [Ake02] compare the performance of MLSR to a network using only LEO satellites and found when the LEO layer ISL utilization approached roughly 96%, a significant decrease in end-to-end delay was achieved by sending the data traffic up to the MEO layer to route using a different path. Once stabilized, the end-to-end (EtE) delay was estimated to be about 130 milliseconds between 105° W, 45° N (Montana/Wyoming border) and 15° W, 15° N (Senegal, Africa). For comparison, the estimated EtE delay for similar distances was approximately 86 milliseconds using only a LEO network, under different loading conditions [HuR06a].

Using the same satellite constellation, an enhancement to the MLSR protocol was adapted to the network [YuE02]. The GEO layer manages groups as well as constructs trees for the LEO and MEO layers. Multicasting using shortest path trees (rooted at the source node on the ground) resulted in a slightly increased delay to gain higher bandwidth efficiency. Using the nearest LEO as the core node for a core based tree multicast, the network and algorithm had worse delay performance and increased link

cost over a non-uniform distribution of members compared to a uniform distribution. However, without further details on the densities and layout of the member nodes, it is difficult to determine if the poor performance is due to the Sparse Mode protocol when a Dense Mode protocol would be more effective, or if the proposed multicasting protocol has a deficiency.

It has been claimed that none of the proposed terrestrial multicast protocols (such as MOSPF, DVMRP, CBT, and the two PIM protocols) are well-suited for use in satellite networks [EkA02]. The main reason is the limited ability for the satellites to establish or maintain the multicast trees in the rapidly changing satellite environment. To the contrary, [HuR06a, Sae03] indicates that with few changes to the protocol, PIM-DM can be adapted to a LEO satellite environment with relatively good performance.

2.3.7 Issues Surrounding Multicast Communications

The two previous sections reflect the results from a significant number of ongoing research efforts in the area of satellite communications architectures and multicasting technologies. However, there are still several areas that impede the extensive deployment of multicast throughout the Internet. There are many reasons why multicasting has been slow to develop.

2.3.7.1 Scalability

The first issue is high scalability [SaM00]. The network must be able to support a large number of users, but without causing excessive delays due to resource limitations or excessively large tree structures (either shared or source-rooted). The overhead of

multiple membership groups, plus multiple trees should not overburden the routing infrastructure.

2.3.7.2 Dynamic Multicast Groups

Multicast protocols should allow members to join and leave groups as necessary, as well as allow members to participate in more than one group at a time. The joining and leaving processes should not burden the existing multicast tree or group members by increasing cost, delays, since the groups can be highly dynamic with numerous joins and leaves occurring throughout a session [SaM00].

2.3.7.3 Survivability

Survivability of a routing protocol is its ability to re-establish connectivity in the event of link or node failures [SaM00]. If the multicasting protocol has its own unicast routing mechanism to establish connectivity, the multicast protocol is as survivable as its unicast counterpart. For multicast protocols that are independent of the unicast routing, such as the PIM protocols, they must implement their own means of protection or restoration in the event of failures.

2.3.7.4 Fairness and Jitter

Depending on the user or customer base of the implemented network, fairness is an issue that has to be addressed [SaM00]. In most cases, each user should receive the same basic quality of service (such as consistent delays), as well access to data at roughly the same time. These can be accomplished by finding delay- and delay-variation-bounded trees for the multicast network. Algorithms that compute the Delay-Bounded

Steiner Tree (DBST) and the Delay-Variation-Bounded Multicast Tree (DVBMT) are beyond the scope of this research [MaG04].

Delay variation is also known as jitter. One cause of jitter is found within the LEO satellite architecture itself [LoL04]. Depending on the instantaneous configuration of satellites, the available routes for a single session may change numerous times, with a different number of hops for each topology change. TCP applications may not be able to tolerate these changes in delays and therefore might timeout or drop connections.

2.3.7.5 Other Related Issues

Still several other issues need to be addressed in multicast protocols. Examples include: IGMP Feedback Implosion, where the multicast receivers send back so many ACKs for the received packets such that memory and processor capacity are exhausted [AkH04, FiD01, SuH03]; asymmetric multicast paths due to terrestrial based-uplinks, where users do not directly uplink to the serving satellite thereby increasing response time [SuH03]; unreliable satellite links due to high bit error rates [AkH04, SuH03]; and flow/congestion control (similar to terrestrial TCP networks). There are numerous research efforts that address TCP flow and congestion control performance in both LEO and GEO satellite network environments [AkJ04, AkM01a, AkM01b, AkX02, BhB01, CrH01, GoJ01, JiA02, KaT04, MaP03, Mar01, MiS01, TsO05, WoP01, ZhB02].

2.4 Multicasting Security

In the early development of multicast, the goals were to provide a means of open communications for a group of interested users that was more efficient than broadcasting. Ease of access and openness were critical to its development [Alm00, DeC90, Dee91].

Ideally, any user could join a multicast group given the multicast address. The user could forward a message with this address to multicast routers that would delivery it to the proper group. Therefore, groups can receive messages from anyone, at anytime, without knowing who sent the messages since registration was not a requirement. Supporting users that joined and left at will gave multicast great flexibility as a means of group communications, but also left it vulnerable to attack.

There has been significant improvement in network security since the early 1990's, much of which has benefited multicast communications. Germane to this discussion are scalability enhancements for security measures. Key management received much attention in the literature, as there are numerous methods of efficiently re-keying a large group, all with benefits and drawbacks depending on the usage model and system requirements [RaH03]. Keying, however, is only one aspect of the multicast system that affects efficiency and scalability. Design of the network topography, both logical and physical, can enhance the overall system security performance of a multicast network.

This subsection discusses the different services required; issues related to scalability for secure multicasting; issues related to Group Membership; and finally relevant secure group communications architectures found in the literature.

2.4.1 General Security Services

Throughout the literature [AgC01, AIE03, AmN05, AvL04, BaB02, BrR02, CaG99, CaW98, DiL00, ElR03, JuA03, KeR05, Kru98, Mit97, PaK98, ShG99, SuH03, XiP05, YaF01], there is general agreement that common network security services are

essential to multicast security including: Confidentiality, Integrity, Access Control, Non-repudiation, Authentication, Traffic Forward Secrecy, Traffic Backward Secrecy, Anonymity, Group Key Management, Group Access Control, and Group Policy. These services can apply to both unicast and multicast networks.

- *Confidentiality*: only the intended parties may read the data. Typically, this is enforced by using one of the many encryption schemes available.
- *Integrity or Data Authentication*: ensures the data that is sent is the same as that which is received (i.e., not altered during transmission). Encrypted checksums or hash functions or keyed hash functions can provide this service.
- *Access control*: only authorized parties may join multicast groups, send messages to multicast groups, or receive data from multicast groups. Methods to control access to the established groups include access control lists and digital signatures.
- *Non-repudiation*: this is the ability of the recipient to prove the sender sent a message even if the sender denies sending it. The typical method used for non-repudiation is a public key infrastructure cryptography, where the sender signs each of the messages with their own private key.
- *Authentication*: ensures that the source of the received message truly is who they claim to be.
- *Key Independence*: ensures that if an outsider can get a set of group keys, he does not have enough information to create either a past or a future key.
- *Traffic Forward Secrecy*: when members leave a group, they should no longer have access to any future group communications.

- *Traffic Backward Secrecy*: when joining a group, a member should not have access to messages that were sent prior to joining the group.
- *Anonymity*: protects both the individual members from knowing who the other members of the group are, as well as preventing outsiders from discovering who the multicast group members are. This, however, conflicts with non-repudiation.
- *Group Key Management*: This is a topic of great interest throughout the literature, since this can greatly affect the scalability and performance of the system. There are numerous proposals for different methods of generating and managing keys [ChB04, HaB01, HaC00, HeS05, HoI04, HuM03, JuL06, JuY06, NgZ05, PaO06, RaH03, RoB01, ScL02, ShG99, WeS03, YaS01, Yuh03].
- *Group Access Control*: This is another area that can affect the scalability and overall performance of the multicast protocol. Group Access Control permits or denies membership into multicast groups according to the particular architecture designs.
- *Group Policy*: this establishes which users have access to which functions, such as signing certificates, key generation and distribution, and maintenance of access control lists.

2.4.2 *Issues Surrounding Multicast Security*

Some of the issues discussed in Section 2.3.7 are directly affected by the level of security implemented in the multicast system. Two of the main concerns that need to be managed are maintaining scalability, and maintaining dynamic group membership in multicasting.

2.4.2.1 Issues Relating to Multicast Scalability

Many issues hinder widespread scalability of secure multicast systems. Limited end node capabilities such as processing power and available storage capacity are one contributor. Another is the Group Key Management protocol, which can consume a lot of bandwidth in a large system.

2.4.2.1.1 Satellite On-board Processing Capabilities

Typical constraints of on-board processing capabilities of many satellite systems are limited memory (for processing and storing), as well as limited processing power [SuH03].

As a related concern, the end users may face a similar limitation on processing and storage capabilities. Any enhancements to the system that benefit the satellite segment should translate to benefits for the end users as well. The terrestrial routers are less constrained than either the satellite or the user nodes. Again, any benefits will apply to the terrestrial routers as well.

2.4.2.1.2 Group Key Management

Perhaps the most critical issue that limits widespread scalability is the group key management scheme used in the system [AgC01, AmN05, JuA02, JuA03, Mit97, ShG99]. Public key infrastructure digital signatures are a secure way of protecting a system; however, they are also computationally expensive. MACs (Message Authentication Codes) with secret keys are less expensive computationally, but are less secure.

If secret keys are loaded onto a satellite before launch, there must be sufficient storage available to have enough keys on board to last the expected lifetime of the satellite. If keys are loaded once a satellite is on orbit, a system of securely re-keying over the air must be implemented.

2.4.2.1.3 Group Key Distribution

To secure a group of users, some type of encryption is generally used. Encryption schemes require key generation and distribution. An overview of several different methods are presented here, adapted from [Kru98]:

- *Manual Key Distribution:* In a manual key distribution scheme, a communications security custodian receives, distributes, stores, and loads keys for all of the cryptographic equipment in a given unit. Since keys are manually distributed, key requirements must be set far in advance, with a sufficient supply requested for a given period of time. A major benefit of this system is that this grade of cryptographic equipment typically operates at line speeds, and hence there is no overhead or delay for using a robust encryption system. The obvious drawback is the labor required to distribute and re-key the equipment. As such, the system has limited scalability. Another downside to the manual system is a significant delay in issuing new keys in the event of compromised keys.
- *Pairwise Keying:* This method of distribution relies on a central entity to generate, distribute, and manage unique keys for each end user of the system. Using public-key infrastructure (PKI) cryptography to establish a secure channel for the distribution of secret group keys to each of the end users is an example of such a system. How well

this system scales depends on the computational power in the central entity and each of the end users that are joining the group. Unless the work of the central entity is distributed to other trusted entities, Pairwise Keying is not efficient enough to scale well.

- *Hierarchical Trees*: This method creates a hierarchical tree of key-encryption-keys (KEKs) for users in the multicast tree. Members are leaves in the tree and have their own KEK. This scheme derives its efficiency by dividing the k-ary tree into smaller subsections. The smaller the subsection of the tree that needs to be re-keyed, the less computationally intensive the re-key will be. This means it will scale very well for large user groups.
- *Secure Lock*: The secure lock uses multicast properties to distribute the keys to interested users. Using the Chinese Remainder Theorem (CRT) [Sti95], a secure lock is constructed to “lock” the deciphering group session key. Those already in the secure group can unlock the group session key, while others cannot. Secure Locks, however, are inherently centralized, and do not scale well.
- *Distributed Registration and Key Distribution (DiRK)*: This architecture spreads the burden of key distribution over several trusted members. Because the system is distributed, it scales well in large networks.

2.4.2.2 *Issues Relating to Group Membership*

Another aspect of group management is determining who the members of the group are. The multicast routing protocol must be aware of group members in the network to deliver packets to them [JuA02, JuA03]. The typical mechanism for this is

the Internet Group Membership Protocol (IGMP), discussed in Section 2.3.5. In the generic group management model, any host can use IGMP to become a member of any IP multicast group, thus exposing the group to eavesdropping or theft of service. Information can be protected by encrypting the multicast data and providing decryption keys to authorized members. Despite the use of encryption, unauthorized users could receive the encrypted data and determine its contents via traffic analysis and/or cryptanalysis. Furthermore, malicious users could launch denial-of-service attacks by either joining several multicast groups and extending the trees, or by filling up the network by sending useless data to known multicast groups. An examination of the Logical Key Hierarchy (LKH) secure multicast protocol revealed security weaknesses in the reliability of the re-keying authentication process [DiC05]. The authors showed that a Denial of Service (DoS) attack could result in a session hijack, but proposed a reliable key authentication scheme that addresses the weaknesses without resorting to public key signatures. In addition, the use of distillation codes have been proposed to detect and resist certain DoS attacks in multicast environments where the end-user devices are resource constrained [DiD03].

One approach to addressing these problems is either to control access to the multicast group, or to control the senders' ability to send data to the established groups. The Gothic architecture provides this type of access control [JuA02]. Gothic's design goals include maintaining or increasing the level of security while providing a scalable system with low computation overhead at the routers, low message overhead, and low support infrastructure requirements by reducing the security processes based on

knowledge of a user's previous or future ability to obtain group data. Relative to two previously proposed systems, Gothic maintained or increased the level of security while increasing scalability. Gothic will be discussed in the following section.

A similar concept is called "GAC/GKM" [XiP05]. GAC/GKM increased overall system efficiency by approximately five times compared to Gothic. This was achieved by using short host identification numbers and group access control server identification numbers instead of digital certificates for authentication and reauthorization. Since the size of the ID numbers is about 40 bits versus the typical 1024 bit digital signatures, the GAC/GKM system uses weaker security to achieve better scalability.

2.4.3 Scalable, Secure Multicast Systems and Architectures

This subsection presents relevant architectures selected from the literature. Each of these proposed architectures improves system scalability and security in different ways.

2.4.3.1 GOTHIC

The functions necessary to provide controlled access to a group are [JuA02]:

1. Group policy specification functions
2. Access request functions
3. Access control functions

The first set of functions is used when a host is designated a group owner. Once designated, that host may set policies for the newly established group. The second set of functions is used to become a member of one or more multicast groups. The third set of functions establishes whether the host can become a member of a particular group.

The functions are divided into two systems: the group policy management system and the group member authorization system. Figure 3 shows the Gothic architecture and its two subsystems. The group policy management system contains the first set of functions, and the group member authorization system contains the last two sets of functions. Gothic interfaces with the routing system as well as any potential group key management systems. Furthermore, Gothic assumes a public-key infrastructure (PKI) complete with a trusted certificate authority is available; however, it can be used without PKI if necessary.

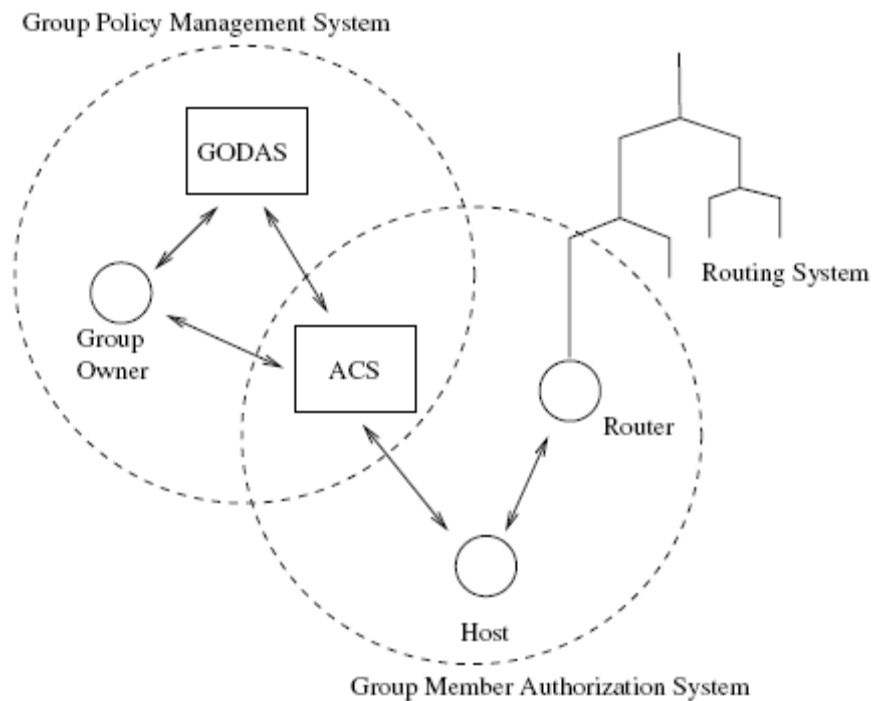


Figure 3 - The Gothic Architecture [JuA02]

2.4.3.1.1 Group Member Authorization System

The group member authorization system (GMAS) controls access to the multicast groups [JuA02]. The main subsystem of the GMAS is an access control server (ACS). Any host that wishes to join or establish a group is authorized and authenticated based on

the host's credentials, such as host IP address (to confirm the user's machine), host certificate and private key (to confirm the individual user), as well as the host's right to join the desired group [JuA02].

2.4.3.1.2 Group Policy Management System

Once a multicast group is established, the group policy management system (GPMS) controls the membership of the established groups based on the group owner's list of authorized users. To ensure the group owner is not corrupted, two methods of determining and authorizing the group owner are proposed: group owner certificates and a group ownership service [JuA02]. The "Group Owner Determination and Authentication Systems," GODAS, ensures the correct host retains the overall access authority to his or her multicast group.

2.4.3.1.3 Reducing Group Keying Overhead

There are literally hundreds of proposals in the literature for various group key management (GKM) schemes; Section 2.4.1 references a small subset of the available literature. Group re-keying can be one of the most expensive operations on the network, and wastes considerable network resources (like bandwidth and processing power) if the groups are dynamic. Generally, most GKMs are designed to efficiently key and re-key large groups of users as their respective groups change either by the addition of new users, departures of former users, or expelling users for various reasons. Depending on the security requirements of the groups, a change in group membership calls for either a full or a partial group re-key to preserve a desired security level for the group.

Some of the burden on the GKM can be alleviated if the system leverages the policies imposed by the GAC to reduce the number of times the system has to re-key [JuA02]. For example, in a typical GKM system, whenever a user joins or leaves a multicast group, the entire system is re-keyed based on the assumption that the new user could have gained access to either the old encrypted data prior to arrival, or to new encrypted data after departure. By leveraging the services of the GAC to ensure no unwanted users have access to the data prior to their validated join or after their departure, the GKM does not have to re-key in either of these situations. As a result, significant overall system efficiency is gained [JuA02].

The feature that is unique to Gothic and applicable to a satellite network, is its use of the “Group Access Control Aware – Group Key Management” system. Gothic’s GACA-GKM can increase the scalability of the proposed architecture. Another feature that can increase scalability is covered in the following section.

2.4.3.2 Iolus

Iolus increases system scalability by breaking up the flat, secure multicast architecture, and creating a hierarchy of independent, secure subgroups [Mit97]. The hierarchy is dubbed a “secure distribution tree,” and acts like a single virtual secure multicast group. There is a single group security controller (GSC) which manages the overall security of the group along with the group security intermediaries (GSI). Generally, GSC and the GSIs are referred to as “group security agents” (GSAs). The subgroups, denoted by clouds in Figure 4, are interconnected by the GSIs, which work together to bridge the local multicast traffic from each subgroup into all of the other

subgroups as needed. GSAs are responsible for managing the re-keying of the clouds, or “clusters,” as needed. The hierarchy is known before the multicast group is initialized, and the GSAs are assigned manually.

By breaking the multicast domain up into hierarchical groups, each managed subgroup can re-key its own subset of the total users, thereby reducing the total overhead on the system. However, a greater amount of trust is placed on the GSAs, which weakens the overall system security [BrR02].

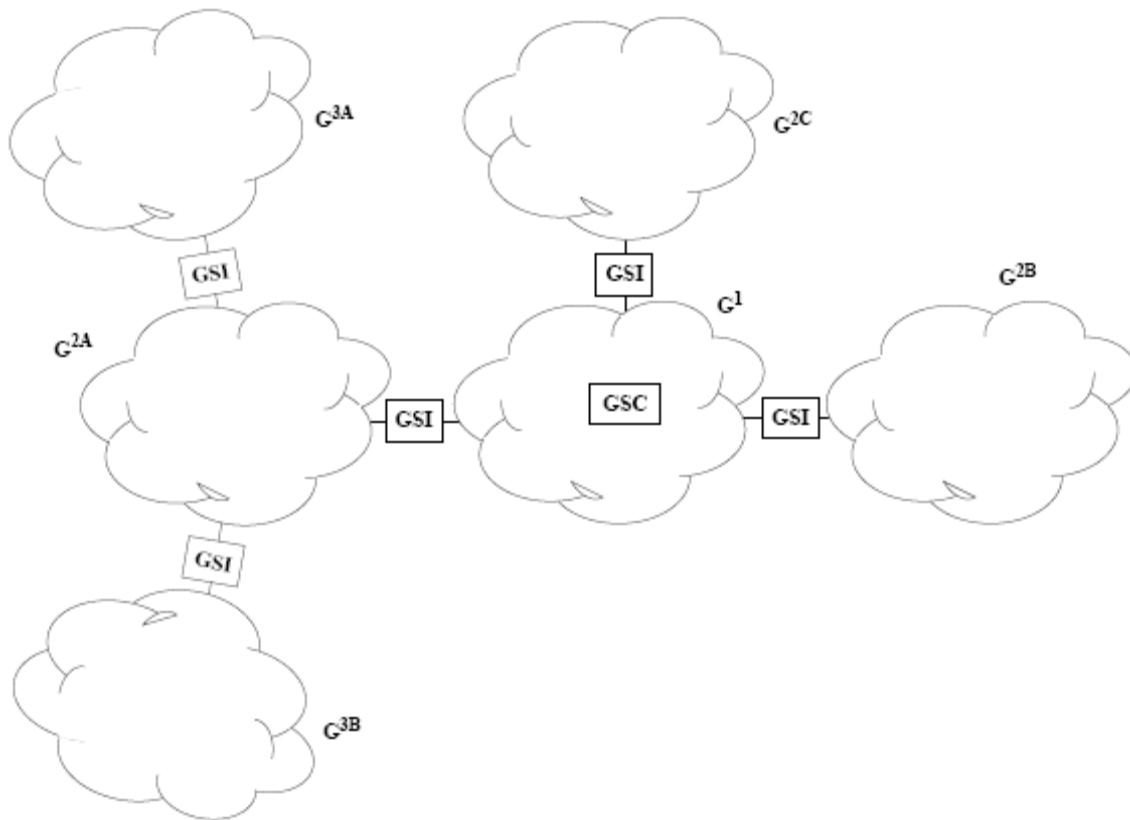


Figure 4 - Example of a Secure Distribution Tree [Mit97]

One concern for implementing security using the Iolus framework was the performance penalty incurred by using the GSAs. To alleviate this concern, a simulation was developed to compare the response time of a multicast network with the Iolus GSAs

in place, and without them (“NOP”). After performing several simulations, it was determined that the average forwarding penalty was approximately 450 microseconds. This is shown in Figure 5, represented by the difference between the NOP and Iolus lines. Almost all of that time is attributable to the cryptographic operations.

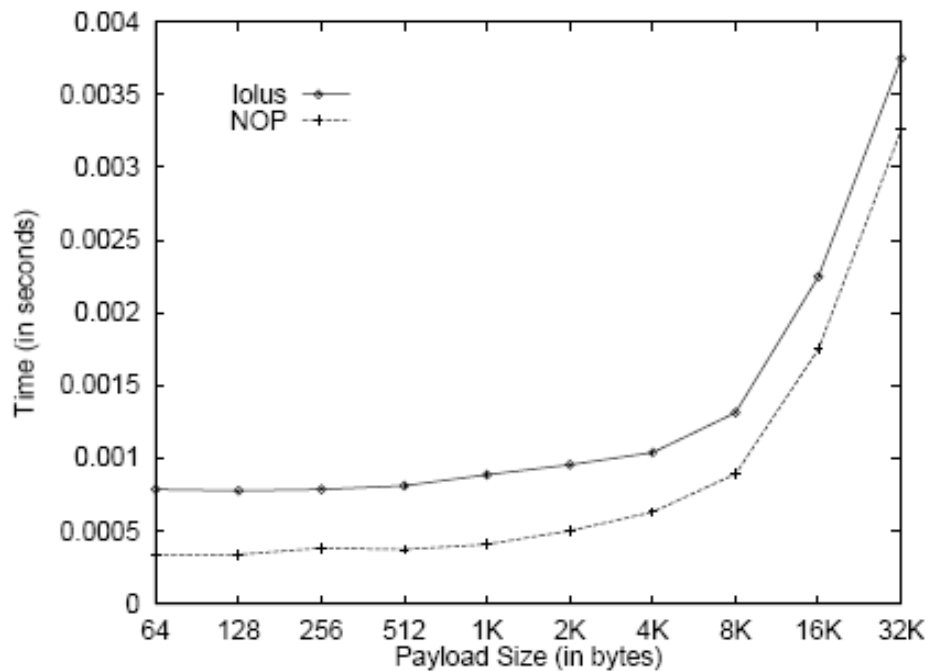


Figure 5 - GSA Multicast Forwarding Performance [Mit97]

2.4.3.3 Spatial Clustering

Iolus increases scalability by using a hierarchical clustering. An increase in multicast scalability is achieved by clustering as well, but the clustering scheme is based on spatial boundaries, and not hierarchy [BaB02]. To form the clusters, the protocol traverses the multicast member tree from the leaves towards the root, assigning members to fixed-size groups as it migrates to the end of the tree. A fixed-size group means re-keying costs are bounded and deterministic. By using spatial clustering, members of the same cluster are near each other in the multicast tree. This proximity allows the re-

keying scheme to be more efficient. Like Iolus, each cluster has a cluster leader that interfaces with other clusters and manages re-keying for the cluster.

The differences between Iolus and Spatial Clustering are subtle [BaB02]. In fact, Spatial Clustering could be used to model Iolus. The two main differences between the architectures are the way the subgroup leaders are assigned and how subgroups are formed. In Iolus, the GSAs are special nodes assigned upon the establishment of the multicast group. In Spatial Clustering, leaders are dynamically assigned, can easily change as the groups change, and are ordinary nodes that happened to be on a cluster boundary in the multicast tree. Regarding the formation of the subgroups, Iolus assigns subgroups based on administrative boundaries, while Spatial Clustering groups are assigned by proximity on the multicast trees [BaB02].

2.4.3.4 Secure Spread

Secure Spread increases the efficiency and scalability of secure multicast [AmN05]. The client-server architecture assigns “heavy-weight” activities to servers, and leaves “light-weight” services to the clients. This architecture is called an “integrated architecture,” where computationally intensive security services are implemented in the servers. A “layered architecture,” in contrast, implements such intensive services in the clients.

To increase performance and scalability, the integrated architecture coupled a small number of servers to execute the computationally expensive services of the distributed protocols, thus removing the burden from the clients. The group key agreement protocols are distributed protocols, and are the most resource intensive of the

services. With a small number of servers in a relatively stable configuration, heavy-weight re-keying between the servers occurs less frequently than the client re-keying. The servers do not need to be re-keyed when a client joins or leaves the group. Servers only re-key if one of the servers leave or join the server group. Also, the server re-keying can be quicker due to needing less keys generated for a small number of servers as compared to a large number of keys for numerous clients.

2.4.4 Deficiencies of Known Scalable, Secure Multicast Systems and Architectures

Most Group Key Management systems are designed to efficiently key and re-key large groups of users as the multicast group membership changes. Even the most efficient GKM, however, will have a fixed cost per user or system to perform the key updates.

Gothic makes use of group membership knowledge and control to reduce re-keying. This provides over an order of magnitude less GKM traffic as compared to a traditional GKM scheme [JuA02]. However, the GACA-GKM is employed across the entire domain, and does not take advantage of physical or logical separation to further enhance the scalability.

Iolus improves re-keying efficiency by dividing the various multicast groups into layered, hierarchical subgroups, connected by GSAs. Spatial Clustering divides the multicast groups into spatial clusters based on proximity in the multicast tree to reduce join and leave re-keying overhead. Neither architecture, however, maintains any Group Access Control Awareness information to reduce the re-keying in the clusters when a previously authenticated and trusted user moves from one cluster to the next. Both

architectures demonstrated improved performance over traditional architectures in fairly static environments where the users primarily join or leave, and not where they move from cluster to cluster.

2.5 Summary

This chapter provides an in-depth look at satellite communications systems as well as the Global Information Grid architecture. This is followed by a discussion on multicast and group management protocols, along with examples of proposed satellite architectures that use multicast. Finally, multicast security was addressed to include required services, group and key management, and architectures germane to the focus of this research. The closing section addresses limitations that the current multicast security architectures faced in a highly mobile user environment.

III. Methodology

3.1 Chapter Overview

This chapter presents the methodology for the development of the secure, scalable Hubenko Security Framework Architecture for LEO satellite-based (LEOSat) networks. The Hubenko Architecture addresses the shortfalls of previous architectures, namely the lack of a secure multicast architecture that scales well for very large numbers (10,000 or more) of highly mobile users. *Highly Mobile Users* change satellite spot beams often, and/or very rapidly. A person walking down the street talking on a satellite telephone would not be considered highly mobile, but the same user in an automobile or an airplane would. A *Highly Mobile Environment* is defined as a group of users in a network that collectively change satellite spot beams often. For example, this could be a large group of slow-moving users, or a small group of rapidly moving users. This chapter begins with the motivation for developing the Hubenko Architecture. The validity of employing a LEO satellite communications network is presented, along with the viability of the PIM-DM multicasting protocol. Next, the development of the Hubenko Security Framework Architecture is presented followed by a detailed discussion of the modeling and simulation environment, along with the descriptions and specific parameters for each of the developed scenarios. The metrics collected and analyzed are defined in this chapter as well. The chapter concludes with the model verification and validation.

3.2 Hubenko LEOSat Security Framework Architecture Motivation

A review of current literature indicates relatively few research efforts can secure group communications while simultaneously scale to very large groups of users (over

10,000 users). A few of the architectures noted earlier make contributions to an overall framework for secure group communications in a multicast network. None, however, specifically addresses a LEOsat network environment, nor do they completely address the issues facing a global user base such as that found in the GIG.

The foundation of any secure group communications is some type of group key distribution and management scheme. As mentioned before, this field is well populated with various concepts for different scenarios and applications, with no one solution meeting all needs. From the standpoint of this research, the actual keying architecture piece, be it a centralized, decentralized, or distributed keying agreement protocol, is transparent to the overall research [ChB04, RaH03]. Therefore, the Hubenko Architecture allows the system developers to insert the group key protocol(s) that best fit their needs.

Several secure group communications architectures improve overall system performance and scalability by dividing the multicast group in various ways. However, breaking the group into progressively smaller units will ultimately reach a point that will begin to negatively affect scalability rather than improve it. Therefore, small cluster sizes alone will not provide sufficient security performance improvement. The developers of the Group Access Control Awareness (GACA) scheme acknowledge that, while capable of improving security performance for a system, GACA is suitable as a module to a larger system, and not a stand-alone solution to security and scalability on its own.

Alone, each of the concepts presented solve parts of the complex security environment faced in the global environment of the GIG. The novel Hubenko Security

Framework Architecture combines several of the features into a coherent solution, presenting a secure architecture adapted to the unique LEOSat environment.

3.3 LEOSat Network Environment Validation

This section establishes the LEO satellite architecture as a viable unsecured baseline solution for meeting the needs of the DoD user community. To assess the relative performance of PIM-DM versus other multicasting protocols (DVMRP and ODMRP), a set of performance metrics are established [Tho01, ThR01, ThR02]. These metrics include: the Data-to-Overhead (DtO) ratio; the Received-to-Sent (RtS) ratio; and the End-to-End (EtE) delay. The Data-to-Overhead ratio indicates how efficiently data is transmitted throughout the network. The higher the ratio, the higher the amount of data as compared to overhead information. The only packet types that contain data are the PIM Packet, RIP Probe, and RIP Report; all other packets are counted as overhead. The Received-to-Sent ratio is an indicator of packet loss, either due to an invalid route, time-to-live expiration, or no next hop available (e.g., a satellite loses communications with the ground station and drops the packet). Packets received compared to total packets transmitted ($p_{\text{recv}}/p_{\text{tot_tx}}$) is a simple means of determining how successfully the multicast system performed. While the sent packet count should always be greater than or equal to the number received, an occasional duplicated packet means this ratio could be slightly greater than one. For example, a source sends a single packet that is later duplicated during a satellite handoff and instead of one of the duplicated packets being properly discarded in the network, both packets are received (which of course the receiver would then be able to discard one of the duplicates). End-to-End delay is a “lower-better” metric,

which indicates the average time a packet was in transit from the source to the subscribers. While each multicasting algorithm may use a different route, the most efficient route is the shortest route with the least number of hops and minimal network congestion along the way.

The PIM-DM protocol's effectiveness can be illustrated by comparing the average values from the simulations for the three defined metrics to earlier work on DVMRP and ODMRP. All three protocols were implemented using the same satellite network model validated in previous work [Tho01, ThR01, ThR02]. However, directly comparing the implementations of PIM-DM, DVMRP, and ODMRP is not possible as the protocols differed considerably in their implementation and execution. This comparison can be accomplished by examining the metrics ranges and bounds of the protocols at comparable loading levels. Table 1 shows the Data-to-Overhead ratio comparison for the target protocols. All of the PIM-DM simulation experiments were repeated three times and a 90% confidence level used. Since the results for DVMRP and ODMRP were gathered from previous work, confidence interval overlap analysis was not performed to ascertain statistical independence.

Table 1 - Data-to-Overhead Comparison

DtO	DVMRP	ODMRP	PIM-DM
Min	0.291817	0.111433	0.645125
Average	0.561919	0.229997	0.82285
Max	0.766399	0.37276	0.910808

As is shown by Table 1, the DtO measurements illustrate that PIM-DM has a 16% higher DtO ratio than DVMRP, and a 59% higher DtO ratio than ODMRP. This is the expected result and is caused by the separation of the routing protocol from the

multicasting protocol. Both DVMRP and ODMRP have the routing protocol information embedded in the multicasting packet. This increases the overall size of the packet, and therefore increases the amount of overhead for the multicasting portion of the protocol. Since PIM-DM simply interfaces with the existing routing protocol and does not have the routing information embedded in the multicasting packets, there is less overhead from the multicasting perspective. The benefit of separating the routing protocol from the multicasting protocol is clear as the DtO ratio increases.

A second strength of PIM-DM is seen from the RtS ratio. Using the “orders of magnitude” reliability terminology from the telecommunications industry, each decimal place in a reliability statistic represents an order of magnitude. For example, a reliability metric of 0.999 is one order of magnitude better than 0.99. Table 2 shows PIM-DM has two orders of magnitude better maximum reliability than ODMRP, and three orders of magnitude better maximum reliability than DVMRP. In addition, the near perfect transmission capability exhibited by PIM-DM is ideal when data integrity is crucial. A protocol with higher RtS not only reliably delivers packets, but decreases retransmission of missed packets. PIM-DM had a tighter range for RtS (99.93%-99.99%) than both DVMRP and ODMRP, regardless of the loading on the network.

Table 2 - Received-to-Sent Comparison

RtS	DVMRP	ODMRP	PIM-DM
Min	0.845103	0.865764	0.999285
Average	0.8950897	0.956833	0.999853
Max	0.9435325	0.996637	0.999939

The EtE delay factor was lower for both ODMRP and DVMRP compared to PIM-DM, as shown in Table 3. This result is surprising, especially when considering that both

DVMRP and PIM-DM build approximately the same length tree structure. The difference can be explained by two factors. First, the additional layer between PIM and RIP introduces a slight delay. Since PIM does not maintain its own routing tables like ODMRP and DVMRP, PIM-DM queries the routing tables to determine the next hop before actually sending the packet, rather than performing the lookup in its own tables. Second, the 99.98% RtS ratio is achieved by PIM-DM at the price of non-optimal paths while the connection between the source and the subscriber was being renegotiated. To avoid dropping packets, an old satellite node would forward packets to the new satellite node until the connection was removed. This forwarding increases the reliability but introduces additional hops along the path leading to higher EtE delays. Therefore, the penalty for the DtO and RtS performance of PIM-DM is, on average, a seven millisecond increase in EtE delays compared to DVMRP and 12 milliseconds increase compared to ODMRP.

Table 3 - End-to-End Delay Comparison

EtE (msec)	DVMRP	ODMRP	PIM-DM
Min	65.9055	56.237	69.488
Avg	69.1706	64.254	76.393
Max	77.326	73.098	86.862

The EtE delays above are well within the typical real-time voice requirements. For example, Nortel research has determined that a delay of 250 milliseconds is the upper delay limit for conversations. If delays exceed that limit, the conversation between two people will be disrupted [NOR05]. Additionally, the EuroSkyWay test-bed analyzed VoIP performance and determined geostationary satellites are capable of providing good quality of service (QoS) in terms of jitter and packet loss, and medium to poor QoS in

terms of packet delay [CrS01]. According to a study on one-way Internet delays, [CoP02] demonstrated that the average delay value for international routes is approximately 110 milliseconds. Consider the case of a global PIM-DM multicast environment, with integrated terrestrial and LEO satellite PIM-DM network segments. Given the EtE performance shown in Table 3, the PIM-DM LEO satellite segment would be transparent to the users in terms of both delay and operation.

Overall, the preliminary work shows that the PIM-DM protocol adapts well to a satellite network environment. The modified PIM-DM protocol provides a scalable framework in a satellite communications environment. The protocol scales with load and provides equivalent performance characteristics regardless of the load on the system. The Data-to-Overhead ratio is on average approximately 80% and increases with a more stable network configuration (i.e., the network converges, with few changes during the simulation period). The Received-to-Sent ratio is 99.98% across all loading levels, so very few packets are dropped with the majority of packets being delivered successfully. Finally, with the End-to-End delay of approximately 76 milliseconds, PIM-DM compares well with longer-range terrestrial networks, and it meets quality of service requirements for packet-based network communications. PIM-DM compares favorably to both DVMRP and ODMRP and surpasses the performance of both protocols. The separation of routing and multicast data simplifies the network and allows the incorporation of other multicast protocols. PIM-DM gives the user superior transmission capability and provides a reliable, scalable network configuration with very little packet loss and excellent responsiveness.

Multicast protocols adapted to a GlobalStar[®]-like LEO satellite environment concluded that multicasting in a LEOSat network provided upwards of 300% increase in efficiency over unicast routing [EkA02].

While the GIG GEO systems use crosslinks to route traffic from one part of the world to another with delays of 250 milliseconds or more, LEO communications systems achieve average end-to-end latencies of less than 100 milliseconds for intercontinental communications using satellite crosslinks [HuR06a, Sae03]. This performance indicates LEO communication satellite systems should be included in an overall GIG architecture to improve end-to-end performance.

3.4 Continued Viability of PIM-DM

PIM-DM has a large following in the commercial world as well as an active Internet Engineering Task Force (IETF) working group [Sav06]. PIM-DM is an excellent choice for adapting to the LEO satellite environment since the protocol is a dense mode protocol, and satellites are capable of interfacing with a large group of users simultaneously. Further, the protocol independence of PIM-DM permits an easier adaptation to a satellite environment, requiring only the multicast portion of the protocol be modified while using the well-established RIP protocol (with minor modifications) for the underlying routing support. From a commercial standpoint, Cisco has incorporated PIM-DM in its routers and Internetwork Operating System (IOS) [CIS07], and the OPNET Modeler [OPN06] software package now has PIM-DM and SM models available. This is not true for other multicast protocols.

Recently, there was a proposal to the IETF to re-classify several of the multicast protocols as historic, indicating they are no longer actively developed and supported [Sav06]. These protocols include Border Gateway Multicast Protocol (BGMP), Core Based Trees (CBT), and Multicast OSPF (MOSPF). In addition, this same document sought to retire the following RFCs: [RFC3913], [RFC2189], [RFC2201], [RFC1584], and [RFC1585] and thus was not considered as the basis of new research.

Despite the fact that PIM-DM is regarded as a protocol that will not work in ISP networks, PIM-DM is a good option in dense end-user environments [Sav06]. Additionally, the comments on the reliance of the complicated *Assert* timing issues causing numerous dropouts and poor routing during satellite handoffs have been satisfactorily addressed in [Sae03]. In the satellite network environment, the satellite routers frequently transition, or “hand-off,” their users to neighboring satellites as the satellites move about their orbits. Typical terrestrial applications of PIM-DM do not experience, and do not account for, the frequent hand-offs encountered in the satellite environment. Therefore, the specified functions of the *Assert* had to be modified to rebuild the links after satellite transitions. The specification uses the *Assert* message to choose between alternate routes to force a specific route configuration, or to determine which node should be the forwarder for the group [AdN05]. The satellite adaptation uses the *Assert* to build a new route since the current route has changed due to satellite movement. Therefore, the *Assert* is accomplishing the same basic function as the specification, but the approach is unique to this satellite network model. Additionally, the RIP Ground message was added to assist with the transition capability. Without these

application-specific modifications, PIM-DM performance in a satellite network would be severely degraded, as noted in the literature.

While not yet obsolete, the use of Distance Vector Multicast Routing Protocol (DVMRP) [RFC1075], first used in the MBone, is on the decline. Most DVMRP applications have been replaced with PIM-SM, leaving DVMRP only in legacy applications for the near term [Sav06].

MOSPF [RFC1584] was used by several vendors in intra-domain networks. Since MOSPF does not scale to the inter-domain case, it is no longer actively deployed.

BGMP [RFC3913] appears to have been supported only in documents. No known implementations or deployments exist [Sav06].

CBT [RFC2201] was an academic project that provided the basis for PIM sparse mode shared trees. As soon as PIM was able to establish the shared tree capability, CBT was no longer needed [Sav06] and hence has not been deployed.

3.5 Hubenko Security Framework Architecture Development

This effort is comprised of three elements: adapt a flat key multicast security architecture to the baseline LEOsat model; enhance this generic architecture by progressively adapting relevant portions of three secure group communications architectures/frameworks (Iolus, Spatial Clustering, and Gothic) to the model; and finally, demonstrate the expected increase in efficiency and overall system scalability performance through discrete event simulation and analysis.

3.5.1 Baseline Security Architecture for the LEO Satellite Environment

This section establishes the baseline security architecture from which security performance improvements will be measured. Since there is a plethora of re-keying protocols, the final selection is left to the system designers implementing an application based on this modular architecture. This allows the applications to drive the selection that best fits the varying power and computational constraints imposed by the system. For example, the choices for re-keying protocols would be considerably different in a mobile communications environment where battery and computational power are less of a concern than in a wireless sensor network environment where every clock cycle must be conserved due to the limited on-board battery size.

Using a generic flat key security system as the basis of a generic security model, the original baseline “LEOsat” model [Fos98, Sae03, Tho01] was adapted to include the basic security functions of key generation, key storage, key agreement, and group key distribution. All members of a multicast group will use the same group key to encrypt or decrypt traffic. This group key is represented by “A” in Figure 6. The lines indicate communication links, the lettered boxes indicate which key is in use to secure that link, and the numbered circles represent the end users. To simplify the model, the processes of encryption and decryption will occur in a fixed unit of time.

Each time a user joins or leaves a multicast group, the entire system will need to re-key with a new group key to maintain the security services such as forward and backward secrecy, and group integrity, mentioned earlier. Re-keying the entire multicast group with a new key is the upper bound, worst-case performance for the system. In

terms of the overall number keys, however, this is the simplest case with a single key shared by all users. The simulations collected the metrics (cf. Section 3.8) relevant to security performance analysis (cf. Chapter IV).

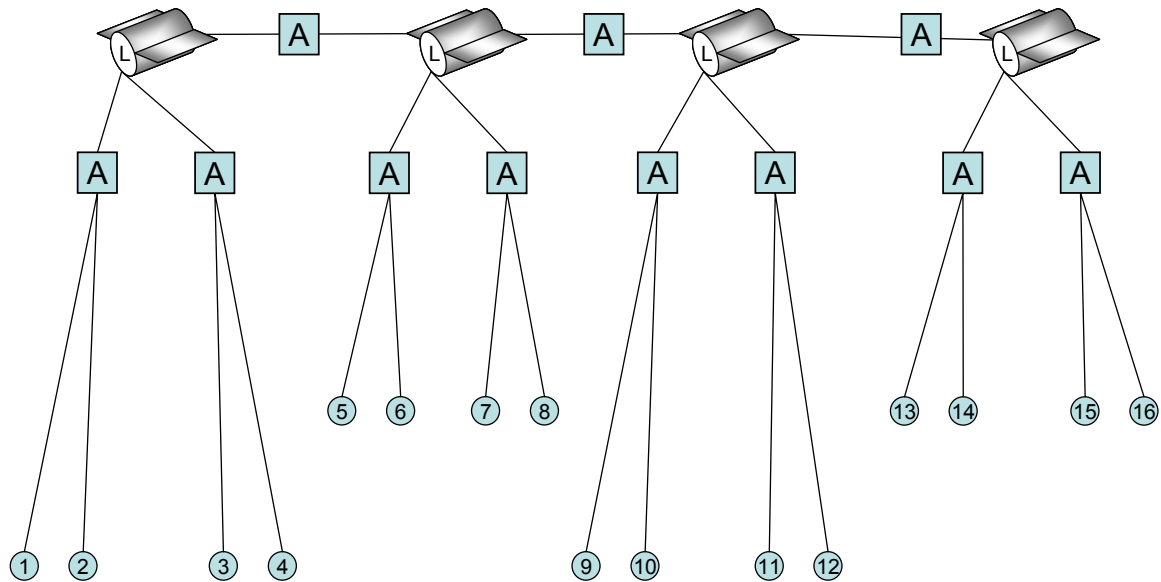


Figure 6 - Baseline LEOsat Security Architecture

Figure 7 through Figure 11 illustrate an example of the baseline architecture. The colors of the beams represent the multicast key in use. For the baseline architecture, all users share the same key, and therefore all the beams are the same color. In Figure 7, all users are connected with the “red” key, and the two aircraft have not yet joined the multicast group.

Upon authentication and authorization, the aircraft are joined to the multicast group in Figure 8. To protect backward traffic secrecy, the entire group is re-keyed with the “magenta” key.

As the aircraft travel along their route, they leave the first spotbeam, and enter a second spot beam, shown in Figure 9. Since there is no tracking enabled in the system,

the entrance into the second spotbeam triggers a new authorization and authentication cycle, and therefore new keys are again issued to the multicast group. For illustration purposes, this is the “blue” key.

Continuing along, the aircraft enter a third spotbeam in Figure 10, and once again a new key (“green”) is issued to the multicast group. Finally, the aircraft depart the multicast group in Figure 11. To protect forward traffic secrecy, the entire remaining multicast group is re-keyed, this time with the “yellow” key, and the two aircraft are not re-keyed.

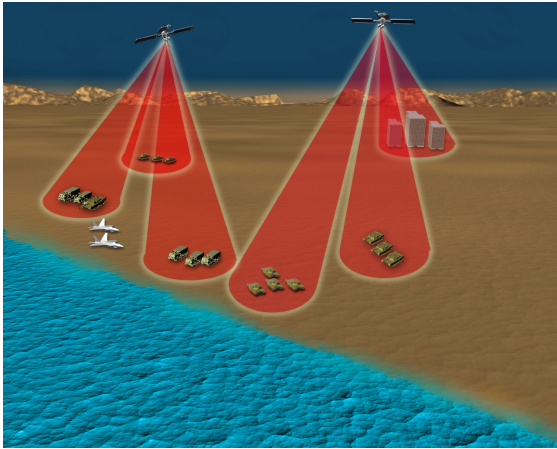


Figure 7 - Initialize Baseline Architecture Example

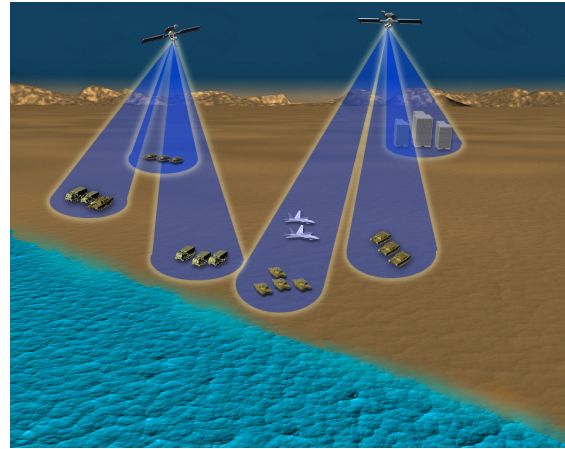


Figure 9 - Baseline Example - Three

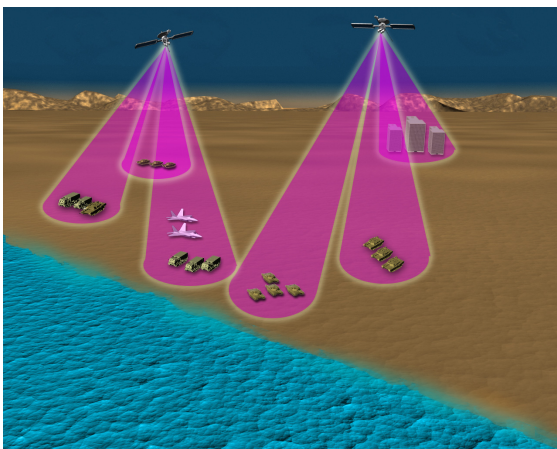


Figure 8 - Baseline Example - Two

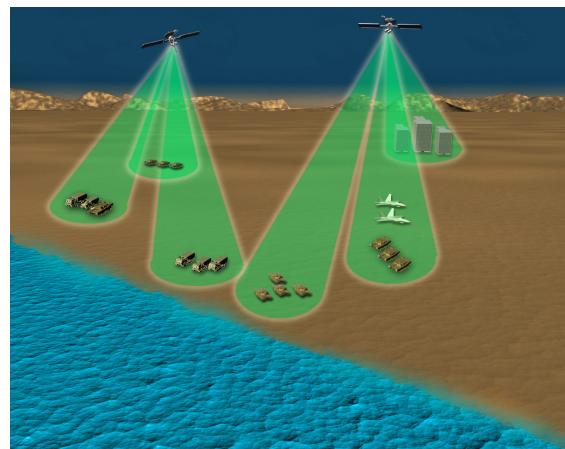


Figure 10 - Baseline Example - Four

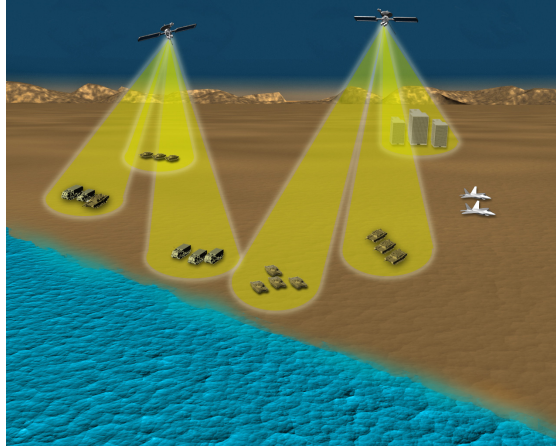


Figure 11 - Baseline Example - Finish

3.5.2 *Clusterized Security Architecture*

With a baseline and minimal security features in place, this section describes how the LEOsat network security architecture was enhanced by using key features of several secure group communications architecture proposals [AmN05, BaB02, JuA02, Mit97]. The first enhancement applies clustering proposed by [BaB02, Mit97].

Iolus, due to its predetermined, static clusters and Group Security Agents (GSA) assignment scheme, adapts well to the satellite environment where satellites follow predetermined orbits with repeating ground tracks, and deterministically hand off users from one satellite to another. The penultimate leaves of the multicast tree, namely the LEO satellites in view of the users, are also static, in a sense, and pre-determined. Although the satellites are actually rapidly moving in and out of view overhead, the user will always be connected to a single satellite. This single satellite, regardless of exactly which satellite unit it is, will appear constant. Furthermore, the satellites naturally act as GSAs, bridging the traffic between clusters (spot beams) and managing the re-keying for each of the clusters.

By dividing the network into two distinct hierarchical groups (“satellites” and “users”) as proposed in the Iolus system, a leave or join by a user will trigger a re-key in the user cluster, but not in the satellite cluster. Similarly, a leave or join by a satellite will trigger a satellite cluster re-key, and not affect the users. However, it is presumed that a leave or join by a satellite is triggered by the need for a satellite’s end-user to leave or join a multicast group since satellites generally are not end users as well as intermediary routers. Therefore, satellite joins or departures independent of user joins or departures should rarely occur. The Satellite Cluster group key is represented by “V” in Figure 12.

To further increase the efficiency of the clustering concept, Spatial Clustering is implemented. Spatial Cluster’s spatial boundaries adapt well to a satellite environment, though the concept of clustering is applied in a slightly different manner from the perspective of the leaves and their relative proximity. In Spatial Cluster, the geographic distances covered within a single cluster vary greatly since fixed-sized clusters are maintained despite variances in user density. Maintaining a fixed-size cluster in the satellite-adapted network, however, is impractical due to the dynamic nature of the mobile user environment. Except in cases with significant spot beam overlap (e.g., in the higher latitudes), users could not switch clusters to modify the cluster sizes. Thus, while the satellite environment can still benefit from the Spatial Cluster concept, fixed geographical boundaries are used rather than fixed cluster user size. The ovals in Figure 12 represent the geographic clustering, with each cluster sharing a user group cluster key, lettered “A” through “H.” This reduces the impact to the system when a new user joins a group, or when a group member leaves. In the initial architecture, the entire system

would need to re-key; in the clusterized architecture, only those users in the affected cluster will need to re-key. When a user joins the multicast group, the LEO satellite system authenticates the user and grants access to the group assuming the proper credentials are presented. Upon admission and registration to the group, the user is assigned to the cluster in which it resides. Due to overlapping satellite spot beams, it is very likely a user may be located within view of several contiguous clusters. Assume, however, that each user is allowed to register in only a single cluster at a time. With seamless, ubiquitous, mobile connectivity on a global scale, each user can be mobile in this system. Some users will be “more mobile” than others; one is walking down the street, while another flies overhead in an airplane. When the users cross cluster boundaries, they are transitioned from one cluster to another. The complexities of channel assignments, hand-off management, and satellite operations are beyond the scope of this research.

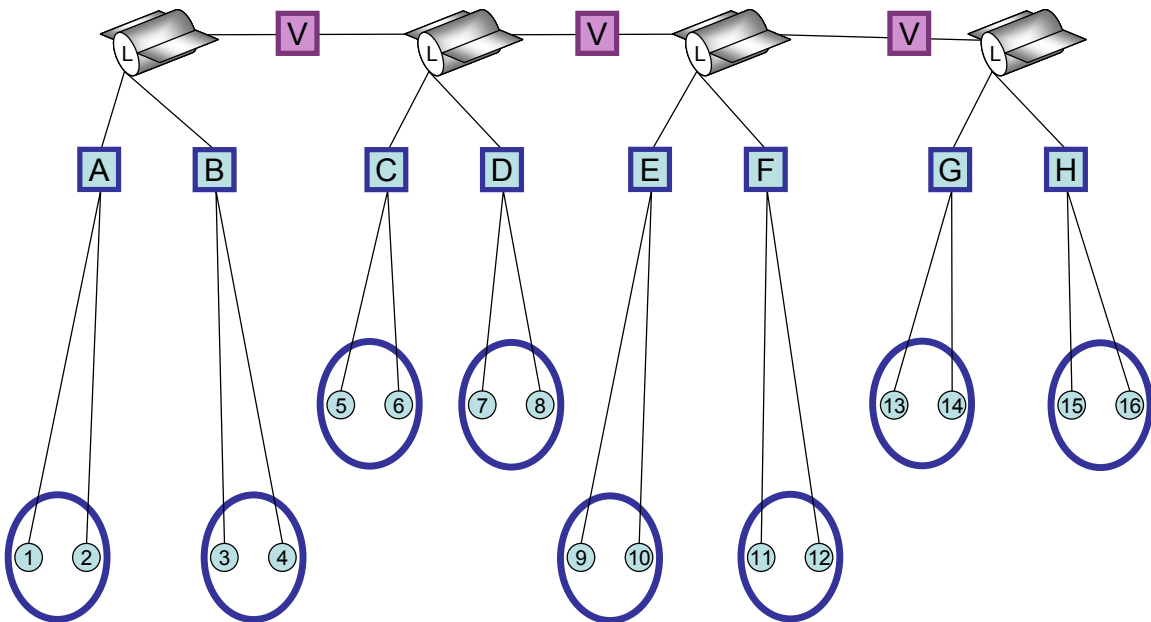


Figure 12 - Clusterized Security Architecture

Figure 13 through Figure 17 illustrate the same scenario as the Baseline example, but with the Clusterized Security Architecture in place. Figure 13 illustrates the initial state of the clusterized multicast group. All users depicted in this figure are communicating in the same multicast group. Each spotbeam, however, is utilizing a different multicast key, represented by a different beam color for illustration purposes. All users within each spotbeam share the same key. The two aircraft are not joined to the multicast group.

When the aircraft join the multicast group and fly into the first spotbeam, only that “teal” cluster needs to re-key, as shown in Figure 14 by the spotbeam turning to a “dark blue” key. Note only those users in the single cluster are now affected by the join, compared to the entire multicast group in the Baseline example.

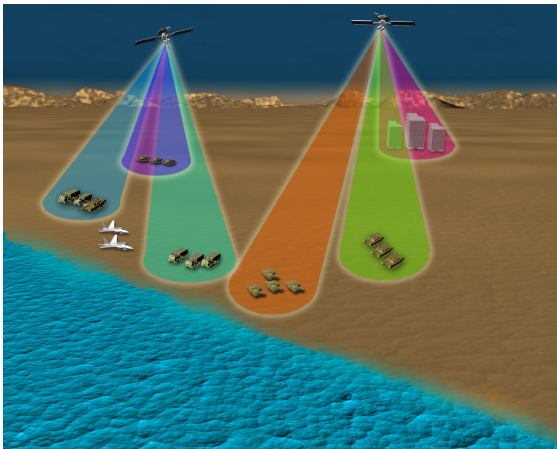


Figure 13 - Initialize Cluster Example

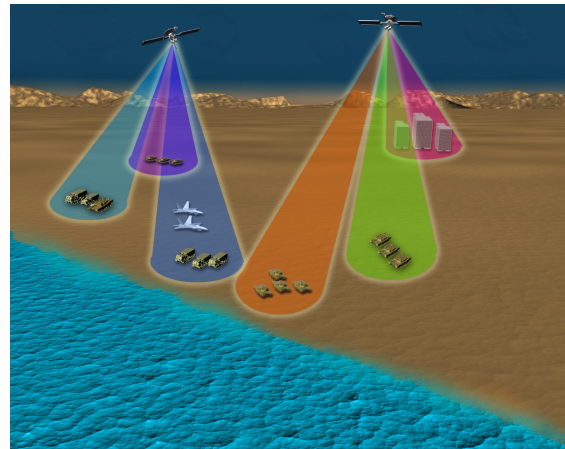


Figure 14 - Cluster Example - Two

When the aircraft fly to the next spotbeam in Figure 15, the old spotbeam changes key to “dark green,” and the new cluster changes key to “tan.” The clusters need to re-key for the same reason as the Baseline example: there is no tracking enabled in the system, the entrance into the second spotbeam triggers a new authorization and

authentication cycle, and therefore new keys issued to the gaining and losing clusters. The difference in the Cluster Architecture is a reduction in the number of affected users, from all of the active multicast group users, to only users in the two affected clusters.

Moving along to another cluster in Figure 16, the aircraft again trigger changes to two clusters. The “tan” cluster re-keys to the “beige” key, and the “light green” cluster re-keys to the “golden” key.

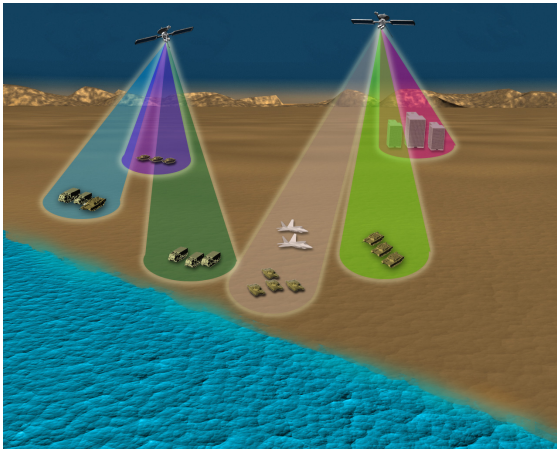


Figure 15 - Cluster Example - Three

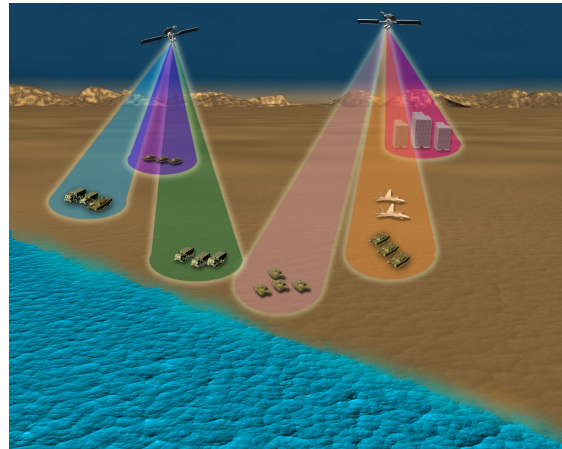


Figure 16 - Cluster Example - Four

Finally, the aircraft leave the multicast group and fly out of the spotbeams. The “golden” keyed cluster re-keys to the “grey” key in Figure 17, completing the example.

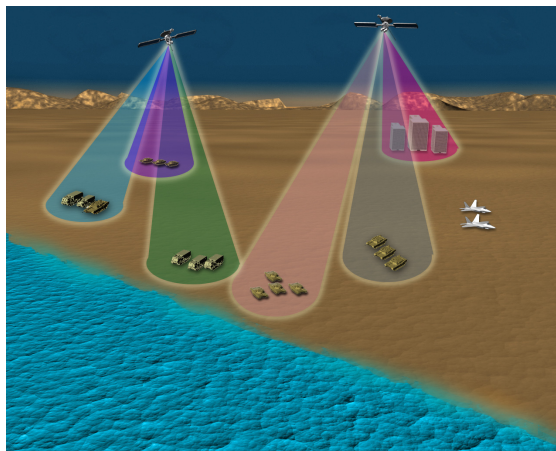


Figure 17 - Cluster Example - Finish

A further enhancement to this scheme divides the satellites into smaller clusters as well. However, it is assumed that the satellites are controlled by a single, trusted entity (in this case the DoD) and there is no need to re-key when a satellite leaves or joins the satellite group.

3.5.3 Hubenko Security Framework Architecture

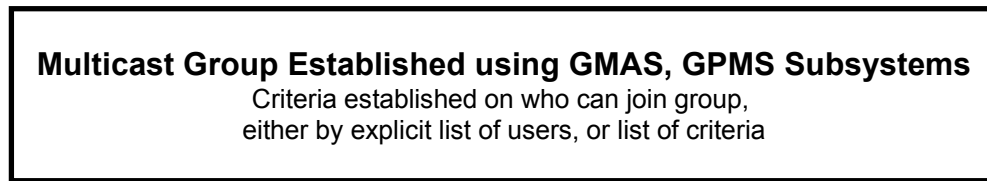
With the “clusterizing” of the multicast network established, the following enhancement adds the “Group Access Control Aware-Group Key Management” feature from Gothic [JuA02]. The satellite environment is an ideal medium capable of centrally sharing the group access awareness information, making Gothic readily adaptable.

When the key functions of Gothic are incorporated into the Hubenko Security Framework Architecture, security performance increases (i.e., re-keying decreases). For example, consider a multicast group established in a deployed location consisting of air-, sea-, and land-based tactical units. The occupied locations spread across an area larger than 50 kilometers in diameter, and therefore is covered by more than a single satellite spot beam. All of the multicast enabled users join the same multicast group. Each of the sea- or land-based users joins the group, clustered in their respective areas. The aircraft flying sorties throughout the region enter and exit the user clusters at a rate much quicker than their ground or sea counterparts. For example, an aircraft flying at 800 kilometers per hour will cross a 50 kilometer spot beam in about three and three quarter minutes at its widest point. During the same period of time, terrestrial users will either appear fixed relative to the spot beam, or occasionally cross into a new spot beam.

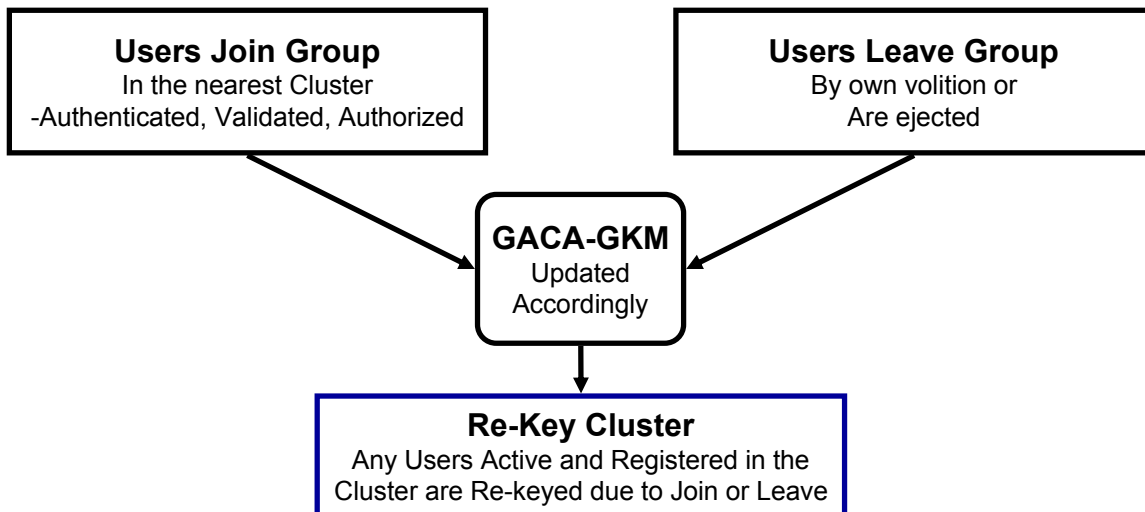
Without clustering, the entire Baseline system would have to re-key when users join or leave a group. With clustering, each cluster is keyed with a separate cluster key. Adding a new user to the cluster, even if it is already joined to the same multicast group in another cluster, requires a re-keying of that new cluster. However, with GACA-GKM support, if the system can establish that a registered user who moves to a new cluster did not have access to data prior to its joining, or will no longer have access after its departure, then the cluster would not need to re-key to incorporate the new user or remove it from the group. Instead, either the new user would be issued a new key upon entry, or the system would simply continue as before so long as the principles of forward- and backward secrecy are maintained.

Figure 18 depicts the flow of the Hubenko Architecture. The top section depicts the initialization process, which follows from the discussion in Sections 2.4.3.1.1 and 2.4.3.1.2. The middle section summarizes the re-keying effects of Joins and Leaves as described in the above paragraphs. The bottom section summarizes the process for re-keying when a user moves to a new cluster.

Group Initialization



Group Membership Changes



Group Member Movement

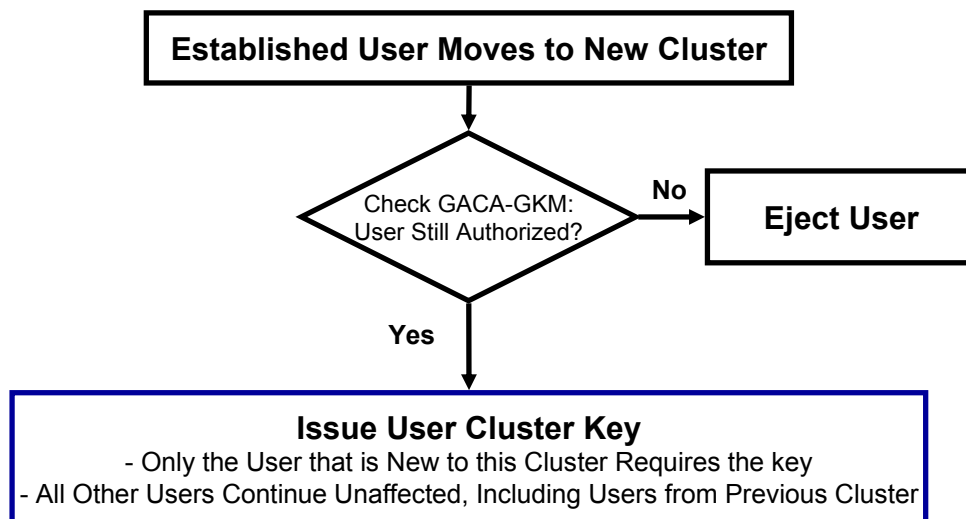


Figure 18 - Hubenko Architecture Flow Chart

Figure 19 depicts the key features of the Hubenko Architecture. The dotted lines represent the Satellite Layer sharing global knowledge of active users through the GACA-GKM. As before, multiple users in the same cluster who are participating in the same multicast group share the same cluster key.

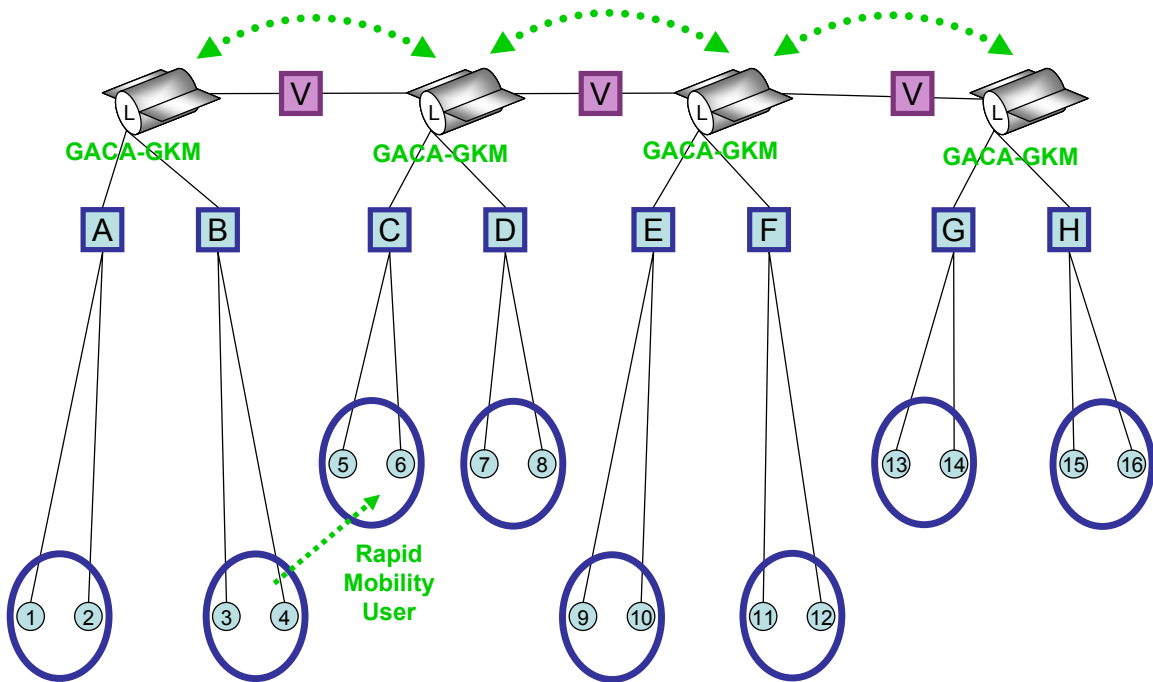


Figure 19 - Hubenko Security Framework Architecture

Assume a mobile user (e.g., User 4 in Figure 19) is registered in cluster “B” in a multicast group, then moves to cluster “C” and joins a different multicast group. With GACA-GKM support, the system would issue the cluster “C” key to User 4 without re-keying the other users in “C” since the system knows that User 4 did not collect any data from the new multicast group in “C” prior to it being granted the “C” key. Further, the system would not need to re-key the users in cluster “B” since User 4 is no longer able to receive the “B” data. For added security, User 4 should destroy the “B” key since it is no longer needed. Since GACA-GKM tracks the locations and group memberships of the

users in the system, it knows when users transition from one cluster to another and are still registered in the same multicast group. Therefore, when registered members of a multicast group move from cluster to cluster, they are issued the new cluster keys without impacting the new or old clusters. Since the user is already a member of the multicast group, and already has the same old data collected in the previous cluster, there is no need to re-key the new cluster since Traffic Backward Secrecy is not violated. Further, there is no need to re-key the old cluster since Traffic Forward Secrecy would not be violated either.

Using the previous sample scenario from the Baseline and Cluster examples, Figure 20 through Figure 23 illustrate the potential savings in re-keying by employing the Hubenko Architecture in a mobile environment. The Hubenko Architecture effectively initializes much like the Cluster Architecture did in Figure 13, with each cluster in Figure 20 utilizing a different key. However, when the two aircraft fly into the first spot beam in Figure 21 and join the multicast group, the system is able to issue the current “dark green” key to the two aircraft, and not have to re-key the whole cluster. This is because the system is able to determine that neither of the two aircraft were previously in a location that was covered by the multicast spotbeams, and therefore would not have been able to collect data from the past.

Upon transitioning to the next cluster in Figure 22, the system again tracks the whereabouts of the aircraft, and is able to issue the “tan” keys to the aircraft, without having to re-key the tan cluster. In addition, the system does not need to re-key the dark

green cluster because the system not only knows that the aircraft are no longer in that cluster, but also to which cluster they are currently assigned.

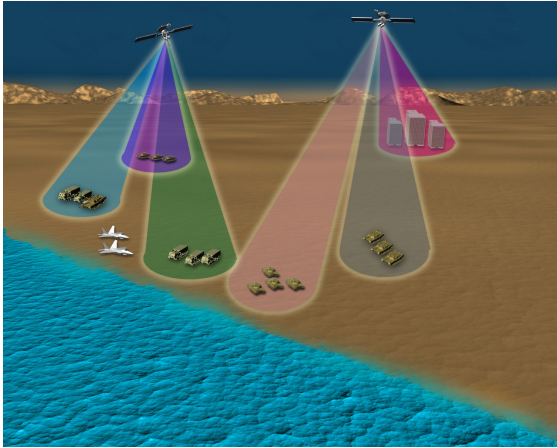


Figure 20 - Initialize Hubenko Architecture

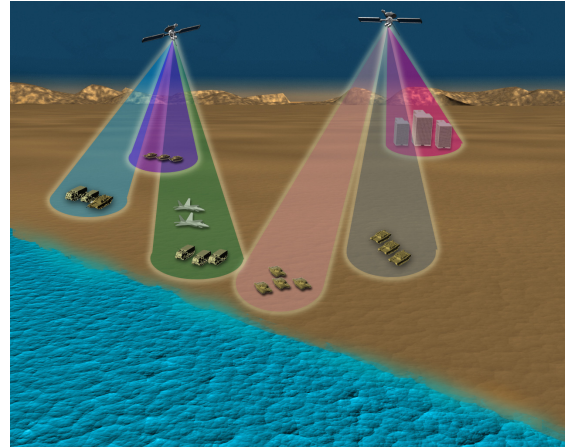


Figure 21 - Hubenko Example - Two

The same situation holds true as the aircraft move into the “grey” cluster in Figure 23. The “tan” cluster does not need to re-key, nor does the “grey” cluster. Finally, as the aircraft leave the multicast group and fly out of the “grey” cluster, they deregister from the multicast group. This Leave triggers the “grey” cluster to re-key to protect forward traffic secrecy.

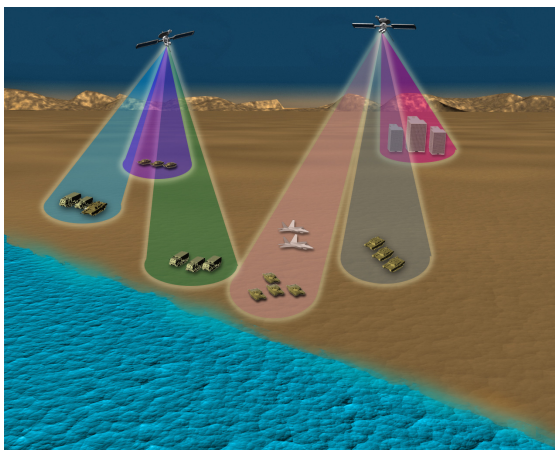


Figure 22 - Hubenko Example - Three

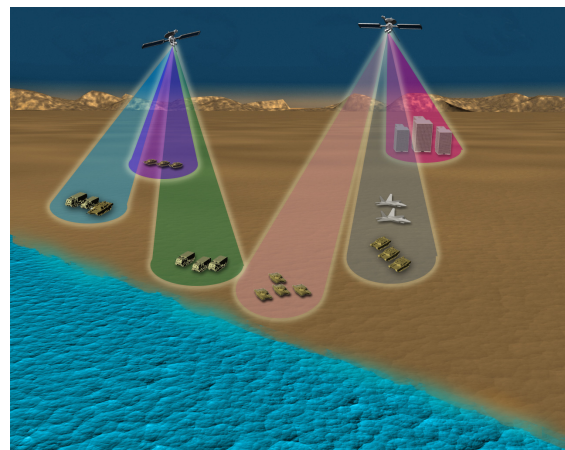


Figure 23 - Hubenko Example - Four

To ensure the integrity of the system, “physical separation” alone cannot be used when a previously unregistered user joins a group due to the broadcast nature of satellite communications and the inability to determine if anyone is “listening” to the transmitted data. Despite the use of relatively small spot beams, a large geographical area is still contained within view of the satellite. Therefore, a user may be out of view of any of the registered users, but well within view of the data transmissions in the cluster. This user can conceivably collect data, and then join the group. If the system did not re-key the cluster upon this new user’s join, the new user would now be able to decrypt the previously collected data with the key it just received. This violates the Traffic Backward Secrecy service provided by the network security system.

The previous cases do not apply if there is only one multicast group on the system. All of the registered users, while communicating with different cluster keys, would be receiving the same multicast data. Therefore, local transitions from spot beam to spot beam without cluster re-keying would be acceptable. However, in a system capable of handling multiple, concurrent, and distinct multicast groups, the former cases would most likely apply.

3.5.4 Demonstrate Improved System Security Performance

The final element of the research and development of the Hubenko Security Framework Architecture demonstrates the overall security performance improvements (i.e., less overall re-keying for the individual users and for the system as a whole) of the enhanced architecture by way of discrete time simulation using MatLab. Architecture models were developed based on the architectures defined above. The design of the

models are discussed in Section 3.6. The results and respective analysis of the simulations are discussed in Chapter IV.

3.6 Simulation Environment and Architecture Models

A discrete time computer simulation was created using MatLab[®] version R2006b [MAT07] to compare the efficiency and scalability performance of three representative architectures. *Efficiency* is defined as a measure of average re-keying experienced by the individual users. That is, the basis for determining efficiency was the number of times each user, on average, had to re-key during a given simulation period. *Scalability* is defined as the overall system-level key count. The more keys distributed per simulation, the less scalable the architecture. Since the number of keys, and not actual packet traffic, was the focus for determining efficiency and scalability, complex event simulators with packet-generation capabilities were not necessary. Instead, the simulation tracks all of the required performance statistics on each of the individual users, and aggregates the results to establish system level performance.

3.6.1 Simulation Environment

In this model, all multicast groups and active users (those registered in the multicast groups) are managed by the satellite infrastructure. If a user decides to initiate a new multicast group, the request is made to the satellite network, and the necessary group ownership information is transferred to the satellite layer for group establishment and subsequent management. For the performance results and analysis discussed in Chapter IV, however, the simulations focused on the steady-state performance, i.e., users joining, leaving, and moving within established multicast groups. When a user joins a

multicast group, it is authenticated through the closest LEO satellite. It is assumed an active user in a multicast group establishes and maintains a connection to the closest LEO satellite, whether or not it is actually transmitting data at the time. Active users require current keys to maintain their connections. When a user leaves (or is forced to leave), the user disconnects from the satellite.

Throughout the rest of this document, the following terms are defined as follows. A *Simulation* refers to a specific MatLab script file to code each of the experiments. A *Scenario* is a given simulation configuration, with certain parameters that remain constant throughout the running of the entire simulation (e.g., the number of time steps to simulate), and certain parameters (e.g., number of users) that vary in a predetermined way throughout the given simulation. Each scenario models a certain user environment with predetermined demographics and characteristics. A *Time Step* is a single unit of time, where all events appear to occur simultaneously. An *Iteration* is the complete execution of a single instance of the scenario, running from time step one through the total number of defined time steps. Within each iteration, the user properties remain constant, and are the same for each of the architectures. This is true because the users are defined first, before the simulation loops through the time steps of the given iteration. The user data structure utilizes a single parameter set for each user, which each architecture references throughout the simulation. The architecture-specific variables for each user are modified by the respective architecture, while the set user parameters are not modified within an iteration. As the simulation executes through the time steps, the appropriate actions are taken for each architecture before proceeding to the next time

step. This ensures each architecture is operating in the same system state, with the same users modeled for each architecture. Further model details are discussed throughout this section, and in Section 3.10.

To determine the performance of the Hubenko Architecture across differing user environments, simulations were created for several hypothetical scenarios involving various types of multicast-enabled users. The simulations modeled various configurations of satellites, spot beams, and other parameters in the different scenarios. The values for the scenario parameters were based on analogies to the physical world and sound engineering judgment. In general, the model is capable of simulating any configuration of satellites, clusters, and user demographics by simply changing the experimental parameters. Furthermore, the time intervals can be appropriately scaled to model different environments to address issues regarding concurrency, race conditions, and convergence. The processes of encryption and decryption are assumed to occur in a fixed unit of time. The System, Scenario, and Iteration Level Parameters and Factors are shown in Table 4. The specific values for the parameters and factors for each scenario are presented in Section 4.2. The only parameters that were held constant throughout all simulations are the individual speed settings for each of the Mobility Categories, and the Join Time Range. The speed settings mimic typical speeds encountered by real-life mobile users, namely users in automobiles, ships, and airplanes, as well as non-moving users. The Join Time Range was held fixed at 10% of the overall length of time in each simulation. This ensured all users were participating in each simulation. The System Level Factors varied between the different scenarios, but some (noted below) were held

constant across all iterations within each specific scenario. The Scenario Level Factors were held constant across all time steps within an iteration, but varied between iterations.

Table 4 - System, Scenario, and Iteration Level Parameters and Factors

<table><tr><td>System Level Parameters (Constant across all Scenarios)</td></tr><tr><td>Mobility Speeds (fixed per category)</td></tr><tr><td>Join Time Range (10% of avail time)</td></tr></table>	System Level Parameters (Constant across all Scenarios)	Mobility Speeds (fixed per category)	Join Time Range (10% of avail time)	<table><tr><td>System Level Factors (Varied across Scenarios)</td></tr><tr><td>Number of Satellites</td></tr><tr><td>Number of Clusters</td></tr><tr><td>Number of Time Steps</td></tr><tr><td>Control Group Size</td></tr><tr><td>Number of Users</td></tr><tr><td>Duration</td></tr><tr><td>Rates of Mobility</td></tr></table>	System Level Factors (Varied across Scenarios)	Number of Satellites	Number of Clusters	Number of Time Steps	Control Group Size	Number of Users	Duration	Rates of Mobility
System Level Parameters (Constant across all Scenarios)												
Mobility Speeds (fixed per category)												
Join Time Range (10% of avail time)												
System Level Factors (Varied across Scenarios)												
Number of Satellites												
Number of Clusters												
Number of Time Steps												
Control Group Size												
Number of Users												
Duration												
Rates of Mobility												
<table><tr><td>Scenario Level Parameters (Constant across all Iterations)</td></tr><tr><td>Number of Satellites</td></tr><tr><td>Number of Clusters</td></tr><tr><td>Number of Time Steps</td></tr><tr><td>Mobility Speeds (per category)</td></tr><tr><td>Control Group Size</td></tr><tr><td>Join Time Range</td></tr></table>	Scenario Level Parameters (Constant across all Iterations)	Number of Satellites	Number of Clusters	Number of Time Steps	Mobility Speeds (per category)	Control Group Size	Join Time Range	<table><tr><td>Scenario Level Factors (Varied across Iterations)</td></tr><tr><td>Number of Users</td></tr><tr><td>Duration</td></tr><tr><td>Rates of Mobility</td></tr></table>	Scenario Level Factors (Varied across Iterations)	Number of Users	Duration	Rates of Mobility
Scenario Level Parameters (Constant across all Iterations)												
Number of Satellites												
Number of Clusters												
Number of Time Steps												
Mobility Speeds (per category)												
Control Group Size												
Join Time Range												
Scenario Level Factors (Varied across Iterations)												
Number of Users												
Duration												
Rates of Mobility												
<table><tr><td>Iteration Level Parameters (Constant across all Time Steps)</td></tr><tr><td>Number of Satellites</td></tr><tr><td>Number of Clusters</td></tr><tr><td>Number of Time Steps</td></tr><tr><td>Mobility Speeds (per category)</td></tr><tr><td>Control Group Size</td></tr><tr><td>Number of Users</td></tr><tr><td>Rate of Mobility</td></tr><tr><td>Duration</td></tr><tr><td>Join Time Range</td></tr></table>	Iteration Level Parameters (Constant across all Time Steps)	Number of Satellites	Number of Clusters	Number of Time Steps	Mobility Speeds (per category)	Control Group Size	Number of Users	Rate of Mobility	Duration	Join Time Range		
Iteration Level Parameters (Constant across all Time Steps)												
Number of Satellites												
Number of Clusters												
Number of Time Steps												
Mobility Speeds (per category)												
Control Group Size												
Number of Users												
Rate of Mobility												
Duration												
Join Time Range												

The basic security functions of key generation, key storage, key agreement, and group key distribution were incorporated into the model. They were implemented through structured arrays, pre-allocated in memory to speed up operation. All of the keying statistics are tracked on a per-user basis, and are easily aggregated to report and

analyze system-level statistics. In addition, multiple fields with multi-dimensional arrays within each structure represented each user's parameters, as described below.

The users are divided into four representative Mobility categories, assigned with varying percentages of each as needed to model each scenario (cf. Section 4.2). The categories were chosen to represent the main types of users commonly operating in a deployed environment. "Stationary" (i.e., non-moving) users represent fixed infrastructure, such as a command post. "Sea" users have slow mobility (e.g., movement between clusters occurs at a relatively slow pace (e.g., several time steps)), and represent ships and amphibious units. "Ground" users move twice as fast as Sea users, and represent vehicles such as tanks, trucks, automobiles. "Air" users move four times as fast as Ground users, and represent airplanes, helicopters, and unmanned aerial vehicles (UAVs). The relative speeds of the categories were derived by analogy to real-world operators, which were then generalized into four distinct groups for simplicity. A ship typically has top speeds near 45 kilometers per hour. Smaller craft can move faster, while some ships have slower top speeds. An automobile or truck can easily reach 90 kilometers per hour, while most tanks cannot. Additionally, 360 kilometers per hour is an easy feat for a jet, but more difficult for UAVs and helicopters to achieve. Should an analysis require a finer granularity of Mobility Categories, each category can easily be broken into subcategories (e.g., "Air" can be divided into UAVs, Helicopters, and Jet Planes for instance). Related to the user Mobility categories is a system-level "Rate of Mobility" (RoM) parameter. A "Rate of Mobility" is defined as the overall percentage of users that are mobile (i.e., Sea, Ground or Air type) for each iteration. For example, a 1%

RoM means that out of one thousand users, an average of ten users would be assigned one of the three mobility categories, with the remaining users assigned a stationary category.

When the simulation initializes an iteration, each user is randomly assigned (using a uniform distribution) to an initial Satellite and respective Cluster; a Join Time; a Duration; and one of the four Mobility categories. In most of the scenarios, the uniform distribution ensured even loading across all of the factors. To investigate targeted areas of interest, certain scenarios reduced the range of factor values to simulate a more concentrated factor loading. For example, in scenarios with numerous satellites, using the uniform distribution allowed level loading across the system, without “overcrowding” any one cluster. Some of the scenarios, however, have only a single satellite for a high user density.

If the node is mobile, it may change to a new cluster during the iteration. The Join Times are uniformly distributed to activate all users within a specified time period, typically within the first one-third of the iteration’s time steps. In general, the Durations (length of time the user is active in the multicast group) are uniformly distributed between one time step to the time remaining until the end of the simulation. Certain scenarios, however, investigated the performance with specified duration lengths, as noted below.

The distributions used ensure a highly active user group with numerous joins and leaves spread throughout the iteration. Besides the joining and leaving activities, the users are able to move between clusters at a rate dependent on their mobility category.

Each user's mobility category is also assigned randomly within the constraint of the overall Rate of Mobility for the given scenario. Once the overall RoM is achieved (e.g., 10% of all active users are Sea, Ground, or Air types), all subsequent users are assigned to the Stationary category. Each of the scenarios used different RoM to simulate different real-life situations. The RoM were derived from knowledge of typical troop, fleet, and squadron sizes found operating within an operational area of responsibility (AOR). For example, a Marine Expeditionary Force (MEF) typically has between 7,000 and 20,000 troops deployed to a region. Along with the troops, the MEF deploys a few squadrons of aircraft and several amphibious units. Additionally, the Marines frequent deploy with the Navy, thus increasing the number of sea vessels and aircraft in the AOR. Out of the total number of troops, not all are in motion simultaneously. Hence, the scenarios all have less than 100% RoM. If, on the other hand, a scenario were to focus specifically on the efficiency and scalability of a mobile ad hoc network (MANET), it would be feasible to have 100% of the users be mobile.

To model the impact each event has on re-keying, the events are logically categorized into two levels. Joins and leaves are categorized as Level 2 events, and movement between clusters is categorized as a Level 1 event. If multiple events occur within a single time step, the highest-level event (i.e., Level 2 > Level 1 > None) takes priority, and only one consequence is modeled for the affected cluster or system as appropriate. In typical multicast systems, the only level that is modeled is Level 2 since movement was not a design criteria as multicast was being developed. Therefore, Level 1 was implemented to account for the movement not seen in other models. As a generic

example, if there are two leaves and a join within the same time step, only one round of re-keying is required to account properly for all three changes in the multicast group instead of three rounds of keying. The sizing of the time step will determine the level of fidelity of multiple events occurring near-simultaneously within a time step.

3.6.2 Architecture Models

3.6.2.1 Baseline Architecture

The first architecture, referred to as the “Baseline” architecture, is a generic multicast network that uses a flat keying system (i.e., all keys shown in Figure 6 are the same). There is no provision for clustering, so a user joining or leaving the network requires a new group key be established and distributed to all users in the system. As a user travels from one location to another, it deregisters from one spot beam, and re-registers in a new one. This is a new join, and again all users need to be re-keyed.

In the Baseline architecture, all events are handled the same since a user joining the multicast group, leaving the multicast group, or moving between satellite spot beams produces the same effect: trigger the multicast group to re-key. When the multicast group re-keys, all active users require a new key, regardless of their spot beam.

3.6.2.2 Cluster Architecture

The second architecture, referred to as the “Cluster” architecture, enables clustering, where each cluster is keyed with a separate cluster key (as shown in Figure 12). Adding a new user to the cluster, even if already joined to the same multicast group but in another cluster, required a re-keying of that cluster. Highly mobile users (e.g., aircraft), enter and exit the user clusters at a much greater rate than their terrestrial

counterparts. Therefore, even a single airplane flying into and out of heavily populated clusters induces a significant amount of re-keying on the cluster users.

In the Cluster architecture, all events again produce the same effect of inducing a re-key; however, the impacts are limited to the users within the same cluster where the event occurs. Therefore, when a user joins or leaves a multicast group, or moves to a new cluster, only that cluster requires the re-key, and not the entire multicast group as in the Baseline architecture.

3.6.2.3 Hubenko Architecture

The third architecture, referred to as the “Hubenko Architecture,” incorporates the GACA-GKM support into the Clustered architecture and is shown in Figure 19. If the system can establish a registered user does not have access to data prior to its joining a cluster, or would no longer have access after its departure, the cluster does not need to re-key. Instead, either the new user is issued a new key upon entry, or the system simply continues as before upon exit.

It is important to note that this implies a level of trust in the GACA subsystem, as well as sufficient trust in the authenticated user. A user will retain old keys for a certain amount of time, and could return to a previous cluster and continue to receive messages. If the user is a legitimate member of the multicast group anyway, the impact is minimal for returning to an old cluster that has not been re-keyed since that user would have collected the same data through another cluster. As a precaution, however, the whole system should establish a policy to re-key periodically, thus ensuring old keys are not used longer than the policy dictates.

Finally, in the Hubenko Architecture, the Level 1 and Level 2 events affect the system differently. Level 2 events (joins and leaves) have the same impacts as the Cluster architecture: the multicast group users in the affected cluster are re-keyed. Level 1 events (movement between clusters), however, do not require a re-key since the movement is tracked within the Group Access Control Awareness (GACA) subsystem. This differs from the Cluster architecture, which does not have the GACA subsystem and therefore cannot correlate a leave in one cluster and a join in another cluster as movement between the two. When multiple events occur within the same cluster and time step in the Hubenko Architecture, the highest Level event will drive how the cluster responds. If there are multiple joins or leaves within the same time step, the entire cluster will re-key once for that time step, and not once per join or leave. If there is movement into or out of the cluster along with a leave or a join in the same time step, then the cluster must re-key once to accommodate the new or departed user. If there are multiple movements that meet the criteria for merely issuing keys to the moved user, then no other user (other than the one that just arrived) within the cluster is affected for that time step.

The complete Hubenko Architecture requires that the ownership determination functions and the group policy specification functions from the Gothic architecture be implemented. Together, these control access to the established multicast groups. However, since the analysis was focused on the long-term, steady-state system, and not the initialization, these functions were not explicitly modeled and simulated. Instead, it was assumed that the complete set of functions were in place, and no distinction was

made between either a user leaving the multicast group of its own volition, or a user being ejected for some other reason.

The following pages depict the flow of the MatLab simulation code (Figure 24). A sample of the complete code is included in Section 6.5. While the specific iteration structure and plotting functions varied between scenarios, the core of the simulation remained the same.

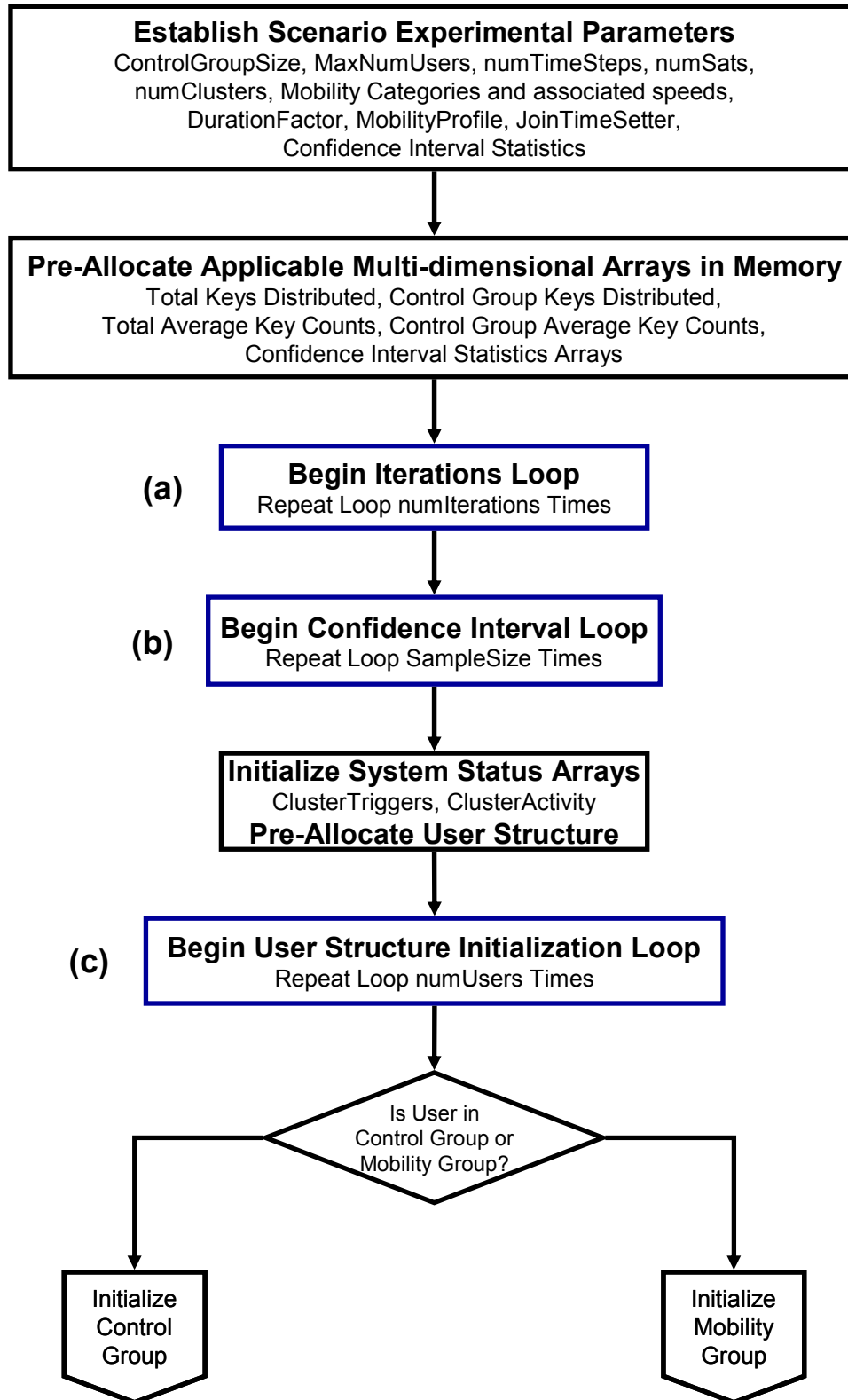


Figure 24 - Flow Diagram for MatLab Simulation Code

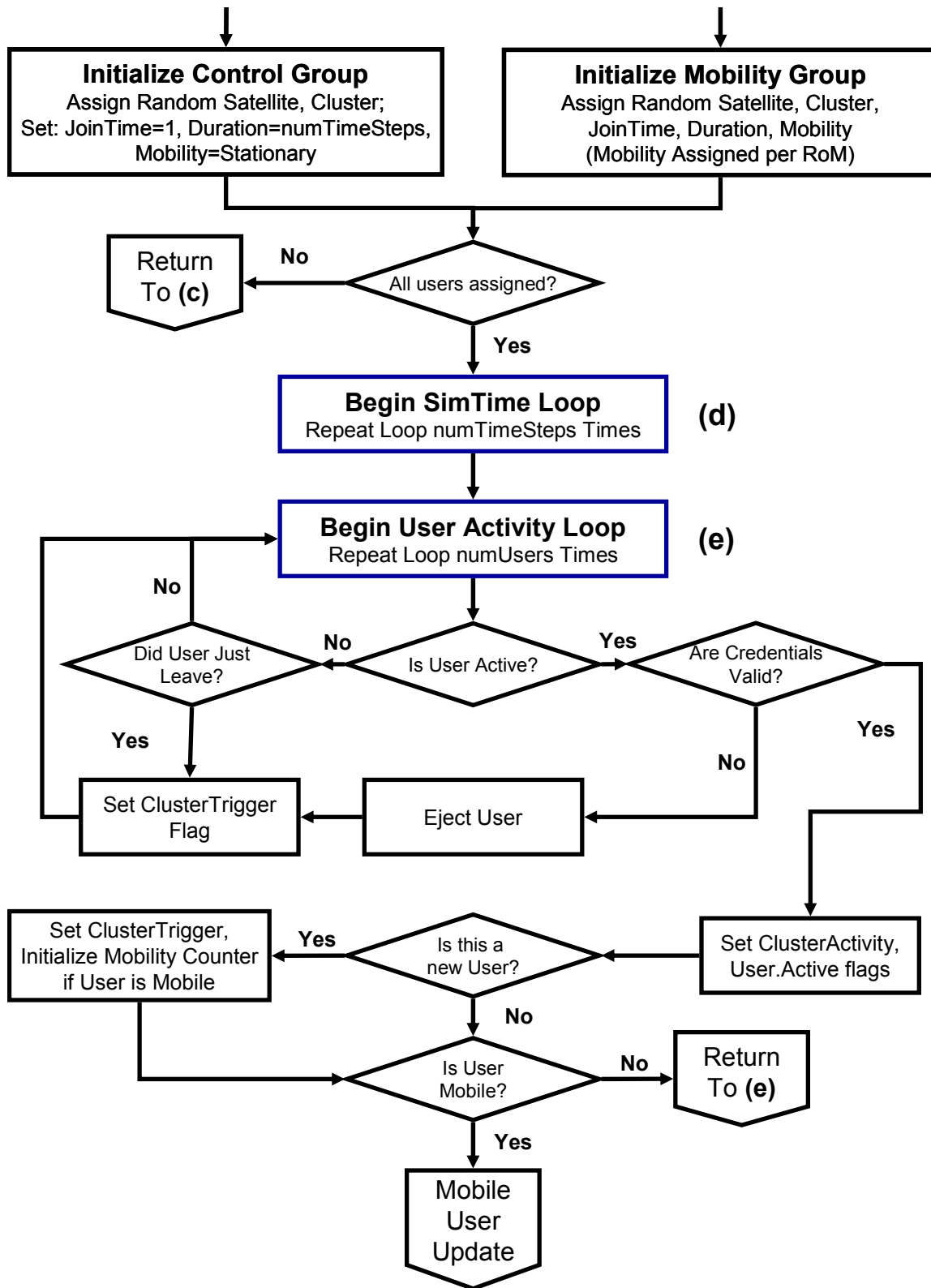


Figure 24 - Flow Diagram for MatLab Simulation Code (Continued)

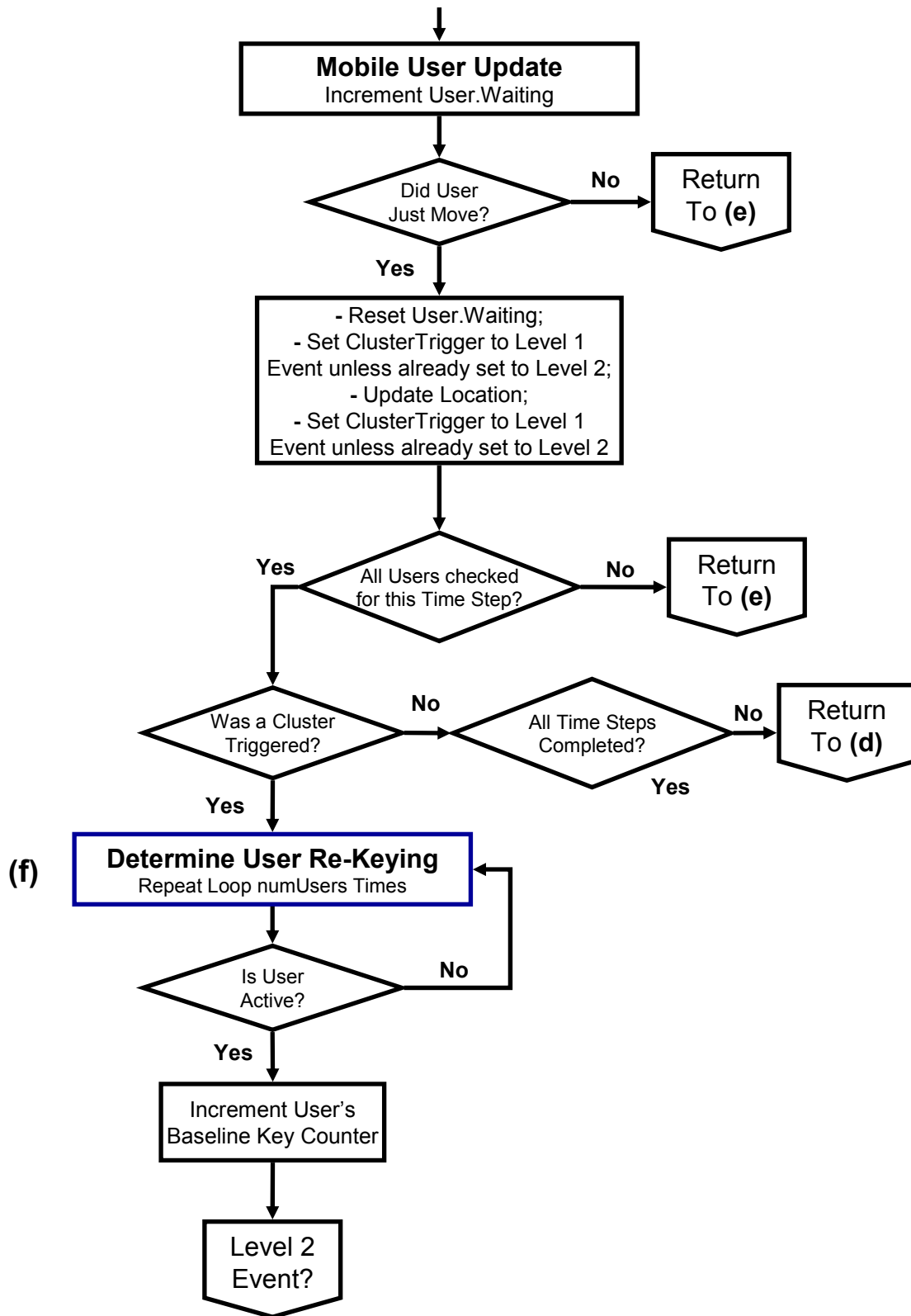


Figure 24 - Flow Diagram for MatLab Simulation Code (Continued)

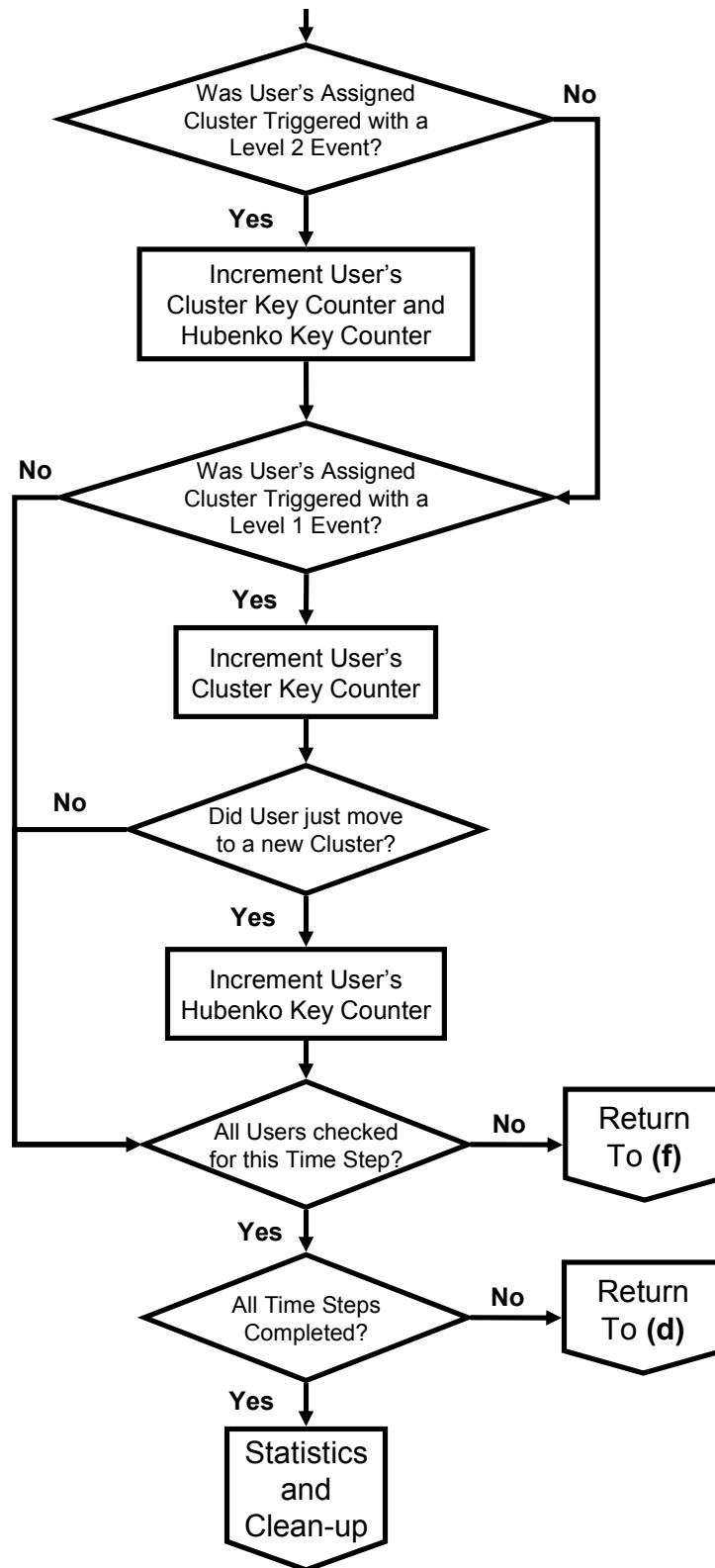


Figure 24 - Flow Diagram for MatLab Simulation Code (Continued)

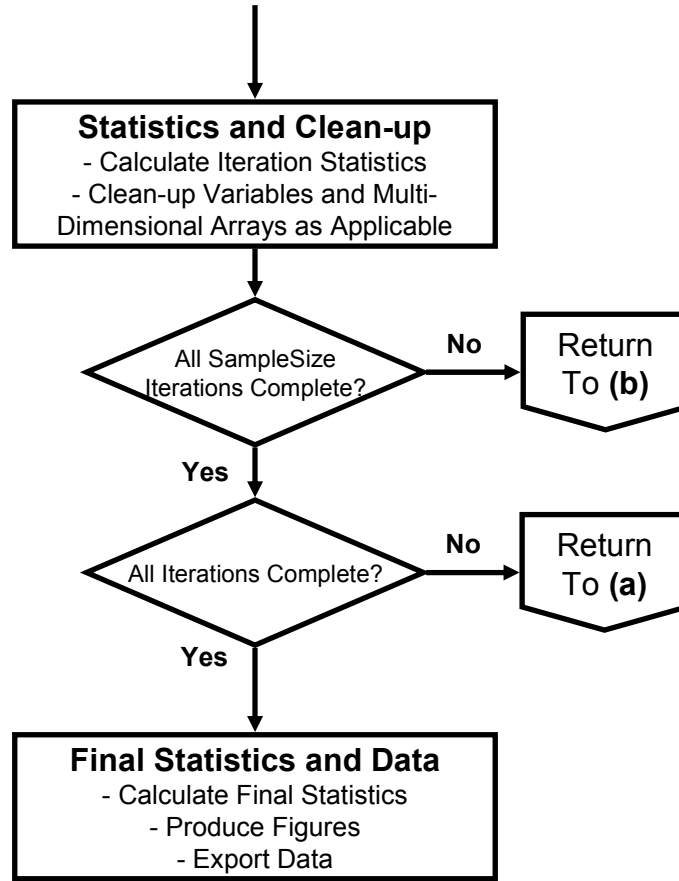


Figure 24 - Flow Diagram for MatLab Simulation Code (Continued)

3.6.3 Confidence Interval

The confidence level for this research is 95%. When an experiment has a 95% confidence level with an interval of plus or minus 10%, there is a 95% probability that the actual mean value of the experiment lies within a range 10% above and 10% below the experimental mean [Jai91]. The confidence interval is given by

$$\left(\bar{x} - z_{1-\frac{\alpha}{2}} \left(\frac{s}{\sqrt{n}} \right), \bar{x} + z_{1-\frac{\alpha}{2}} \left(\frac{s}{\sqrt{n}} \right) \right) \quad (1)$$

where \bar{x} is the sample mean, $z_{1-\frac{\alpha}{2}}$ is the $(1-\frac{\alpha}{2})$ quantile of a unit normal variate (1.960

for 95% confidence if more than 30 samples are used), s is the standard deviation, and n

is the number of samples. If the means of two experiments fall within the confidence intervals of each other, then the two items being compared are statistically not different. If the confidence interval does not contain the mean, then the items being compared may be statistically different at this confidence level and a t-test would need to be performed.

The Coefficient of Variation (C.O.V.) [Jai91], is the ratio of the sample standard deviation to the sample mean

$$C.O.V. = \frac{s}{\bar{x}} \quad (2)$$

A C.O.V. of less than 10% is generally used as the stopping criteria for simulations. Results collected for analysis in Section 4.2 indicated three repetitions were sufficient to achieve non-overlapping interval bounds for the scenarios with 10,000 users at 95% confidence, while five repetitions were necessary for the scenarios with fewer users.

3.7 Simulation Equipment

The research and development computer was a XEON workstation with two three-gigahertz “Dual-Core” Hyper Threaded XEON CPUs, along with 4 gigabytes of random access memory and dual 75 gigabyte hard drives. This computer is typically capable of running upwards of eight simultaneous MatLab simulations, due to its eight virtual CPUs, with no apparent slowdown.

The elapsed time for simulations to complete varied from as little as less than a day, to more than four weeks. The longest simulations were the ones that modeled 10,000 users for 10,000 time steps, with three repetitions to achieve the desired non-overlapping 95% confidence interval bounds. The only technical issue that arose due to

computer equipment and/or software occurred during the execution of the 10,000 user/10,000 time step simulations. MatLab running on Microsoft Windows®-based computers has a two billion data element limitation. The simulations were coded in such a way as to maximize the full set of available data elements, without exceeding the limit. However, after approximately three weeks into the execution, the workstation experienced a memory error and reboot, thereby not completing the simulation. The page file statistics never surpassed two gigabytes during the executions; however, Windows XP does not have a native utility to track actual system memory usage or history, so there may have been an error that was not tracked. The only logged error that was reported related to the Symantec “quarantine scan” operation. The machine was removed from the local area network, and all anti-virus and security software was uninstalled. This solved the problem.

3.8 Metrics for Security Performance Evaluation and Analysis

The overall objective of this research effort is the development of an efficient and scalable multicast security framework architecture for a LEOsat environment that provides improved performance over current secure group communications architectures. *Efficiency* is defined as a measure of average re-keying experienced by the individual users. That is, the basis for determining efficiency is the number of times each user, on average, has to re-key during a given simulation period. *Scalability* is defined as a measure of the overall system-level key count. The more keys that have to be distributed per simulation, the less scalable the architecture. Therefore, the following metrics are used throughout the following simulations and analysis:

- Average number of times each user is re-keyed during an iteration.
- Total number of keys distributed in the system during an iteration

These metrics are similar in concept to related research efforts and are germane to determining potential security performance improvements [HoI04, RaH03].

3.9 Time Scaling for Modeling Expediency

Time scaling is a technique that has been successfully used in the past to reduce simulation times by appropriately adjusting packet sizes, delays, etc [Fos98, Sae03, Tho01]. This was helpful for analyzing end-to-end delays in prior research. The focus of this research, however, was on the effects joining, leaving, and moving of users had on re-keying operations. In this research, time was normalized to uniform time steps, and all events occurred within those steps. The time steps can be enlarged to the order of seconds or even minutes to model broad, large-scale environments such as the global LEOSat network, or reduced to milliseconds to analyze small, localized networks in greater detail.

3.10 Model Verification

Model verification was accomplished using a systematic approach. MatLab code was used for the modeling and simulation of the Hubenko Security Framework Architecture. A spiral testing and verification method was employed on the architecture. Problems with syntax and illegal statements were identified and corrected after each section of code was written. Further, each section of code was checked for proper, expected execution to ensure each progressive feature was correct before the next section was developed.

During development, most of the errors involved logical issues with the boundary conditions, such as properly accounting for the start or finish of a user's duration, incorrectly incrementing re-key counts just before a user's joining, or just after a user's leaving the multicast group. These errors were identified by stepping through the code by hand, using the results of the user structure population and comparing the output of functions with the expected output. Figure 25 through Figure 30 (excluding Figure 28) graphically display contents of the Satellite, Cluster, Mobility, Join Time, and Duration fields for each of the individual users' random assignments, summarized from the structured array. Plots similar to these were used throughout the development and testing to ensure the expected randomization occurred, ensure the assignments were within the expected bounds, and to verify that the code was executing properly given certain values in the user structured arrays. Figure 25 shows the satellites that each user is assigned to at the start of the simulation. Figure 26 shows the respective cluster assignments for each user. Combining the cluster assignment with the satellite assignment, each user's location can be identified throughout the simulation. Figure 28 is an aggregate of the data from the User.Mobility field (plotted as a bar plot in Figure 27), and verifies the distribution of the user Mobility Categories. The distribution of the user mobility is used to define the specific "Rate of Mobility" for each of the model scenarios. Each user's Join Time and Duration assignments are shown in Figure 29 and Figure 30, respectively. These two fields dictate when the users join, and how long they remain active, thus allowing a verification of each user's activity (or lack thereof) for each time slot.

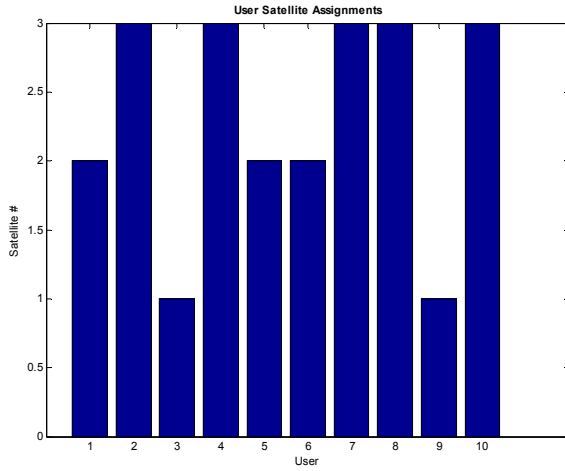


Figure 25 - User Satellite Assignments

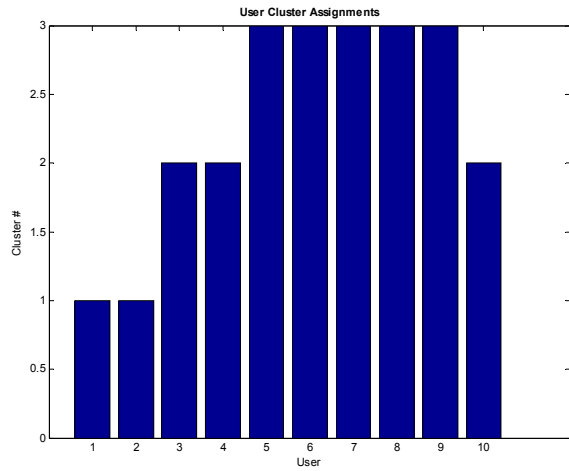


Figure 26 - User Cluster Assignments

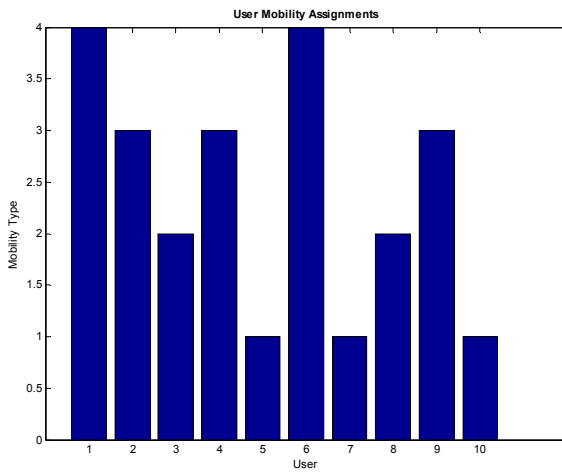


Figure 27 - User Mobility Assignments

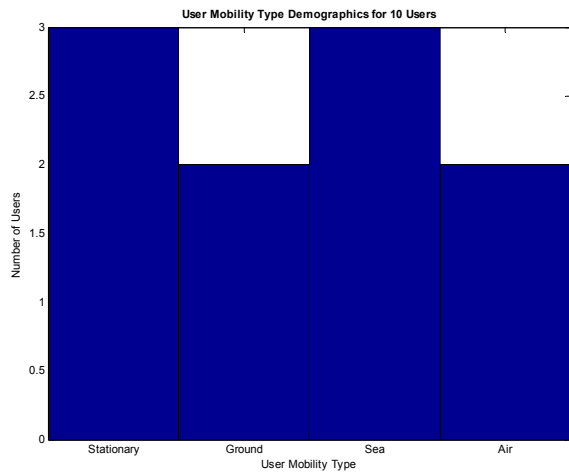


Figure 28 - User Mobility Verification

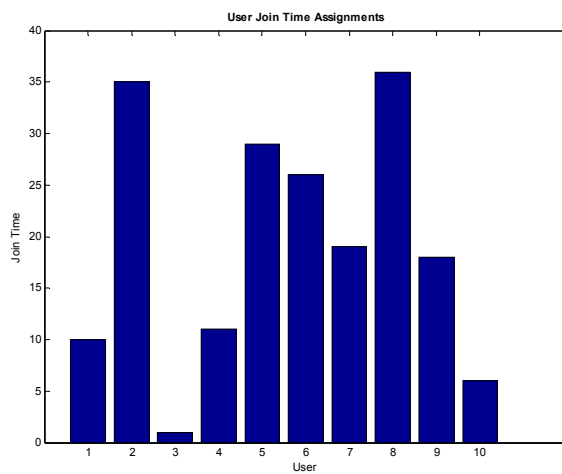


Figure 29 - User Join Time Assignments

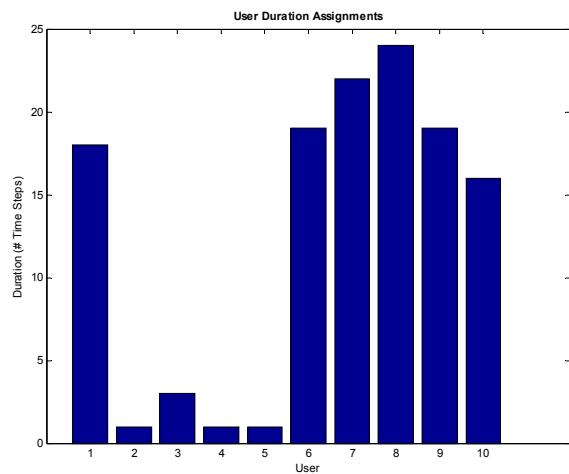


Figure 30 - User Duration Assignments

Critical to the operation of the code is the identification of when users are active and when they are not. As discussed in Section 3.6.1, all active users receive new keys upon the appropriate system or cluster re-key, whether or not they are transmitting data at that time. Therefore, it is imperative to ensure the system is properly tracking each user's current state of activity. To verify the correct operation of simulated user activity, the user structure was examined with the help of spreadsheets, along with graphical plots such as Figure 31. This figure shows the Join Times (positive slopes) as well as the Departures (negative slopes) of the ten users being examined. Join Time plus Duration equals Departure Time.

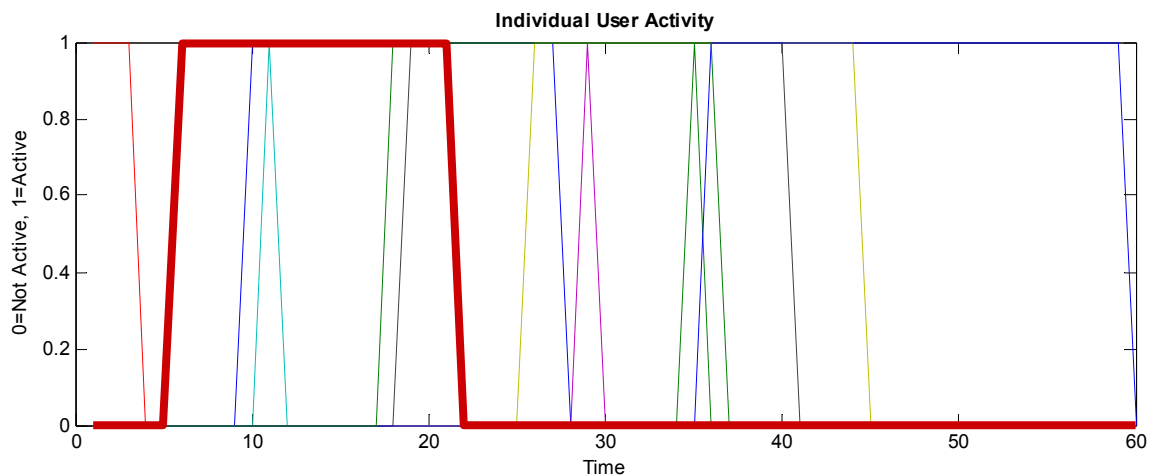


Figure 31 - User Activity Verification

To illustrate, User 10, depicted with the bold red line, had a Join Time of six (cf. Figure 29) and a Duration of sixteen (cf. Figure 30) for a Departure Time of twenty-two. Note the first descending line in Figure 31. This line is associated with User 3. User 3's Join Time was set at Time Step one, and therefore there is no ascending line associated with the Join since the user initialized as active. However, User 3 in the plotted example case had a Departure of Time Step four, and its respective descending line is clearly

identified. Therefore, the plot shows nine ascending lines (indicating the Joins) and ten descending lines (indicating the Departures).

Along with Joins and Departures, Mobile users can move between clusters. This information was tracked in another multidimensional array and combined with the Join and Departure information to yield a set of “triggers” used to establish when clusters or systems would need to re-key. Plots similar to Figure 32, along with exporting the arrays to a spreadsheet, were used to verify the correct operation of the Join, Leave, and Movement triggers. Figure 32 is the aggregate of all users across all clusters in the system, for the sixty simulated Time Steps. The height of the bars (either one or two) correlate to the Level One and Level Two events described earlier in Section 3.6.1. Note that there are only nineteen Level Two events (Joins or Leaves) since there is a simultaneous Join and Leave at Time Step Thirty Five. In addition, any movement that occurs within the same Time Step that a Join or Leave occurs will be masked by the higher priority event (i.e., a Join or a Leave).

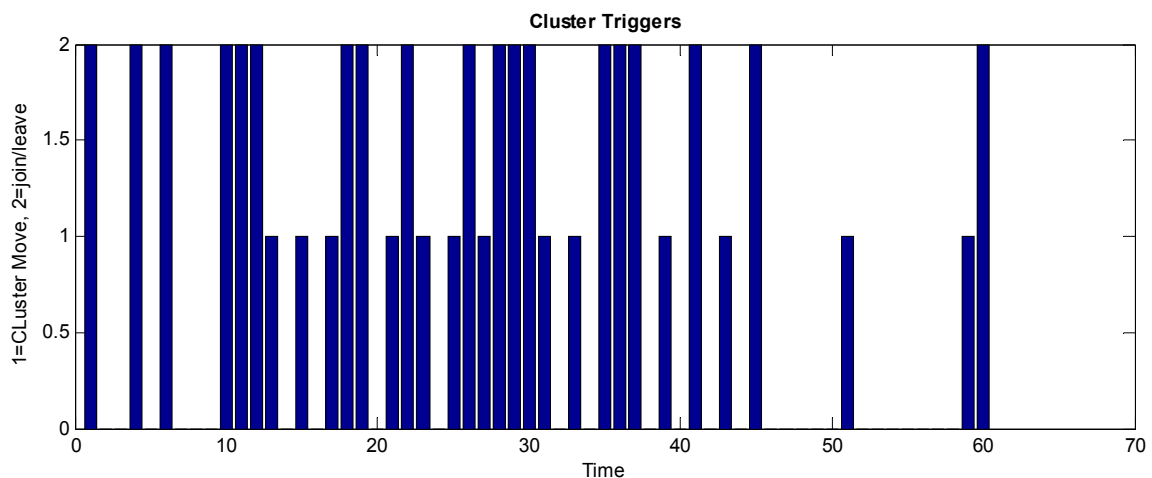


Figure 32 - Cluster Trigger Verification

Returning to the examples of Users 3 and 10, Figure 32 was used to verify the Joins and Departures. The Level 2 events shown at Time Steps 1, 4, 6, and 22 correspond to the User 3 Join, User 3 Departure, User 10 Join, and User 10 Departure, respectively.

Each successive step in the development ultimately led to the final performance statistics, namely, Average Per-User re-keying, and Total System Keys Distributed, shown in Figure 33 and Figure 34, respectively. For the development and testing phases, the data was drawn in bar graphs for simplicity of analysis. Further, there was only one iteration at a time under investigation. Therefore, line plots similar to those shown in Section 4.2, which represent multiple iterations demonstrating the performance of the systems as the number of users grow, were unnecessary and impractical. Bar graphs for each iteration would have been prohibitively cluttered for analysis beyond a few iterations.

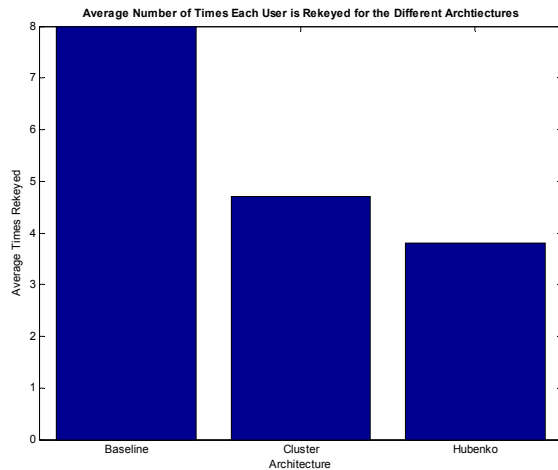


Figure 33 - Average Per-User Re-keying

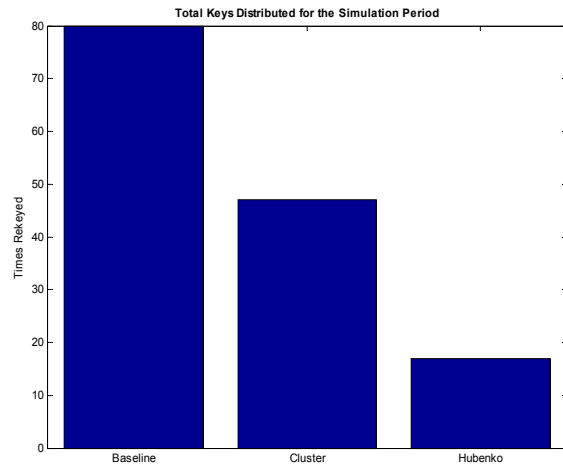


Figure 34 - Total System Keys

During the initial stages of model development, there were multiple active multicast groups in each iteration. This modeled multiple multicast groups co-existing

within the same satellites and clusters. This allows accurate modeling of the physical properties (e.g., time, frequency, and/or code division multiple access technologies) available on current and future satellite systems. However, as the number of users and time steps increased, this method became too resource intensive in terms of the number of MatLab data elements required to execute the code. The number of MatLab data elements is roughly two billion when operating on a Windows-based computing platform. The removal of the concurrent multicast groups conserved sufficient data space to allow the execution of larger numbers of concurrent users over longer simulated periods of time.

Another tool used to verify the model development was the random number generator state control. There are several options available in MatLab for manipulating the pseudorandom events. Only two methods, however, were used in this model. They were resetting the state to zero, and choosing a random seed for each simulation, as shown below.

```
% Return RAND to its default initial state to
allow for repeatability
rand('state',0);

% Initialize RAND to a different state each time.
rand('state',sum(100*clock))
```

Setting the random number generator back to the same state on successive simulation executions allowed testing of certain functions, features, and changes in parameters through replication of the user assignments. This was especially helpful when removing sections of code (such as the multiple multicast group feature), or adding the next successive feature. The simulations could be run using the same user population on

the before and after code, and the results compared to verify the correct operation of the new features.

Enabling different states between successive executions ensured different user initialization parameters, thereby generating slightly different results. MatLab can ensure a new seed each time by utilizing the current time of the system clock as a function for seed generation. The MatLab function “clock” outputs the current time as a six element date vector with the year, month, day, hour, minute, and seconds, each in decimal form. Each element is multiplied by 100 to ensure integer values, and then are summed into a single scalar value to be used as the seed. Since time is monotonically increasing, the seed does not duplicate on successive iterations.

3.11 Model Validation

Model validation was difficult since there are no known physical implementations of similar secure multicasting group architectures. Therefore, the Hubenko Security Framework Architecture model was validated against one of the other architectures found in the literature, namely the Spatial Cluster architecture. A comparison with the Iolus architecture was not possible since the article discussing the Iolus architecture did not perform any simulations examining average or total system re-keying. Instead, time delays incurred by using the group security agents (GSA) were measured.

Full replication of the simulation experiments to validate the Hubenko model with the Gothic architecture model was not possible due to lack of complete environment data (e.g., user parameters, mission trace data) used in [JuA02]. Additionally, the exceptionally long periods of simulated time (almost 700,000 time steps) used in the

Gothic analysis would have to be compressed and the data aggregated because the Hubenko model simulations were only capable of extending to approximately 10,000 time steps and still complete in a reasonable amount of time (e.g., several weeks).

The results found in [JuA02], shown in Figure 35 and Figure 36, demonstrate a trend similar to the results found when the Hubenko model incorporated the GACA-GKM features. Figure 35 shows that Gothic provided approximately an order of magnitude less cumulative key traffic in a live trace of data captured from a space shuttle mission as compared to a key management model that does not employ the group access control awareness features of Gothic. While still favorable, the results are less impressive when Gothic is compared to the same architecture in a simulated trace, shown in Figure 36. Figure 35 and Figure 36 show that Gothic provides a marked performance improvement when employed in a security architecture. Similarly, the Hubenko Architecture provides results (cf. Section 4.2) of similar magnitude and form, and thus the Hubenko model is accurately modeling the simulated environment as specified.

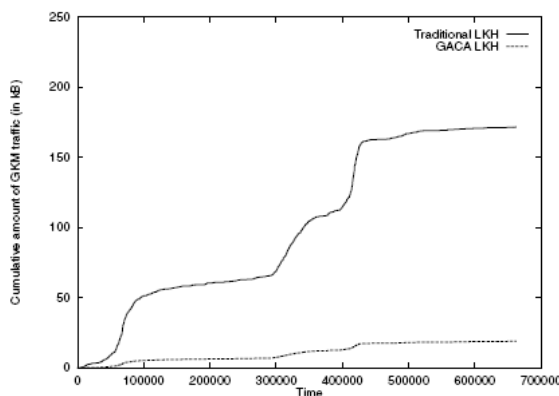


Figure 35 - Group Key Management Overhead - Actual Trace [JuA02]

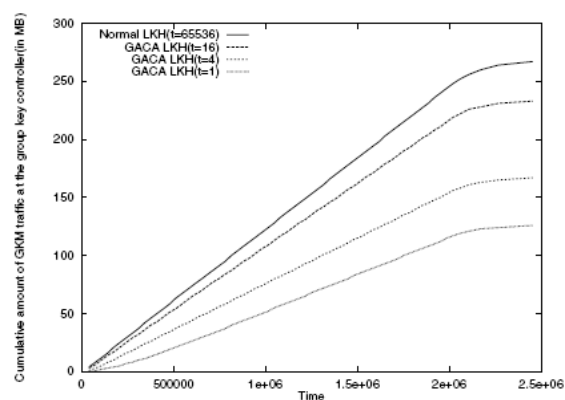


Figure 36 - Group Key Management Overhead - Simulated Trace [JuA02]

The Hubenko model performs better than the Gothic model due to clustering which the Gothic architecture lacks. An example of this is shown in Figure 37 for

comparison. The Hubenko Architecture provides a greater degree of improvement over the Clustered architecture (Figure 37) than the Gothic architecture provides over the Normal LKH architecture (Figure 36). As an aside, the effect of increasing mobility in the simulations is apparent in Figure 37. The average keys distributed in the 1% (iterations 1 through 200) and 10% (iterations 201 through 400) RoM sets begin at or near zero, while the average keys distributed starts off higher in the 25% (iterations 401 through 600) and the 75% (iterations 601 through 800) RoM sets. From the very first iterations (401 and 601, respectively), there is significantly more movement throughout the 25% and 75% RoM sets as compared to the 1% and 10% RoM beginning iterations (1 and 201, respectively).

Note in all figures created during the course of this research, the transitions between different “iteration sets” (e.g., between two consecutive RoM sets) are drawn. This transition appears as a drop in key counts, but it is due only to the graphical process used to create each figure. The most logical presentation for the data was using line graphs. MatLab plotted the data as continuous functions rather than breaking the lines at each set transition. At each transition point within the scenarios, the lines dip in the Hubenko plot due to the resetting of the user population. When the user population drops from the maximum number of users in the last iteration of one set, to the minimum number of users in the first iteration of the next set, the Hubenko key counts all go down as well. In the scenarios where the RoM changes, the Baseline and Cluster plot lines also drop at the transition. However, in the Short versus Long Duration scenarios, the

Hubenko key count goes down on the first iteration of the Long set, while the Baseline and Cluster counts go up.

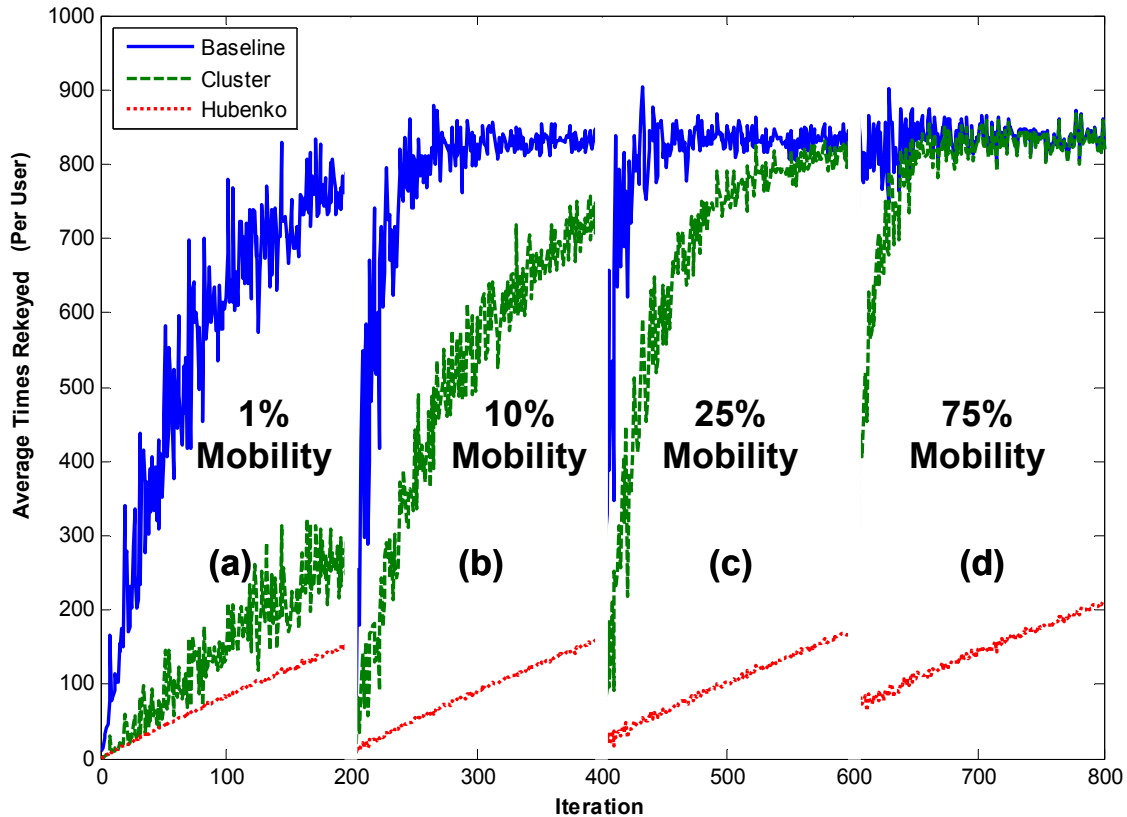


Figure 37 - Average Keys Distributed in a Highly Mobile Environment

The final source for validating the Hubenko model comes from the results demonstrated in the Spatial Clustering experiments [BaB02] shown in Figure 38. This figure demonstrates the near-constant key loading of the Spatial Cluster architecture as an increasing number of users simultaneously depart a multicast group consisting of 24,000 users. In [BaB02], keys were normalized to one byte each to allow different keying methods to be represented. In Figure 38, the line with the square markers is the performance of Spatial Clustering with a single multicast address used for all 24,000 users. The 100 level indicates approximately 100 keys generated per iteration. Due to

clustering, as the number of users simultaneously departing the multicast group increases, the key counts remain approximately the same.

The validation simulations had the following characteristics. The Hubenko Architecture had 2,112 clusters while Spatial Clustering states it had approximately 3,100 clusters (and approximately 17,000 routers). The Hubenko experiments used 23,323 users (versus 24,000 users) for an average of eleven users per cluster. The simulation focused on the steady state (i.e., all users already joined to group) just like Spatial Cluster, with no other events occurring except the noted departures. There was no movement for this validation experiment, and hence no observed difference between the Cluster and Hubenko performance results.

Under similar conditions as the experiments in [BaB02], the Hubenko Architecture also has a near-constant key loading for increased simultaneous departing users as shown in Figure 39.

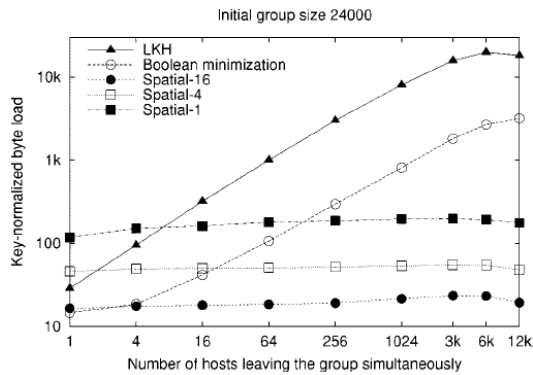


Figure 38 - Spatial Clustering- Varying the Number of Hosts Leaving [BaB02]

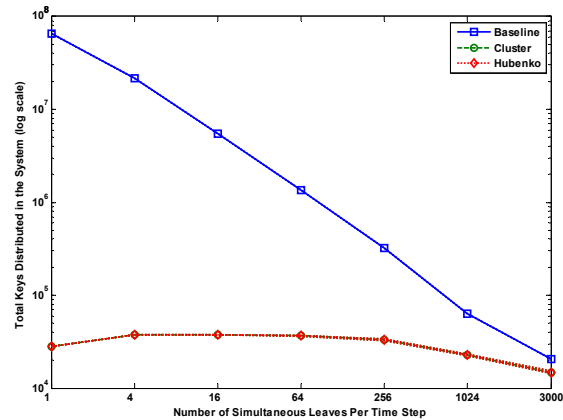


Figure 39 - Hubenko Model - Varying the Number of Hosts Leaving

Close inspection of Figure 38 and Figure 39 reveals several differences. First and foremost, the demonstrated key loading (on the \log_{10} scale) for the Spatial Cluster

architecture is approximately 10^2 keys, while the loading for the Hubenko results is approximately 10^4 keys. The reason for this difference is due to which keys are being considered in each case. The Spatial Clustering experiments measured the keys distributed through the tree routers which does not include the final leaf routers, or the end users (hosts). On the other hand, the Hubenko experiments measure the keys distributed through to the end users. Furthermore, Spatial Clustering does not count any replicated keys sent to the individual users in each cluster. This accounts for one order of magnitude of the difference since the approximate loading of each cluster is between eight and fifteen users. The Hubenko Architecture assumes that across the domain of the 24,000 users, the overall cluster loading average is eleven (which is roughly 10^1).

The second order of magnitude difference is not as clearly explained due to insufficient information on the Spatial Cluster implementation, network topology, and other key parameters. Therefore, it is assumed that unique keys are counted for the key hierarchy (where several users utilize the same sets of keys), and not the total number of keys distributed to each individual user. Even so, since the keys are multicast to the group, there is no additional load on the network for sending multiple keys. The values reported by Spatial Cluster are normalized byte loads, and not necessarily the number of keys distributed to all users. In Figure 38, for example, one hundred keys are clearly not sufficient to re-key the remaining 12,000 users when 12,000 users simultaneously depart. Assuming a uniform distribution of users departing the group, there is no way to have 12,000 users distributed among different clusters, with an average loading of approximately eleven users per cluster, and yet only require one hundred keys for said

users and clusters. However, it is possible to contrive scenarios where the users that are simultaneously departing are all leaving from the same clusters. In this case, all of the empty clusters would simply be pruned from the multicast tree rather than require any new keys to be issued. It might then be possible that of the 12,000 users that departed, only 100 clusters of the remaining users were affected (i.e., only one or two users from a select few clusters left the group). The Hubenko simulation did not contrive such a scenario; rather, it employed a uniform random distribution for the user departures.

The trend of the results shown in Figure 39, compared to the results shown in Figure 38, validates the clustering portion of the Hubenko Security Framework Architecture model. Similarly, the trends of the Gothic architecture, shown in Figure 35 and Figure 36 above, validate the GACA portion of the Hubenko model results.

3.12 Summary

This chapter presents the methodology for the development of the secure, scalable Hubenko Security Framework Architecture for LEO satellite-based networks (LEOsat), and addresses the lack of a secure multicast architecture that scales well for very large numbers (10,000 or more) of highly mobile users. The motivation for developing the Hubenko Architecture, along with the validity of employing a LEO satellite communications network is presented. Additionally, the metrics that were collected and analyzed were defined in this chapter as well. This chapter concludes with the model verification and validation.

IV. Performance Results and Analysis

4.1 Chapter Overview

This chapter discusses the modeling and simulation performance results. Analysis of the results confirms the re-keying advantages provided by the Hubenko Architecture over other secure group communications architectures in all of the simulated user environments. Various user environment scenarios are presented with their corresponding simulation performance results, along with analysis and discussion. Finally, the performance results are summarized.

4.2 Model Scenarios

To determine the performance of the Hubenko Architecture over the Baseline and Clustered architectures, several scenarios are developed and analyzed. In each scenario, the basic models are the same as those discussed in Section 3.6.2. The only changes are to the values in the specified parameters for each scenario, as noted in each scenario discussion below.

4.2.1 Highly Mobile User Environment (Four Different RoM)

The first simulation scenario represented four independent Rates of Mobility (RoM) for a moderate user population size. To contain the user movement in a relatively small geographical area, only a single satellite with ten active spot beams (clusters) is simulated. This models a geographical coverage area that would encompass a typical theater of operations (e.g., deployed military operations overseas, or a widespread disaster recovery area). In general, the model is capable of simulating any configuration of satellites and clusters by simply changing the experimental parameters. However,

these scenarios used a single satellite because aircraft do not typically fly with sufficient speed or range to significantly impact terrestrial-based users over a larger area. The first RoM, 1%, represents a user environment with little mobility, such as when all users are in garrison, and their movements do not cause them to cross into neighboring clusters. Subsequent RoM incrementally increase the user mobility (10%, and 25%), ending with a 75% RoM to characterize the Hubenko Architecture in a highly mobile environment. Figure 40 shows the representative distribution of the users' mobility categories (from the final iteration of each iteration set) for each of the four different Rates of Mobility, marked (a) through (d).

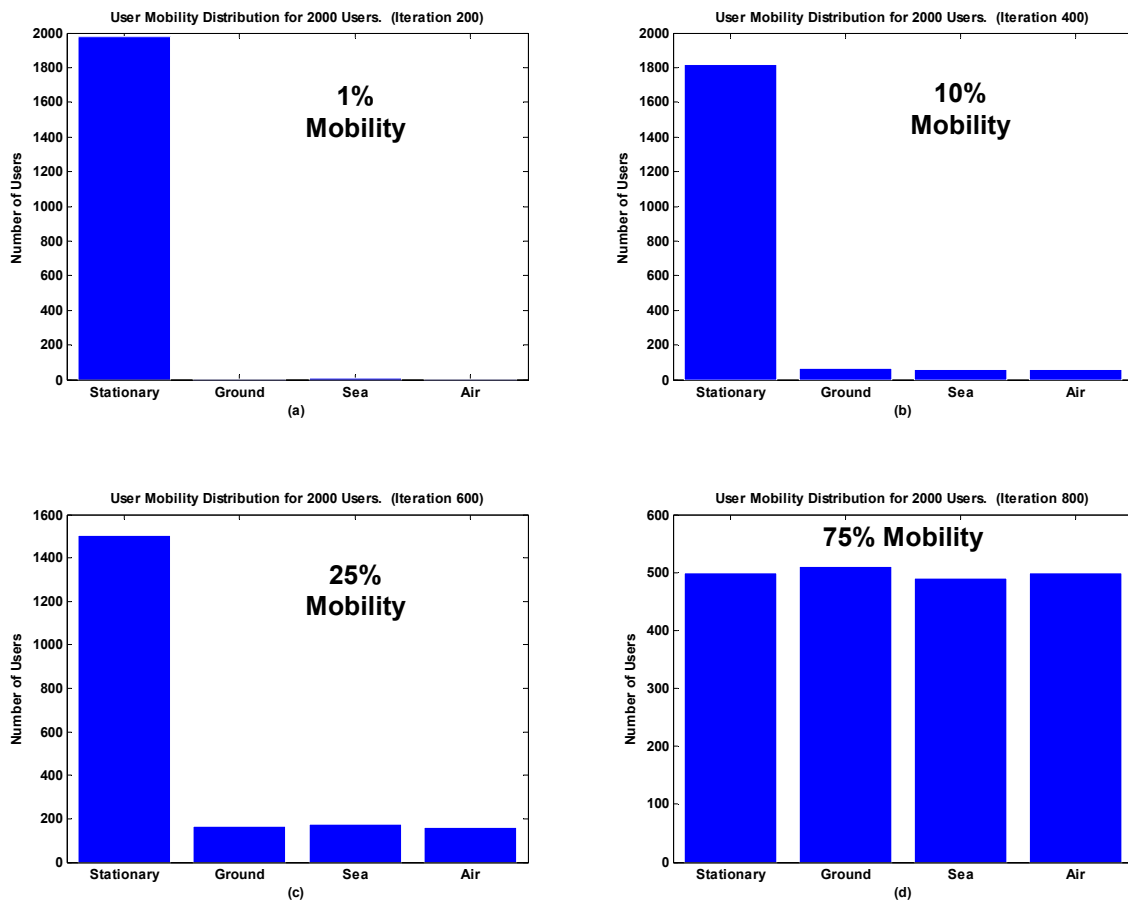


Figure 40 - Rates of Mobility for Highly Mobile Scenario

The distinct sections (“iteration sets”) marked (a) through (d) in Figure 41 and Figure 42 correspond to the four different Rates of Mobility (1%, 10%, 25%, and 75%), respectively. Section (a) has iterations 1 through 200, section (b) iterations 201 through 400, and so on. From left to right in Figure 41 and Figure 42, as the iteration count increased, the number of users in the system also increased. For example, iterations 1, 201, 401, and 601 had ten users total, for an average cluster density of one user per cluster. The maximum average cluster density for each simulation set (iterations 200, 400, 600, and 800) was two hundred users, for a total of two thousand users across the ten satellite clusters. The RoM was constant for all iterations within each iteration set. When the two hundredth iteration within each set completed, the RoM was increased to the next level and the number of users reset to an average cluster density of one user per cluster. The key simulation parameters are summarized in Table 5.

Table 5 - Highly Mobile User Environment Parameters

Satellites	1
Clusters	10
Maximum Users	2000
Time Steps	2000
Rates of Mobility (%)	1, 10, 25, 75
Features	Mobile users evenly divided between Sea, Ground, and Air

With low overall mobility, both the Cluster and the Hubenko Architectures demonstrated significant improvement over the Baseline architecture in terms of average re-keys per user (Figure 41) and total keys distributed in each system (Figure 42). Since there was relatively little movement with the 1% RoM, the Hubenko Architecture offered little improvement over the Cluster architecture. The Group Access Control Awareness –

Group Key Management (GACA-GKM) did not have an opportunity to provide any benefits for supporting mobile users. However, as the Rate of Mobility increased (shown in Figure 41 and Figure 42 (b) through (d)), the performance gains due to the inclusion of the GACA-GKM in the Hubenko Architecture also increased. This is demonstrated by observing the difference in re-keying between the Cluster and the Hubenko architectures in the 1% mobility sections (~150 average re-keys), to the difference in the 75% mobility sections (~625 average re-keys). The performance gain from the Hubenko Architecture is approximately 400%.

Saturation is defined as each user being re-keyed at every time step. The Baseline architecture results in saturation which a re-key of each user occurs per each time step. Adding more users increases the Total Keys Distributed, but does not increase the Per-User Average Re-key result, which equals the number of time steps. This is because at least one event occurs in each time step, and one or more events trigger a re-key, and at most one re-key can occur per time step. Therefore, the maximum number of keys that can be distributed in a system in a single iteration is the number of active users times the number of time steps. Additionally, *Maximum Capacity* of an architecture is defined as the number of users that drives the respective architecture to its saturation point. Beyond the maximum capacity, the architecture continues to re-key each user at each time step. The per-user average re-keying will remain constant, roughly equal to the number of Time Steps (dependent on the average Duration for the users). The Total Keys Distributed, however, will continue to increase as the number of users increases.

In this scenario, the Baseline architecture reached the “saturation” level near iteration 250 for the 10% RoM, the iteration 425 for the 25% RoM, and near iteration 608 for the 75% RoM. The saturation was driven by the increased movement coupled by the user joins and leaves. This can be seen in Figure 41 by the increased average user re-keys in iterations with lower cluster densities (i.e., the left side of section (d) is much higher than the corresponding left side of sections (a) and (b)).

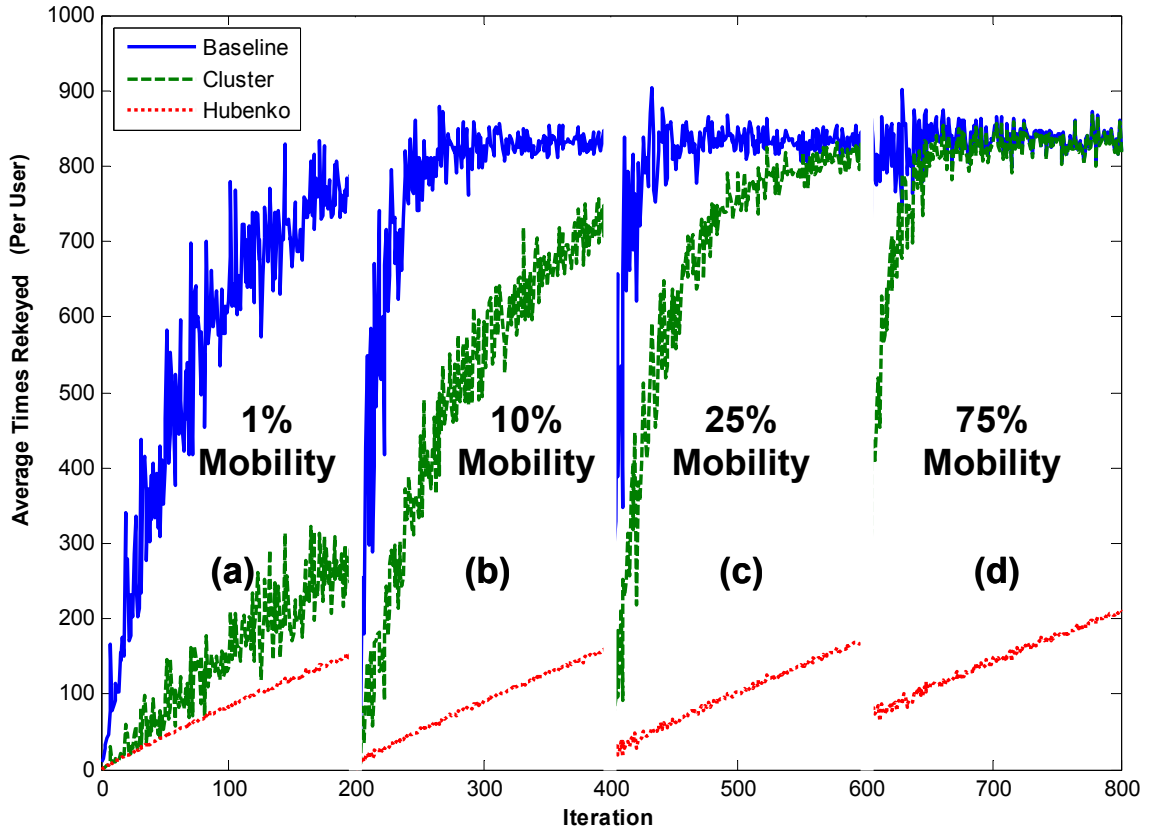


Figure 41 - Average Times Each User is Re-Keyed (from 10 to 2000 Users, 2000 Time Steps, Highly Mobile User Environment Scenario)

The Cluster architecture approached the saturation level at a slower rate due to the reduced size of impacted users in each cluster affected by the increased mobility. However, by approximately iteration 50 (iteration 650 overall) of the 75% RoM set, the Cluster architecture was also saturated, due mostly by the frequent user movement into

and out of the clusters. This means that the Cluster system reaches maximum capacity with only five hundred active users. Meanwhile, in the final iteration (iteration 800), the Hubenko system was operating at approximately 22% capacity with four times as many users. The values in the final iteration of the 75% RoM are: 2,000 Users, 137 Average Hubenko Keys, and 825 Average Cluster Keys. Extrapolating this performance (shown in Equation 3), an estimate of approximately 12,000 users may be sufficient to saturate the Hubenko Architecture. This is a 650% performance increase given a highly mobile user environment.

$$\frac{2000Users}{137AverageKeys} = \frac{xUsers}{825AverageKeys} \quad (3)$$

Had the Cluster and Baseline systems not saturated due to the MatLab simulation code limitations, the Hubenko Architecture improvement likely would have been demonstrated to be considerably larger. In an attempt to demonstrate this improvement, sensitivity analysis was performed. The size of the system (e.g., number of clusters) was increased to reduce the overall cluster densities. However, as the density was reduced, the Hubenko Architecture once again performed better. As the number of users was increased, the Cluster architecture saturated again. The cycle of increasing the number of clusters to reduce the amount of Cluster re-keying, followed by increasing the overall cluster densities was repeated until the maximum number of Matlab elements was attained. At this point (35,494 users, 5,000 clusters) the Hubenko Architecture could still not be saturated.

Recall the transitions from last iteration of a RoM set to the first of the next RoM set (e.g., 200 to 201) is seen as a sharp drop. This apparent transition is an artifact of the

MatLab graphical process of plotting the lines as continuous functions, and not allowing breaks between sets.

Confidence Intervals are not plotted in the scenarios that have several hundred iterations due to visual cluttering. Confidence Intervals are plotted in scenarios that contain 10,000 users and were executed with only thirty or so iterations because they were more visually reasonable.

The overall performance improvements can also be seen in total number of keys distributed in each system, shown in Figure 42. Again, the Baseline architecture approaches the saturation point quickly where the number of keys distributed is no longer affected by movement since the joins and leaves are enough to cause the frequent re-keying of the system. With increased movement in the 2,000 user iterations, the Cluster architecture suffers an order of magnitude more re-keying than the Hubenko Architecture.

Note that the Hubenko Architecture has a slow growth in the total number of keys distributed. This growth is due to the high number of users that are individually keyed as they move into new clusters. With large numbers of mobile users, the issuance of single keys begins to add up to a significant amount. This, of course, is still a much slower growth of total system keys than that experienced in either the Baseline or Cluster architectures.

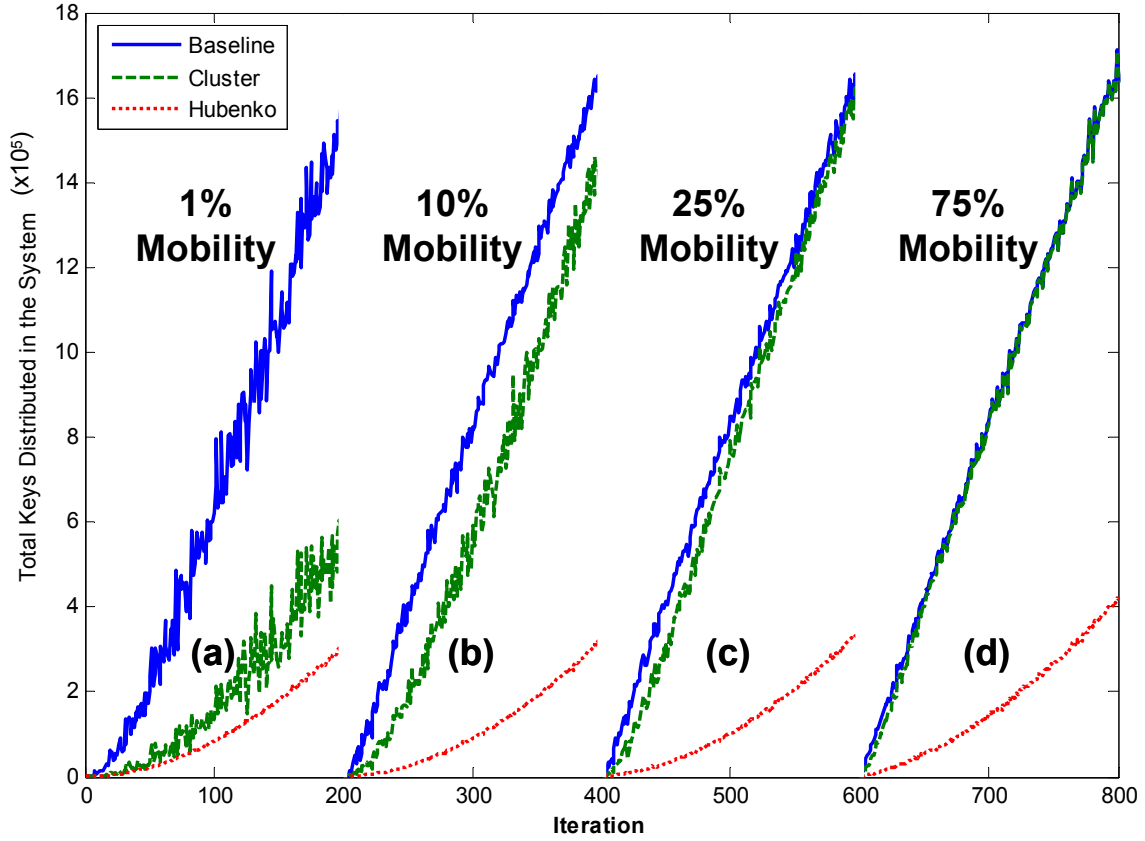


Figure 42 - Total Keys Distributed in Each Architecture (from 10 to 2000 Users, 2000 Time Steps, Highly Mobile User Environment Scenario)

As seen in Figure 42, section (a), with only 1% mobility, the Hubenko Architecture issues approximately 300,000 keys in iteration 200. Since there is little movement (i.e., 1%), the vast majority of the keys are issued due to the join or leave of users in each of the clusters, and not from movement. Since the join and leave distribution are statistically the same across all iterations, the iteration 800 of Figure 42, section (d), with 75% mobility, would also have approximately 300,000 keys issued in the Hubenko Architecture due to joins and leaves. Therefore, the additional 100,000 keys (for a total of 400,000 Hubenko Architecture keys) are due to individual key updates to mobile users as the mobile users travel to new clusters. Comparing the same iterations of

the Cluster Architecture, there were 500,000 keys issued in iteration 200, and 1.6 million keys issued in iteration 800. The difference due to the increased mobility is 1.1 million more Cluster Architecture keys. The Hubenko Architecture, therefore, has a ten-fold improvement over the Cluster architecture with the same user joins, leave, and mobility.

4.2.2 Short versus Long Duration

The next simulation modeled two scenarios that also had a single satellite with ten spot beams, each spot beam representing a different cluster. Using Total Keys Distributed and Per-User Average Re-keying as the figures of merit for comparison, the two scenarios demonstrate the performance improvements offered by the Hubenko Architecture with varying user duration characteristics. The first scenario modeled a Rate of Mobility (RoM) of 1%, and the second scenario modeled a RoM of 50%. The 1% RoM is the low mobility environment, and 50% RoM is the high mobility environment. The focus of this investigation is the impact of changing the Duration factor of the mobile users rather than increasing the Rate of Mobility. The longer the users persist, the larger the number of re-keys is expected.

Due the length of time to accomplish each experiment, a full factorial design was not used in all scenarios. However, a full factorial design was used for the analysis of variance to investigate interactions.

To investigate the impact a few aircraft flying over numerous terrestrial users have on re-keying, a “Control Group” of users is set aside in each scenario. The users in the control group were assigned: a Join Time of one (became active in the first time step); a Duration equal to the number of Time Steps that kept the users active until the last time

step; and a Mobility category of Stationary. The size of the control group varied across the scenarios, as noted below. During the course of the simulations, the metrics were tracked for all users combined, as well as for just the control group users.

For the first scenario, the number of users increase from as low as ten users in the system, to as high as one thousand. With ten clusters in the system, there is a maximum average cluster density of 100 users per cluster in the 1000 user case. In this case, increasing the user density beyond this number saturates the system for the Cluster architecture.

The first scenario models a user population with 1% overall mobility. The control group size was held constant at 50% of the total user population. In this scenario, the Stationary mobility category was used to model the ground troop component of a deployed contingency, and not a stationary infrastructure. With respect to fast-moving vehicles and aircraft, troops appear stationary. The value of 50% of the population allows the non-control group users to generate significant movement, and therefore mimic real-life situations where aircraft and vehicles are continuously moving throughout a theater of operations. This scenario ran for two hundred iterations. During each iteration, the user assignments remained constant for all three architectures. For each successive iteration, the user population received an entirely new set of uniformly distributed assignments. In the first one hundred iterations, the number of users increased from ten users to one thousand users in steps of ten. In addition, each user's Duration was set to a relatively "Short" period of time (approximately 20% of the total simulation time). Within the second set of one hundred iterations, the number of users was reset to

begin at ten users again, and continue to one thousand in increments of ten users per successive iteration. The user Durations for this second set of iterations were set to relatively “Long” periods of time (approximately 80% of the total simulation time). During the early stages of development, a sensitivity analysis was performed to investigate the trends produced by varying the Duration length. The results indicated no significant knees in the curve, and therefore the values of 20% and 80% were chosen using sound engineering judgment as logical breakpoints to define “Short” and “Long,” respectively. Table 6 summarizes the parameters for this scenario. The two distinct sets of iterations can be seen in Figure 43, with the Short Durations on the left (Iterations 1 through 100), and the Long Durations on the right (Iterations 101 through 200). Iteration 1 has ten users, iteration one hundred has one thousand users. Similarly, iteration one hundred one has ten users, and iteration two hundred has one thousand users.

Table 6 - First Short vs. Long Duration Scenario Parameters

Satellites	1
Clusters	10
Maximum Users	1000
Time Steps	1000
Rates of Mobility (%)	1
Features	Short Duration=20%*TimeSteps Long Duration=80%*TimeSteps Control Group = 50%

Figure 43 shows the total number of keys distributed to all users in each of the architectures. Clustering provided about a half order of magnitude reduction in total keys distributed within the Cluster and Hubenko Architectures over the Baseline architecture. With relatively little movement between clusters, the Hubenko Architecture’s use of the Group Access Control Awareness subsystem provided a statistically insignificant benefit

over the Cluster architecture in the Short Duration iterations. The benefits of the GACA subsystem emerged in the Long Duration iterations where there was slightly more movement due to users being active long enough to make a slight impact. One percent mobility was not sufficient to saturate the Baseline architecture with re-keying activity since there is less than $(\text{number of users}) \times (\text{one thousand time steps})$ total keys distributed in each iteration.

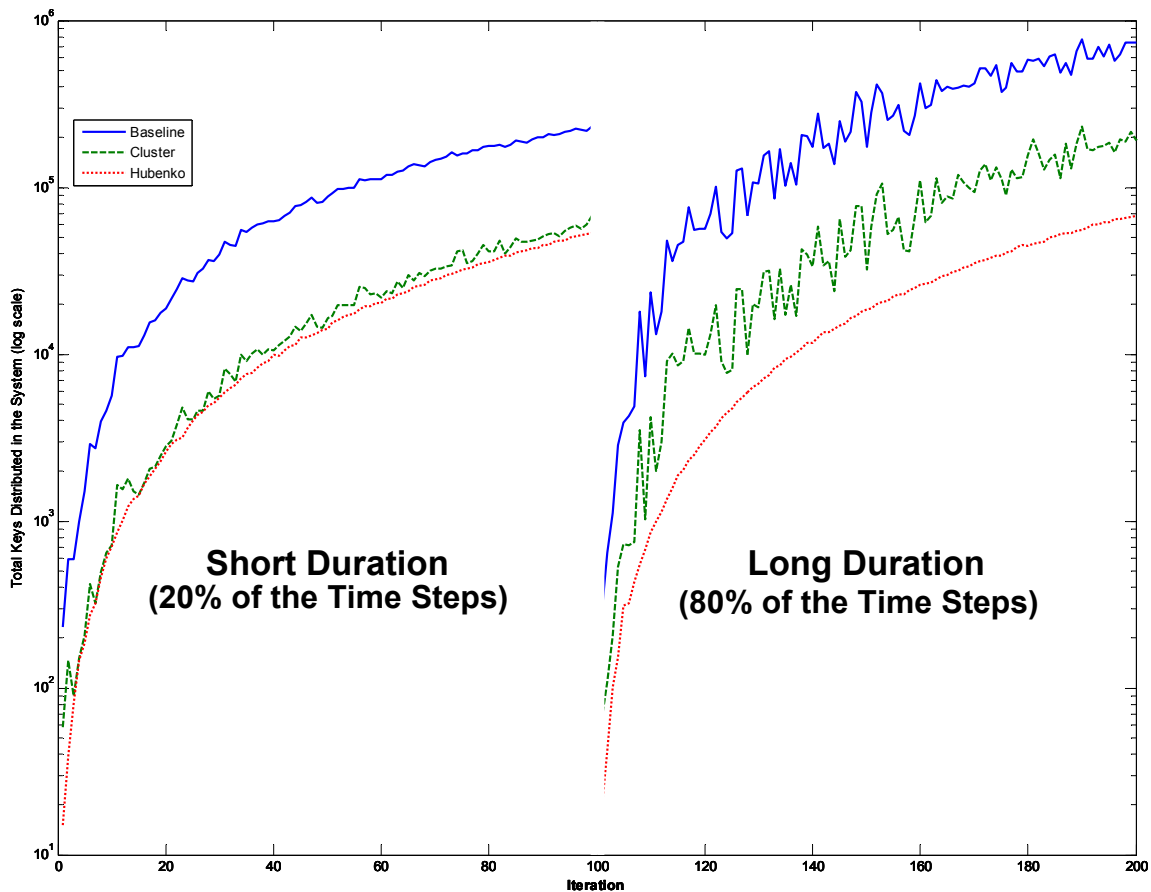


Figure 43 - Total Keys Distributed - 1% Mobility (from 10 to 1000 Users, 1000 Time Steps, Short versus Long Duration Scenario 1)

The three data lines on the left side of Figure 43 (iterations 1 through 100, “Short Duration”) are relatively smooth since at most only 1% of the users were mobile, and they were active for only a short time. This limited the overall mobility and therefore

variability across the iterations. The lines on the right side (iterations 101 through 200, “Long Duration”) fluctuated more due to increased variability in the mobility between iterations. The mobile users were not only active for longer periods of time, but the speeds at which they moved between clusters varied based on the mobility category. Therefore, if one iteration had five ground or sea users and only one aircraft, it would have fewer movement triggers than an iteration with five aircraft users.

For the second Short versus Long Duration scenario, the number of users was increased to 10,000, the number of time steps was increased to 10,000, and the Rate of Mobility was increased to 50%. The control group size was held constant at 50% of the total user population like the previous scenario. Therefore, the remaining 50% of the users were randomly assigned to the three mobility categories. Table 7 summarizes the parameters for this scenario.

Table 7 - Second Short vs. Long Duration Scenario Parameters

Satellites	1
Clusters	10
Maximum Users	10,000
Time Steps	10,000
Rates of Mobility (%)	50
Features	Short Duration=20%*TimeSteps Long Duration=80%*TimeSteps Control Group = 50%

The performance of the Cluster architecture thus far was following a trend of saturating long before the Hubenko Architecture. In Figure 44, for example, with one thousand users maximum simulated over one thousand time steps, with a 50% RoM. Even with a relatively small user population, the Cluster architecture approaches saturation, while the Hubenko Architecture performs at approximately one-ninth

capacity. Therefore, increasing the number of users and time steps will determine the Hubenko performance under stress.

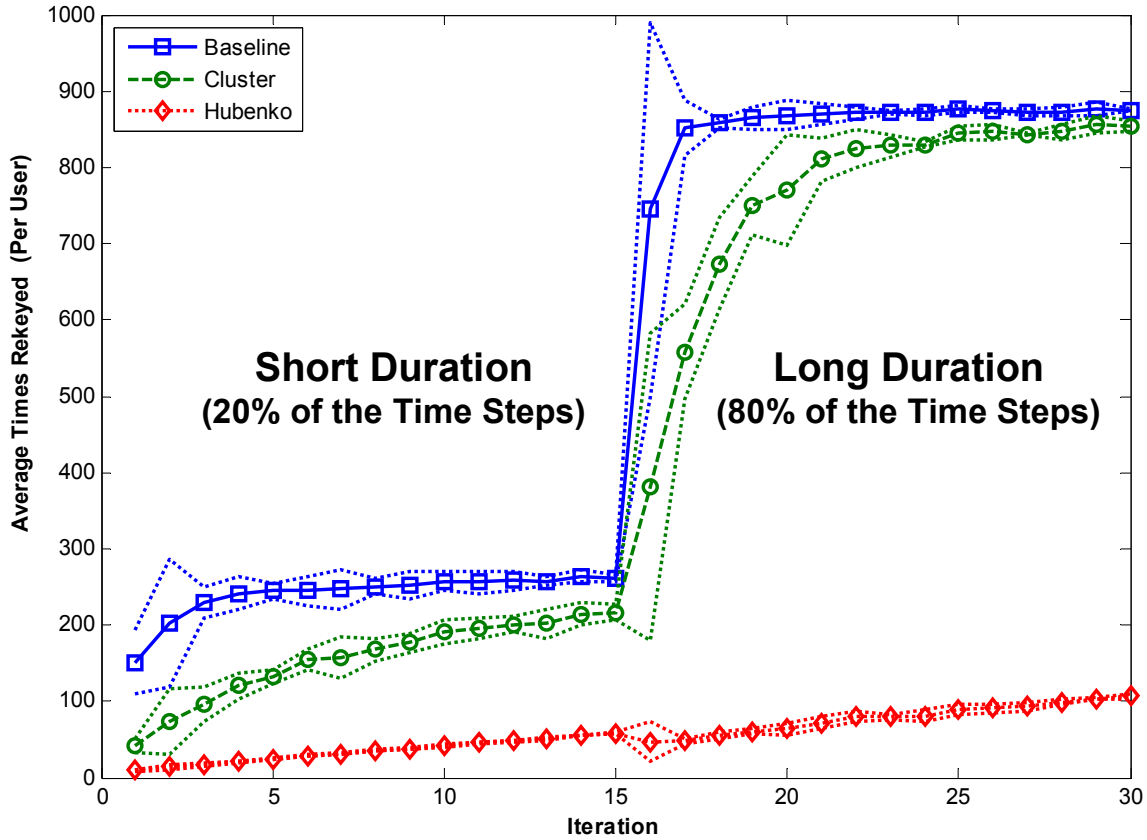


Figure 44 - Average Per-User Re-Key - 50% Mobility (from 10 to 1000 Users, 1000 Time Steps, Short versus Long Duration Scenario 1)

The apparent step increase that occurs in Iterations 16 through 30 is due to the increased length of time a mobile user remains active. On average, they remain active four times longer in the Long Duration than the Short Duration. Correspondingly, the average re-keying experienced per user also increases an average of four times as compared to the respective Short Duration iteration (e.g., Iterations 5 and 20 have the same number of users).

Note the difference in the plots between Figure 43 and Figure 44. In preparation for simulating a much larger user population for a much larger number of time steps, the number of iterations is decreased (from 200 in Scenario 1 to 30 in Scenario 2). The decrease was necessary to allow the simulations to complete in a reasonable amount of time (measured in weeks). The decrease in step resolution, however, still produced sufficient data points to analyze the trends and detect significant changes. Based on the results from previous scenarios, the trends had only minor variations due to random distributions as the population size grew. Little certainty, if any, is lost by the decrease in granularity. Along with the increased user population and increased time steps, the number of replications was increased from one simulation to three. Running three replications of the 10,000 user simulations resulted in non-overlapping bounds at a 95% confidence interval (illustrated as dotted lines of the same color surrounding the main plot lines of interest). The scenarios with 2,000 or less users required a sample size of five for non-overlapping confidence interval bounds, and therefore resulted in statistically different performance for the different architectures. In the scenarios with 10,000 mobile users, three replications generally yielded Coefficients of Variance of less than 0.1%.

Figure 45 demonstrates that the Short Duration iterations still do not have enough event activity to saturate the Baseline architecture which is operating at only about one-third capacity. However, the Long Duration iterations approach the maximum possible total keys distributed (approximately 8,700 out of 10,000 possible). With increased mobility, the Cluster architecture shows significant increases in total keys distributed for both the Short and Long Durations from the 1% mobility scenario. Despite the benefits

of the smaller clusters limiting the impact of local joins and leaves, the Cluster architecture also approaches the saturation point in the Long Duration iterations. This occurs due to the frequent movement of the users throughout the simulation. Despite the increased movement, the performance of the Hubenko Architecture remains nearly stable in this scenario, as it did in the 1% mobility scenario. The main reason for this stability is due to the GACA subsystem tracking users as they move between clusters. If users are able to maintain their credentials and meet the requirements for being able to transfer between clusters, the GACA subsystem issues the moving users keys without re-keying the entire old and new clusters.

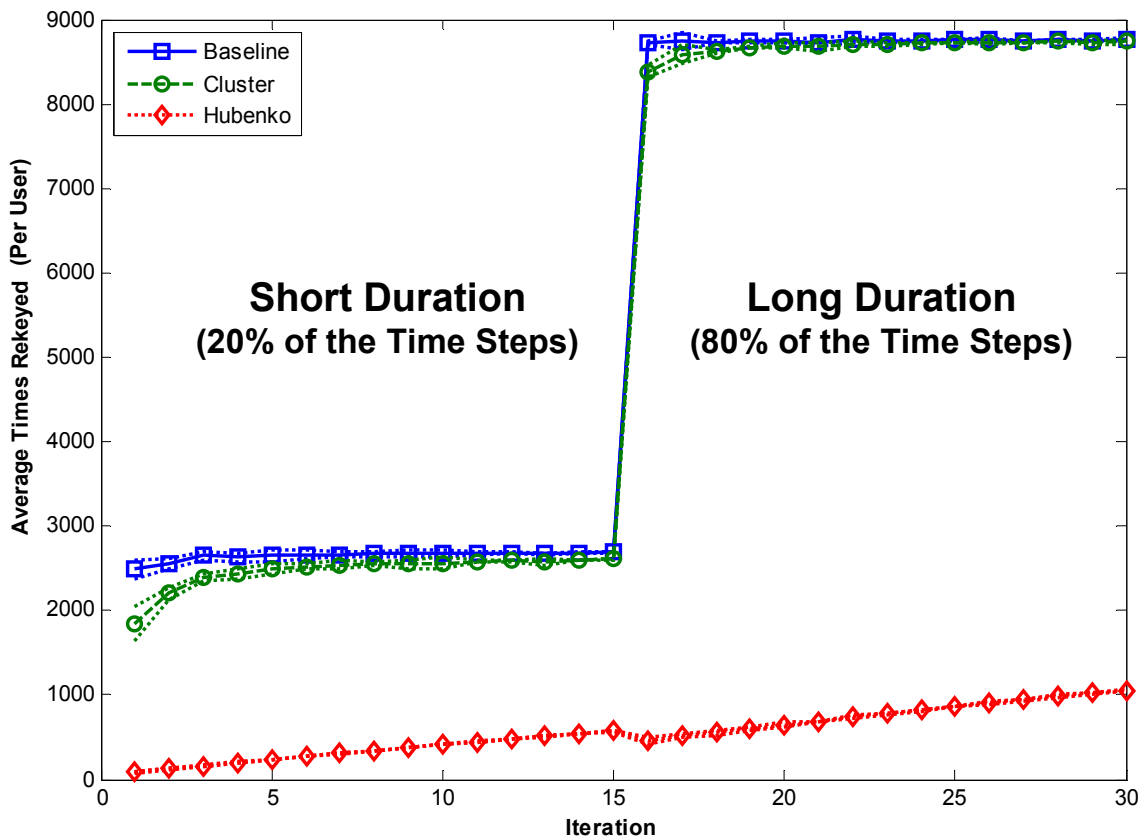


Figure 45 - Average Per-User Re-Key - 50% Mobility (from 10 to 10,000 Users, 10,000 Time Steps, Short versus Long Duration Scenario 2)

The Total Keys Distributed count in Figure 46 demonstrates nearly an order of magnitude fewer keys distributed between the Hubenko Architecture and the Baseline and Cluster architectures at Iteration 30. Figure 46 shows all of the keys distributed for each of the architectures in the second Short versus Long Duration scenario. The results for the Cluster and Baseline key counts are statistically equivalent due to their overlapping confidence interval bounds. The Hubenko Architecture, however, distributes almost 80 million less keys to all users in the same span of time.

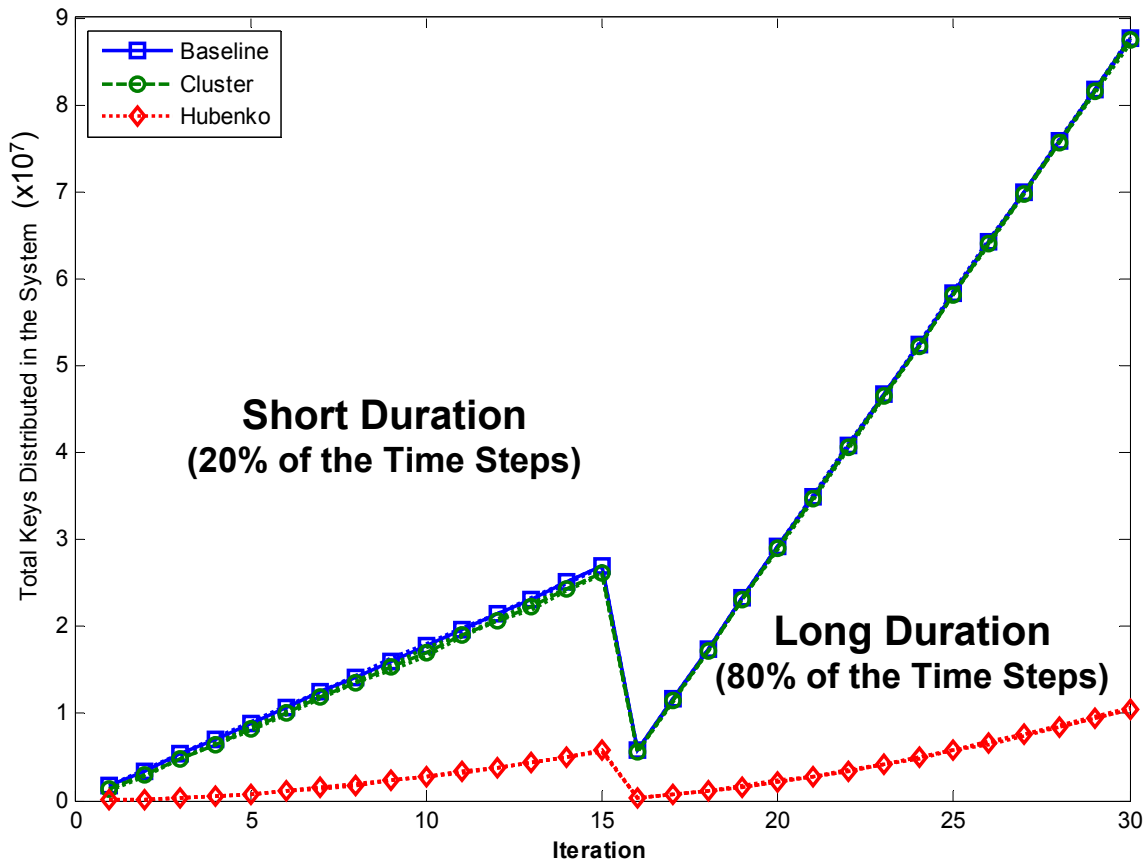


Figure 46 - Total Keys Distributed - All Users (from 10 to 10,000 Users, 10,000 Time Steps, Short versus Long Duration Scenario 2)

Figure 47 shows the number of keys distributed to the Control Group (50% of the user population). Since the Control Group persists for the entire simulation while the

mobile users leave after 20% or 80% of the available time, the Control Group would have, on average, more keys distributed to them than the mobile, non-control users.

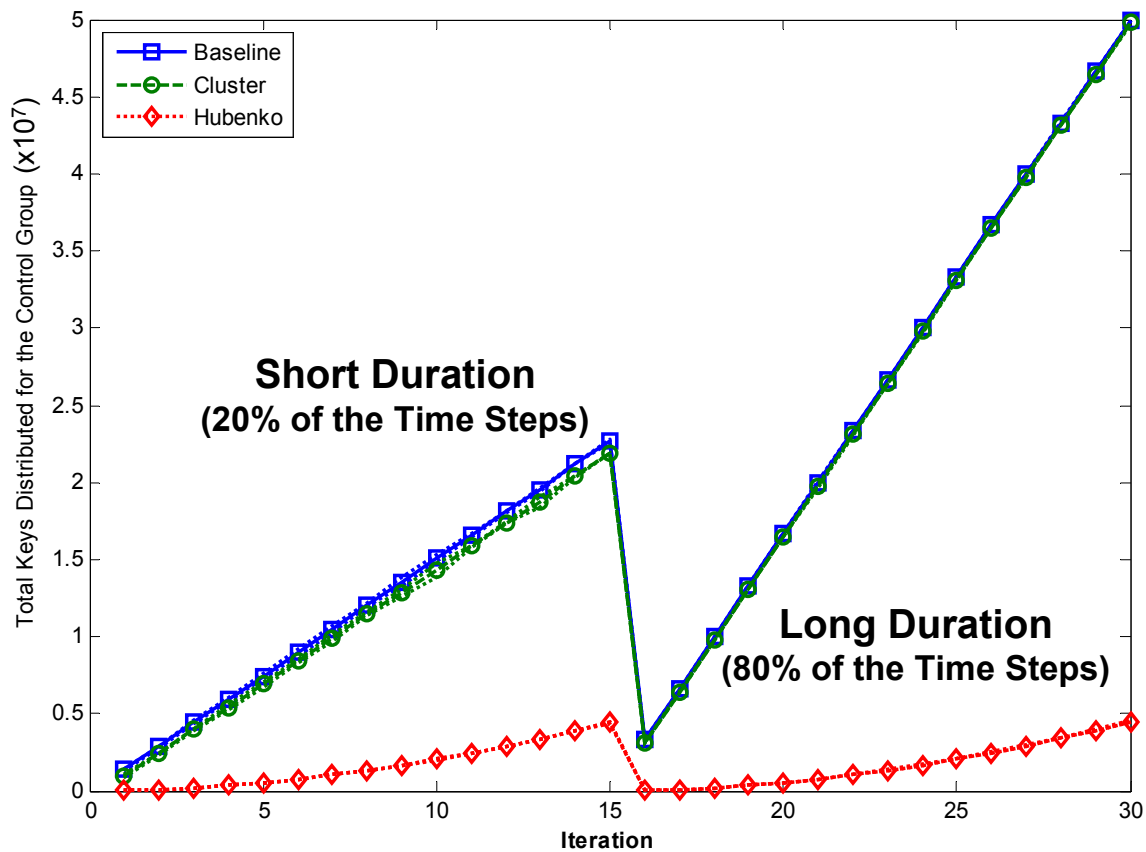


Figure 47 - Total Keys Distributed - Control Group (from 10 to 10,000 Users, 10,000 Time Steps, Short versus Long Duration Scenario 2)

While this is true with the Baseline and Cluster cases, the Hubenko Control Group actually has slightly less keys on average due to the mobile users getting new keys each time they move from cluster to cluster. For example, the Control Group of users in the Hubenko Architecture received approximately 4.4 million keys during the entire final iteration. The total number of users acquired slightly more than 10 million keys. Therefore, the mobile users account for the 5.6 million remaining keys, with approximately 1 million keys issued due to movement between clusters. The Baseline

and Cluster architectures, on the other hand, have 50 million keys issued to the Control Groups, but only about 37 million keys issued to the mobile users. Therefore, implementing the Hubenko Architecture reduces the re-keying burden on the Control Group as well as reducing the overall re-keying for the system. This reduced re-keying overall enhances scalability and increases the efficiency of the system.

4.2.3 *Increasing Aircraft over Stationary Users*

This set of scenarios determines any reduction in re-keying for terrestrial-based users provided by the Hubenko Architecture in a highly mobile environment. A *Highly Mobile Environment* is a group of users in a network that collectively change satellite spot beams often. These scenarios simulated a large population of terrestrial users with several aircraft flying overhead, continuously moving between the clusters. The control group size was held constant at 85% of the total user population, and their Duration lasts for the entire number of time steps. The Control Group's Mobility Category is Stationary Users. The Duration for the remaining 15% of users is at Long (up to 80% of the total possible time steps). Six iteration sets were run with increasing overall average mobility as follows: 1%, 3%, 5%, 7%, 10%, and 15%. If a user is mobile, its mobility category is set to Aircraft. The first scenario was run with 1,000 users for 1,000 time steps to observe the behavior of the Cluster architecture in addition to the Hubenko Architecture. Table 8 summarizes the scenario parameters. The sample size of five replications prevents significant overlap in the confidence interval bounds of the three architectures under the lower RoM. The second scenario was run with 10,000 users and 5,000 time steps to demonstrate the performance of the Hubenko Architecture in a heavily populated

environment. Due to the significantly larger number of users and time steps, three replications were sufficient.

Table 8 - Increasing Aircraft Parameters - Scenario 1

Satellites	1
Clusters	10
Maximum Users	1,000
Time Steps	1,000
Rates of Mobility (%)	1, 3, 5, 7, 10, 15
Features	Control Group = 85% Mobile User Duration = Long

Observing the per-user average re-keying for all of the users in Figure 48, the Baseline architecture quickly saturates in all but the first iteration set (1% mobility). The Cluster architecture shows modest improvement under low mobility. By 7% mobility, clustering alone is insufficient to prevent re-keying saturation. The Hubenko Architecture provides the most stable operation in the heavily mobile environment, with approximately one and a half orders of magnitude less average user re-keying. The slow growth in the average number of re-keys in the respective iterations across the iteration sets was due to the increasing amount of movement in the mobile user population.

By comparison, Figure 49 shows that the results are nearly identical for the Control Group under all simulated RoM, as demonstrated by the same average re-keying per user for each of the different RoM. This is due to the randomization of the mobile users' joins and departures that, with a uniform distribution, appear constant over the course of numerous iterations. What is absent is the excessive re-keying caused by the frequent movement of the mobile users due to the GACA-GKM sub-system. The trend is similar for the Control Group results of the Total Keys Distributed, shown in Figure 51.

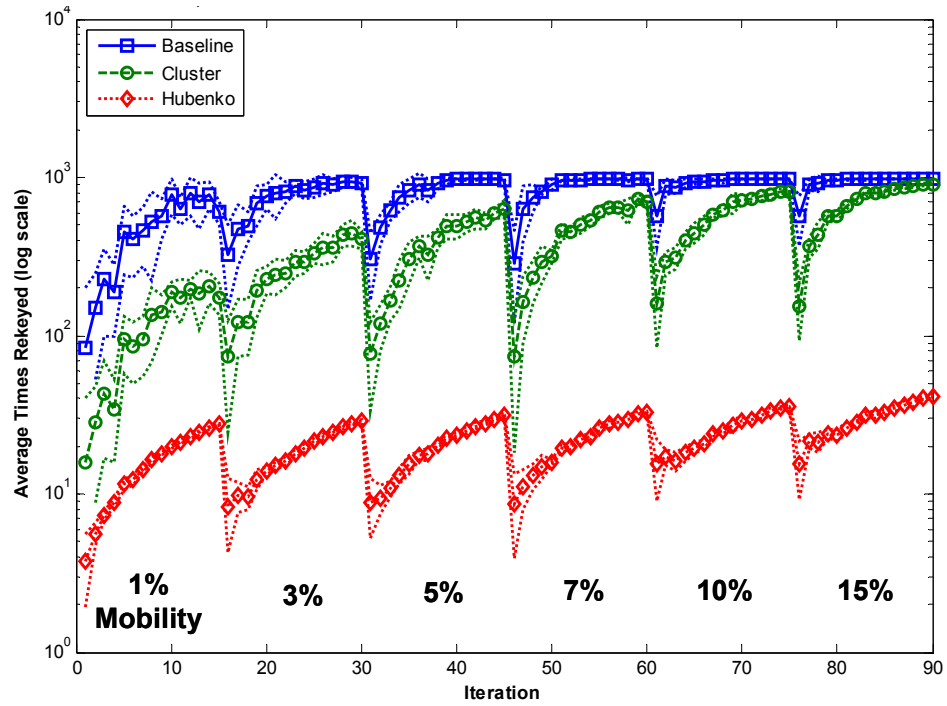


Figure 48 - Average Per-User Re-Key - All Users (from 10 to 1000 Users, 1000 Time Steps, Increasing Aircraft Scenario 1)

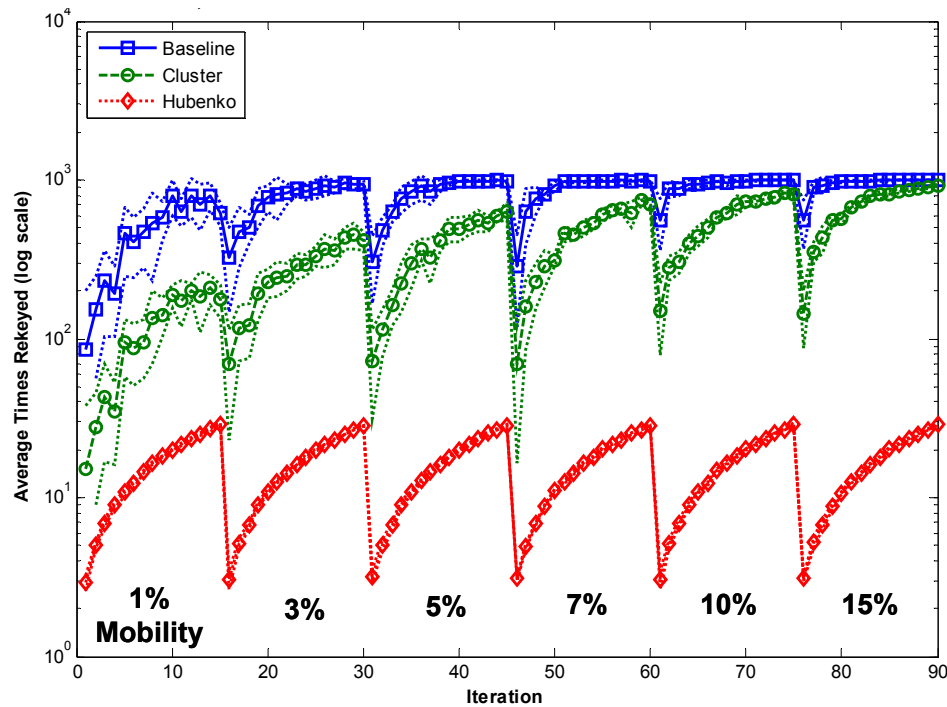


Figure 49 - Average Per-User Re-Key - Control Group (from 10 to 1000 Users, 1000 Time Steps, Increasing Aircraft Scenario 1)

Figure 50 shows the slight growth in the Total Keys Distributed for all users in the Hubenko Architecture, while the results are fairly constant across all RoM for the control group in Figure 51.

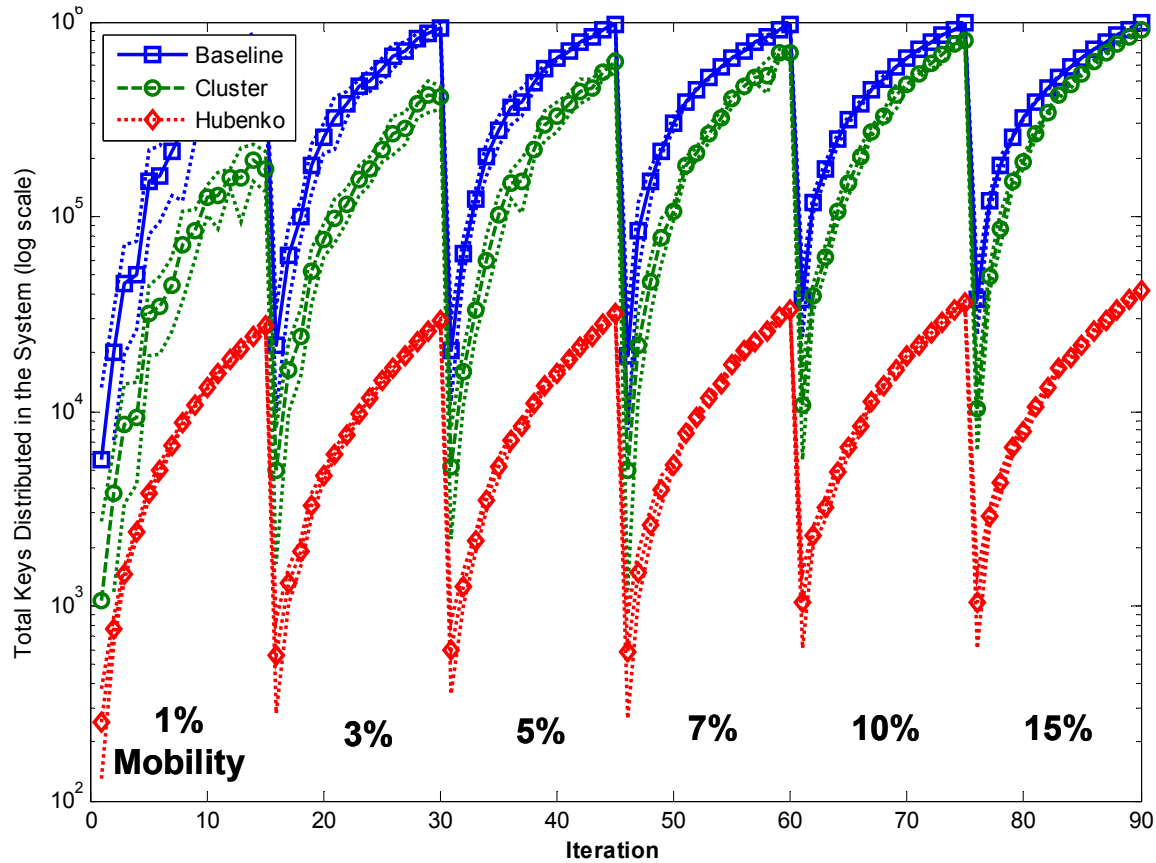


Figure 50 - Total Keys Distributed - All Users (from 10 to 1000 Users, 1000 Time Steps, Increasing Aircraft Scenario 1)

Increasing the RoM has virtually no effect on the stationary terrestrial user, which was the goal of the Hubenko Architecture. Due to the GACA-GKM subsystem, the large amount of stationary users (e.g., a brigade of Marines in a deployed AOR) does not need to re-key every time an aircraft flies overhead. The Hubenko Architecture effectively buffers the non- or slow-moving users from the impacts of the rapidly-moving user. In fact, the Control Group users could have been randomly assigned the Stationary, Sea, or

Ground Mobility Category instead of just Stationary, and the results would have been approximately the same. There would be little change with the exception of the additional keys incurred by the individual Control Group users moving from one cluster to another. The Air users flying overhead would not induce any additional re-keying on the non-stationary users, just as they induce no re-keying on the Stationary users (assuming those fast-moving aircraft have the proper credentials such that the GACA-GKM subsystem can transparently authenticate, validate, and authorize them into the new clusters).

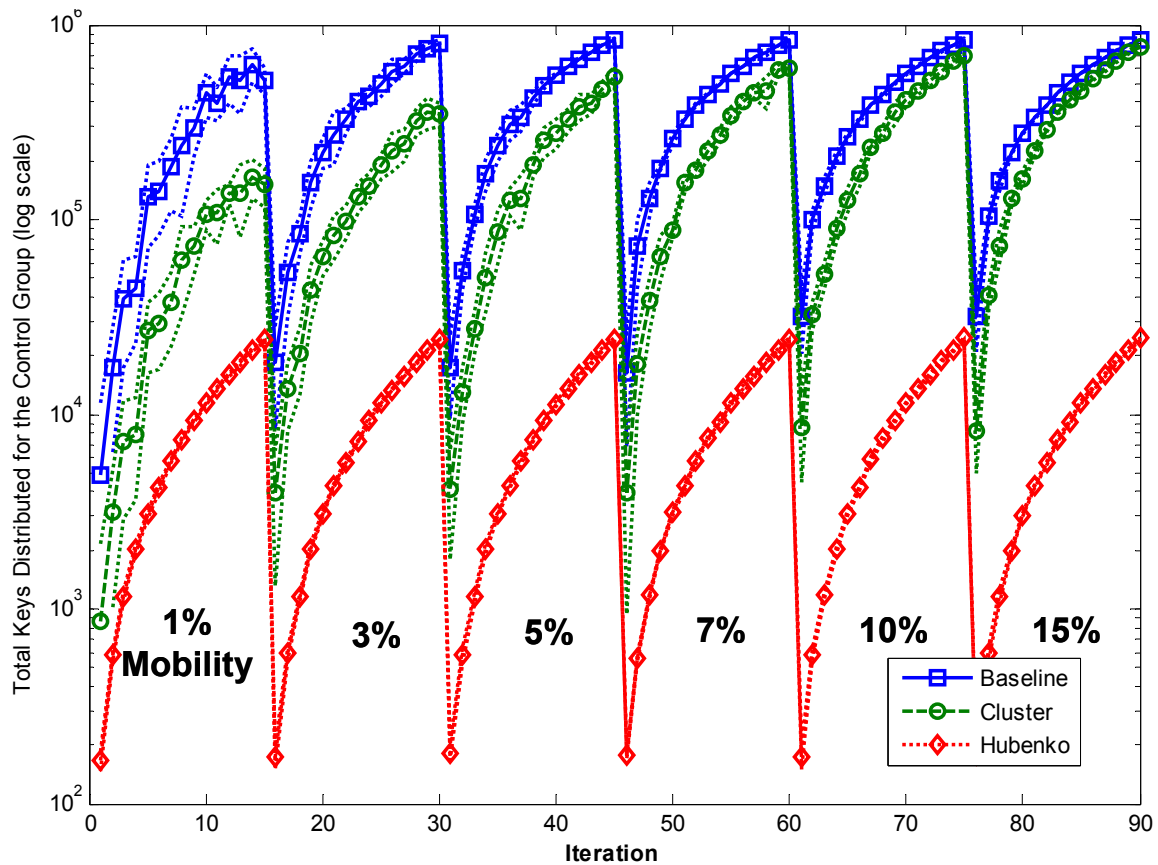


Figure 51 - Total Keys Distributed - Control Group (from 10 to 1000 Users, 1000 Time Steps, Increasing Aircraft Scenario 1)

The Baseline architecture is saturated, and therefore no change is observed with increased RoM. The Cluster architecture saturates on the higher number iterations within each iteration set (the ones with a higher number of active users), and increasingly approaches the saturation point in the iterations with lower RoM. The overall results indicate that if the system designers implemented the Hubenko Architecture, terrestrial-based users would experience reduced re-keying in environments where numerous aircraft are flying overhead. If the Hubenko Architecture were not employed, each over-flight would cause a re-key in the local cluster, thus increasing overhead and reducing system efficiency and scalability.

In an effort to analyze the Hubenko Architecture under a higher user loading level, Scenario 2 with 10,000 users for 5,000 time steps was executed. A sample size of three replications was sufficient to generate statistically different results for the Baseline and Cluster architectures, even for the 1% RoM. The parameters are summarized in Table 9.

Table 9 - Increasing Aircraft Parameters - Scenario 2

Satellites	1
Clusters	10
Maximum Users	10,000
Time Steps	5,000
Rates of Mobility (%)	1, 3, 5, 7, 10, 15
Features	Control Group = 85% Mobile User Duration = Long

As expected, the Cluster and Baseline architectures quickly saturate in the 3% RoM and beyond, while the Hubenko Architecture experiences linear growth in the Total

Keys Distributed, as shown in Figure 52. There is approximately 15% growth in the total number of keys distributed, which corresponds to the representative increase in mobility.

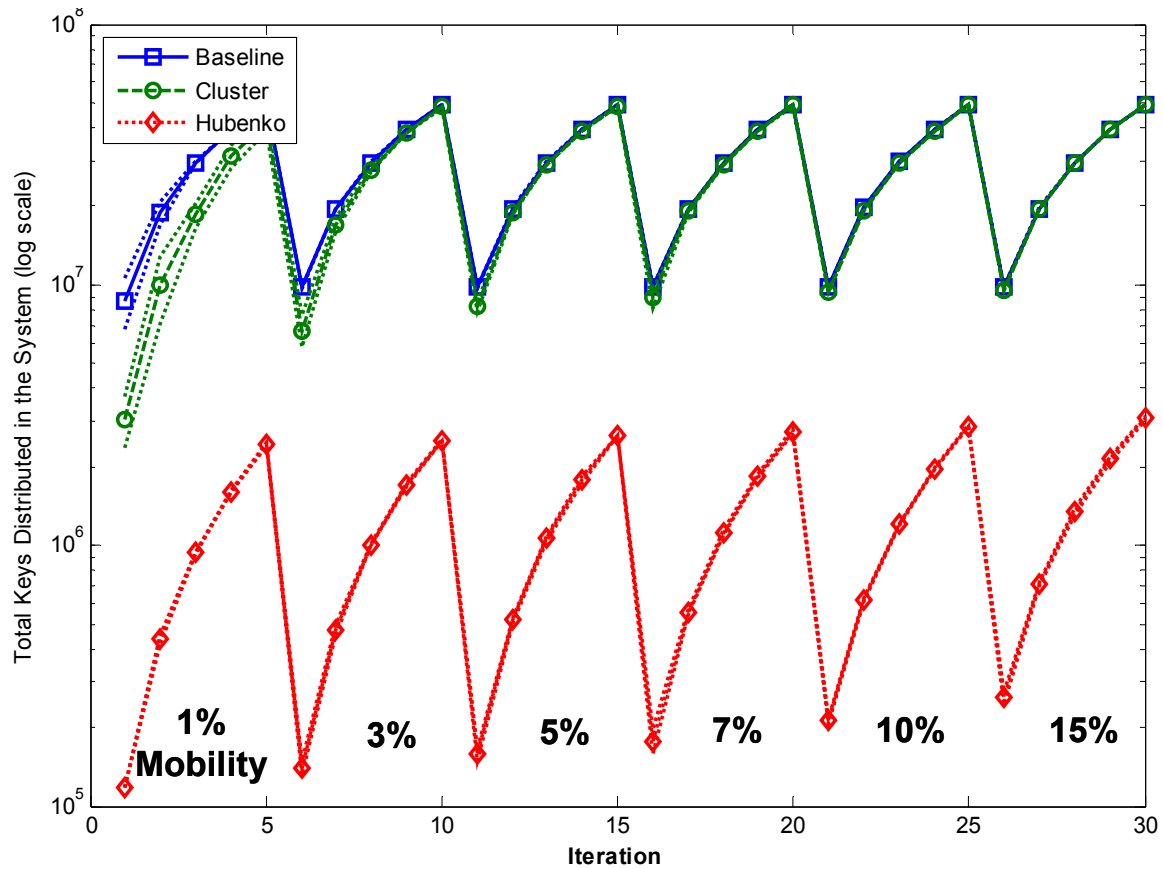


Figure 52 - Total Keys Distributed - All Users (from 10 to 10,000 Users, 10,000 Time Steps, Increasing Aircraft Scenario 2)

The average per-user re-keying displays similar performance in Figure 53, with the Cluster architecture operating within 2% of complete saturation, and the Baseline architecture re-keying during almost every single time step. On the other hand, the Hubenko Architecture utilized only approximately 6% of the total possible re-keying capacity operating under the exact same environmental conditions.

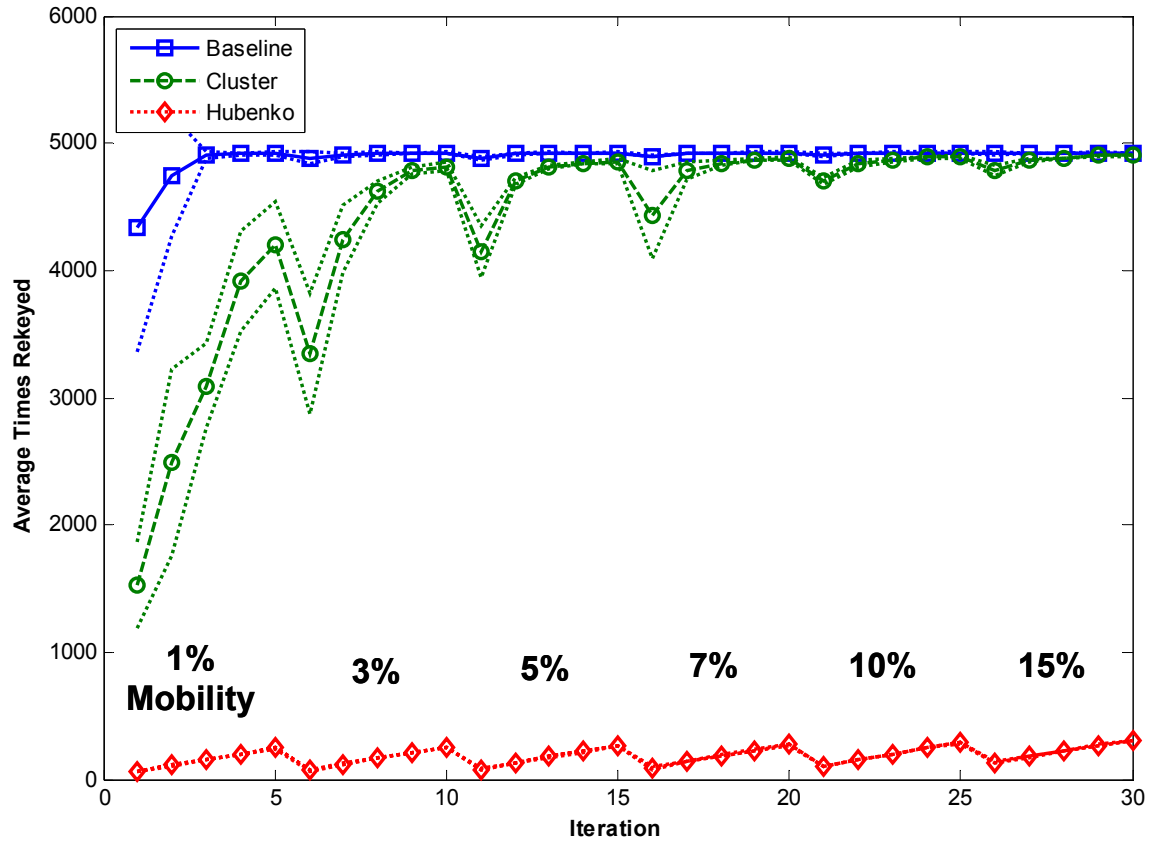


Figure 53 - Average Per-User Re-Key - All Users (from 10 to 10,000 Users, 10,000 Time Steps, Increasing Aircraft Scenario 2)

4.2.4 Varied Air Content Rate of Mobility

The final investigative experiment simulated five distinct RoM sets with the final RoM allocating 40% of the total user population to the Air mobility category. At the beginning of each iteration, the users were assigned a mobility category using the weighted uniform random distribution shown in Table 10. This weighting allows the growth in mobility to be controlled over the various RoM, thus allowing a comparison on the effects of the overall increase in movement on the system. These RoM distributions are hypothetical, and are meant to stress the system with an increasing amount of mobility and plot the results side by side for analysis.

Table 10 - Rates of Mobility (Varied Air Content)

Iteration	User Type Demographics
1 through 100	All Stationary
101 through 200	~1/2 Stationary, 1/2 Ground
201 through 300	~1/3 Stationary, Ground, Sea
301 through 400	~1/4 Stationary, Ground, Sea, Air
401 through 500	~1/5 Stationary, Ground, Sea; 2/5 Air

Within each RoM set, the user population is steadily increased from one through one hundred average users per cluster, for a total maximum user population of 2,000 users. Table 11 summarizes the scenario parameters. This scenario analyzes the Hubenko Architecture performance in a heavily mobile environment with increasing air assets. This scenario had the heaviest amount of mobility of all the modeled scenarios, with only 20% of the users stationary in the final RoM.

Table 11 - Varied Air Content RoM Parameters

Satellites	2	
Clusters	10	
Maximum Users	2000	
Time Steps	2000	
Rates of Mobility (%)	0, 50, 66, 75, 80	
Features	1 through 100	All Stationary
	101 through 200	~1/2 Stationary, 1/2 Ground
	201 through 300	~1/3 Stationary, Ground, Sea
	301 through 400	~1/4 Stationary, Ground, Sea, Air
	401 through 500	~1/5 Stationary, Ground, Sea; 2/5 Air

Since there is no movement in the first iteration set (iterations 1 through 100 in Figure 54), the GACA-GKM provides no additional benefit in the Hubenko system compared to the Clustered system. The steady growth in re-keying for all three architectures is due to the steady growth in overall number of active users in each system and their respective joins and leaves.

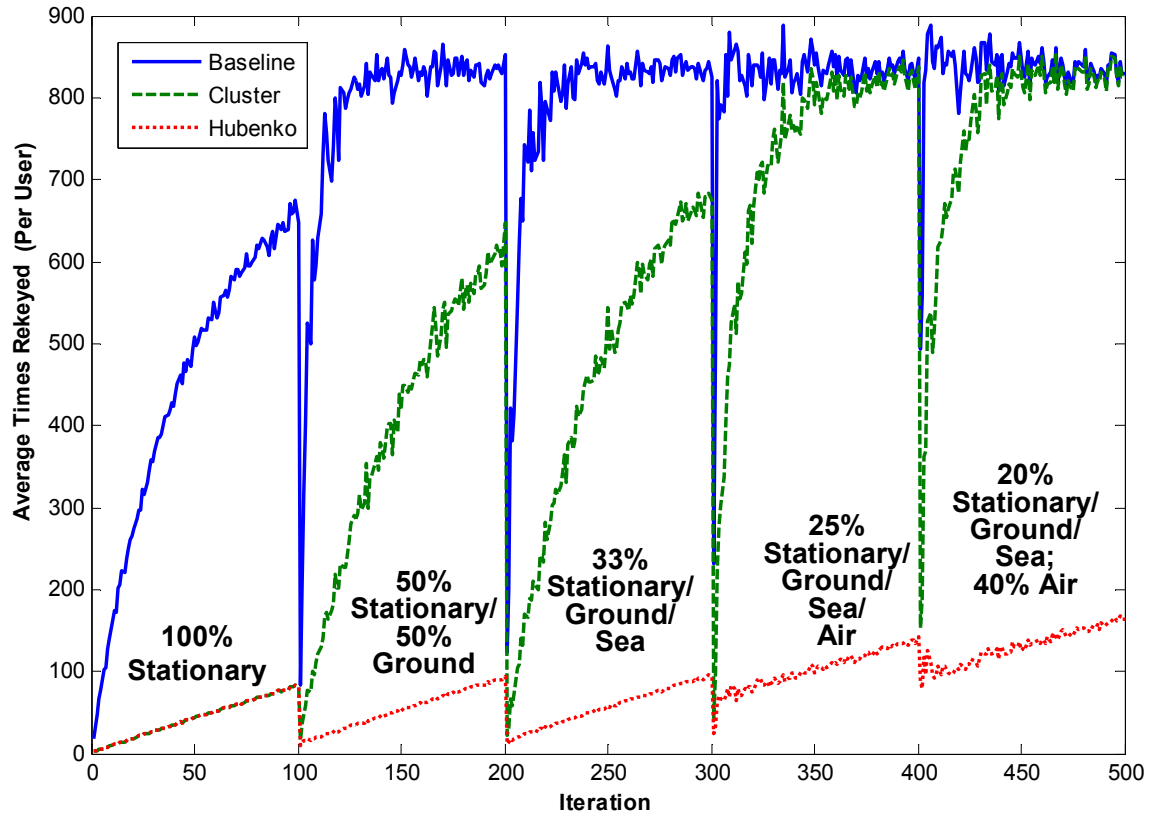


Figure 54 - Per-User Average Re-Key Results - All Users (from 10 to 2000 Users, 2000 Time Steps, Varied Air Content Scenario)

As mobility increases from left to right in Figure 54, so does the amount of average re-keying for the Baseline and Clustered architectures. The flat architecture reaches its maximum due to the numerous joins and leaves throughout the system as early as the 50% RoM with only the relatively slow moving Ground users. Beyond this level of mobility, the re-keying only gets worse if the system is not already saturated.

The Clustered architecture, while performing under the saturation level in the first three RoM, saturates in the 75% RoM. The Cluster architecture is able to avoid saturation in the 50% and 66% RoM sets because the movers were relatively slow (numerous time steps pass before the user moves to a new cluster). None of the mobile users was the Air category. Therefore, while the overall RoM for this scenario was the

same or higher than the scenario RoM in Sections 4.2.2 and 4.2.3, the speed at which the users changed clusters was considerably slower on average with no Air users. Correspondingly, the per-user average re-keying experience was lower in this scenario for the second and third RoM sets than in the previous scenarios. With the introduction of the Air category of users in the fourth RoM (iterations 301 through 400), the Cluster architecture once again saturates beyond an average cluster density of fifty users per cluster. The same is also true when the RoM increases to 80% and the allocation of Air users increases to 40%.

The Hubenko Architecture experiences a considerably smaller rate of increase in per-user average re-keying in the respective RoM sets, clearly demonstrating the combined benefits of the clustering and GACA-GKM features. Having a 50% mobile user population only increases average re-keying 10% over the all stationary case (iterations 1 through 100). This relatively small increase is due to the mobile users changing clusters rather slowly, since none of the mobile users were rapidly moving users. The 66% RoM has an increase of 15%; again a small increase due to the lack of Air users in the RoM allocation. Increasing the RoM to 75% with 25% of the total user population being allocated to the rapid moving user category (Air) increases the average re-keying by about 50%. Similarly, increasing the RoM to 80% with 40% of the total population becoming Air users increased the average re-keying by about 65% over the stationary case. While this performance compared to the Stationary RoM appears significantly impacted, comparing the Hubenko performance to the respective Cluster performance demonstrates an improvement in re-keying performance. The true

performance increase is masked by the Cluster architecture saturating under the given scenario parameters.

4.3 Performance Conclusions

Reducing the number of total keys distributed in each architecture to increase scalability was one focus for this research, while minimizing the re-keying impact (and hence increasing efficiency) for the individual terrestrial user was another.

4.3.1 Re-Keying Performance Results

First and foremost, regardless of the scenario, the Hubenko Architecture always performed better than either the Cluster or the Baseline architectures. Table 12 summarizes the average re-keying counts of the individual users in the different scenarios. The data is from the iteration of each scenario with the maximum number of users simulated.

Table 12 - Per-User Average Re-Keying Summary

Control Group Size	Rate of Mobility	Duration	Max # Users	Time Steps	Hubenko		Cluster		Baseline	
					All Users	Control Group	All Users	Control Group	All Users	Control Group
50%	1%	Short	1,000	1,000	55	89	63	102	230	382
		Long			68	90	190	216	738	841
	50%	Short	10,000	10,000	574	884	2,609	4,382	2,689	4,541
		Long			1,058	900	8,736	9,956	8,757	9,997
85%	1%	Long	10,000	5,000	244	259	4,206	4,248	4,921	4,994
	3%				254	259	4,818	4,876	4,926	4,999
	5%				264	260	4,859	4,921	4,924	4,997
	7%				274	260	4,883	4,949	4,925	4,998
	10%				288	259	4,897	4,964	4,927	4,999
	15%				309	257	4,906	4,976	4,926	4,999

For the first scenario with 1% RoM, there is an extremely low overall mobility. In the Short duration iterations, All Users averaged less individual re-keying than the Control Group because the non-control group was active for a relatively short time, and therefore only re-keyed a few times. Only active users re-key. The Control Group, on

the other hand, was always active and so gathered many more keys. Averaging the two groups together lowered the overall average number. There was very little change in the Long duration iterations since there was very little movement overall.

In the 50% RoM scenario, the Short duration again produced a lower average re-keying for All Users compared to the Control Group in the Hubenko Architecture for similar reasons to the 1% RoM scenario. However, the Long duration had significantly more movement for a longer period of time. Therefore, more keys were distributed, on average, to All Users as compared to the Control Group. This occurred because each individual mobile user would acquire a new key upon entry to a cluster (due to movement, not a new Join), whereas the Control Group was stationary and did not gain any more keys other than those which were assigned to the clusters as a whole (for a Join or a Leave). The mobile users in the same clusters also receive a new key as well, and therefore the net sum for that case is the same between the two groups. Comparing the Long to the Short durations for the 50% RoM, the All Users average doubles while the Control Group remains effectively the same. The difference between the two All Users statistics is due to the increased individual movement. The difference between the two Control Group statistics is due to the random distribution of Join and Leave times. The number of time steps (i.e., 10,000) gives sufficient range for the users to individually join and leave at different time steps. The difference of sixteen keys falls within the confidence interval bounds at a 95% confidence level, and therefore the two results are not different.

In the Increasing Aircraft scenario with the 85% Control Group size, extrapolating the results gives the crossover point to be about 4% Rate of Mobility for the Control Group and the All Users averages to be even, despite the 15/85 split in user population size. With more than 4% RoM, however, the All Users average is larger than the Control Group average due to the extra keys generated by the moving users. Compared to the other scenarios, similar trends are observed as the overall RoM increases: the Control Group averages remain statistically equivalent between RoM, and the All User average increases as the RoM increases.

In all scenarios, the Hubenko Control Group average re-keying count was virtually unaffected by increasing Rates of Mobility, which was the research goal of the Hubenko Architecture. In contrast, the Control Group averages doubled for both the Cluster and the Baseline architectures in the Short/Long scenarios. The number would have been larger for the Cluster and the Baseline counts had those systems not saturated.

Using the same scenarios as above, Table 13 summarizes the Total Keys Distributed for the three architectures. The first observation to note is that, unlike the averages in Table 12, the All Users entries are always higher than the corresponding Control Group entries. This is expected since the All Users value includes the key count for the Control Group. The difference between the All Users value and the Control Group value is the number of keys distributed to the mobile users in each of the simulations.

Table 13 - Total Keys Distributed Summary

Control Group Size	Rate of Mobility	Duration	Max # Users	Time Steps	Hubenko		Cluster		Baseline	
					All Users	Control Group	All Users	Control Group	All Users	Control Group
50%	1%	Short	1,000	1,000	54,698	44,428	62,980	50,960	230,019	191,000
		Long			67,523	44,883	189,988	108,249	737,977	420,500
	50%	Short	10,000	10,000	5,740,023	4,417,780	26,090,714	21,909,020	26,891,443	22,703,333
		Long			10,577,002	4,499,922	87,363,595	49,782,164	87,568,289	49,985,000
85%	1%	Long	10,000	5,000	2,444,874	2,200,596	42,055,851	36,107,938	49,214,102	42,449,000
	3%				2,536,541	2,200,724	48,179,126	41,450,189	49,257,760	42,488,667
	5%				2,638,523	2,206,712	48,593,570	41,831,655	49,244,917	42,471,667
	7%				2,742,361	2,208,028	48,830,033	42,069,857	49,251,433	42,485,833
	10%				2,877,280	2,201,124	48,965,305	42,190,781	49,268,474	42,491,500
	15%				3,087,913	2,185,256	49,057,807	42,293,289	49,257,078	42,491,500

In the 1% RoM scenario, with low mobility and short duration, the Hubenko Architecture All Users count has 25% growth over the Control Group count. Although 50% of the total users were active at some point during the iteration, they were only active for at most 20% of the total available number of Time Steps. This was not long enough either to allow the mobile users to generate significant cluster activity, or to collect numerous keys as they moved between clusters. Similarly, the key count for All Users in the Long duration does not increase significantly. While those mobile users were active for up to 80% of the total available time, the 1% mobility still limits the potential number of keys that could have been generated. Even with the limited mobility, the Hubenko Architecture collected one-third as many keys in the same iteration as the Cluster architecture, and one-tenth as many as the Baseline architecture. Therefore, the Hubenko Architecture begins to improve scalability and efficiency even with extremely low mobility.

In the 50% RoM scenario, the Hubenko Architecture's All Users key count experiences a 30% growth over the Control Group key count for the Short Duration iteration, and 135% growth for the Long Duration iteration. Comparing the same statistics for the Cluster and Baseline architectures, they both experienced only 18% key

growth for the Short Duration, and only 76% key growth for the Long Duration. The reason for the comparatively low percentage increases is that the two systems reached the saturation points, as discussed earlier, and therefore the counts ceased to increase. The efficiency and scalability benefits of the Hubenko Architecture are obvious when the total counts of the three systems are compared. The Hubenko Architecture produced four and a half times less keys overall for the Short Duration, and eight and a quarter times less keys for the Long Duration. Again, if the model's data element limitations could be lifted, these numbers would have been even better.

The Hubenko Architecture has modest growth as the RoM steadily increases from 1% to 15% in the "Increasing Aircraft" scenario. The growth is strictly due to the mobile users moving to new clusters and gathering new keys as they enter each new cluster (assuming, of course, the users are properly authorized to do so). The results are similar to the Per User Average Re-keying just discussed. With the exception of the 1% RoM, there is no further increase in total key count in either the Cluster or Baseline architecture for the increased RoM due to the saturation of those architectures.

Though the results were not tabularized, the performance in the "Varied Air Content" scenario also demonstrates the superior performance of the Hubenko Architecture, this time in an excessively (80%) mobile scenario. Even in the most mobile case simulated in that scenario, the Hubenko Architecture still did not double the amount of re-keying, while the Cluster and Baseline architectures saturated with the introduction of the Air users.

4.3.2 *Hubenko Saturation*

In all simulated scenarios, the Hubenko Architecture outperformed the Baseline and the Cluster architectures with fewer re-keys individually and at the system level. By observing the trend of increased re-keying with increasing numbers of users, one can predict that the Hubenko Architecture too will eventually saturate. Due to the two billion data element limit of MatLab, however, it was not possible to simulate a scenario with any appreciable length of time where the Hubenko Architecture saturates. This was because of the need for very large numbers of users (e.g., in the “Varied Air Content” scenario, beyond 50,000 users). At that point, though, there would no longer be any benefit to implementing either a Hubenko or a Clustered architecture. Therefore, in the case of an excessively saturated system, the simplest solution becomes the most efficient: re-key the entire system simultaneously on a pre-determined scheduled that meets the required security level. For any system loading less than this, however, the Hubenko Architecture is the superior choice for systems with highly mobile users.

4.3.3 *RoM Sensitivity*

From the validation simulation (Section 3.11) where all users were set to Stationary, and the 0% RoM iteration set in the Varied Air Content RoM scenario (Section 4.2.4), it is clear that without movement, the Hubenko Architecture provides no re-keying performance increase over the Cluster architecture. With the introduction of mobility come the scalability and efficiency benefits provided by the Hubenko Architecture.

In the Short versus Long Duration scenario with 1% RoM (Section 4.2.2), the Short Duration iteration set demonstrated statistically insignificant differences in the Cluster and Hubenko performances. This was due to the Short Duration parameter not allowing the mobile users to move between clusters often enough to impact the re-keying results. Keeping the RoM at 1% while increasing the Duration to Long yielded approximately a half order of magnitude performance increase for the Hubenko Architecture. Movement was not the only factor to influence the performance of the Hubenko Architecture. Increasing the length of time that users were active increased the amount of overall movement throughout the simulation led to the observation of the increased re-keying performance in the Hubenko Architecture. Therefore, overall movement is the main contributor to being able to discern the benefits of implementing the Hubenko Architecture.

The results of the other scenarios corroborate this conclusion. In all simulated scenarios, the more movement that occurred during the simulation, the better the Hubenko Architecture performed compared to the Baseline and Cluster architectures. The increase in movement could come from either an increase in the RoM (more users moving throughout the simulation period), or an increase in the length of time the moving users are allowed to move about, or the overall relative speeds at which the mobile users are allowed to move. Consider the case shown in Figure 54. Iterations 101 through 200 have 50% Stationary/50% Ground users, and iterations 201 through 300 having one third each Stationary, Ground, and Sea users. While the overall RoM for the sets are 50% and

66% respectively, the Cluster architecture did not saturate until the Air category was added (Iterations 301 through 400).

The driver to the above results was the overall “Mobility Content” of the RoM. Each time a user moves from one cluster to another is considered one move. *Mobility Content* is the overall expected average number of collective moves by the mobile users,

$$Mobility\ Content = \sum_{i=2}^4 \frac{TimeSteps \times AvgDuration \times NumberUsers_i}{Speed_i} \quad (4)$$

where i is the Mobility Category, and 2 equals Ground, 3 equals Sea, and 4 equals Air. The Stationary users do not contribute to the Mobility Content and therefore are not included in this calculation. The Speed of the user is the number of Time Steps that pass between successive moves. The lower the number, the faster the user is moving. The numbers were selected based on the descriptions of the Mobility Categories and their analogous physical world representations.

The Mobility Content for the final iteration of each RoM set for the Varied Air Content Scenario is shown in Table 14. The Average Duration for the mobile users was set at 50% of the Time Steps for all of the Rates of Mobility in this scenario.

Table 14 - Mobility Content for Varied Air Content Scenario

Average Mobile User Duration		50%	Rate of Mobility											Mobility Content
			Stationary		Ground			Sea			Air			
Users	Time Steps		Rate	Users	Rate	Users	Speed	Rate	Users	Speed	Rate	Users	Speed	
2000	2000		100%	2000	0%	0	20	0%	0	40	0%	0	5	0
			50%	1000	50%	1000		0%	0		0%	0		50000
			33%	667	33%	667		33%	667		0%	0		50000
			25%	500	25%	500		25%	500		25%	500		137500
			20%	400	20%	400		20%	400		40%	800		190000
2000	2000		60%	1200							40%	800	5	160000

Note the Mobility Content for the second and third sets (50% and 66% RoM) are equal despite the third RoM having 16% more active mobile users. The reason for the equivalent Mobility Content is the Sea users move more slowly, and therefore contribute less movement to the overall scenario as compared to the Ground users. One might then expect that the two RoM sets might produce equivalent re-keying statistics. This is not true. The latter RoM set, with 16% more users, induced approximately 15% more re-keying due to the additional joins and leaves of the extra users, shown again in Figure 55.

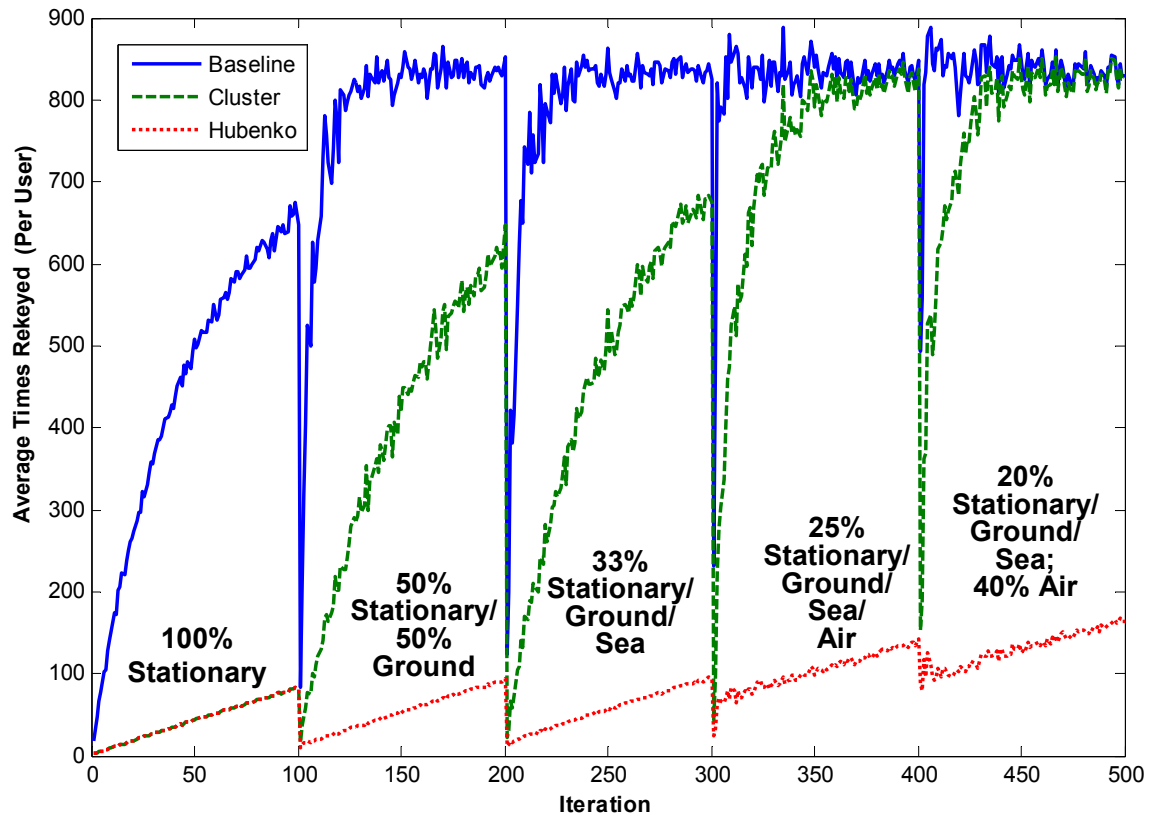


Figure 55 - Varied Air Content RoM Scenario Revisited (from 10 to 2000 Users, 2000 Time Steps)

Increasing the RoM by 9% with the inclusion of the Air users more than doubled the Mobility Content, and caused the Cluster Architecture to saturate while the Hubenko Architecture increased by 50% over the Stationary RoM set. To demonstrate that the

main contributor to the Cluster's saturation was the Air user, this scenario should have included a RoM with 40% Air users and the rest Stationary. The last row in Table 14 is the expected Mobility Content. The Cluster architecture would have saturated due to the more than tripling of Mobility Content as compared to the 50% Ground RoM iteration. Therefore, the main contributor to the increased re-keying is the Mobility Content of each Scenario.

4.4 Analysis of Variance

In general, experiments are used to study the performance of processes and systems. Experiments consist of several inputs, of which some variables are controllable, and others are not. These inputs are processed by the system, and a response is observed. To increase the fidelity of the system analysis, multiple replications of the same experiment can be processed, and the observations recorded and analyzed. One method of analyzing the data is through the Analysis of Variance, or ANOVA. This allows the complexities of the numerous observations to be divided into manageable groups with definable impacts on the system.

There are three main Factors that were controlled throughout the simulations: Duration, RoM, and Number of Users. In the ANOVA analysis that follows, the three factors each had three levels of input: Duration (0.2, 0.5, 0.8); RoM (25%, 50%, 75%); and Number of Users (200, 600, 1000). Alone, each Factor may have an effect, or Factors may combine through interactions.

In the following ANOVA tables, the observations are the total keys distributed for the Baseline, Cluster, and Hubenko architectures, respectively. The raw data collected is

listed in Table 30. For the first ANOVA table, the Duration was held constant at 20% of the available simulation time, giving the users a short period in which to interact. With the Join Time held at 10% to ensure all users would be active at some point during each simulation, having a Duration of 20% means all users will Join and Leave a multicast group during the simulation. Therefore, the Joins and Leaves had more of an impact than the amount of movement. Unfortunately, the amount of re-keying due to Joins and Leaves versus the amount of re-keying due to movement was not captured during the simulations, so there is no definite proof that this statement is true. However, observing the F-statistics and the P-values the Summary ANOVA table in Table 15, we see that the Number of Users in the Baseline architecture is a significant factor, while the RoM and the interaction of the RoM and Number of Users are not. A significant factor at the 95% confidence level is one having a P-value less than or equal to 0.05. For the Hubenko and Cluster Architectures, where the systems are less sensitive to motion, both the Number of Users and the RoM are significant factors, as well as their interactions.

Table 15 - ANOVA with Duration = 0.2

Baseline						
<i>Source of Variation</i>	<i>SS</i>	<i>df</i>	<i>MS</i>	<i>F</i>	<i>P-value</i>	<i>F crit</i>
Number of Users	4.16E+12	2	2.08E+12	318945.839	0.000	3.259
RoM	5.69E+06	2	2.84E+06	0.436	0.650	3.259
Interaction	6.80E+07	4	1.70E+07	2.609	0.052	2.634
Error	2.35E+08	36	6.51E+06			
Total	4.16E+12	44				

Cluster						
<i>Source of Variation</i>	<i>SS</i>	<i>df</i>	<i>MS</i>	<i>F</i>	<i>P-value</i>	<i>F crit</i>
Number of Users	4.46E+12	2	2.23E+12	35480.347	0.000	3.259
RoM	8.84E+09	2	4.42E+09	70.300	0.000	3.259
Interaction	1.66E+09	4	4.16E+08	6.617	0.000	2.634
Error	2.26E+09	36	6.29E+07			
Total	4.48E+12	44				

Hubenko						
<i>Source of Variation</i>	<i>SS</i>	<i>df</i>	<i>MS</i>	<i>F</i>	<i>P-value</i>	<i>F crit</i>
Number of Users	6.05E+10	2	3.02E+10	14129.994	0.000	3.259
RoM	1.92E+09	2	9.59E+08	448.136	0.000	3.259
Interaction	5.39E+08	4	1.35E+08	62.909	0.000	2.634
Error	7.71E+07	36	2.14E+06			
Total	6.30E+10	44				

Increasing the Duration to 50% of the available simulation time means that there was more time for the users to move about and interact, thus making the RoM more significant of a factor in the Baseline Architecture. However, the interaction between the Number of Users and the RoM was not significant in the Baseline and Cluster Architectures, as shown in Table 16.

Table 16 - ANOVA with Duration = 0.5

Baseline						
<i>Source of Variation</i>	<i>SS</i>	<i>df</i>	<i>MS</i>	<i>F</i>	<i>P-value</i>	<i>F crit</i>
Number of Users	3.57E+12	2	1.79E+12	120246.946	0.000	3.259
RoM	1.91E+08	2	9.56E+07	6.430	0.004	3.259
Interaction	2.04E+08	4	5.11E+07	3.439	0.018	2.634
Error	5.35E+08	36	1.49E+07			
Total	3.57E+12	44				

Cluster						
<i>Source of Variation</i>	<i>SS</i>	<i>df</i>	<i>MS</i>	<i>F</i>	<i>P-value</i>	<i>F crit</i>
Number of Users	3.67E+12	2	1.84E+12	39613.784	0.000	3.259
RoM	1.35E+10	2	6.73E+09	145.058	0.000	3.259
Interaction	4.59E+08	4	1.15E+08	2.472	0.062	2.634
Error	1.67E+09	36	4.64E+07			
Total	3.69E+12	44				

Hubenko						
<i>Source of Variation</i>	<i>SS</i>	<i>df</i>	<i>MS</i>	<i>F</i>	<i>P-value</i>	<i>F crit</i>
Number of Users	5.71E+10	2	2.86E+10	15831.566	0.000	3.259
RoM	1.24E+09	2	6.19E+08	342.914	0.000	3.259
Interaction	3.46E+08	4	8.65E+07	47.939	0.000	2.634
Error	6.50E+07	36	1.80E+06			
Total	5.88E+10	44				

Finally, the Duration was increased to 80%, and the Number of Users and the RoM were significant factors for all three architectures. The interactions, however, were only significant for the Hubenko Architecture, as shown in Table 17.

Table 17 - ANOVA with Duration = 0.8

Baseline						
<i>Source of Variation</i>	<i>SS</i>	<i>df</i>	<i>MS</i>	<i>F</i>	<i>P-value</i>	<i>F crit</i>
Number of Users	3.02E+12	2	1.51E+12	39745.053	0.000	3.259
RoM	3.40E+08	2	1.70E+08	4.468	0.018	3.259
Interaction	2.48E+08	4	6.21E+07	1.632	0.187	2.634
Error	1.37E+09	36	3.80E+07			
Total	3.02E+12	44				

Cluster						
<i>Source of Variation</i>	<i>SS</i>	<i>df</i>	<i>MS</i>	<i>F</i>	<i>P-value</i>	<i>F crit</i>
Number of Users	3.00E+12	2	1.50E+12	14541.172	0.000	3.259
RoM	2.00E+10	2	1.00E+10	96.948	0.000	3.259
Interaction	1.54E+09	4	3.85E+08	3.729	0.012	2.634
Error	3.71E+09	36	1.03E+08			
Total	3.02E+12	44				

Hubenko						
<i>Source of Variation</i>	<i>SS</i>	<i>df</i>	<i>MS</i>	<i>F</i>	<i>P-value</i>	<i>F crit</i>
Number of Users	5.22E+10	2	2.61E+10	25127.946	0.000	3.259
RoM	8.63E+08	2	4.32E+08	415.784	0.000	3.259
Interaction	2.51E+08	4	6.27E+07	60.399	0.000	2.634
Error	3.74E+07	36	1.04E+06			
Total	5.33E+10	44				

4.5 Summary

Analysis was performed on four different user scenarios, simulating a wide array of potential communications environments. In all simulated cases, the Hubenko Architecture demonstrated superior re-keying efficiency and scalability results over the Cluster and Baseline architectures. As the Mobility Content of the scenarios increased, the Hubenko Architecture steadily increased as well, rather than saturating like the Cluster and Baseline architectures. Within the data capacity limitations of the MatLab

software operating on a Windows platform, the Hubenko Architecture could not be saturated, whereas the Cluster and Baseline architectures readily saturated with moderate Mobility Content. The primary objective of the Hubenko Architecture was achieved, as shown by the minimal re-keying impact on the Control Group users when numerous rapidly moving users were present in the system.

V. Conclusion

5.1 Summary of Research

Relatively few research efforts are aimed at securing group communications while scaling well to large groups of highly mobile users. A few of the architectures noted in Chapter II contribute pieces to an overall framework for secure group communications in a multicast network. None of the research, though, specifically addressed a LEOsat network environment, nor do they completely address the issues facing a global, highly mobile user base dependent on a LEO communications satellite system as their best means for infrastructure.

After a rigorous search through the literature to survey the history and determine the state-of-the-art of satellite multicasting and secure group communications, this research provides an efficient and scalable secure multicasting in the LEO satellite network environment by developing the novel “Hubenko Security Framework Architecture.”

This research develops and analyzes the Baseline, Cluster, and Hubenko Architectures in multiple mobile communication environment scenarios, and consistently demonstrates the superior re-keying advantage offered by the “Hubenko Security Framework Architecture.”

This research was the basis for several publications, as noted in Section 5.3. Further, this research has been used in the development of an application of the Hubenko Architecture to the unmanned aerial vehicle environment at the Master’s degree level.

5.2 Research Contributions

In today's highly mobile world of deployed communications, security and efficiency are critical requirements that must be met. Employing a security scheme that negatively impacts the user's network experience is undesirable. Leveraging multicast architectures that provide disparate scalability benefits in non-mobile environments, the Hubenko Architecture provides efficient security in a mobile multicast environment using a low earth orbit satellite-based infrastructure. The aforementioned simulations demonstrate the Hubenko Architecture's results in significantly less re-keying for both the individual user and the overall system. Less re-keying means less system overhead which corresponds to better network throughput and lower mean delay. An example of the increased efficiency is the 835% reduction of individual re-keying in the Varied Air Content scenario. An example of the increased scalability is the Hubenko Architecture operating at 22% capacity with four times the number of users that caused the Cluster architecture to saturate.

This research produced a novel architecture that can be applied to numerous group communications environments to reduce the re-keying overhead (increased efficiency) and increase the number of supportable users (increased scalability). Increased efficiency means smaller devices that are battery-dependent can re-key less often, which translates to longer battery life for performing more sensing operations. Users in the field connected via low-rate secure links will effectively have more bandwidth due to less time wasted on repeatedly transferring new keys. Larger numbers of supportable users means the network can support a larger number of sensors, or accommodate an order of magnitude of more users in the same network.

5.3 Publications

The number of refereed publications in international journals and conference proceedings demonstrates the novelty of this research. To date, five papers have been published including two journal articles [HuR06a, HuR06b, HuR07a, HuR07b, HuR08]. Specific titles and publication venues are listed at the end of this chapter.

5.4 Recommendations for Future Research

5.4.1 *Adapt Hubenko Security Framework Architecture to Other Environments*

With relatively minor adjustments, the Hubenko Architecture can be applied to several other areas of communications, namely unmanned aerial vehicle (UAV) swarms, wireless sensor networks (WSN), and mobile ad hoc networks. Master's level research is currently underway in applying the Hubenko Architecture to a UAV environment, with a goal of assessing battery life and communications overhead performance gains.

Additionally, the Hubenko Architecture could be applied to wireless sensor networks in a heterogeneous environment to reduce the amount of re-keying on the WSN when mobile units pass through the WSN field. Another potential application is to use an Air Battle Node instead of a LEO satellite network. This would bring the main infrastructure closer to the tactical theater network, reducing propagation delays even more.

5.4.2 *Incorporate Features from the Integrated Architecture Concept*

Another area of potential interest for increasing system scalability and efficiency makes use of the “integrated architecture” concept from [AmN05]. This concept removes some of the security processing burden from the users, as shown in Figure 56. By centralizing the key agreement and distribution across the satellite group versus the

user group, a further increase in system scalability should be achieved due to less processing requirements being placed on the end users. Incidentally, a corollary benefit from implementing the integrated architecture is the potential for bringing the GIG's "Power to the Edge" by allowing the end users to upload heavyweight processing tasks to the satellites for computation. The radio frequency propagation time for the user to send data to the LEO system and receive a reply (a single round trip; up once and down once) is between 1.33 and 13.33 milliseconds. This shifts ground-based processing tasks performed by deployed tactical users to more capable orbital resources. This corollary is based on the assumption that the next generation LEO satellite system processes and downloads large amounts of data more quickly than the tactical ground system and independently of satellite handoff delays. Leveraging the capabilities of the satellite infrastructure to perform the "heavy lifting" computations for reduced-capability mobile terrestrial users is a potential benefit inherent in the overall system with minimal adaptation required.

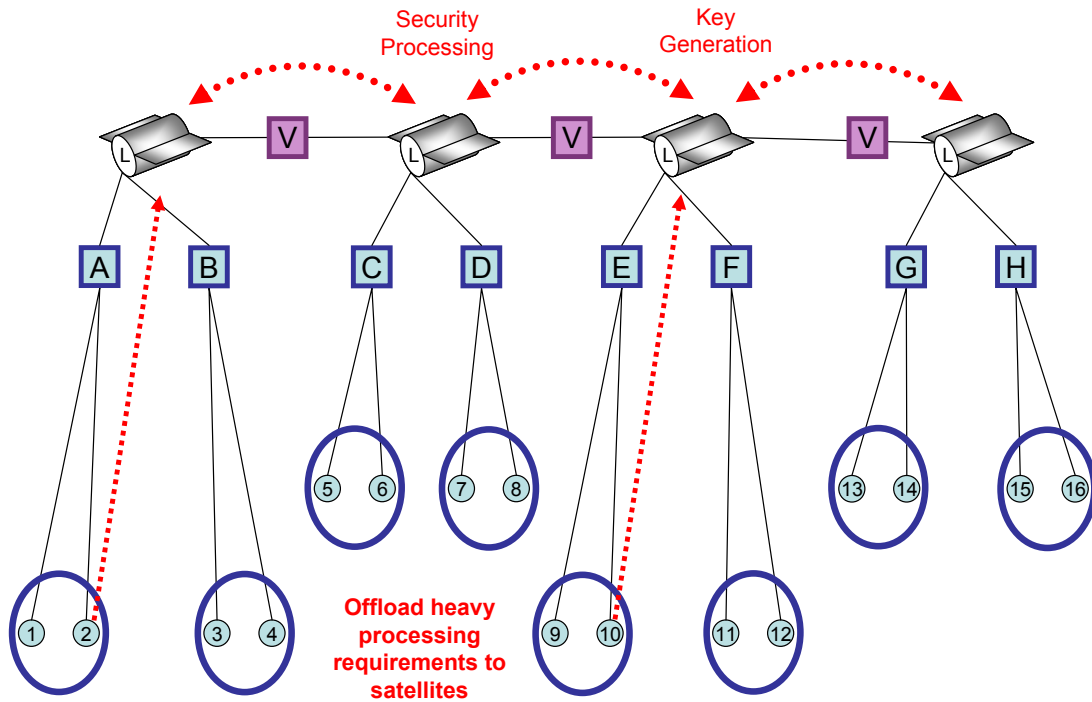


Figure 56 - Integrated Architecture Services Added

5.4.3 Re-establish Original LEOSat Baseline with Hubenko Architecture

With the Hubenko Security Framework Architecture complete, a port of the MatLab simulations to the OPNET [OPN06] environment for more detailed analysis at the packet level would be beneficial. One could re-investigate the End-to-End, Received-to-Sent, and Data-to-Overhead ratio performance with a more detailed packet- and system-level analysis of the architecture.

Publications

Published (5):

- [HuR06a] Hubenko Jr., Victor P., Richard A. Raines, Michael A. Temple, Robert F. Mills, and Mark D. Saeger, "Adaptation, Modeling, and Analysis of PIM-DM in a LEO Satellite Network Environment," *Proceedings of the IEEE Aerospace Conference*, Big Sky, Montana, 2006.
- [HuR06b] Hubenko Jr., Victor P., Richard A. Raines, Robert F. Mills, Rusty O. Baldwin, Barry E. Mullins, and Michael R. Grimaila, "Improving the Global Information Grid's Performance Through Satellite Communications Layer Enhancements," *IEEE Communications*, vol. 44, no. 11, pp. 66-72, 2006. (Approximately 5% Acceptance Rate)
- [HuR07a] Hubenko Jr., Victor P., Richard A. Raines, Rusty O. Baldwin, Barry E. Mullins, Robert F. Mills, and Michael R. Grimaila, "Improving Satellite Multicast Security Scalability by Reducing Re-keying Requirements," *IEEE Network*, vol. 21, no. 4, pp. 51-56, 2007. (Approximately 5% Acceptance Rate)
- [HuR07b] Hubenko Jr., Victor P., Richard A. Raines, Rusty O. Baldwin, Barry E. Mullins, Robert F. Mills, and Michael R. Grimaila, "Applying a Secure and Efficient Low Earth Orbit Satellite-Based Multicast Architecture in a Deployed Environment," *Proceedings of the MILCOM 2007*, pp. 1-7, Orlando, Florida, 2007
- [HuR08] Hubenko Jr., Victor P., Richard A. Raines, Rusty O. Baldwin, Barry E. Mullins, Robert F. Mills, and Michael R. Grimaila, "A Secure and Efficient Satellite-based Multicast Architecture," *Proceedings of the IEEE Radio and Wireless Symposium*, pp. 227-230, Orlando, Florida, 2008 (Winner, Third Best Student Paper)

VI. Appendix

This section presents the raw data tables and a printout of the MatLab code. The only tables included here are for the three scenarios that had thirty iterations. Due to their large size, each of the tables for the other scenarios, with ninety or more iterations, are available in softcopy. A sample printout of the MatLab code is also attached in this section. Numerous versions of the code were used throughout development. Within each version, the outer loops of the code (illustrated in Figure 24) were modified as needed to accommodate the parameter changes for each scenario. The core architectural portion of the code, however, was not modified after verification and validation, and was carried through in each version unaltered.

6.1 Short versus Long Duration Scenario 1 (Section 4.2.2)

**Table 18 - Total Keys Distributed (All Users,
Short vs. Long Duration Scenario 1)**

Iteration	Coeff of Variance			Sample Standard Dev			Mean		
	Baseline	Cluster	Hubenko	Baseline	Cluster	Hubenko	Baseline	Cluster	Hubenko
1	0.1134	0.0785	0.0446	1,148	221	30	10,131	2,818	662
2	0.1649	0.2358	0.0892	4,482	2,340	164	27,178	9,923	1,842
3	0.0345	0.0932	0.0389	1,582	1,801	136	45,889	19,324	3,485
4	0.0351	0.0553	0.0190	2,268	1,781	107	64,630	32,198	5,650
5	0.0168	0.0287	0.0230	1,370	1,264	185	81,764	43,979	8,040
6	0.0313	0.0364	0.0131	3,069	2,247	150	98,073	61,804	11,506
7	0.0423	0.0707	0.0080	4,870	5,195	118	115,201	73,432	14,743
8	0.0150	0.0366	0.0117	2,012	3,280	221	133,960	89,656	18,834
9	0.0299	0.0261	0.0111	4,523	2,765	254	151,078	105,908	22,916
10	0.0192	0.0321	0.0215	3,304	4,091	610	171,998	127,295	28,313
11	0.0243	0.0287	0.0055	4,564	4,125	183	187,664	143,656	33,331
12	0.0188	0.0208	0.0110	3,877	3,350	427	206,772	160,803	38,712
13	0.0076	0.0377	0.0143	1,691	6,596	630	223,545	175,030	44,099
14	0.0111	0.0283	0.0059	2,734	5,685	306	247,133	200,620	51,572
15	0.0065	0.0188	0.0077	1,687	4,076	443	261,293	216,475	57,767
16	0.1329	0.2125	0.2180	6,632	5,419	688	49,913	25,495	3,156
17	0.0173	0.0446	0.0337	1,974	3,333	215	114,203	74,794	6,389
18	0.0025	0.0355	0.0380	430	4,784	418	171,567	134,790	11,004
19	0.0067	0.0203	0.0224	1,555	4,074	364	230,844	200,323	16,268
20	0.0092	0.0379	0.0459	2,677	9,747	979	290,027	257,069	21,311
21	0.0062	0.0138	0.0469	2,162	4,483	1,345	348,178	324,141	28,688
22	0.0037	0.0122	0.0341	1,521	4,699	1,274	406,813	385,056	37,316
23	0.0006	0.0070	0.0179	270	3,116	765	465,786	442,460	42,654
24	0.0022	0.0015	0.0370	1,168	747	1,807	522,956	497,912	48,760
25	0.0022	0.0040	0.0341	1,309	2,257	2,031	584,313	563,508	59,511
26	0.0008	0.0047	0.0235	486	2,904	1,565	642,065	621,087	66,617
27	0.0022	0.0007	0.0254	1,540	459	1,903	697,785	674,657	74,859
28	0.0025	0.0049	0.0111	1,925	3,599	952	756,834	733,793	86,077
29	0.0039	0.0057	0.0038	3,230	4,519	369	818,866	799,647	96,531
30	0.0004	0.0031	0.0105	366	2,617	1,115	874,995	853,895	106,548

**Table 19 - Total Keys Distributed (Control Group Users,
Short vs. Long Duration Scenario 1)**

Iteration	Coeff of Variance			Sample Standard Dev			Mean		
	Baseline	Cluster	Hubenko	Baseline	Cluster	Hubenko	Baseline	Cluster	Hubenko
1	0.1185	0.0739	0.0520	963	150	14	8,129	2,034	263
2	0.1646	0.2328	0.0381	3,628	1,769	37	22,043	7,599	971
3	0.0394	0.0979	0.0049	1,480	1,489	10	37,600	15,203	2,058
4	0.0389	0.0601	0.0147	2,066	1,539	53	53,111	25,594	3,584
5	0.0281	0.0155	0.0134	1,899	547	72	67,691	35,251	5,386
6	0.0246	0.0304	0.0082	2,000	1,518	65	81,400	49,887	7,887
7	0.0444	0.0718	0.0079	4,252	4,250	82	95,763	59,196	10,391
8	0.0239	0.0364	0.0021	2,674	2,653	29	112,051	72,860	13,662
9	0.0359	0.0317	0.0102	4,543	2,741	172	126,400	86,420	16,919
10	0.0200	0.0325	0.0180	2,884	3,366	376	143,856	103,631	20,872
11	0.0302	0.0387	0.0160	4,733	4,533	398	156,831	117,220	24,872
12	0.0194	0.0232	0.0159	3,355	3,056	465	173,067	131,829	29,266
13	0.0127	0.0373	0.0170	2,385	5,372	574	188,211	144,196	33,715
14	0.0091	0.0261	0.0161	1,887	4,321	637	208,126	165,638	39,614
15	0.0068	0.0251	0.0068	1,500	4,457	301	219,000	177,836	44,388
16	0.1251	0.2180	0.0247	3,363	2,770	7	26,884	12,708	263
17	0.0153	0.0439	0.0031	981	1,736	3	64,030	39,554	927
18	0.0052	0.0327	0.0243	503	2,380	49	97,167	72,692	2,022
19	0.0047	0.0204	0.0089	609	2,208	31	130,473	108,280	3,479
20	0.0047	0.0376	0.0094	771	5,275	52	164,606	140,387	5,559
21	0.0048	0.0181	0.0074	945	3,243	58	197,733	178,941	7,791
22	0.0020	0.0105	0.0055	466	2,249	59	231,602	213,295	10,656
23	0.0020	0.0086	0.0129	534	2,106	175	265,131	245,582	13,601
24	0.0012	0.0038	0.0109	346	1,058	187	298,300	276,737	17,146
25	0.0015	0.0049	0.0224	509	1,534	473	331,779	313,363	21,115
26	0.0025	0.0061	0.0137	924	2,099	343	365,410	346,826	25,052
27	0.0015	0.0032	0.0098	611	1,206	291	397,867	377,165	29,703
28	0.0025	0.0066	0.0150	1,090	2,729	518	431,124	410,427	34,514
29	0.0006	0.0026	0.0147	270	1,160	582	465,755	448,308	39,586
30	0.0006	0.0038	0.0070	289	1,812	315	499,167	479,751	45,032

**Table 20 - Average Per-User Re-Key (All Users,
Short vs. Long Duration Scenario 1)**

Iteration	Coeff of Variance			Sample Standard Dev			Mean		
	Baseline	Cluster	Hubenko	Baseline	Cluster	Hubenko	Baseline	Cluster	Hubenko
1	0.1134	0.0785	0.0446	17.14	3.30	0.44	151	42	10
2	0.1649	0.2358	0.0892	33.45	17.46	1.23	203	74	14
3	0.0345	0.0932	0.0389	7.91	9.00	0.68	229	97	17
4	0.0351	0.0553	0.0190	8.50	6.67	0.40	242	121	21
5	0.0168	0.0287	0.0230	4.10	3.78	0.55	245	132	24
6	0.0313	0.0364	0.0131	7.67	5.62	0.38	245	155	29
7	0.0423	0.0707	0.0080	10.43	11.12	0.25	247	157	32
8	0.0150	0.0366	0.0117	3.77	6.14	0.41	251	168	35
9	0.0299	0.0261	0.0111	7.54	4.61	0.42	252	177	38
10	0.0192	0.0321	0.0215	4.95	6.13	0.91	258	191	42
11	0.0243	0.0287	0.0055	6.22	5.62	0.25	256	196	45
12	0.0188	0.0208	0.0110	4.85	4.19	0.53	258	201	48
13	0.0076	0.0377	0.0143	1.95	7.61	0.73	258	202	51
14	0.0111	0.0283	0.0059	2.93	6.09	0.33	265	215	55
15	0.0065	0.0188	0.0077	1.69	4.08	0.44	261	216	58
16	0.1329	0.2125	0.2180	98.98	80.88	10.27	745	381	47
17	0.0173	0.0446	0.0337	14.73	24.88	1.61	852	558	48
18	0.0025	0.0355	0.0380	2.15	23.92	2.09	858	674	55
19	0.0067	0.0203	0.0224	5.82	15.26	1.36	865	750	61
20	0.0092	0.0379	0.0459	8.02	29.18	2.93	868	770	64
21	0.0062	0.0138	0.0469	5.40	11.21	3.36	870	810	72
22	0.0037	0.0122	0.0341	3.26	10.06	2.73	871	825	80
23	0.0006	0.0070	0.0179	0.51	5.84	1.43	872	829	80
24	0.0022	0.0015	0.0370	1.95	1.25	3.01	872	830	81
25	0.0022	0.0040	0.0341	1.96	3.38	3.04	876	845	89
26	0.0008	0.0047	0.0235	0.66	3.96	2.13	875	846	91
27	0.0022	0.0007	0.0254	1.92	0.57	2.38	872	843	94
28	0.0025	0.0049	0.0111	2.22	4.15	1.10	873	846	99
29	0.0039	0.0057	0.0038	3.46	4.84	0.39	877	856	103
30	0.0004	0.0031	0.0105	0.37	2.62	1.12	875	854	107

**Table 21 - Average Per-User Re-Key (Control Group Users,
Short vs. Long Duration Scenario 1)**

Iteration	Coeff of Variance			Sample Standard Dev			Mean		
	Baseline	Cluster	Hubenko	Baseline	Cluster	Hubenko	Baseline	Cluster	Hubenko
1	0.1185	0.0739	0.0520	28.76	4.49	0.41	243	61	8
2	0.1646	0.2328	0.0381	54.15	26.40	0.55	329	113	14
3	0.0394	0.0979	0.0049	14.80	14.89	0.10	376	152	21
4	0.0389	0.0601	0.0147	15.48	11.53	0.39	398	192	27
5	0.0281	0.0155	0.0134	11.37	3.28	0.43	405	211	32
6	0.0246	0.0304	0.0082	10.00	7.59	0.32	407	249	39
7	0.0444	0.0718	0.0079	18.21	18.20	0.35	410	254	45
8	0.0239	0.0364	0.0021	10.02	9.93	0.11	420	273	51
9	0.0359	0.0317	0.0102	15.14	9.14	0.57	421	288	56
10	0.0200	0.0325	0.0180	8.65	10.09	1.13	431	311	63
11	0.0302	0.0387	0.0160	12.90	12.35	1.08	427	319	68
12	0.0194	0.0232	0.0159	8.39	7.64	1.16	433	330	73
13	0.0127	0.0373	0.0170	5.50	12.39	1.32	434	333	78
14	0.0091	0.0261	0.0161	4.04	9.25	1.36	446	355	85
15	0.0068	0.0251	0.0068	3.00	8.91	0.60	438	356	89
16	0.1251	0.2180	0.0247	100.38	82.69	0.19	803	379	8
17	0.0153	0.0439	0.0031	14.64	25.91	0.04	956	590	14
18	0.0052	0.0327	0.0243	5.03	23.80	0.49	972	727	20
19	0.0047	0.0204	0.0089	4.57	16.54	0.23	977	811	26
20	0.0047	0.0376	0.0094	4.62	31.59	0.31	986	841	33
21	0.0048	0.0181	0.0074	4.73	16.22	0.29	989	895	39
22	0.0020	0.0105	0.0055	2.00	9.63	0.25	992	913	46
23	0.0020	0.0086	0.0129	2.00	7.89	0.66	993	920	51
24	0.0012	0.0038	0.0109	1.15	3.53	0.62	994	922	57
25	0.0015	0.0049	0.0224	1.53	4.60	1.42	995	940	63
26	0.0025	0.0061	0.0137	2.52	5.72	0.93	996	945	68
27	0.0015	0.0032	0.0098	1.53	3.02	0.73	995	943	74
28	0.0025	0.0066	0.0150	2.51	6.30	1.19	995	947	80
29	0.0006	0.0026	0.0147	0.58	2.48	1.25	997	960	85
30	0.0006	0.0038	0.0070	0.58	3.62	0.63	998	960	90

6.2 Short versus Long Duration Scenario 2 (Section 4.2.2)

**Table 22 - Total Keys Distributed (All Users,
Short vs. Long Duration Scenario 2)**

Iteration	Coeff of Variance			Sample Standard Dev			Mean		
	Baseline	Cluster	Hubenko	Baseline	Cluster	Hubenko	Baseline	Cluster	Hubenko
1	0.0183	0.0433	0.0553	30,387	53,151	3,285	1,661,172	1,226,265	59,351
2	0.0099	0.0131	0.0170	33,605	38,596	2,795	3,410,688	2,935,814	164,514
3	0.0083	0.0076	0.0145	43,726	36,575	4,702	5,294,894	4,783,084	324,829
4	0.0074	0.0099	0.0166	52,041	64,736	8,852	7,008,409	6,513,867	533,315
5	0.0105	0.0107	0.0031	92,975	88,962	2,451	8,851,142	8,327,963	795,164
6	0.0078	0.0047	0.0030	83,311	46,993	3,280	10,637,850	10,072,815	1,084,649
7	0.0039	0.0068	0.0076	48,052	80,884	10,948	12,435,709	11,874,432	1,449,019
8	0.0039	0.0033	0.0027	56,194	45,029	4,847	14,248,129	13,623,667	1,826,417
9	0.0074	0.0078	0.0008	119,049	119,129	1,852	16,059,457	15,311,133	2,271,602
10	0.0057	0.0106	0.0038	101,588	180,271	10,339	17,859,429	17,072,154	2,745,599
11	0.0029	0.0016	0.0059	56,133	31,149	19,133	19,640,751	18,947,681	3,269,541
12	0.0011	0.0018	0.0031	23,675	36,891	11,794	21,493,120	20,755,037	3,838,068
13	0.0024	0.0066	0.0014	56,414	146,353	6,368	23,124,297	22,329,092	4,416,859
14	0.0009	0.0012	0.0014	22,197	29,339	7,127	25,056,137	24,233,676	5,066,143
15	0.0012	0.0020	0.0036	32,866	51,068	20,789	26,891,443	26,090,714	5,740,023
16	0.0010	0.0035	0.0363	5,639	19,454	11,078	5,816,340	5,591,317	304,988
17	0.0047	0.0053	0.0150	54,213	60,802	10,416	11,656,030	11,453,313	692,885
18	0.0008	0.0010	0.0240	13,435	16,705	26,624	17,465,774	17,264,926	1,111,409
19	0.0008	0.0004	0.0113	19,227	8,566	18,212	23,326,603	23,121,042	1,616,300
20	0.0009	0.0016	0.0153	26,182	47,787	33,135	29,184,609	28,974,514	2,163,270
21	0.0024	0.0026	0.0015	84,754	89,706	4,178	34,929,849	34,699,256	2,724,421
22	0.0018	0.0017	0.0117	72,387	70,384	40,301	40,874,192	40,668,990	3,446,372
23	0.0012	0.0010	0.0068	57,003	46,167	28,072	46,662,197	46,458,033	4,146,359
24	0.0005	0.0003	0.0046	27,470	15,474	22,674	52,509,643	52,291,032	4,906,205
25	0.0005	0.0002	0.0027	26,606	12,282	15,822	58,391,091	58,197,611	5,766,391
26	0.0015	0.0016	0.0077	94,048	100,309	50,990	64,226,145	64,020,551	6,622,766
27	0.0002	0.0004	0.0054	13,273	25,565	40,619	69,988,711	69,789,077	7,538,044
28	0.0005	0.0004	0.0058	37,933	29,955	49,615	75,926,247	75,743,459	8,537,221
29	0.0007	0.0008	0.0064	56,403	63,710	61,429	81,712,054	81,499,750	9,532,191
30	0.0009	0.0013	0.0058	82,644	109,593	61,331	87,568,289	87,363,595	10,577,002

**Table 23 - Total Keys Distributed (Control Group Users,
Short vs. Long Duration Scenario 2)**

Iteration	Coeff of Variance			Sample Standard Dev			Mean		
	Baseline	Cluster	Hubenko	Baseline	Cluster	Hubenko	Baseline	Cluster	Hubenko
1	0.0227	0.0423	0.0015	31,317	42,080	34	1,381,395	994,705	22,448
2	0.0066	0.0085	0.0024	19,034	20,533	214	2,866,321	2,424,052	87,917
3	0.0104	0.0085	0.0004	46,458	33,555	87	4,453,667	3,962,800	195,752
4	0.0083	0.0111	0.0039	48,668	60,024	1,358	5,894,526	5,414,396	344,642
5	0.0105	0.0102	0.0023	78,497	70,845	1,237	7,457,047	6,945,763	533,802
6	0.0101	0.0067	0.0023	90,561	56,402	1,724	8,984,667	8,429,919	760,599
7	0.0077	0.0098	0.0016	80,963	97,225	1,643	10,461,950	9,909,673	1,030,454
8	0.0053	0.0040	0.0026	64,027	45,943	3,498	12,047,728	11,431,506	1,329,609
9	0.0075	0.0079	0.0040	102,059	100,824	6,765	13,564,000	12,824,160	1,672,945
10	0.0067	0.0127	0.0029	101,369	181,969	6,021	15,078,492	14,300,051	2,045,510
11	0.0033	0.0014	0.0049	55,046	21,514	12,089	16,569,951	15,883,761	2,448,507
12	0.0015	0.0015	0.0057	28,000	26,725	16,461	18,116,000	17,384,439	2,894,303
13	0.0021	0.0070	0.0007	41,334	130,668	2,375	19,498,500	18,710,533	3,359,104
14	0.0003	0.0016	0.0019	7,129	32,111	7,539	21,181,957	20,365,983	3,884,750
15	0.0014	0.0003	0.0039	32,532	7,275	17,163	22,703,333	21,909,020	4,417,780
16	0.0022	0.0023	0.0055	7,212	7,134	122	3,293,370	3,099,634	22,357
17	0.0022	0.0029	0.0067	14,352	18,680	592	6,629,313	6,439,848	88,379
18	0.0009	0.0004	0.0055	8,622	3,563	1,086	9,967,333	9,775,485	196,101
19	0.0015	0.0001	0.0032	19,787	1,596	1,115	13,295,786	13,097,456	347,714
20	0.0003	0.0010	0.0040	4,812	16,941	2,172	16,652,774	16,447,879	536,905
21	0.0011	0.0018	0.0010	22,716	36,014	745	19,974,000	19,748,673	766,169
22	0.0006	0.0008	0.0021	12,849	19,636	2,219	23,319,113	23,117,654	1,039,744
23	0.0003	0.0005	0.0061	8,148	13,121	8,135	26,623,772	26,423,277	1,341,442
24	0.0002	0.0005	0.0035	6,245	14,333	5,873	29,978,000	29,762,559	1,688,906
25	0.0002	0.0006	0.0038	5,091	20,553	7,798	33,315,557	33,124,632	2,073,335
26	0.0001	0.0002	0.0053	2,117	7,562	13,269	36,654,110	36,450,991	2,483,995
27	0.0003	0.0007	0.0021	10,066	26,456	6,296	39,978,667	39,781,343	2,936,168
28	0.0003	0.0001	0.0008	10,904	5,375	2,737	43,314,112	43,133,423	3,436,971
29	0.0002	0.0004	0.0038	10,778	16,930	15,033	46,654,443	46,444,294	3,936,133
30	0.0000	0.0006	0.0043	0	27,686	19,145	49,985,000	49,782,164	4,499,922

**Table 24 - Average Per-User Re-Key (All Users,
Short vs. Long Duration Scenario 2)**

Iteration	Coeff of Variance			Sample Standard Dev			Mean		
	Baseline	Cluster	Hubenko	Baseline	Cluster	Hubenko	Baseline	Cluster	Hubenko
1	0.0183	0.0433	0.0553	45.56	79.69	4.93	2,491	1,838	89
2	0.0099	0.0131	0.0170	25.19	28.93	2.10	2,557	2,201	123
3	0.0083	0.0076	0.0145	21.86	18.29	2.35	2,647	2,392	162
4	0.0074	0.0099	0.0166	19.51	24.27	3.32	2,628	2,442	200
5	0.0105	0.0107	0.0031	27.89	26.68	0.74	2,655	2,498	239
6	0.0078	0.0047	0.0030	20.83	11.75	0.82	2,659	2,518	271
7	0.0039	0.0068	0.0076	10.30	17.33	2.35	2,665	2,544	310
8	0.0039	0.0033	0.0027	10.54	8.44	0.91	2,671	2,554	342
9	0.0074	0.0078	0.0008	19.84	19.85	0.31	2,677	2,552	379
10	0.0057	0.0106	0.0038	15.24	27.04	1.55	2,679	2,561	412
11	0.0029	0.0016	0.0059	7.65	4.25	2.61	2,678	2,584	446
12	0.0011	0.0018	0.0031	2.96	4.61	1.47	2,687	2,594	480
13	0.0024	0.0066	0.0014	6.51	16.89	0.73	2,668	2,576	510
14	0.0009	0.0012	0.0014	2.38	3.14	0.76	2,684	2,596	543
15	0.0012	0.0020	0.0036	3.29	5.11	2.08	2,689	2,609	574
16	0.0010	0.0035	0.0363	8.45	29.17	16.61	8,720	8,383	457
17	0.0047	0.0053	0.0150	40.64	45.58	7.81	8,738	8,586	519
18	0.0008	0.0010	0.0240	6.72	8.35	13.31	8,733	8,632	556
19	0.0008	0.0004	0.0113	7.21	3.21	6.83	8,746	8,669	606
20	0.0009	0.0016	0.0153	7.85	14.33	9.94	8,754	8,691	649
21	0.0024	0.0026	0.0015	21.19	22.43	1.04	8,732	8,675	681
22	0.0018	0.0017	0.0117	15.51	15.08	8.64	8,758	8,714	738
23	0.0012	0.0010	0.0068	10.69	8.66	5.26	8,748	8,710	777
24	0.0005	0.0003	0.0046	4.58	2.58	3.78	8,752	8,715	818
25	0.0005	0.0002	0.0027	3.99	1.84	2.37	8,758	8,729	865
26	0.0015	0.0016	0.0077	12.82	13.68	6.95	8,757	8,729	903
27	0.0002	0.0004	0.0054	1.66	3.20	5.08	8,749	8,724	942
28	0.0005	0.0004	0.0058	4.38	3.46	5.72	8,760	8,739	985
29	0.0007	0.0008	0.0064	6.04	6.83	6.58	8,754	8,731	1,021
30	0.0009	0.0013	0.0058	8.26	10.96	6.13	8,757	8,736	1,058

**Table 25 - Average Per-User Re-Key (Control Group Users,
Short vs. Long Duration Scenario 2)**

Iteration	Coeff of Variance			Sample Standard Dev			Mean		
	Baseline	Cluster	Hubenko	Baseline	Cluster	Hubenko	Baseline	Cluster	Hubenko
1	0.0227	0.0423	0.0015	93.90	126.18	0.10	4,142	2,983	67
2	0.0066	0.0085	0.0024	28.54	30.78	0.32	4,297	3,634	132
3	0.0104	0.0085	0.0004	46.46	33.55	0.09	4,454	3,963	196
4	0.0083	0.0111	0.0039	36.50	45.01	1.02	4,420	4,060	258
5	0.0105	0.0102	0.0023	47.09	42.50	0.74	4,473	4,167	320
6	0.0101	0.0067	0.0023	45.28	28.20	0.86	4,492	4,215	380
7	0.0077	0.0098	0.0016	34.70	41.66	0.70	4,483	4,247	442
8	0.0053	0.0040	0.0026	24.01	17.23	1.31	4,517	4,286	499
9	0.0075	0.0079	0.0040	34.02	33.61	2.25	4,521	4,275	558
10	0.0067	0.0127	0.0029	30.41	54.59	1.81	4,523	4,290	614
11	0.0033	0.0014	0.0049	15.01	5.87	3.30	4,519	4,332	668
12	0.0015	0.0015	0.0057	7.00	6.68	4.12	4,529	4,346	724
13	0.0021	0.0070	0.0007	9.54	30.15	0.55	4,499	4,318	775
14	0.0003	0.0016	0.0019	1.53	6.88	1.62	4,539	4,364	832
15	0.0014	0.0003	0.0039	6.51	1.45	3.43	4,541	4,382	884
16	0.0022	0.0023	0.0055	21.62	21.39	0.37	9,875	9,294	67
17	0.0022	0.0029	0.0067	21.52	28.01	0.89	9,939	9,655	133
18	0.0009	0.0004	0.0055	8.62	3.56	1.09	9,967	9,775	196
19	0.0015	0.0001	0.0032	14.84	1.20	0.84	9,971	9,822	261
20	0.0003	0.0010	0.0040	2.89	10.16	1.30	9,990	9,867	322
21	0.0011	0.0018	0.0010	11.36	18.01	0.37	9,987	9,874	383
22	0.0006	0.0008	0.0021	5.51	8.41	0.95	9,993	9,907	446
23	0.0003	0.0005	0.0061	3.06	4.92	3.05	9,983	9,907	503
24	0.0002	0.0005	0.0035	2.08	4.78	1.96	9,993	9,921	563
25	0.0002	0.0006	0.0038	1.53	6.17	2.34	9,994	9,937	622
26	0.0001	0.0002	0.0053	0.58	2.06	3.62	9,996	9,940	677
27	0.0003	0.0007	0.0021	2.52	6.61	1.57	9,995	9,945	734
28	0.0003	0.0001	0.0008	2.52	1.24	0.63	9,995	9,953	793
29	0.0002	0.0004	0.0038	2.31	3.63	3.22	9,997	9,952	843
30	0.0000	0.0006	0.0043	0.00	5.54	3.83	9,997	9,956	900

6.3 Increasing Aircraft Over Stationary Users Scenario 2 (Section 4.2.3)

**Table 26 - Total Keys Distributed (All Users,
Increasing Aircraft Over Stationary Users Scenario 2)**

Iteration	Coeff of Variance			Sample Standard Dev			Mean		
	Baseline	Cluster	Hubenko	Baseline	Cluster	Hubenko	Baseline	Cluster	Hubenko
1	0.0904	0.0897	0.0023	784,829	274,033	275	8,681,369	3,055,333	117,732
2	0.0407	0.1177	0.0152	772,818	1,173,413	6,646	18,976,685	9,970,518	437,455
3	0.0018	0.0431	0.0025	53,566	800,236	2,317	29,433,570	18,562,466	940,188
4	0.0003	0.0404	0.0044	10,262	1,263,530	7,033	39,320,710	31,313,357	1,608,110
5	0.0007	0.0324	0.0071	34,017	1,361,841	17,303	49,214,102	42,055,851	2,444,874
6	0.0035	0.0569	0.0231	34,400	380,817	3,230	9,770,308	6,687,975	139,861
7	0.0011	0.0251	0.0195	22,200	425,981	9,252	19,609,750	16,984,644	473,900
8	0.0009	0.0075	0.0036	26,589	208,018	3,619	29,520,563	27,701,209	1,006,610
9	0.0002	0.0025	0.0055	9,491	96,303	9,387	39,379,345	38,265,499	1,702,262
10	0.0002	0.0032	0.0012	7,713	154,483	2,920	49,257,760	48,179,126	2,536,541
11	0.0010	0.0202	0.0218	9,728	167,167	3,459	9,761,333	8,293,889	158,682
12	0.0008	0.0025	0.0099	15,507	46,824	5,109	19,659,593	18,822,068	518,121
13	0.0006	0.0011	0.0072	16,456	31,920	7,623	29,535,431	28,846,826	1,060,091
14	0.0002	0.0008	0.0114	5,989	29,226	20,325	39,391,169	38,757,835	1,783,214
15	0.0003	0.0014	0.0025	16,778	68,131	6,575	49,244,917	48,593,570	2,638,523
16	0.0006	0.0314	0.0420	5,667	279,120	7,442	9,788,197	8,876,319	177,390
17	0.0000	0.0052	0.0099	976	99,539	5,534	19,676,719	19,142,139	556,938
18	0.0002	0.0012	0.0082	4,753	35,696	9,177	29,534,553	29,074,184	1,122,987
19	0.0003	0.0002	0.0045	11,313	8,768	8,248	39,395,378	38,967,151	1,839,463
20	0.0004	0.0009	0.0116	17,796	41,728	31,904	49,251,433	48,830,033	2,742,361
21	0.0009	0.0025	0.0096	8,935	23,533	2,026	9,822,170	9,404,468	211,796
22	0.0001	0.0026	0.0066	1,976	49,842	4,105	19,688,321	19,352,214	622,009
23	0.0002	0.0008	0.0035	5,392	22,836	4,155	29,553,302	29,207,472	1,201,793
24	0.0004	0.0002	0.0024	13,963	8,793	4,646	39,393,821	39,096,376	1,969,192
25	0.0001	0.0012	0.0047	7,355	60,835	13,404	49,268,474	48,965,305	2,877,280
26	0.0011	0.0036	0.0213	11,052	34,605	5,545	9,831,126	9,575,730	259,776
27	0.0005	0.0009	0.0055	10,650	18,365	3,900	19,682,966	19,467,606	709,542
28	0.0000	0.0002	0.0102	1,191	6,918	13,743	29,545,568	29,301,262	1,349,402
29	0.0003	0.0007	0.0084	12,390	26,241	18,085	39,409,317	39,218,908	2,145,057
30	0.0001	0.0006	0.0040	5,036	28,360	12,442	49,257,078	49,057,807	3,087,913

**Table 27 - Total Keys Distributed (Control Group Users,
Increasing Aircraft Over Stationary Users Scenario 2)**

Iteration	Coeff of Variance			Sample Standard Dev			Mean		
	Baseline	Cluster	Hubenko	Baseline	Cluster	Hubenko	Baseline	Cluster	Hubenko
1	0.0904	0.0901	0.0126	674,779	235,371	1,256	7,465,833	2,613,564	99,820
2	0.0402	0.1173	0.0106	657,918	1,001,880	4,076	16,348,333	8,542,335	385,210
3	0.0017	0.0428	0.0039	42,466	681,868	3,254	25,375,900	15,916,084	841,788
4	0.0002	0.0403	0.0027	6,800	1,083,386	3,878	33,904,800	26,874,601	1,440,893
5	0.0007	0.0326	0.0060	29,445	1,176,173	13,210	42,449,000	36,107,938	2,200,596
6	0.0038	0.0570	0.0125	32,300	326,376	1,244	8,418,400	5,728,202	99,719
7	0.0014	0.0254	0.0130	24,122	369,534	5,050	16,903,667	14,565,260	387,465
8	0.0010	0.0079	0.0068	25,669	188,972	5,765	25,460,900	23,789,119	848,794
9	0.0002	0.0028	0.0055	6,800	90,976	7,965	33,959,200	32,900,293	1,455,898
10	0.0001	0.0035	0.0029	4,907	143,850	6,306	42,488,667	41,450,189	2,200,724
11	0.0011	0.0202	0.0102	8,833	143,706	1,021	8,409,900	7,102,288	100,134
12	0.0007	0.0025	0.0035	11,940	39,913	1,337	16,951,267	16,165,912	384,375
13	0.0006	0.0011	0.0017	15,581	27,851	1,419	25,471,100	24,805,061	838,692
14	0.0001	0.0009	0.0061	3,926	28,921	8,929	33,975,067	33,354,936	1,457,823
15	0.0001	0.0015	0.0028	4,907	62,574	6,271	42,471,667	41,831,655	2,206,712
16	0.0011	0.0325	0.0028	8,996	247,237	277	8,437,100	7,610,948	100,467
17	0.0003	0.0055	0.0020	5,194	89,699	763	16,971,667	16,457,992	389,310
18	0.0002	0.0013	0.0043	5,100	33,277	3,668	25,474,500	25,023,431	847,141
19	0.0003	0.0002	0.0058	10,387	8,326	8,332	33,984,133	33,562,246	1,443,860
20	0.0001	0.0011	0.0111	4,907	46,662	24,403	42,485,833	42,069,857	2,208,028
21	0.0010	0.0027	0.0065	8,500	21,593	649	8,467,700	8,074,409	100,624
22	0.0002	0.0030	0.0129	3,926	49,773	4,970	16,985,267	16,655,744	386,205
23	0.0002	0.0010	0.0035	5,100	25,709	2,977	25,489,800	25,148,962	845,165
24	0.0003	0.0002	0.0087	10,387	5,070	12,642	33,984,133	33,689,599	1,445,425
25	0.0000	0.0013	0.0037	0	54,912	8,253	42,491,500	42,190,781	2,201,124
26	0.0009	0.0037	0.0013	7,852	30,083	132	8,475,633	8,228,259	100,677
27	0.0005	0.0011	0.0058	8,996	18,061	2,244	16,976,200	16,763,702	384,039
28	0.0001	0.0002	0.0046	2,944	4,016	3,852	25,486,400	25,244,285	840,838
29	0.0002	0.0006	0.0026	7,852	20,685	3,715	33,988,667	33,799,540	1,443,188
30	0.0000	0.0005	0.0027	0	23,186	5,843	42,491,500	42,293,289	2,185,256

**Table 28 - Average Per-User Re-Key (All Users,
Increasing Aircraft Over Stationary Users Scenario 2)**

Iteration	Coeff of Variance			Sample Standard Dev			Mean		
	Baseline	Cluster	Hubenko	Baseline	Cluster	Hubenko	Baseline	Cluster	Hubenko
1	0.0904	0.0897	0.0023	392.41	137.02	0.14	4,341	1,528	59
2	0.0407	0.1177	0.0152	193.20	293.35	1.66	4,744	2,493	109
3	0.0018	0.0431	0.0025	8.93	133.37	0.39	4,906	3,094	157
4	0.0003	0.0404	0.0044	1.28	157.94	0.88	4,915	3,914	201
5	0.0007	0.0324	0.0071	3.40	136.18	1.73	4,921	4,206	244
6	0.0035	0.0569	0.0231	17.20	190.41	1.62	4,885	3,344	70
7	0.0011	0.0251	0.0195	5.55	106.50	2.31	4,902	4,246	118
8	0.0009	0.0075	0.0036	4.43	34.67	0.60	4,920	4,617	168
9	0.0002	0.0025	0.0055	1.19	12.04	1.17	4,922	4,783	213
10	0.0002	0.0032	0.0012	0.77	15.45	0.29	4,926	4,818	254
11	0.0010	0.0202	0.0218	4.86	83.58	1.73	4,881	4,147	79
12	0.0008	0.0025	0.0099	3.88	11.71	1.28	4,915	4,706	130
13	0.0006	0.0011	0.0072	2.74	5.32	1.27	4,923	4,808	177
14	0.0002	0.0008	0.0114	0.75	3.65	2.54	4,924	4,845	223
15	0.0003	0.0014	0.0025	1.68	6.81	0.66	4,924	4,859	264
16	0.0006	0.0314	0.0420	2.83	139.56	3.72	4,894	4,438	89
17	0.0000	0.0052	0.0099	0.24	24.88	1.38	4,919	4,786	139
18	0.0002	0.0012	0.0082	0.79	5.95	1.53	4,922	4,846	187
19	0.0003	0.0002	0.0045	1.41	1.10	1.03	4,924	4,871	230
20	0.0004	0.0009	0.0116	1.78	4.17	3.19	4,925	4,883	274
21	0.0009	0.0025	0.0096	4.47	11.77	1.01	4,911	4,702	106
22	0.0001	0.0026	0.0066	0.49	12.46	1.03	4,922	4,838	156
23	0.0002	0.0008	0.0035	0.90	3.81	0.69	4,926	4,868	200
24	0.0004	0.0002	0.0024	1.75	1.10	0.58	4,924	4,887	246
25	0.0001	0.0012	0.0047	0.74	6.08	1.34	4,927	4,897	288
26	0.0011	0.0036	0.0213	5.53	17.30	2.77	4,916	4,788	130
27	0.0005	0.0009	0.0055	2.66	4.59	0.98	4,921	4,867	177
28	0.0000	0.0002	0.0102	0.20	1.15	2.29	4,924	4,884	225
29	0.0003	0.0007	0.0084	1.55	3.28	2.26	4,926	4,902	268
30	0.0001	0.0006	0.0040	0.50	2.84	1.24	4,926	4,906	309

**Table 29 - Average Per-User Re-Key (Control Group Users,
Increasing Aircraft Over Stationary Users Scenario 2)**

Iteration	Coeff of Variance			Sample Standard Dev			Mean		
	Baseline	Cluster	Hubenko	Baseline	Cluster	Hubenko	Baseline	Cluster	Hubenko
1	0.0904	0.0901	0.0126	396.93	138.45	0.74	4,392	1,537	59
2	0.0402	0.1173	0.0106	193.51	294.67	1.20	4,808	2,512	113
3	0.0017	0.0428	0.0039	8.33	133.70	0.64	4,976	3,121	165
4	0.0002	0.0403	0.0027	1.00	159.32	0.57	4,986	3,952	212
5	0.0007	0.0326	0.0060	3.46	138.37	1.55	4,994	4,248	259
6	0.0038	0.0570	0.0125	19.00	191.99	0.73	4,952	3,370	59
7	0.0014	0.0254	0.0130	7.09	108.69	1.49	4,972	4,284	114
8	0.0010	0.0079	0.0068	5.03	37.05	1.13	4,992	4,665	166
9	0.0002	0.0028	0.0055	1.00	13.38	1.17	4,994	4,838	214
10	0.0001	0.0035	0.0029	0.58	16.92	0.74	4,999	4,876	259
11	0.0011	0.0202	0.0102	5.20	84.53	0.60	4,947	4,178	59
12	0.0007	0.0025	0.0035	3.51	11.74	0.39	4,986	4,755	113
13	0.0006	0.0011	0.0017	3.06	5.46	0.28	4,994	4,864	164
14	0.0001	0.0009	0.0061	0.58	4.25	1.31	4,996	4,905	214
15	0.0001	0.0015	0.0028	0.58	7.36	0.74	4,997	4,921	260
16	0.0011	0.0325	0.0028	5.29	145.43	0.16	4,963	4,477	59
17	0.0003	0.0055	0.0020	1.53	26.38	0.22	4,992	4,841	115
18	0.0002	0.0013	0.0043	1.00	6.52	0.72	4,995	4,907	166
19	0.0003	0.0002	0.0058	1.53	1.22	1.23	4,998	4,936	212
20	0.0001	0.0011	0.0111	0.58	5.49	2.87	4,998	4,949	260
21	0.0010	0.0027	0.0065	5.00	12.70	0.38	4,981	4,750	59
22	0.0002	0.0030	0.0129	1.15	14.64	1.46	4,996	4,899	114
23	0.0002	0.0010	0.0035	1.00	5.04	0.58	4,998	4,931	166
24	0.0003	0.0002	0.0087	1.53	0.75	1.86	4,998	4,954	213
25	0.0000	0.0013	0.0037	0.00	6.46	0.97	4,999	4,964	259
26	0.0009	0.0037	0.0013	4.62	17.70	0.08	4,986	4,840	59
27	0.0005	0.0011	0.0058	2.65	5.31	0.66	4,993	4,931	113
28	0.0001	0.0002	0.0046	0.58	0.79	0.76	4,997	4,950	165
29	0.0002	0.0006	0.0026	1.15	3.04	0.55	4,998	4,971	212
30	0.0000	0.0005	0.0027	0.00	2.73	0.69	4,999	4,976	257

6.4 Analysis of Variance Data

Table 30 - Data in Raw Format for use in ANOVA

DURATION = 0.8											
HubenkoKeys	0.25	0.5	0.75	ClusterKeys	0.25	0.5	0.75	BaselineKeys	0.25	0.5	0.75
1000	78705	96077	96539	1000	678480	727819	751231	1000	780039	771508	784647
	80187	93370	96289		694094	740147	749768		774599	779642	785121
	82611	95486	99117		715227	745256	759803		786635	780241	786688
	82798	95729	96551		717437	749569	750438		786870	785123	790336
	80328	95047	95869		703392	746920	741463		786768	783815	777905
200	6409	9495	10867	200	76347	112138	123405	200	138653	151657	158605
	5983	8350	9922		76190	102476	115171		150363	151019	154580
	6890	9407	8970		88997	107686	104683		144765	155989	143972
	6643	9351	8382		86878	111108	104525		147129	152841	152870
	5802	8601	9691		65519	98375	112416		124882	140072	149441
600	32936	43346	43080	600	348562	430105	425057	600	450133	466361	462598
	33518	42874	42817		372809	418082	421233		465622	462892	465291
	33539	44514	44686		374467	438655	430816		464372	474679	469654
	32935	44100	42714		354295	429474	418483		450464	466626	461737
	34963	42289	43076		390184	426299	431277		463910	465025	468947

DURATION = 0.5											
HubenkoKeys	0.25	0.5	0.75	ClusterKeys	0.25	0.5	0.75	BaselineKeys	0.25	0.5	0.75
1000	86396	102936	103496	1000	804281	832975	831874	1000	852191	859060	854526
	83452	102418	104980		803760	825468	819547		856372	850410	848034
	83300	103212	101494		806027	838547	826800		855043	859267	853373
	83967	101947	102635		798536	834741	831642		852950	856949	854613
	82946	103504	98948		793114	824300	823272		855147	851912	849878
200	7002	11431	11052	200	97543	135558	138206	200	159692	167489	170433
	6168	11735	9050		81536	140216	118701		152752	170230	161093
	7426	11118	11757		99265	135499	135425		164819	165724	165422
	6699	11307	11572		83309	135302	134502		147497	167374	167217
	7132	12049	10464		97895	131714	130681		160683	167690	167498
600	37593	48308	47614	600	459543	480248	485931	600	513106	504398	513162
	37314	47585	47160		436552	482656	480814		502764	511364	510648
	36669	47932	46620		437864	489190	483317		509750	515704	509550
	35508	46129	46962		433769	489641	487819		510790	516069	514236
	37656	44985	51763		454465	478111	491065		506198	510161	510793

DURATION = 0.2											
HubenkoKeys	0.25	0.5	0.75	ClusterKeys	0.25	0.5	0.75	BaselineKeys	0.25	0.5	0.75
1000	87451	105485	105656	1000	900834	907866	915652	1000	927558	923079	928342
	84191	108622	108244		902430	915710	912431		928957	926334	925213
	82584	109975	107839		898208	912661	914815		929441	925012	926635
	86055	109757	105374		897640	914624	916090		927184	926510	928024
	83551	108729	106264		894082	915006	915966		925934	927601	928174
200	7620	11906	11502	200	116975	151883	151606	200	181335	182648	183438
	6343	13656	11606		83983	160799	153013		168162	183902	185226
	7671	13220	13412		114657	157223	153972		185090	185144	184077
	8243	13467	10438		123471	160494	144516		183311	185474	183871
	6364	10171	13341		93729	138507	159756		180862	182688	183080
600	40656	52254	53048	600	527847	542282	544162	600	558364	555703	556938
	36294	52303	52093		500028	543180	539710		557349	557388	555623
	40153	50335	52523		522066	538361	537698		556304	555800	553446
	38156	51677	55220		516321	542177	546951		557758	556073	557402
	38079	52637	51474		507080	543549	540104		554970	556329	556133

6.5 MatLab Code from Increasing Aircraft Over Stationary Users Scenario 2 (Section 4.2.3)

```
% Maj Victor Hubenko
clear; clc;
tic
RunVersion = 'CI 6sets 10kU 5kTS SS3 2007 06 11 WS';
VersionName = strrep(RunVersion, ' ', '');
TimeStamp=num2str(datestr(now));

warning off MATLAB:xlswrite:AddSheet

% EXPERIMENTAL PARAMETERS
```

```

ControlGroupSize=0.85; %sets the control group size. 0.5 = 50% of the users
%are stationary and being counted for the impacts
MaxNumUsers=10000; %Maximum possible number of users for final iterations
numTimeSteps=5000;

numSets=6; % Number of sets. e.g. use '2' for Short and Long, or '6' for the Milcom
Increase AC experiment
% NOTE: If more than 2, need to modify 'MobilityFactor'
numDataPoints=5; % Number of Data Points within each Set
numIterations=numSets*numDataPoints; %NOTE: Must be EVEN!!

%Now can plot with different markers at each data point
numSats=1;
numClusters=10;
numMoving=4;
numWait=5; %the Lower the number, the more frequent the cluster changing
numSpeed=8; % Difference in speed between Mobility 2/3 vs Mobility 4
% NOTE: numWait*numSpeed must be even!

DurationFactor=0.1; % The higher the number, the longer the "Short" duration, and the
shorter the "Long" duration
%JoinFactor=0.3; % The lower the number, the more users join earlier

MobilityProfile=[0.01 0.03 0.05 0.07 0.1 0.15]; % This gives mobility profiles for all
experiment sets

%MobilityProfile=[0.01 .1 .25 .75]; % This gives the mobility profiles for sets
% of experiments, 1, 10, 25 and 75% total mobility

IterationsAxis=zeros(numIterations,1, 'uint16');%5June zeros(numIterations,1, 'uint16');
JoinTimeSetter=0.1; % This has everyone join within the first 10% of the simulation

% STATISTICS:
SampleSize= 3; %number of times to run each complete set. Also number of samples of data
for each identical run
sqrtofn=sqrt(SampleSize);
% df --> 1 2 3 4 5 6 7 8 9
10 11 12 13 14 15 16 17 18 19 20
21 22 23 24 25 26 27 28 29 30
alpha05= [6.314 2.92 2.353 2.132 2.015 1.943 1.895 1.86 1.833 1.812
1.796 1.782 1.771 1.761 1.753 1.746 1.74 1.734 1.729 1.725 1.721
1.717 1.714 1.711 1.708 1.706 1.703 1.701 1.699 1.697];
alpha025= [12.706 4.303 3.182 2.776 2.571 2.447 2.365 2.306 2.262 2.228
2.201 2.179 2.16 2.145 2.131 2.12 2.11 2.101 2.093 2.086 2.08
2.074 2.069 2.064 2.06 2.056 2.052 2.048 2.045 2.042];
% use alpha05 for 90% CI, alpha025 for 95% CI
tAlphaHalf= alpha025(SampleSize-1); %Value of t Alpha over 2 per table

%FirstStep=numSats*numClusters; %5June
%LastStep=FirstStep*numIterations; %5June

% numIterSteps=1; %number of steps to test the join factor (.1, .2, .3, etc)

% numIterations=ceil(numIterSteps*numIterFactor*2/numDataPoints); % number of times to
run this analysis experiment
% This ensures divisible by 4 for creation of JoinFactor,
% and must be even for MobilityFactor. The *2 is to allow
% the MobilityFactor to repeat after half of the iterations

% CONSTANTS
numArchitectures=3; % Baseline, Clustered, Hubenko

MobilityBins=[1 2 3 4]; % 1=Stationary, 2=Ground, 3=Sea, 4=Air
MobilityHistPlot=zeros(numIterations,4);
AvgKeySummaryPlot1=zeros(numIterations,4); % Average Re-keys per Mobility Type for
Baseline
AvgKeySummaryPlot2=zeros(numIterations,4); % Average Re-keys per Mobility Type for
Cluster

```

```

AvgKeySummaryPlot3=zeros(numIterations,4); % Average Re-keys per Mobility Type for
Hubenko

TotalKeysDistribCount=zeros(numIterations,numArchitectures,SampleSize);
% Total Number of keys distributed in a MCast Group for the simulation
% period. Single dimension array, running tally. Count all of the new keys
% that are distributed to all users, satellites each time a new key is
% distributed for the MCast Group. 1=baseline, 2=clusters, 3=Hubenko

TotalHalfKeysDistribCount=zeros(numIterations,numArchitectures,SampleSize);
% Total Number of keys distributed for the Stationary "control group" users

DensityVsRekeys=zeros(numIterations,numArchitectures,SampleSize);
DensityVsHalfRekeys=zeros(numIterations,numArchitectures,SampleSize);

% [+ B - + C - + H - ...] Where B, C, H are the means for the SampleSize,
% + is the Top of the confidence interval, - is the Bottom of the
% Confidence Interval
TotalKeysDistribCountPlot=zeros(numIterations,3*numArchitectures);
TotalHalfKeysDistribCountPlot=zeros(numIterations,3*numArchitectures);
DensityVsRekeysPlot=zeros(numIterations,3*numArchitectures);
DensityVsHalfRekeysPlot=zeros(numIterations,3*numArchitectures);

% xMeanArray is the mean array for each of the above arrays
TKDMeanArray=zeros(numIterations,numArchitectures);
THKDMeanArray=zeros(numIterations,numArchitectures);
DVRMeanArray=zeros(numIterations,numArchitectures);
DVHRMeanArray=zeros(numIterations,numArchitectures);

% xSampleSDArray is the sample standard deviation array for each of the above arrays
TKDSampleSDArray=zeros(numIterations,numArchitectures);
THKDSampleSDArray=zeros(numIterations,numArchitectures);
DVRSampleSDArray=zeros(numIterations,numArchitectures);
DVHRSampleSDArray=zeros(numIterations,numArchitectures);

% % The Coefficient of Variation (C.O.V.) [Jai91], is the ratio of standard
% deviation to sample mean: xSampleSDArray/xMeanArray.
COVTKD=zeros(numIterations,numArchitectures);
COVTHKD=zeros(numIterations,numArchitectures);
COVDVR=zeros(numIterations,numArchitectures);
COVDVHR=zeros(numIterations,numArchitectures);

FigNum=0;
index = datestr(clock);
index = strrep(index, ' ', '-');
index = strrep(index, ':', '-');

% % Return RAND to its default initial state to allow for repeatability
% rand('state',0);

% Initialize RAND to a different state each time.
rand('state',sum(100*clock))

for IterAxisMaker=1:numIterations
    IterationsAxis(IterAxisMaker,1)=IterAxisMaker;
end

MobilityFactor=zeros(numIterations,1);
MFactorCount=1;
for MobilityMaker=1:numIterations % (numIterations/2)
    MobilityFactor(MobilityMaker,1)=MobilityProfile(MFactorCount);
    if mod(MobilityMaker,numDataPoints)==0
        MFactorCount=MFactorCount+1;
    end
end
% JoinFactor=zeros(numIterations,1);
% multiplier=0.1;
% for JoinMaker=1:numIterations
%     JoinFactor(JoinMaker,1)=multiplier;
%     if mod(JoinMaker,numDataPoints)==0

```

```

% multiplier=multiplier+0.1;
% end
% end
% Note: FirstStep=numSats*numClusters; LastStep=FirstStep*numIterations;
for h=1:numIterations %FirstStep:hStepSize:LastStep

% ModTest1=h/FirstStep;
ModTest2=mod(h,numDataPoints);
if ModTest2==0
    IterRep=numDataPoints;
else IterRep=ModTest2;
end

% numUsers=h;
numUsers=ceil(IterRep*MaxNumUsers/numDataPoints)
% Rate of Mobility is held for numDataPoints times

for g=1:SampleSize % Start Loop for run repetition for Statistics calculations
    pause(0);
ClusterActivity=zeros((numSats*numClusters)+1,numTimeSteps, 'uint16');
%ClusterActivity=zeros((numSats*numClusters)+1,numMCGroups,numTimeSteps, 'uint16');
% Tracks when a user joins or leaves a specific Cluster within a Multicast
% Group. As a user joins or leaves, increment/decrement as appropriate.
% The last element {(numSats*numClusters)+1} in each set is the
% total count of Active Users in that MCGroup across all satellites and
% clusters.

ClusterTriggers=zeros((numSats*numClusters)+1,numTimeSteps, 'uint8');
%ClusterTriggers=zeros((numSats*numClusters)+1,numMCGroups,numTimeSteps, 'uint8');
% Tracks when a cluster needs to be rekeyed. When a new user first joins
% or leaves the system, the corresponding cluster element is set to 1. If
% a registered mobile user enters or leaves the cluster, the cluster
% element is set to 2. The last
% element {(numSats*numClusters)+1} in each set is the "MCGroup Rekey
% Trigger Flag," which is set to the max of that MCGroup (0, 1, or 2). 0
% means no joins, leaves, or mobile users entering/exiting; 1 means a user
% registered or deregistered from the system; 2 means a mobile user entered
% or left the cluster.

% Initialize Users
UserMoverPercent=0;
MFcalc=MobilityFactor(h);

%Initialize User Structure
User=repmat(struct('Satellite',int8(0),'Cluster',int8(0),...
    'TimesRekeyed1',0,'TimesRekeyed2',0,'TimesRekeyed3',0,'JoinTime',int16(0),...
    'Duration',int16(0),'Mobility',int8(0),'Waiting',int8(0),'Active',zeros(numTimeSteps,1,
    'uint8')),1,numUsers);
for i=1:numUsers
    pause(0);
    User(i).Satellite = ceil(rand*numSats);
    User(i).Cluster = ceil(rand*numClusters);
% The following were initialized in the repmat(struct) statement
% User(i).TimesRekeyed1 = 0; % Baseline System Rekey Count
% User(i).TimesRekeyed2 = 0; % Cluster System Rekey Count
% User(i).TimesRekeyed3 = 0; % Hubenko System Rekey Count
    if i<=(numUsers*ControlGroupSize)
        % For the first half of the users, set them to Join at one, and
        % stay the whole time. Also set them to Stationary
        User(i).JoinTime = 1; %ceil(rand*numTimeSteps*JoinTimeSetter);
        User(i).Duration = numTimeSteps-1;
        User(i).Mobility = 1;
    else % Otherwise, set them to Join randomly in 1st third, Short and Long Durations,
        % and random mobility up to the Mobility Profile
        User(i).JoinTime = ceil(rand*numTimeSteps*JoinTimeSetter);
        if h <= (numIterations/2)
            % User(i).Duration = ceil(rand*DurationFactor*(numTimeSteps-
            User(i).JoinTime)); % "Short"
        else

```

```

        User(i).Duration = ceil((1-rand*DurationFactor)*(numTimeSteps-User(i).JoinTime));
    % "Long"
    %         end %if for Duration assignment
        %         % Uniformly assign durations to be within remaining time, under the
        %         % constraint of "Short" or "Long" DurationFactor
        if UserMoverPercent < (MFcalcd*numUsers)
            UserMover=rand;
            %         if UserMover > MFcalcd % if UserMover is greater than the Mobility Profile
            %         %for this increment, then set the user to Stationary
            %         User(i).Mobility = 1;
            %         else % Otherwise, uniformly assign it to either Sea, Ground, or Air
            %         User(i).Mobility = 1+ceil(rand*3);
            %         UserMoverPercent=UserMoverPercent+1;
            %         %end % if/else UserMover > MFcalcd
        else User(i).Mobility = 1;
            end %if/else UserMoverPercent < (MFcalcd*numUsers)
        end %Of the if/else for i<=(numUsers*ControlGroupSize)

    % Both of the following were initialized in the repmat(struct) statement
    %     User(i).Waiting = 0; %holder for how long to wait until moving to next cluster
    %     User(i).Active=zeros(numTimeSteps,1, 'uint8'); % Initialize to all
    %     % zeros indicating not active. When Active, each slot will be set to 1.

% if mod(i,1800)==0
%     InitializeUsersLoopsTaken=i
% end

end %for i=numUsers Loop

MobilityHist=[User.Mobility];
MobilityHistPlot(h,:)=hist(MobilityHist,MobilityBins);

% Below is to check to ensure random spread in the correct ranges
%     Lo=Locator;
%     figure, mesh(Lo); %meshc gives contour plot under mesh
%figure,surf(Lo);
% Sa = [User.Satellite]
% Cl = [User.Cluster]
% MC = [User.MCGroup]
% JT = [User.JoinTime]
% Du = [User.Duration];
% Mo = [User.Mobility]

% figure,bar(Du)
% xlabel('User #');
% ylabel('Duration Value');
% title(['User.Duration for iteration ',num2str(ModTest1)])

% Start stepping through "Time."
% Array indexing starts at "1"; nomenclature is (rows, columns)
% Joins and leaves are edge triggered. Can not join and leave in
% same time step. Can have join duration of one time step, but not less.

for simTime=1:numTimeSteps
    % timeis=simTime
    for j=1:numUsers
        % First check if each User is Active
        if ((User(j).JoinTime <= simTime) && (simTime <= (User(j).JoinTime +
User(j).Duration - 1))) % changed from & to && based on auto-recommendation
            % If Active, load the User's location based on the Satellite and Cluster
            % Line below assumes User can only be in one MCGroup at a time
            ClusterActivity(((User(j).Satellite-
1)*numClusters)+User(j).Cluster,simTime)=ClusterActivity(((User(j).Satellite-
1)*numClusters)+User(j).Cluster,simTime)+1;
%ClusterActivity(((User(j).Satellite-
1)*numClusters)+User(j).Cluster,User(j).MCGroup,simTime)=ClusterActivity(((User(j).Satell
ite-1)*numClusters)+User(j).Cluster,User(j).MCGroup,simTime)+1;
            User(j).Active(simTime,1)=1; % Set User Active Flag since it is active

```



```

        % Then check if user just became active during this time slot. If
        % so, then process the rekeying as appropriate.
        if (User(j).JoinTime == simTime) % if true, this is a new user to the
group/cluster
            % Set the flag for the new user
            ClusterTriggers((User(j).Satellite-
1)*numClusters)+User(j).Cluster,simTime)=2;
%ClusterTriggers((User(j).Satellite-
1)*numClusters)+User(j).Cluster,User(j).MCGroup,simTime)=2;
            if User(j).Mobility >1
                User(j).Waiting=1;
            end
            end % Check if just became Active

            if User(j).Mobility >1
                User(j).Waiting=User(j).Waiting+1;
                if (User(j).Mobility==2) % This is the Ground User; 2xfaster than
Sea User
                    if User(j).Waiting ==(numWait*numSpeed*0.5)
                        User(j).Waiting=1;
%if ClusterTriggers((User(j).Satellite-
1)*numClusters)+User(j).Cluster,User(j).MCGroup,simTime)~=2
                        if ClusterTriggers((User(j).Satellite-
1)*numClusters)+User(j).Cluster,simTime)~=2
                            %This triggers the current cluster for the
                            %departing user.
%ClusterTriggers((User(j).Satellite-
1)*numClusters)+User(j).Cluster,User(j).MCGroup,simTime)=1;
                            ClusterTriggers((User(j).Satellite-
1)*numClusters)+User(j).Cluster,simTime)=1;
                        end
                        %Now get a new location, and set the trigger
                        User(j).Satellite = ceil(rand*numSats);
                        User(j).Cluster = ceil(rand*numClusters);
%if ClusterTriggers((User(j).Satellite-
1)*numClusters)+User(j).Cluster,User(j).MCGroup,simTime)~=2
%ClusterTriggers((User(j).Satellite-
1)*numClusters)+User(j).Cluster,User(j).MCGroup,simTime)=1;
                        if ClusterTriggers((User(j).Satellite-
1)*numClusters)+User(j).Cluster,simTime)~=2
                            ClusterTriggers((User(j).Satellite-
1)*numClusters)+User(j).Cluster,simTime)=1;
                            %This triggers the new cluster for the user
                        end
                        end%if User Waiting

                    elseif (User(j).Mobility==3) % This is the Sea User; half as fast as
Ground User
                        if User(j).Waiting ==(numWait*numSpeed)
                            User(j).Waiting=1;
                            if ClusterTriggers((User(j).Satellite-
1)*numClusters)+User(j).Cluster,simTime)~=2
%if ClusterTriggers((User(j).Satellite-
1)*numClusters)+User(j).Cluster,User(j).MCGroup,simTime)~=2
                                %This triggers the current cluster for the
                                %departing user.
                                ClusterTriggers((User(j).Satellite-
1)*numClusters)+User(j).Cluster,simTime)=1;
                            end
                            %Now get a new location, and set the trigger
                            User(j).Satellite = ceil(rand*numSats);
                            User(j).Cluster = ceil(rand*numClusters);
                            if ClusterTriggers((User(j).Satellite-
1)*numClusters)+User(j).Cluster,simTime)~=2
                                ClusterTriggers((User(j).Satellite-
1)*numClusters)+User(j).Cluster,simTime)=1;
                                %This triggers the new cluster for the user
                            end
                            end%if User Waiting

```

```

elseif User(j).Mobility==4 % This is the Air Mover, so moves in
fewest # of TimeSteps
    if User(j).Waiting ==numWait
        User(j).Waiting=1;
        if ClusterTriggers(((User(j).Satellite-
1)*numClusters)+User(j).Cluster,simTime)~=2
            %This triggers the current cluster for the
            %departing user.
            ClusterTriggers(((User(j).Satellite-
1)*numClusters)+User(j).Cluster,simTime)=1;
            end
            %Now get a new location, and set the trigger
            User(j).Satellite = ceil(rand*numSats);
            User(j).Cluster = ceil(rand*numClusters);
            if ClusterTriggers(((User(j).Satellite-
1)*numClusters)+User(j).Cluster,simTime)~=2
                ClusterTriggers(((User(j).Satellite-
1)*numClusters)+User(j).Cluster,simTime)=1;
                %This triggers the new cluster for the user
            end
        end%if User Waiting
    end%if & elseif
end%if User Mobility >1

% Check to see if User just left the MCGroup/System
elseif (simTime == (User(j).JoinTime + User(j).Duration))
    % Set the flag for the leaving user
    ClusterTriggers(((User(j).Satellite-
1)*numClusters)+User(j).Cluster,simTime)=2;

    % Decrement the User's instant key count. If the user leaves,
    % it will definitely drop the key regardless if the
    % Group/Cluster rekeys or not

end %if & elseif

end %j
pause(0);

% Check for joins and leaves. If either a join, a leave, or both
% in the MC Group, then rekey. Otherwise, no need to rekey.

ClusterActivity((numSats*numClusters)+1,simTime)=sum(ClusterActivity(1:(numSats*numClusters),simTime));

ClusterTriggers((numSats*numClusters)+1,simTime)=max(ClusterTriggers(1:(numSats*numClusters),simTime));

if ClusterTriggers((numSats*numClusters)+1,simTime)>=1
    % If true, this means there was some kind of activity in
    % the MCGroup, so all active users must rekey for the Baseline system.
    if ClusterTriggers((numSats*numClusters)+1,NewKeyCheckLoop,simTime)==2
        %If true, there was a new or departing user, so all
        %active users must rekey for the Baseline system.
    end
end

TotalKeysDistribCount(NewKeyCheckLoop,1)=TotalKeysDistribCount(NewKeyCheckLoop,1)+Cluster
Activity((numSats*numClusters)+1,NewKeyCheckLoop,simTime);
% end

% First check which users were active, then see who was
% affected.
for k=1:numUsers
    if User(k).Active(simTime,1)==1
        %If the user is Active, continue. Otherwise move
        %on to next user.
        if ClusterTriggers((numSats*numClusters)+1,simTime)>=1
            %If true, this means a new user joined or left
            %the MCGroup, and therefore all users in the
            %baseline must rekey, as well as all users in
            %the Cluster must key

```

```

%
TotalKeysDistribCount(NewKeyCheckLoop,1)=TotalKeysDistribCount(NewKeyCheckLoop,1)+1;
User(k).TimesRekeyed1 = User(k).TimesRekeyed1+1; % Baseline
System Rekey Count
    end%if ClusterTriggers >=1 at the MCGroup level

    if ClusterTriggers(((User(k).Satellite-
1)*numClusters)+User(k).Cluster,simTime)==2
        %If ClusterTriggers for this cluster==2, then
        %a new user joined or a non-mobile user left.
        %Therefore, both Cluster and Hubenko rekey
        User(k).TimesRekeyed2 = User(k).TimesRekeyed2+1; % Cluster
System Rekey Count
%
TotalKeysDistribCount(NewKeyCheckLoop,2)=TotalKeysDistribCount(NewKeyCheckLoop,2)+1;
%zeros(numMCGroups,numArchitectures);
%
%         if (User(j).JoinTime ~= simTime) && User(j).Waiting~=1
%
%         % If the User did not just join right
%
%         % now, and if the User didn't just move right now,
%
%         % then increment its Hubenko Key count
%
%         User(j).Waiting~=1
%
%         User(k).TimesRekeyed3 = User(k).TimesRekeyed3+1; %
Hubenko System Rekey Count
%
%         end
%
%
TotalKeysDistribCount(NewKeyCheckLoop,3)=TotalKeysDistribCount(NewKeyCheckLoop,3)+1;

    elseif ClusterTriggers(((User(k).Satellite-
1)*numClusters)+User(k).Cluster,simTime)==1
        %If ClusterTriggers for this cluster==1, then
        %a mobile user joined or left the cluster.
        %Therefore, only Cluster rekeys, along with any users that
just moved in the Hubenko case.
        User(k).TimesRekeyed2 = User(k).TimesRekeyed2+1; % Cluster
System Rekey Count
        if User(k).Waiting == 1 % If true, the user just moved, so
increment Hubenko key count
            User(k).TimesRekeyed3 = User(k).TimesRekeyed3+1; %
Hubenko System Rekey Count
        end

%
TotalKeysDistribCount(NewKeyCheckLoop,2)=TotalKeysDistribCount(NewKeyCheckLoop,2)+1;
    end%if ClusterTriggers == 2 or 1
    end%ifActive & MCGroup
    end% for k
end%If Cluster Triggers

% if mod(simTime,3000)==0
%     SimTimeLoopsTaken=simTime
% end

pause(0);
end %simTime

%*****
% Figure out how many times, on average, each mobility type re-keyed

MobilityHist=[User.Mobility]; %this gives # of each type

for i=1:numUsers
    if User(i).Mobility == 1
        AvgKeySummaryPlot1(h,1)=AvgKeySummaryPlot1(h,1)+User(i).TimesRekeyed1;
        AvgKeySummaryPlot2(h,1)=AvgKeySummaryPlot2(h,1)+User(i).TimesRekeyed2;
        AvgKeySummaryPlot3(h,1)=AvgKeySummaryPlot3(h,1)+User(i).TimesRekeyed3;
    elseif User(i).Mobility == 2
        AvgKeySummaryPlot1(h,2)=AvgKeySummaryPlot1(h,2)+User(i).TimesRekeyed1;
        AvgKeySummaryPlot2(h,2)=AvgKeySummaryPlot2(h,2)+User(i).TimesRekeyed2;
        AvgKeySummaryPlot3(h,2)=AvgKeySummaryPlot3(h,2)+User(i).TimesRekeyed3;
    elseif User(i).Mobility == 3

```

```

        AvgKeySummaryPlot1(h,3)=AvgKeySummaryPlot1(h,3)+User(i).TimesRekeyed1;
        AvgKeySummaryPlot2(h,3)=AvgKeySummaryPlot2(h,3)+User(i).TimesRekeyed2;
        AvgKeySummaryPlot3(h,3)=AvgKeySummaryPlot3(h,3)+User(i).TimesRekeyed3;
    else
        AvgKeySummaryPlot1(h,4)=AvgKeySummaryPlot1(h,4)+User(i).TimesRekeyed1;
        AvgKeySummaryPlot2(h,4)=AvgKeySummaryPlot2(h,4)+User(i).TimesRekeyed2;
        AvgKeySummaryPlot3(h,4)=AvgKeySummaryPlot3(h,4)+User(i).TimesRekeyed3;
    end %end if

end %for i=numUsers Loop
% Now average each of the summaries out using the precalculated number in
% each mobility type
pause(0);
AvgKeySummaryPlot1(h,:)=AvgKeySummaryPlot1(h,:)./MobilityHistPlot(h,:);
AvgKeySummaryPlot2(h,:)=AvgKeySummaryPlot2(h,:)./MobilityHistPlot(h,:);
AvgKeySummaryPlot3(h,:)=AvgKeySummaryPlot3(h,:)./MobilityHistPlot(h,:);
%*****

% All of the User's different Keys
UserKeys1=[User.TimesRekeyed1];
UserKeys2=[User.TimesRekeyed2];
UserKeys3=[User.TimesRekeyed3];
% Only the Control Group's keys
HalfUserKeys1=UserKeys1(1:(numUsers*ControlGroupSize));
HalfUserKeys2=UserKeys2(1:(numUsers*ControlGroupSize));
HalfUserKeys3=UserKeys3(1:(numUsers*ControlGroupSize));

SumUserKeys1=sum(UserKeys1);
SumUserKeys2=sum(UserKeys2);
SumUserKeys3=sum(UserKeys3);
SumHalfUserKeys1=sum(HalfUserKeys1);
SumHalfUserKeys2=sum(HalfUserKeys2);
SumHalfUserKeys3=sum(HalfUserKeys3);

TotalKeysDistribCount(h,:,g)=[SumUserKeys1 SumUserKeys2 SumUserKeys3];
TotalHalfKeysDistribCount(h,:,g)=[SumHalfUserKeys1 SumHalfUserKeys2 SumHalfUserKeys3];

AverageUserKeys1=SumUserKeys1/numUsers;
AverageUserKeys2=SumUserKeys2/numUsers;
AverageUserKeys3=SumUserKeys3/numUsers;
AverageUserKeys=[AverageUserKeys1 AverageUserKeys2 AverageUserKeys3];
AverageHalfUserKeys1=SumHalfUserKeys1/(numUsers*ControlGroupSize);
AverageHalfUserKeys2=SumHalfUserKeys2/(numUsers*ControlGroupSize);
AverageHalfUserKeys3=SumHalfUserKeys3/(numUsers*ControlGroupSize);
AverageHalfUserKeys=[AverageHalfUserKeys1 AverageHalfUserKeys2 AverageHalfUserKeys3];

figure,bar(AverageUserKeys)
xlabel('Architecture');
set(gca,'XTickLabel',{'Baseline','Cluster','Hubenko'})
ylabel('Average Times Rekeyed');
% XMinorTick off
% YMinorTick off
title(['Average Number of Times Each User is Rekeyed'];['for the Different Architectures'];['Time Steps:',num2str(numTimeSteps),', Users:',num2str(numUsers),', MCGroups:',num2str(numMCGroups),', Sats:',num2str(numSats),', Clust:',num2str(numClusters)];[' Baseline:',num2str(AverageUserKeys1),', Cluster:',num2str(AverageUserKeys2),', Hubenko:',num2str(AverageUserKeys3)]])
set(gcf, 'PaperPositionMode', 'manual');
set(gcf, 'PaperUnits', 'inches');
set(gcf, 'PaperPosition', [1 1 4.9 3.7]);

PlotJoinTimeUserKeys=[User.TimesRekeyed1; User.TimesRekeyed2; User.TimesRekeyed3; User.JoinTime];
figure,bar(PlotJoinTimeUserKeys')
title(['Join Time Vs User Times Rekeyed'])
legend('Baseline Keys','Cluster Keys','Hubenko Keys','Time Joined');

PlotClusterActivity=zeros(1,numTimeSteps);
PlotClusterActivity(:,:)=ClusterActivity((numSats*numClusters)+1,1,:);
figure,plot(PlotClusterActivity)

```

```

xlabel('Time Step');
ylabel('Number of Current Active Users');
title(['Number of Current Active Users Out of ',num2str(numUsers),' Possible Users'];
['Time Steps:',num2str(numTimeSteps),' Satellites:',num2str(numSats),' Clusters:',num2str(numClusters)];
%
PlotClusterTriggers=zeros(1,numTimeSteps);
PlotClusterTriggers(:,:)=ClusterTriggers((numSats*numClusters)+1,1,:);
figure,plot(PlotClusterTriggers)
xlabel('Time Step');
ylabel('Cluster Trigger');
title(['Cluster Triggers. 2 = new or leave, 1 = moving, 0 = no change']))

DensityVsRekeys(h,:,g)=AvearageUserKeys;
DensityVsHalfRekeys(h,:,g)=AvearageHalfUserKeys;

% path = 'D:\Victor Data\1 - Dissertation Work\Matlab Files\';
path = 'D:\Victor Workstation Data\Workstation Matlab Files\';
% %
filename = [path 'Mobility Analysis-Sat-' num2str(numSats) '-Clus-'
num2str(numClusters) '-Mov-' num2str(numMoving) '-Its-' num2str(numIterations) '-TS-'
num2str(numTimeSteps) '-' index '.txt'];
dlmwrite(filename, AvearageUserKeys, '-append', 'delimiter', '\t', 'precision', 6);

% Clear EVERYTHING except "DensityVsRekeys"
% Changed 27 Feb 07 clear numUsers;
%clear UserKeyCount;
%clear MCGroupKeys;
%clear TotalKeysDistribCount;
clear ClusterActivity;
clear ClusterTriggers;
clear User;
clear SimTimeLoopsTaken;
clear InitializeUsersLoopsTaken;
clear simTime;
%clear NewKeyCheckLoop;
clear i;
clear j;
clear k;
% clear TotalKeyscheckfor1;
% clear TotalKeyscheckfor2;
% clear TotalKeyscheckfor3;
clear UserKeys1;
clear UserKeys2;
clear UserKeys3;
clear HalfUserKeys1;
clear HalfUserKeys2;
clear HalfUserKeys3;
clear AverageUserKeys1;
clear AverageUserKeys2;
clear AverageUserKeys3;
clear AvearageUserKeys;
clear AverageHalfUserKeys1;
clear AverageHalfUserKeys2;
clear AverageHalfUserKeys3;
clear AvearageHalfUserKeys;

clear PlotClusterActivity;
clear MobilityHist;

pause(0);

end % for g=1:SampleSize loop

if mod(h,20)==0
    IterationsTaken=h
    NumberOfIterations=numIterations
    toc
end

```

```

UpdateNote=strcat('cmd /c "net send /domain:enxp401x "Iteration #',num2str(iter),'
completed."');
system(UpdateNote);    %USE THIS ONE FOR AN UPDATE ON EACH TRIAL

if mod(h,numDataPoints)==0
    UpdateNote=strcat('cmd /c "net send /domain:enxp401x "Iter# ',num2str(h),' of
',num2str(numIterations),'-',VersionName,'."');
    system(UpdateNote);
end

%end "h" loop here for iterations of number of users, then plot out results
end

% Now Compute the Confidence Intervals:
% % [+ B - + C - + H - ...] Where B, C, H are the means for the SampleSize,
% % + is the Top of the confidence interval, - is the Bottom of the
% % Confidence Interval
% TotalKeysDistribCountPlot=zeros(numIterations,3*numArchitectures);
% TotalHalfKeysDistribCountPlot=zeros(numIterations,3*numArchitectures);
% DensityVsRekeysPlot=zeros(numIterations,3*numArchitectures);
% DensityVsHalfRekeysPlot=zeros(numIterations,3*numArchitectures);

% xMeanArray is the mean array for each of the above arrays
% NOTE: mean(x,3) produces the mean in the third dimension, namely the repeated samples
TKDMeanArray=mean(TotalKeysDistribCount,3);
THKDMeanArray=mean(TotalHalfKeysDistribCount,3);
DVRMeanArray=mean(DensityVsRekeys,3);
DVHRMeanArray=mean(DensityVsHalfRekeys,3);

% % xSampleSDArray is the sample standard deviation array for each of the above arrays
% NOTE: s = std(X,flag,dim) computes the standard deviations along the
% dimension of X specified by scalar dim. Set flag to 0 to normalize
% Y by n-1; set flag to 1 to normalize by n.
% Using std(x,0,3) for ssd across the sample size
TKDSampleSDArray=std(TotalKeysDistribCount,0,3);
THKDSampleSDArray=std(TotalHalfKeysDistribCount,0,3);
DVRSampleSDArray=std(DensityVsRekeys,0,3);
DVHRSampleSDArray=std(DensityVsHalfRekeys,0,3);

% % The Coefficient of Variation (C.O.V.) [Jai91], is the ratio of standard
% deviation to sample mean: xSampleSDArray/xMeanArray.
COVTKD=TKDSampleSDArray./TKDMeanArray;
COVTHKD=THKDSampleSDArray./THKDMeanArray;
COVDVR=DVRSampleSDArray./DVRMeanArray;
COVDVHR=DVHRSampleSDArray./DVHRMeanArray;

% XBar= ; %means for each set of identical runs
%n=SampleSize
%sqrtofn=sqrt(SampleSize)
%SampleSD= Sample Standard Deviation
%use alpha05 for 90% CI, alpha025 for 95% CI
%tAlphaHalf= alpha025(SampleSize-1); %Value of t Alpha over 2 per table

% Confidence Interval (+) = Xbar + (tAlphaHalf*SampleSD/sqrtofn)
% Confidence Interval (-) = Xbar - (tAlphaHalf*SampleSD/sqrtofn)

for statA=1:numArchitectures

    %Put the Means in place:
    TotalKeysDistribCountPlot(:,(3*statA)-1)=TKDMeanArray(:,statA);
    TotalHalfKeysDistribCountPlot(:,(3*statA)-1)=THKDMeanArray(:,statA);
    DensityVsRekeysPlot(:,(3*statA)-1)=DVRMeanArray(:,statA);
    DensityVsHalfRekeysPlot(:,(3*statA)-1)=DVHRMeanArray(:,statA);

    %Now Calculate the + CI Bounds
    TotalKeysDistribCountPlot(:,(3*statA)-2)=TotalKeysDistribCountPlot(:,(3*statA)-
1)+(tAlphaHalf*TKDSampleSDArray(:,statA)/sqrtofn);
    TotalHalfKeysDistribCountPlot(:,(3*statA)-
2)=TotalHalfKeysDistribCountPlot(:,(3*statA)-
1)+(tAlphaHalf*THKDSampleSDArray(:,statA)/sqrtofn);

```

```

        DensityVsRekeysPlot(:, (3*statA)-2)=DensityVsRekeysPlot(:, (3*statA)-
1)+(tAlphaHalf*DVRSampleSDArray(:,statA)/sqrtofn);
        DensityVsHalfRekeysPlot(:, (3*statA)-2)=DensityVsHalfRekeysPlot(:, (3*statA)-
1)+(tAlphaHalf*DVHRSampleSDArray(:,statA)/sqrtofn);

        %Now Calculate the - CI Bounds
        TotalKeysDistribCountPlot(:, (3*statA))=TotalKeysDistribCountPlot(:, (3*statA)-1)-
(tAlphaHalf*TKDSampleSDArray(:,statA)/sqrtofn);

TotalHalfKeysDistribCountPlot(:, (3*statA))=TotalHalfKeysDistribCountPlot(:, (3*statA)-1)-
(tAlphaHalf*THKDSampleSDArray(:,statA)/sqrtofn);
        DensityVsRekeysPlot(:, (3*statA))=DensityVsRekeysPlot(:, (3*statA)-1)-
(tAlphaHalf*DVRSampleSDArray(:,statA)/sqrtofn);
        DensityVsHalfRekeysPlot(:, (3*statA))=DensityVsHalfRekeysPlot(:, (3*statA)-1)-
(tAlphaHalf*DVHRSampleSDArray(:,statA)/sqrtofn);

        end % for statA

pause(0);

figurebox = figure;
subplot(2,2,1),bar(MobilityHistPlot(ceil(numDataPoints*0.25),:))%,MobilityBins)    Changed
from Hist to Bar
    xlabel(' (a) ', 'FontWeight','bold');
    set(gca,'XTickLabel',{'Stationary';'Ground';'Sea';'Air'}, 'FontWeight','bold')
    ylabel('Number of Users', 'FontWeight','bold');
    title(['User Mobility Distribution for
???' num2str(numSats*numClusters*numDataPoints*0.25), ' Users. (Iteration
',num2str(numDataPoints*0.25),')'], 'FontWeight','bold');
%See if need to reset numUsers with numUsers=FirstStep*numDataPoints
    hfinder = findobj(gca,'Type','patch');
    set(hfinder,'FaceColor','b','EdgeColor','w')

    subplot(2,2,2),bar(MobilityHistPlot(ceil(numDataPoints*0.5),:))%,MobilityBins)
    xlabel(' (b) ', 'FontWeight','bold');
    set(gca,'XTickLabel',{'Stationary';'Ground';'Sea';'Air'}, 'FontWeight','bold')
    ylabel('Number of Users', 'FontWeight','bold');
    title(['User Mobility Distribution for
???' num2str(numSats*numClusters*numDataPoints*0.5), ' Users. (Iteration
',num2str(numDataPoints*0.5),')'], 'FontWeight','bold');
    hfinder = findobj(gca,'Type','patch');
    set(hfinder,'FaceColor','b','EdgeColor','w')

    subplot(2,2,3),bar(MobilityHistPlot(ceil(numDataPoints*0.75),:))%,MobilityBins)
    xlabel(' (c) ', 'FontWeight','bold');
    set(gca,'XTickLabel',{'Stationary';'Ground';'Sea';'Air'}, 'FontWeight','bold')
    ylabel('Number of Users', 'FontWeight','bold');
    title(['User Mobility Distribution for
???' num2str(numSats*numClusters*numDataPoints*0.75), ' Users. (Iteration
',num2str(numDataPoints*0.75),')'], 'FontWeight','bold');
    hfinder = findobj(gca,'Type','patch');
    set(hfinder,'FaceColor','b','EdgeColor','w')

    subplot(2,2,4),bar(MobilityHistPlot(numDataPoints,:))%,MobilityBins)
    xlabel(' (d) ', 'FontWeight','bold');
    set(gca,'XTickLabel',{'Stationary';'Ground';'Sea';'Air'}, 'FontWeight','bold')
    ylabel('Number of Users', 'FontWeight','bold');
    title(['User Mobility Distribution for ???' num2str(numSats*numClusters*numDataPoints), '
Users. (Iteration ',num2str(numDataPoints),')'], 'FontWeight','bold');
    hfinder = findobj(gca,'Type','patch');
    set(hfinder,'FaceColor','b','EdgeColor','w')

% Create textbox
annotation1 = annotation(...
    figurebox,'textbox',...
    'LineStyle','none',...    % no outline box
    'Position',[0.417 0.96 0.2 0.02],...    % [left, bottom, width, height]
    'HorizontalAlignment','center',...
    'FontWeight','bold',...
    'FitHeightToText','off',...

```

```

    'String', {num2str(TimeStamp)});

DateStamp=num2str(datestr(now,30));
FigNum=FigNum+1;
FigName=strcat(DateStamp,VersionName,num2str(FigNum),'.fig');
saveas(gcf,FigName)
%print('-dmeta', '-r1200', FigName);

tickmarksforx=zeros(1,numIterations);
for tickmaker=1:numIterations
    tickmarksforx(1,tickmaker)=tickmaker;
end

%figure,[AX,H1,H2] = plotyy(X,Y1,X,Y2,DensityVsRekeys,JoinFactor); %,'plot');
% Turn Plot Colors on and off
%set(0,'DefaultAxesLineStyleOrder',{'-',':','--'}) % setting a default value for the
axes LineStyleOrder property
% s = square, o = o, d = diamond
%set(0,'DefaultAxesColorOrder',[0,0,0]) % Sets default line color to black (see
"ColorSpec" for colors)
% set(0,'DefaultAxesLineStyleOrder','-|---|:',...
% 'DefaultLineLineWidth',1.5) %'DefaultAxesColorOrder',[1 0 0;0
1 0;0 0 1],...
% '-',':o','--x' {'-*',':','o'} , 'LineWidth',2
% % Dual plot on single axes
% figure,[ax,h1,h2] = plotyy(IterationsAxis, JoinFactor, IterationsAxis,
DensityVsRekeys);
% % grid on
% ylabel('Rate of Mobility','FontWeight','bold'); % puts a label on the left axis.
% axes(ax(2)) % makes the 2nd yaxis the current axis.
% xlabel('Iteration','FontWeight','bold'); % puts a label on the X axis
% ylabel('Average Times Rekeyed','FontWeight','bold'); % puts a label on the right axis
% legend('Baseline','Cluster','Hubenko');
% %title({'Average Number of Times Each User is Rekeyed vs. increasing Join Factor
(Higher JF=Slower Join Rate)'};['JoinFactor Varies and Nobody Leaves. Last Iteration
Average Users per Cluster= ',num2str(numUsers/(numSats*numClusters))];['Time
Steps:',num2str(numTimeSteps),', Satellites:',num2str(numSats),',
Clusters:',num2str(numClusters),', numMoving:',num2str(numMoving)];['IterFactor:
',num2str(numDataPoints),', IterSteps:',num2str(numIterSteps),',
numWait:',num2str(numWait),', numSpeed:',num2str(numSpeed))])
% % title({'Average Number of Times Each User is Rekeyed vs. increasing Join Factor
(Higher JF=Slower Join Rate)'};['JoinFactor Varies and Nobody Leaves. Last Iteration
Average Users per Cluster= ',num2str(numUsers/(numSats*numClusters))];['Time
Steps:',num2str(numTimeSteps),', Satellites:',num2str(numSats),',
Clusters:',num2str(numClusters),', numMoving:',num2str(numMoving),',
numWait:',num2str(numWait),', numSpeed:',num2str(numSpeed)];['IterFactor:
',num2str(numDataPoints),', IterSteps:',num2str(numIterSteps),',
RunVersion=',RunVersion]})
% title({'Average Number of Times Each User is Rekeyed vs. Increasing Mobility and
Increasing User Density'};['Last Iteration Average Users per Cluster =
',num2str(numUsers/(numSats*numClusters)),'. JoinFactor held constant at
',num2str(JoinTimeSetter)];['Time Steps: ',num2str(numTimeSteps),', Satellites:
',num2str(numSats),', Clusters: ',num2str(numClusters),', numMoving:
',num2str(numMoving),', numWait: ',num2str(numWait),', numSpeed:
',num2str(numSpeed)];['IterFactor: ',num2str(numDataPoints),', IterSteps:
',num2str(numIterSteps),', RunVersion = ',RunVersion,
',num2str(TimeStamp)]}, 'FontWeight','bold')

set(0,'DefaultLineLineWidth',1.5)
%figure,plot(IterationsAxis, DensityVsRekeys);

%*****
% These lines below name each on of the lines, and gives them their
% linestyle. They will then show up in the legend with the given names.
% set(plot2(2),'DisplayName','Baseline');
% set(plot2(5),'DisplayName','Cluster','LineStyle','--');
% set(plot2(8),'DisplayName','Hubenko','LineStyle',':');
%
% xlabel('Iteration','FontWeight','bold');
% ylabel('Average Times Rekeyed','FontWeight','bold');

```



```

%
% %These lines below turn off the HandleVisibility for the lines that I don't
% %want to show up in the legend. Be sure to call Legend after the lines are
% %"shut off" otherwise the lines will still end up in the legend.
% set(plot2(1),'HandleVisibility','off');
% set(plot2(3),'HandleVisibility','off');
% set(plot2(4),'HandleVisibility','off');
% set(plot2(6),'HandleVisibility','off');
% set(plot2(7),'HandleVisibility','off');
% set(plot2(9),'HandleVisibility','off');
% legend('Location','NorthWest');
%*****

% s = square, o = o, d = diamond
%set(0,'DefaultAxesColorOrder',[0,0,0]) % Sets default line color to black (see
"ColorSpec" for colors)
% set(0,'DefaultAxesLineStyleOrder','-|--|:',...
% 'DefaultLineLineWidth',1.5) %'DefaultAxesColorOrder',[1 0 0;0
1 0;0 0 1],...
% '-','o','--x' {'-*',':', 'o'} style color marker

figure,plot2 = plot(IterationsAxis, DensityVsRekeysPlot);
set(plot2(2),'DisplayName','Baseline','LineStyle','-','Marker','s','Color','b');
set(plot2(5),'DisplayName','Cluster','LineStyle','--','Marker','o','Color',[0 0.5 0]);
set(plot2(8),'DisplayName','Hubenko','LineStyle',':', 'Marker','d','Color','r');
set(plot2(1),'LineStyle',':', 'Color','b','HandleVisibility','off');
set(plot2(3),'LineStyle',':', 'Color','b','HandleVisibility','off');
set(plot2(4),'LineStyle',':', 'Color',[0 0.5 0],'HandleVisibility','off');
set(plot2(6),'LineStyle',':', 'Color',[0 0.5 0],'HandleVisibility','off');
set(plot2(7),'LineStyle',':', 'Color','r','HandleVisibility','off');
set(plot2(9),'LineStyle',':', 'Color','r','HandleVisibility','off');
legend('Location','NorthWest');
xlabel('Iteration','FontWeight','bold');
ylabel('Average Times Rekeyed','FontWeight','bold');
%legend('Baseline','Cluster','Hubenko','Location','NorthWest');
%title(['Average Number of Times Each User is Rekeyed vs. increasing Join Factor (Higher
JF=Slower Join Rate)'];['JoinFactor Varies and Nobody Leaves. Last Iteration Average
Users per Cluster= ',num2str(numUsers/(numSats*numClusters))];['Time
Steps:',num2str(numTimeSteps)', ' Satellites:',num2str(numSats)',
Clusters:',num2str(numClusters)', ' numMoving:',num2str(numMoving)];['IterFactor:
',num2str(numDataPoints)', ' IterSteps:',num2str(numIterSteps)',
numWait:',num2str(numWait)', ' numSpeed:',num2str(numSpeed)])
% title(['Average Number of Times Each User is Rekeyed vs. increasing Join Factor
(Higher JF=Slower Join Rate)'];['JoinFactor Varies and Nobody Leaves. Last Iteration
Average Users per Cluster= ',num2str(numUsers/(numSats*numClusters))];['Time
Steps:',num2str(numTimeSteps)', ' Satellites:',num2str(numSats)',
Clusters:',num2str(numClusters)', ' numMoving:',num2str(numMoving)',
numWait:',num2str(numWait)', ' numSpeed:',num2str(numSpeed)];['IterFactor:
',num2str(numDataPoints)', ' IterSteps:',num2str(numIterSteps)',
RunVersion=',RunVersion'])
title(['Average Number of Times Each User is Rekeyed (All Users)'];['Last Iteration
Average Users per Cluster = ',num2str(numUsers/(numSats*numClusters))', ' JoinFactor held
constant at ',num2str(JoinTimeSetter)];['Time Steps: ',num2str(numTimeSteps)',
Satellites: ',num2str(numSats)', ' Clusters: ',num2str(numClusters)', ' numMoving:
',num2str(numMoving)', ' numWait: ',num2str(numWait)', ' numSpeed:
',num2str(numSpeed)];['Number of Data Points: ',num2str(numDataPoints)', ' Number of Sets:
',num2str(numSets)', ' RunVersion = ',RunVersion,
',num2str(TimeStamp)]','FontWeight','bold')

FigNum=FigNum+1;
FigName=strcat(DateStamp,VersionName,num2str(FigNum),'.fig');
saveas(gcf, FigName)
%print('-dmeta', '-r1200', FigName);

%figure,semilogy(IterationsAxis, DensityVsRekeys);
figure,semilogy3 = semilogy(IterationsAxis, DensityVsRekeysPlot);
set(semilogy3(2),'DisplayName','Baseline','LineStyle','-','Marker','s','Color','b');
set(semilogy3(5),'DisplayName','Cluster','LineStyle','--','Marker','o','Color',[0 0.5
0]);
set(semilogy3(8),'DisplayName','Hubenko','LineStyle',':', 'Marker','d','Color','r');

```

```

set(semilogy3(1),'LineStyle',':', 'Color','b','HandleVisibility','off');
set(semilogy3(3),'LineStyle',':', 'Color','b','HandleVisibility','off');
set(semilogy3(4),'LineStyle',':', 'Color',[0 0.5 0],'HandleVisibility','off');
set(semilogy3(6),'LineStyle',':', 'Color',[0 0.5 0],'HandleVisibility','off');
set(semilogy3(7),'LineStyle',':', 'Color','r','HandleVisibility','off');
set(semilogy3(9),'LineStyle',':', 'Color','r','HandleVisibility','off');
legend('Location','NorthWest');
xlabel('Iteration','FontWeight','bold');
ylabel('Average Times Rekeyed (log scale)','FontWeight','bold');
%legend('Baseline','Cluster','Hubenko','Location','NorthWest');
%title(['Average Number of Times Each User is Rekeyed vs. increasing Join Factor (Higher
JF=Slower Join Rate)'];['JoinFactor Varies and Nobody Leaves. Last Iteration Average
Users per Cluster= ',num2str(numUsers/(numSats*numClusters))];['Time
Steps:',num2str(numTimeSteps),', Satellites:',num2str(numSats),',
Clusters:',num2str(numClusters),', numMoving:',num2str(numMoving)];['IterFactor:
',num2str(numDataPoints),', IterSteps:',num2str(numIterSteps),',
numWait:',num2str(numWait),', numSpeed:',num2str(numSpeed)]]);
% title(['Average Number of Times Each User is Rekeyed vs. increasing Join Factor
(Higher JF=Slower Join Rate)'];['JoinFactor Varies and Nobody Leaves. Last Iteration
Average Users per Cluster= ',num2str(numUsers/(numSats*numClusters))];['Time
Steps:',num2str(numTimeSteps),', Satellites:',num2str(numSats),',
Clusters:',num2str(numClusters),', numMoving:',num2str(numMoving),',
numWait:',num2str(numWait),', numSpeed:',num2str(numSpeed)];['IterFactor:
',num2str(numDataPoints),', IterSteps:',num2str(numIterSteps),',
RunVersion=',RunVersion]]);
title(['Average Number of Times Each User is Rekeyed (All Users)'];['Last Iteration
Average Users per Cluster = ',num2str(numUsers/(numSats*numClusters)),'. JoinFactor held
constant at ',num2str(JoinTimeSetter)];['Time Steps: ',num2str(numTimeSteps),',
Satellites: ',num2str(numSats),', Clusters: ',num2str(numClusters),', numMoving:
',num2str(numMoving),', numWait: ',num2str(numWait),', numSpeed:
',num2str(numSpeed)];['Number of Data Points: ',num2str(numDataPoints),', Number of Sets:
',num2str(numSets),', RunVersion = ',RunVersion,
',num2str(TimeStamp)]'],'FontWeight','bold')

FigNum=FigNum+1;
FigName=strcat(DateStamp,VersionName,num2str(FigNum),'.fig');
saveas(gcf,FigName)
%print('-dmeta', '-r1200', FigName);

%figure,plot(IterationsAxis, DensityVsHalfRekeys);
figure,plot4 = plot(IterationsAxis, DensityVsHalfRekeysPlot);
set(plot4(2),'DisplayName','Baseline','LineStyle','-', 'Marker','s','Color','b');
set(plot4(5),'DisplayName','Cluster','LineStyle','--', 'Marker','o','Color',[0 0.5 0]);
set(plot4(8),'DisplayName','Hubenko','LineStyle',':', 'Marker','d','Color','r');
set(plot4(1),'LineStyle',':', 'Color','b','HandleVisibility','off');
set(plot4(3),'LineStyle',':', 'Color','b','HandleVisibility','off');
set(plot4(4),'LineStyle',':', 'Color',[0 0.5 0],'HandleVisibility','off');
set(plot4(6),'LineStyle',':', 'Color',[0 0.5 0],'HandleVisibility','off');
set(plot4(7),'LineStyle',':', 'Color','r','HandleVisibility','off');
set(plot4(9),'LineStyle',':', 'Color','r','HandleVisibility','off');
legend('Location','NorthWest');
xlabel('Iteration','FontWeight','bold');
ylabel('Average Times Rekeyed','FontWeight','bold');
%legend('Baseline','Cluster','Hubenko','Location','NorthWest');
%title(['Average Number of Times Each User is Rekeyed vs. increasing Join Factor (Higher
JF=Slower Join Rate)'];['JoinFactor Varies and Nobody Leaves. Last Iteration Average
Users per Cluster= ',num2str(numUsers/(numSats*numClusters))];['Time
Steps:',num2str(numTimeSteps),', Satellites:',num2str(numSats),',
Clusters:',num2str(numClusters),', numMoving:',num2str(numMoving)];['IterFactor:
',num2str(numDataPoints),', IterSteps:',num2str(numIterSteps),',
numWait:',num2str(numWait),', numSpeed:',num2str(numSpeed)]]);
% title(['Average Number of Times Each User is Rekeyed vs. increasing Join Factor
(Higher JF=Slower Join Rate)'];['JoinFactor Varies and Nobody Leaves. Last Iteration
Average Users per Cluster= ',num2str(numUsers/(numSats*numClusters))];['Time
Steps:',num2str(numTimeSteps),', Satellites:',num2str(numSats),',
Clusters:',num2str(numClusters),', numMoving:',num2str(numMoving),',
numWait:',num2str(numWait),', numSpeed:',num2str(numSpeed)];['IterFactor:
',num2str(numDataPoints),', IterSteps:',num2str(numIterSteps),',
RunVersion=',RunVersion]]);

```

```

title({'Average Number of Times Each User is Rekeyed (Control Group=
',num2str(ControlGroupSize*100),'% of all Users)'};['Last Iteration Average Users per
Cluster = ',num2str(numUsers/(numSats*numClusters))','. JoinFactor held constant at
',num2str(JoinTimeSetter)];['Time Steps: ',num2str(numTimeSteps),'', Satellites:
',num2str(numSats),'', Clusters: ',num2str(numClusters),'', numMoving:
',num2str(numMoving),'', numWait: ',num2str(numWait),'', numSpeed:
',num2str(numSpeed)];['Number of Data Points: ',num2str(numDataPoints),'', Number of Sets:
',num2str(numSets),' RunVersion = ',RunVersion,'
',num2str(TimeStamp)]},'FontWeight','bold')

FigNum=FigNum+1;
FigName=strcat(DateStamp,VersionName,num2str(FigNum),'.fig');
saveas(gcf, FigName)
%print('-dmeta', '-r1200', FigName);

%figure,semilogy(IterationsAxis, DensityVsHalfRekeys);
figure,semilogy5 = semilogy(IterationsAxis, DensityVsHalfRekeysPlot);
set(semilogy5(2),'DisplayName','Baseline','LineStyle','-','Marker','s','Color','b');
set(semilogy5(5),'DisplayName','Cluster','LineStyle','--','Marker','o','Color',[0 0.5
0]);
set(semilogy5(8),'DisplayName','Hubenko','LineStyle',':', 'Marker','d','Color','r');
set(semilogy5(1),'LineStyle',':', 'Color','b','HandleVisibility','off');
set(semilogy5(3),'LineStyle',':', 'Color','b','HandleVisibility','off');
set(semilogy5(4),'LineStyle',':', 'Color',[0 0.5 0],'HandleVisibility','off');
set(semilogy5(6),'LineStyle',':', 'Color',[0 0.5 0],'HandleVisibility','off');
set(semilogy5(7),'LineStyle',':', 'Color','r','HandleVisibility','off');
set(semilogy5(9),'LineStyle',':', 'Color','r','HandleVisibility','off');
legend('Location','NorthWest');
xlabel('Iteration','FontWeight','bold');
ylabel('Average Times Rekeyed (log scale)','FontWeight','bold');
%legend('Baseline','Cluster','Hubenko','Location','NorthWest');
%title({'Average Number of Times Each User is Rekeyed vs. increasing Join Factor (Higher
JF=Slower Join Rate)'};['JoinFactor Varies and Nobody Leaves. Last Iteration Average
Users per Cluster= ',num2str(numUsers/(numSats*numClusters))];['Time
Steps: ',num2str(numTimeSteps),'', Satellites:',num2str(numSats),'',
Clusters:',num2str(numClusters),'', numMoving:',num2str(numMoving)];['IterFactor:
',num2str(numDataPoints),'', IterSteps:',num2str(numIterSteps),'',
numWait:',num2str(numWait),'', numSpeed:',num2str(numSpeed)])
% title({'Average Number of Times Each User is Rekeyed vs. increasing Join Factor
(Higher JF=Slower Join Rate)'};['JoinFactor Varies and Nobody Leaves. Last Iteration
Average Users per Cluster= ',num2str(numUsers/(numSats*numClusters))];['Time
Steps: ',num2str(numTimeSteps),'', Satellites:',num2str(numSats),'',
Clusters:',num2str(numClusters),'', numMoving:',num2str(numMoving),'',
numWait:',num2str(numWait),'', numSpeed:',num2str(numSpeed)];['IterFactor:
',num2str(numDataPoints),'', IterSteps:',num2str(numIterSteps),'',
RunVersion=',RunVersion']})
title({'Average Number of Times Each User is Rekeyed (Control Group=
',num2str(ControlGroupSize*100),'% of all Users)'};['Last Iteration Average Users per
Cluster = ',num2str(numUsers/(numSats*numClusters))','. JoinFactor held constant at
',num2str(JoinTimeSetter)];['Time Steps: ',num2str(numTimeSteps),'', Satellites:
',num2str(numSats),'', Clusters: ',num2str(numClusters),'', numMoving:
',num2str(numMoving),'', numWait: ',num2str(numWait),'', numSpeed:
',num2str(numSpeed)];['Number of Data Points: ',num2str(numDataPoints),'', Number of Sets:
',num2str(numSets),' RunVersion = ',RunVersion,'
',num2str(TimeStamp)]},'FontWeight','bold')

FigNum=FigNum+1;
FigName=strcat(DateStamp,VersionName,num2str(FigNum),'.fig');
saveas(gcf, FigName)
%print('-dmeta', '-r1200', FigName);

% set(0,'DefaultLineLineWidth',1.5)
% figure,plot(IterationsAxis, DensityVsRekeys);
% % ylabel('Rate of Mobility','FontWeight','bold'); % puts a label on the left axis.
% % axes(ax(2)) % makes the 2nd yaxsis the current axis.
% xlabel('Iteration','FontWeight','bold');
% ylabel('Average Times Rekeyed','FontWeight','bold');
% legend('Baseline','Cluster','Hubenko');
% %title({'Average Number of Times Each User is Rekeyed vs. increasing Join Factor
(Higher JF=Slower Join Rate)'};['JoinFactor Varies and Nobody Leaves. Last Iteration

```

```

Average Users per Cluster= ',num2str(numUsers/(numSats*numClusters))');['Time
Steps:',num2str(numTimeSteps),',', Satellites:',num2str(numSats),',',
Clusters:',num2str(numClusters),',', numMoving:',num2str(numMoving)];['IterFactor:
',num2str(numDataPoints),',', IterSteps:',num2str(numIterSteps),',',
numWait:',num2str(numWait),',', numSpeed:',num2str(numSpeed)]]))
% % title({'Average Number of Times Each User is Rekeyed vs. increasing Join Factor
(Higher JF=Slower Join Rate)'};['JoinFactor Varies and Nobody Leaves. Last Iteration
Average Users per Cluster= ',num2str(numUsers/(numSats*numClusters))');['Time
Steps:',num2str(numTimeSteps),',', Satellites:',num2str(numSats),',',
Clusters:',num2str(numClusters),',', numMoving:',num2str(numMoving),',',
numWait:',num2str(numWait),',', numSpeed:',num2str(numSpeed)'];['IterFactor:
',num2str(numDataPoints),',', IterSteps:',num2str(numIterSteps),',',
RunVersion=',RunVersion']]
% title({'Average Number of Times Each User is Rekeyed vs. Increasing Mobility and
Increasing User Density'};['Last Iteration Average Users per Cluster =
',num2str(numUsers/(numSats*numClusters)),'. JoinFactor held constant at
',num2str(JoinTimeSetter)];['Time Steps: ',num2str(numTimeSteps),',', Satellites:
',num2str(numSats),',', Clusters: ',num2str(numClusters),',', numMoving:
',num2str(numMoving),',', numWait: ',num2str(numWait),',', numSpeed:
',num2str(numSpeed)'];['IterFactor: ',num2str(numDataPoints),',', IterSteps:
',num2str(numIterSteps),',', RunVersion = ',RunVersion,',
',num2str(TimeStamp)]],'FontWeight','bold')

% % plot(DensityVsRekeys)
% % % Plotting Multiple Plots with Different Axis Limits on same Plot
% % ax1 = gca;
% % ax2 = axes('Position',get(ax1,'Position'),...
% % 'XAxisLocation','bottom',...
% % 'YAxisLocation','right'); %,...
% % 'Color','none',...
% % % 'XColor','k','YColor','k');
% % plot(JoinFactor,ax2)
% xlabel('Average Number of Users per Cluster');
% ylabel('Average Times Rekeyed');
% legend('Baseline','Cluster','Hubenko');
% title({'Average Number of Times Each User is Rekeyed'};['Versus increasing User
Cluster Density'];['JoinFactor Varies and Nobody Leaves'];['Time
Steps:',num2str(numTimeSteps),',', Satellites:',num2str(numSats),',',
Clusters:',num2str(numClusters)];['numMoving:',num2str(numMoving),',',
numWait:',num2str(numWait),',', numSpeed:',num2str(numSpeed)]]))
%set(gca, 'xtick',tickmarksforx,'xminortick', 'off')
%set(gca, 'yminortick', 'off')

% figure,bar(DensityVsRekeys)
% %title({'Average Number of Times Each User is Rekeyed vs. increasing Join Factor
(Higher JF=Slower Join Rate)'};['JoinFactor Varies and Nobody Leaves. Last Iteration
Average Users per Cluster= ',num2str(numUsers/(numSats*numClusters))');['Time
Steps:',num2str(numTimeSteps),',', Satellites:',num2str(numSats),',',
Clusters:',num2str(numClusters),',', numMoving:',num2str(numMoving),',',
numWait:',num2str(numWait),',', numSpeed:',num2str(numSpeed)'];['IterFactor:
',num2str(numDataPoints),',', IterSteps:',num2str(numIterSteps),',',
RunVersion=',RunVersion']]
% title({'Average Number of Times Each User is Rekeyed vs. Increasing Mobility and
Increasing User Density'};['Last Iteration Average Users per Cluster =
',num2str(numUsers/(numSats*numClusters)),'. JoinFactor held constant at
',num2str(JoinTimeSetter)];['Time Steps: ',num2str(numTimeSteps),',', Satellites:
',num2str(numSats),',', Clusters: ',num2str(numClusters),',', numMoving:
',num2str(numMoving),',', numWait: ',num2str(numWait),',', numSpeed:
',num2str(numSpeed)'];['IterFactor: ',num2str(numDataPoints),',', IterSteps:
',num2str(numIterSteps),',', RunVersion = ',RunVersion,',
',num2str(TimeStamp)]],'FontWeight','bold')
% %title({'Average Number of Times Each User is Rekeyed vs. increasing Join Factor
(Higher JF=Slower Join Rate)'};['JoinFactor Varies and Nobody Leaves. Last Iteration
Average Users per Cluster= ',num2str(numUsers/(numSats*numClusters))');['Time
Steps:',num2str(numTimeSteps),',', Satellites:',num2str(numSats),',',
Clusters:',num2str(numClusters),',', numMoving:',num2str(numMoving)];['IterFactor:
',num2str(numDataPoints),',', IterSteps:',num2str(numIterSteps),',',
numWait:',num2str(numWait),',', numSpeed:',num2str(numSpeed)]]))
% % XMinorTick off
% % YMinorTick off

```

```

% xlabel('Iteration','FontWeight','bold'); % puts a label on the X axis
% ylabel('Average Times Rekeyed','FontWeight','bold'); % puts a label on the right axis
% legend('Baseline','Cluster','Hubenko');

% figure,bar(DensityVsRekeys')
% title(['Average Number of Times Each User is Rekeyed vs. Increasing Mobility and
Increasing User Density'];['Last Iteration Average Users per Cluster =
',num2str(numUsers/(numSats*numClusters)),'. JoinFactor held constant at
',num2str(JoinTimeSetter)];['Time Steps: ',num2str(numTimeSteps),', Satellites:
',num2str(numSats),', Clusters: ',num2str(numClusters),', numMoving:
',num2str(numMoving),', numWait: ',num2str(numWait),', numSpeed:
',num2str(numSpeed)];['IterFactor: ',num2str(numDataPoints),', IterSteps:
',num2str(numIterSteps),', RunVersion = ',RunVersion,
',num2str(TimeStamp)]], 'FontWeight','bold')
% set(gca,'XTickLabel',{'Baseline';'Cluster';'Hubenko'})

%figure,plot(TotalKeysDistribCount)
figure,plot6 = plot(TotalKeysDistribCountPlot);
set(plot6(2),'DisplayName','Baseline','LineStyle','-', 'Marker','s','Color','b');
set(plot6(5),'DisplayName','Cluster','LineStyle','--','Marker','o','Color',[0 0.5 0]);
set(plot6(8),'DisplayName','Hubenko','LineStyle',':', 'Marker','d','Color','r');
set(plot6(1),'LineStyle',':', 'Color','b','HandleVisibility','off');
set(plot6(3),'LineStyle',':', 'Color','b','HandleVisibility','off');
set(plot6(4),'LineStyle',':', 'Color',[0 0.5 0],'HandleVisibility','off');
set(plot6(6),'LineStyle',':', 'Color',[0 0.5 0],'HandleVisibility','off');
set(plot6(7),'LineStyle',':', 'Color','r','HandleVisibility','off');
set(plot6(9),'LineStyle',':', 'Color','r','HandleVisibility','off');
legend('Location','NorthWest');
xlabel('Iteration','FontWeight','bold');
ylabel('Total Keys Distributed in the System');
%legend('Baseline','Cluster','Hubenko','Location','NorthWest');
% set(gca,'XTickLabel',{'Baseline';'Cluster';'Hubenko'})
title(['Total Keys Distributed in the System'];['Users:',num2str(numUsers),',
Sats:',num2str(numSats),', Clust:',num2str(numClusters)];['
Mobility:',num2str(numMoving),', Wait:',num2str(numWait),',
Speed:',num2str(numSpeed)];['Number of DataPoints: ',num2str(numDataPoints),', Number of
Sets: ',num2str(numSets),', RunVersion = ',RunVersion, ' ',num2str(TimeStamp)]])
% set(gcf, 'PaperPositionMode', 'manual');
% set(gcf, 'PaperUnits', 'inches');
% set(gcf, 'PaperPosition', [1 5 4.9 3.7]); % space from left edge, space
% from bottom, width, height
FigNum=FigNum+1;
FigName=strcat(DateStamp,VersionName,num2str(FigNum),'.fig');
saveas(gcf, FigName)
%print('-dmeta', '-r1200', FigName);

%figure,semilogy(TotalKeysDistribCount)
figure,semilogy7 = semilogy(TotalKeysDistribCountPlot);
set(semilogy7(2),'DisplayName','Baseline','LineStyle','-', 'Marker','s','Color','b');
set(semilogy7(5),'DisplayName','Cluster','LineStyle','--','Marker','o','Color',[0 0.5
0]);
set(semilogy7(8),'DisplayName','Hubenko','LineStyle',':', 'Marker','d','Color','r');
set(semilogy7(1),'LineStyle',':', 'Color','b','HandleVisibility','off');
set(semilogy7(3),'LineStyle',':', 'Color','b','HandleVisibility','off');
set(semilogy7(4),'LineStyle',':', 'Color',[0 0.5 0],'HandleVisibility','off');
set(semilogy7(6),'LineStyle',':', 'Color',[0 0.5 0],'HandleVisibility','off');
set(semilogy7(7),'LineStyle',':', 'Color','r','HandleVisibility','off');
set(semilogy7(9),'LineStyle',':', 'Color','r','HandleVisibility','off');
legend('Location','NorthWest');
xlabel('Iteration','FontWeight','bold');
ylabel('Total Keys Distributed in the System (log scale)');
%legend('Baseline','Cluster','Hubenko','Location','NorthWest');
% set(gca,'XTickLabel',{'Baseline';'Cluster';'Hubenko'})
title(['Total Keys Distributed in the System'];['Users:',num2str(numUsers),',
Satellites:',num2str(numSats),',
Clusters:',num2str(numClusters)];['Mobility:',num2str(numMoving),',
Wait:',num2str(numWait),', Speed:',num2str(numSpeed)];['Number of DataPoints:
',num2str(numDataPoints),', Number of Sets: ',num2str(numSets),', RunVersion =
',RunVersion, ' ',num2str(TimeStamp)]])

```

```

FigNum=FigNum+1;
FigName=strcat(DateStamp,VersionName,num2str(FigNum),'.fig');
saveas(gcf, FigName)
%print('-dmeta', '-r1200', FigName);

%figure,plot(TotalHalfKeysDistribCount)
figure,plot8 = plot(TotalHalfKeysDistribCountPlot);
set(plot8(2),'DisplayName','Baseline','LineStyle','-','Marker','s','Color','b');
set(plot8(5),'DisplayName','Cluster','LineStyle','--','Marker','o','Color',[0 0.5 0]);
set(plot8(8),'DisplayName','Hubenko','LineStyle',':','Marker','d','Color','r');
set(plot8(1),'LineStyle',':','Color','b','HandleVisibility','off');
set(plot8(3),'LineStyle',':','Color','b','HandleVisibility','off');
set(plot8(4),'LineStyle',':','Color',[0 0.5 0],'HandleVisibility','off');
set(plot8(6),'LineStyle',':','Color',[0 0.5 0],'HandleVisibility','off');
set(plot8(7),'LineStyle',':','Color','r','HandleVisibility','off');
set(plot8(9),'LineStyle',':','Color','r','HandleVisibility','off');
legend('Location','NorthWest');
xlabel('Iteration','FontWeight','bold');
ylabel('Total Keys Distributed for the Control Group');
%legend('Baseline','Cluster','Hubenko','Location','NorthWest');
% set(gca,'XTickLabel',{'Baseline','Cluster','Hubenko'})
title(['Total Keys Distributed for the Control Group ('num2str(ControlGroupSize*100),'%
of all Users)'];['Users:',num2str(numUsers),' Sats:',num2str(numSats),'
Clust:',num2str(numClusters)];['Mobility:',num2str(numMoving),'
Wait:',num2str(numWait),' Speed:',num2str(numSpeed)];['Number of DataPoints:
',num2str(numDataPoints),' Number of Sets: ',num2str(numSets),' RunVersion =
',RunVersion,' ',num2str(TimeStamp)]]);
% set(gcf,'PaperPositionMode','manual');
% set(gcf,'PaperUnits','inches');
% set(gcf,'PaperPosition',[1 5 4.9 3.7]); % space from left edge, space
% from bottom, width, height

FigNum=FigNum+1;
FigName=strcat(DateStamp,VersionName,num2str(FigNum),'.fig');
saveas(gcf, FigName)
%print('-dmeta', '-r1200', FigName);

%figure,semilogy(TotalHalfKeysDistribCount)
figure,semilogy9 = semilogy(TotalHalfKeysDistribCountPlot);
set(semilogy9(2),'DisplayName','Baseline','LineStyle','-','Marker','s','Color','b');
set(semilogy9(5),'DisplayName','Cluster','LineStyle','--','Marker','o','Color',[0 0.5
0]);
set(semilogy9(8),'DisplayName','Hubenko','LineStyle',':','Marker','d','Color','r');
set(semilogy9(1),'LineStyle',':','Color','b','HandleVisibility','off');
set(semilogy9(3),'LineStyle',':','Color','b','HandleVisibility','off');
set(semilogy9(4),'LineStyle',':','Color',[0 0.5 0],'HandleVisibility','off');
set(semilogy9(6),'LineStyle',':','Color',[0 0.5 0],'HandleVisibility','off');
set(semilogy9(7),'LineStyle',':','Color','r','HandleVisibility','off');
set(semilogy9(9),'LineStyle',':','Color','r','HandleVisibility','off');
legend('Location','NorthWest');
xlabel('Iteration','FontWeight','bold');
ylabel('Total Keys Distributed for the Control Group (log scale)');
%legend('Baseline','Cluster','Hubenko','Location','NorthWest');
% set(gca,'XTickLabel',{'Baseline','Cluster','Hubenko'})
title(['Total Keys Distributed for the Control Group ('num2str(ControlGroupSize*100),'%
of all Users)'];['Users:',num2str(numUsers),' Satellites:',num2str(numSats),'
Clusters:',num2str(numClusters)];['Mobility:',num2str(numMoving),'
Wait:',num2str(numWait),' Speed:',num2str(numSpeed)];['Number of DataPoints:
',num2str(numDataPoints),' Number of Sets: ',num2str(numSets),' RunVersion =
',RunVersion,' ',num2str(TimeStamp)]]);
FigNum=FigNum+1;
FigName=strcat(DateStamp,VersionName,num2str(FigNum),'.fig');
saveas(gcf, FigName)
%print('-dmeta', '-r1200', FigName);

% figure,bar(AvgKeySummaryPlot1)
% title(['Average Number of Times Each User Type is Rekeyed for the Baseline
Architecture'];['Last Iteration Average Users per Cluster =
',num2str(numUsers/(numSats*numClusters)),'. JoinFactor held constant at
',num2str(JoinTimeSetter)];['Time Steps: ',num2str(numTimeSteps),' Satellites:

```

```

',num2str(numSats),' Clusters: ',num2str(numClusters),' numMoving:
',num2str(numMoving),' numWait: ',num2str(numWait),' numSpeed:
',num2str(numSpeed)];['IterFactor: ',num2str(numDataPoints),' IterSteps:
',num2str(numSets),' RunVersion = ',RunVersion,
',num2str(TimeStamp)]},'FontWeight','bold')
%
% figure,bar(AvgKeySummaryPlot2)
% title(['Average Number of Times Each User Type is Rekeyed for the Clustered
Architecture'];['Last Iteration Average Users per Cluster =
',num2str(numUsers/(numSats*numClusters)),'. JoinFactor held constant at
',num2str(JoinTimeSetter)];['Time Steps: ',num2str(numTimeSteps),' Satellites:
',num2str(numSats),' Clusters: ',num2str(numClusters),' numMoving:
',num2str(numMoving),' numWait: ',num2str(numWait),' numSpeed:
',num2str(numSpeed)];['IterFactor: ',num2str(numDataPoints),' IterSteps:
',num2str(numSets),' RunVersion = ',RunVersion,
',num2str(TimeStamp)]},'FontWeight','bold')
%
% figure,bar(AvgKeySummaryPlot3)
% title(['Average Number of Times Each User Type is Rekeyed for the Hubenko
Architecture'];['Last Iteration Average Users per Cluster =
',num2str(numUsers/(numSats*numClusters)),'. JoinFactor held constant at
',num2str(JoinTimeSetter)];['Time Steps: ',num2str(numTimeSteps),' Satellites:
',num2str(numSats),' Clusters: ',num2str(numClusters),' numMoving:
',num2str(numMoving),' numWait: ',num2str(numWait),' numSpeed:
',num2str(numSpeed)];['IterFactor: ',num2str(numDataPoints),' IterSteps:
',num2str(numSets),' RunVersion = ',RunVersion,
',num2str(TimeStamp)]},'FontWeight','bold')

%*****
%NOW WRITE ALL ARRAYS TO Excel TO SAVE THE RAW DATA
XLFileName=strcat(DateStamp,VersionName,'.xls');
% % % CONFIDENCE INTERVALS:
% % % % [+ B - + C - + H - ...] Where B, C, H are the means for the SampleSize,
% % % % + is the Top of the confidence interval, - is the Bottom of the
% % % % Confidence Interval; "half" = control group

InfoRow1={'Each Row is an Iteration'};
HeaderRow1={'Baseline + CI','Baseline','Baseline - CI','Cluster + CI','Cluster','Cluster
- CI','Hubenko + CI','Hubenko','Hubenko - CI'};
HeaderRow2={'Baseline','Cluster','Hubenko'};

xlswrite(XLFileName, InfoRow1,'TotalKeysDistribCountPlot','C4');
xlswrite(XLFileName, HeaderRow1,'TotalKeysDistribCountPlot','C5');
xlswrite(XLFileName, TotalKeysDistribCountPlot, 'TotalKeysDistribCountPlot','C6');

xlswrite(XLFileName, {'Coeff of Variance'},'TotalKeysDistribStats','C4');
xlswrite(XLFileName, HeaderRow2,'TotalKeysDistribStats','C5');
xlswrite(XLFileName, COVTKD, 'TotalKeysDistribStats','C6');

xlswrite(XLFileName, {'Sample Standard Dev'},'TotalKeysDistribStats','I4');
xlswrite(XLFileName, HeaderRow2,'TotalKeysDistribStats','I5');
xlswrite(XLFileName, TKDSampleSDArray, 'TotalKeysDistribStats','I6');

xlswrite(XLFileName, {'Mean'},'TotalKeysDistribStats','O4');
xlswrite(XLFileName, HeaderRow2,'TotalKeysDistribStats','O5');
xlswrite(XLFileName, TKDMeanArray, 'TotalKeysDistribStats','O6');

xlswrite(XLFileName, InfoRow1,'TotalHalfKeysDistribCountPlot','C4');
xlswrite(XLFileName, HeaderRow1,'TotalHalfKeysDistribCountPlot','C5');
xlswrite(XLFileName, TotalHalfKeysDistribCountPlot,
'TotalHalfKeysDistribCountPlot','C6');

xlswrite(XLFileName, {'Coeff of Variance'},'TotalHalfKeysDistribStats','C4');
xlswrite(XLFileName, HeaderRow2,'TotalHalfKeysDistribStats','C5');
xlswrite(XLFileName, COVTHKD, 'TotalHalfKeysDistribStats','C6');

xlswrite(XLFileName, {'Sample Standard Dev'},'TotalHalfKeysDistribStats','I4');
xlswrite(XLFileName, HeaderRow2,'TotalHalfKeysDistribStats','I5');
xlswrite(XLFileName, THKDSampleSDArray, 'TotalHalfKeysDistribStats','I6');

```

```

xlswrite(XLFileName, {'Mean'}, 'TotalHalfKeysDistribStats', 'O4');
xlswrite(XLFileName, HeaderRow2, 'TotalHalfKeysDistribStats', 'O5');
xlswrite(XLFileName, THKDMeanArray, 'TotalHalfKeysDistribStats', 'O6');

xlswrite(XLFileName, InfoRow1, 'DensityVsRekeysPlot', 'C4');
xlswrite(XLFileName, HeaderRow1, 'DensityVsRekeysPlot', 'C5');
xlswrite(XLFileName, DensityVsRekeysPlot, 'DensityVsRekeysPlot', 'C6');

xlswrite(XLFileName, {'Coeff of Variance'}, 'DensityVsRekeysStats', 'C4');
xlswrite(XLFileName, HeaderRow2, 'DensityVsRekeysStats', 'C5');
xlswrite(XLFileName, COVDVR, 'DensityVsRekeysStats', 'C6');

xlswrite(XLFileName, {'Sample Standard Dev'}, 'DensityVsRekeysStats', 'I4');
xlswrite(XLFileName, HeaderRow2, 'DensityVsRekeysStats', 'I5');
xlswrite(XLFileName, DVRSampleSDArray, 'DensityVsRekeysStats', 'I6');

xlswrite(XLFileName, {'Mean'}, 'DensityVsRekeysStats', 'O4');
xlswrite(XLFileName, HeaderRow2, 'DensityVsRekeysStats', 'O5');
xlswrite(XLFileName, DVRMeanArray, 'DensityVsRekeysStats', 'O6');

xlswrite(XLFileName, InfoRow1, 'DensityVsHalfRekeysPlot', 'C4');
xlswrite(XLFileName, HeaderRow1, 'DensityVsHalfRekeysPlot', 'C5');
xlswrite(XLFileName, DensityVsHalfRekeysPlot, 'DensityVsHalfRekeysPlot', 'C6');

xlswrite(XLFileName, {'Coeff of Variance'}, 'DensityVsHalfRekeysStats', 'C4');
xlswrite(XLFileName, HeaderRow2, 'DensityVsHalfRekeysStats', 'C5');
xlswrite(XLFileName, COVDVHR, 'DensityVsHalfRekeysStats', 'C6');

xlswrite(XLFileName, {'Sample Standard Dev'}, 'DensityVsHalfRekeysStats', 'I4');
xlswrite(XLFileName, HeaderRow2, 'DensityVsHalfRekeysStats', 'I5');
xlswrite(XLFileName, DVHRSampleSDArray, 'DensityVsHalfRekeysStats', 'I6');

xlswrite(XLFileName, {'Mean'}, 'DensityVsHalfRekeysStats', 'O4');
xlswrite(XLFileName, HeaderRow2, 'DensityVsHalfRekeysStats', 'O5');
xlswrite(XLFileName, DVHRMeanArray, 'DensityVsHalfRekeysStats', 'O6');
pause(0);

% The rawest of the raw data. Multidimensional arrays with depth "SampleSize"
for XL=1:SampleSize
    NameOfSheet=strcat('TotalKeysDistribCount', num2str(XL));
    xlswrite(XLFileName, InfoRow1, NameOfSheet, 'C4');
    xlswrite(XLFileName, HeaderRow2, NameOfSheet, 'C5');
    xlswrite(XLFileName, TotalKeysDistribCount(:, :, XL), NameOfSheet, 'C6');
    NameOfSheet1=strcat('TotalHalfKeysDistribCount', num2str(XL));
    xlswrite(XLFileName, InfoRow1, NameOfSheet1, 'C4');
    xlswrite(XLFileName, HeaderRow2, NameOfSheet1, 'C5');
    xlswrite(XLFileName, TotalHalfKeysDistribCount(:, :, XL), NameOfSheet1, 'C6');
    NameOfSheet2=strcat('DensityVsRekeysCount', num2str(XL));
    xlswrite(XLFileName, InfoRow1, NameOfSheet2, 'C4');
    xlswrite(XLFileName, HeaderRow2, NameOfSheet2, 'C5');
    xlswrite(XLFileName, DensityVsRekeys(:, :, XL), NameOfSheet2, 'C6');
    NameOfSheet3=strcat('DensityVsHalfRekeysCount', num2str(XL));
    xlswrite(XLFileName, InfoRow1, NameOfSheet3, 'C4');
    xlswrite(XLFileName, HeaderRow2, NameOfSheet3, 'C5');
    xlswrite(XLFileName, DensityVsHalfRekeys(:, :, XL), NameOfSheet3, 'C6');
    pause(0);
end% for XL=1:SampleSize
xlswrite(XLFileName, HeaderRow, DateStamp, 'A4')
xlswrite(XLFileName, ResultsTable, DateStamp, 'A8')
toc
system('cmd /c "net send /domain:enxp401x "Finished!""');
FinishedNote=strcat('cmd /c "net send /domain:enxp401x "Finished ', RunVersion, '! TS-
', num2str(numTimeSteps), ' ', IF-', num2str(numDataPoints), '."");
system(FinishedNote);

```


VII. Bibliography

- [AdN05] Protocol Independent Multicast - Dense Mode (PIM-DM): Protocol Specification (Revised) (RFC 3973), <http://tools.ietf.org/wg/pim/draft-ietf-pim-dm-new-v2/rfc3973.txt>, Accessed: May 15, 2006.
- [AgC01] Agarwal, D. A., O. Chevassut, M. R. Thompson, and G. Tsudik, "An integrated solution for secure group communication in wide-area networks," *Proceedings of the Sixth IEEE Symposium on Computers and Communications, 2001*, Hammamet, 2001.
- [AkE02] Akyildiz, I. F., E. Ekici, and M. D. Bender, "MLSR: a novel routing algorithm for multilayered satellite IP networks," *Networking, IEEE/ACM Transactions on*, vol. 10, no. 3, pp. 411-424, 2002.
- [AkH04] Akkor, Gun, Michael Hadjithediosiou, and John S. Baras, "Transport protocols in multicast via satellite," *International Journal of Satellite Communications and Networking*, vol. 22, no. 6, pp. 611-627, 2004.
- [AlH03] Alberts, David S. and Richard E. Hayes, *Power to the Edge: Command and Control in the Information Age*. Washington, DC: DoD Command and Control Research Project, 2003.
- [Alm00] Almeroth, Kevin C., "The evolution of multicast: from the MBone to interdomain multicast to Internet2 deployment," *IEEE Network*, vol. 14, no. 1, pp. 10-20, 2000.
- [AmN05] Amir, Yair, Cristina Nita-Rotaru, Jonathan Stanton, and Gene Tsudik, "Secure Spread: An Integrated Architecture for Secure Group Communication " *IEEE TDSC*, vol. 2, no. 3, pp. 248-261, 2005.
- [BaB02] Banerjee, Suman and Bobby Bhattacharjee, "Scalable secure group communication over IP multicast," *IEEE Journal on Selected Areas in Communications*, vol. 20, no. 8, pp. 1511-1527, 2002.
- [BaL03] Barnett, C. A. and K. J. R. Liu, "Resource efficient multicast for 3G UMTS wireless networks," *Proceedings of the VTC*, 2003.
- [Bal97] Core Based Trees (CBT version 2) Multicast Routing (RFC 2189), <http://www.ietf.org/rfc/rfc2189.txt?number=2189>, Accessed: May 15, 2006.
- [Bar04] Barani, Bernard, "Satellite communications: the contribution of the 5th framework programme and future perspectives," *International Journal of Satellite Communications and Networking*, vol. 22, no. 1, pp. 5-18, 2004.
- [BeF99] Bever, Mark, Joseph Freitag, Stuart Linsky, James M. Myers, Raymond M. Nuber, Jaime L. Prieto Jr, and Eric R. Wiswell, "Fast-packet vs circuit switch

- and bent pipe satellite network architectures," *International Journal of Satellite Communications*, vol. 17, no. 2-3, pp. 83-105, 1999.
- [BhH02] Bhasin, Kul and Jeffrey L. Hayden, "Space Internet architectures and technologies for NASA enterprises," *International Journal of Satellite Communications*, vol. 20, no. 5, pp. 311-332, 2002.
- [BrR02] Bruschi, Danilo and Emilia Rosti, "Secure multicast in wireless networks of mobile hosts: protocols and issues," *Mobile Networks and Applications*, vol. 7, no. 6, pp. 503-511, 2002.
- [CaD02] IETF, RFC 3376: Internet Group Management Protocol, Version 3, <http://www.ietf.org/rfc/rfc3376.txt>, Accessed: May 22, 2006.
- [CaL99] Carducci, F. and G. Losquadro, "The EuroSkyWay worldwide system providing broadband service to fixed and mobile end-users," *International Journal of Satellite Communications*, vol. 17, no. 2-3, pp. 143-154, 1999.
- [ChB04] Challal, Yacine, Hatem Bettahar, and Abdelmadjid Bouabdallah, "SAKM: a scalable and adaptive key management approach for multicast communications," *ACM SIGCOMM Computer Communication Review*, vol. 34, no. 2 (April 2004), pp. 55-70, 2004.
- [ChE02] Chao, Chen, Ekici Eylem, and F. Akyildiz Ian, "Satellite grouping and routing protocol for LEO/MEO satellite IP networks," *Proceedings of the 5th ACM international workshop on Wireless mobile multimedia*, Atlanta, Georgia, USA, 2002.
- [CIS07] Cisco Systems, Inc., Cisco Internetwork Operating System (Cisco IOS), San Jose, CA, <http://www.cisco.com>, Accessed: August 30, 2007.
- [CoP02] 53rd IETF, Statistics of One-Way Internet Packet Delays, Minneapolis, MN
- [CrS01] Cruickshank, H., Z. Sun, F. Carducci, and A. Sanchez, "Analysis of IP voice conferencing over EuroSkyWay satellite system," *IEEE Communications*, vol. 148, no. 4, pp. 202-206, 2001.
- [DeC90] Deering, Stephen and D. Cheriton, "Multicast Routing in Datagram Internetworks and Extended LANs," *ACM Transactions on Computer Systems*, pp. 85-111, 1990.
- [Dee91] Deering, Stephen, "Multicast Routing in a Datagram Internetwork," Ph.D., Stanford University, 1991.
- [DeE96] Deering, S., D. L. Estrin, D. Farinacci, V. Jacobson, Liu Ching-Gung, and Wei Liming, "The PIM architecture for wide-area multicast routing," *Networking, IEEE/ACM Transactions on*, vol. 4, no. 2, pp. 153-162, 1996.

- [DeF99] IETF, Multicast Listener Discovery (MLD) for IPv6, <http://tools.ietf.org/html/2710>, Accessed: May 22, 2006.
- [DiC05] Di Pietro, Roberto, Stefano Chessa, and Piero Maestrini, "Computation, Memory and Bandwidth Efficient Distillation Codes to Mitigate DoS in Multicast," *Proceedings of the First International Conference on Security and Privacy for Emerging Areas in Communications Networks (SECURECOMM'05)*, Athens, Greece, 2005.
- [DiD03] Di Pietro, Roberto, Antonio Durante, and Luigi V. Mancini, "A reliable key authentication schema for secure multicast communications," *Proceedings of the 22nd International Symposium on Reliable Distributed Systems (SRDS'03)*, Florence, Italy, 2003.
- [Dij59] Dijkstra, E. W., "A Note on Two Problems in Connexion with Graphs," *Numerische Mathematik*, vol. 1, pp. 269-271, 1959.
- [DoD02] Department of Defense, *Global Information Grid (GIG) Overarching Policy*, DoD Directive 8100.1, (Arlington, VA).
- [DTI05] Transformational SATCOM (TSAT) - PE NUMBER: 0603845F, <http://www.dtic.mil/descriptivesum/Y2006/AirForce/0603845F.pdf>, Washington, DC, Accessed: April 17, 2006.
- [EkA02] Ekici, E., I. F. Akyildiz, and M. D. Bender, "A multicast routing algorithm for LEO satellite IP networks," *Networking, IEEE/ACM Transactions on*, vol. 10, no. 2, pp. 183-192, 2002.
- [Ela05] Elangovan, A., "Efficient multicasting and broadcasting in layer 2 provider backbone networks," *IEEE Comm*, vol. 43, no. 11, pp. 166-170, 2005.
- [EIR03] El-Sayed, A., V. Roca, and L. Mathy, "A survey of proposals for an alternative group communication service," *IEEE Network*, vol. 17, no. 1, pp. 46-51, 2003.
- [FeH04] IETF, IGMP/MLD-based Multicast Forwarding ("IGMP/MLD Proxying"), <http://tools.ietf.org/pdf/draft-ietf-magma-igmp-proxy-06.pdf>, Accessed: 2006.
- [FeH06] Protocol Independent Multicast - Sparse Mode (PIM-SM): Protocol Specification (Revised), <http://tools.ietf.org/wg/pim/draft-ietf-pim-sm-v2-new/draft-ietf-pim-sm-v2-new-12.txt>, Accessed: May 15, 2006.
- [Fen02] IETF, RFC 3228: IANA Considerations for IPv4 Internet Group Management Protocol (IGMP), <http://tools.ietf.org/pdf/rfc3228.pdf>, Accessed: 2006.
- [FiD01] Filali, F. and W. Dabbous, "Issues on the IP multicast service behaviour over the next-generation satellite-terrestrial hybrid networks," *Proceedings of the Sixth IEEE Symposium on Computers and Communications*, 2001.

- [FoR98] Fossa Jr., C. E., R. A. Raines, G. H. Gunsch, and M. A. Temple, "An overview of the IRIDIUM (R) low Earth orbit (LEO) satellite system," *Proceedings of the IEEE 1998 National Aerospace and Electronics Conference*, Dayton, OH, USA, 1998.
- [Fos98] Fossa Jr, Carl E., "A Performance Analysis of the IRIDIUM Low Earth Orbit Satellite System," Master's thesis, Air Force Institute of Technology, 1998, AFIT/GE/ENG/98J-01.
- [FrH99] Freitag, Joe, Peter Hadinger, Hau Ho, and Eric Wiswell, "Global EHF satellite network for delivering fibre optic capacity world wide," *International Journal of Satellite Communications*, vol. 17, no. 2-3, pp. 73-81, 1999.
- [GAO04] United States Government Accountability Office, *Defense Acquisitions: the Global Information Grid and challenges facing its implementation*, GAO-04-858, (Washington, DC: July 28, 2004).
- [GhS99] Ghedia, Lalji, Keith Smith, and Gary Titzer, "Satellite PCN - the ICO system," *Intl Journal of Satellite Communications*, vol. 17, no. 4, pp. 273-289, 1999.
- [HaB01] Hardjono, T., M. Baugher, and H. Harney, "Group Key Management for IP Multicast: Model & Architecture," *Proceedings of the 10th IEEE International Workshops on Enabling Technologies*, 2001.
- [Hab03] IETF, RFC 3590: Source Address Selection for the Multicast Listener Discovery (MLD) Protocol, <http://tools.ietf.org/html/3590>, Accessed: 2006.
- [HaC00] Hardjono, T. and B. Cain, "Key establishment for IGMP authentication in IP multicast," *Proceedings of the ECUMN 2000*, 2000.
- [HaM03] IETF, IGMPv3/MLDv2 and Multicast Routing Protocol Interaction, <http://tools.ietf.org/pdf/draft-ietf-magma-igmpv3-and-routing-05.pdf>, Accessed: May 22, 2006.
- [HeS05] Heeyoul, Kim, Hong Seong-min, H. Yoon, and J. W. Cho, "Secure group communication with multiplicative one-way functions," *Proceedings of the International Conference on Information Technology*, 2005.
- [HoC04] IETF, IGMPv3/MLDv2 for SSM, <http://tools.ietf.org/pdf/draft-holbrook-idmr-igmpv3-ssm-08.pdf>, Accessed: May 22, 2006.
- [HoI04] Howarth, M. P., S. Iyengar, Z. Sun, and H. Cruickshank, "Dynamics of key management in secure satellite multicast," *Selected Areas in Communications, IEEE Journal on*, vol. 22, no. 2, pp. 308-319, 2004.
- [Hub97] Hubbel, Y. C., "A comparison of the IRIDIUM and AMPS systems," *IEEE Network*, vol. 11, no. 2, pp. 52-59, 1997.

- [HuM03] Huang, J. H. and S. Mishra, "Mykil: a highly scalable key distribution protocol for large group multicast," *Proceedings of the GLOBECOM 2003*, 2003.
- [HuR06a] Hubenko Jr., Victor P., Richard A. Raines, Michael A. Temple, Robert F. Mills, and Mark D. Saeger, "Adaptation, Modeling, and Analysis of PIM-DM in a LEO Satellite Network Environment," *Proceedings of the IEEE Aerospace Conference*, Big Sky, Montana, 2006.
- [HuR06b] Hubenko Jr., Victor P., Richard A. Raines, Robert F. Mills, Rusty O. Baldwin, Barry E. Mullins, and Michael R. Grimaila, "Improving the Global Information Grid's Performance Through Satellite Communications Layer Enhancements," *IEEE Communications*, vol. 44, no. 11, pp. 66-72, 2006.
- [HuR07a] Hubenko Jr., Victor P., Richard A. Raines, Rusty O. Baldwin, Barry E. Mullins, Robert F. Mills, and Michael R. Grimaila, "Improving Satellite Multicast Security Scalability by Reducing Re-keying Requirements," *IEEE Network*, vol. 21, no. 4, pp. 51-56, 2007.
- [HuR07b] Hubenko Jr., Victor P., Richard A. Raines, Rusty O. Baldwin, Barry E. Mullins, Robert F. Mills, and Michael R. Grimaila, "Applying a Secure and Efficient Low Earth Orbit Satellite-Based Multicast Architecture in a Deployed Environment," *Proceedings of the MILCOM 2007*, Orlando, Florida, 2007.
- [HuR08] Hubenko Jr., Victor P., Richard A. Raines, Rusty O. Baldwin, Barry E. Mullins, Robert F. Mills, and Michael R. Grimaila, "A Secure and Efficient Satellite-based Multicast Architecture," *Proceedings of the IEEE Radio and Wireless Symposium*, Orlando, Florida, 2008.
- [Jai91] Jain, Raj, *The Art of Computer Systems Performance Analysis*. New York, New York: John Wiley & Sons, 1991.
- [JaK99] Jancso, James D. and Bruce Kraselsky, "The Constellation LEO satellite system: a wide-area solution to telecom needs in underserved areas worldwide," *International Journal of Satellite Communications*, vol. 17, no. 4, pp. 257-271, 1999.
- [JuA02] Judge, Paul and Mostafa Ammar, "Gothic: a group access control architecture for secure multicast and anycast," *Proceedings of the IEEE INFOCOM*, New York City, NY, USA, 2002.
- [JuA03] Judge, Paul and Mostafa Ammar, "Security issues and solutions in multicast content distribution: a survey," *IEEE Network*, vol. 17, no. 1, pp. 30-36, 2003.

- [JuL06] Jung, Eunjin, Alex X. Liu, and Mohamed G. Gouda, "Key bundles and parcels: Secure communication in many groups," *Computer Networks*, vol. 50, no. 11, pp. 1781-1798, 2006.
- [JuY06] Jun, Zhang, Zhou Yu, Ma Fanyuan, Gu Dawu, and Bai Yingcai, "An extension of secure group communication using key graph," *Information Sciences*, vol. 176, no. 20, pp. 3060-3078, 2006.
- [KaH04] Karaliopoulos, M., P. Henrio, K. Narenthiran, E. Angelou, and B. G. Evans, "Packet scheduling for the delivery of multicast and broadcast services over S-UMTS," *International Journal of Satellite Communications and Networking*, vol. 22, no. 5, pp. 503-532, 2004.
- [KaK01] Kamata, Minoru, Tetsuya Kawase, Akira Watanabe, and Iwao Sasase, "Proposal and analysis of multicast communication method in a department VPN," *Electronics and Communications in Japan (Part I: Communications)*, vol. 84, no. 7, pp. 45-56, 2001.
- [Kru98] Kruus, Peter S., "A Survey of Multicast Security Issues and Architectures," *Proceedings of the 21st National Information Systems Security Conference*, Arlington, Virginia, USA, 1998.
- [LaD98] Lai, Yuan-Cheng, Ying-Dar Lin, and Wei-Che Yu, "GMNF-DVMRP: an enhanced version of distance vector multicast routing protocol," *International Journal of Communication Systems*, vol. 11, no. 2, pp. 93-101, 1998.
- [LeK00] Lee, Jaeook and Sun Kang, "Satellite over satellite (SOS) network: a novel architecture for satellite network," *Proceedings of the IEEE INFOCOM 2000; Nineteenth Annual Joint Conference of the IEEE Computer and Communications Societies*, Tel Aviv, Israel, 2000.
- [LeL00] Lee, Jae-Wook, Jun-Woo Lee, Tae-Wan Kim, and Dae-Ung Kim, "Satellite over satellite (SOS) network: a novel concept of hierarchical architecture and routing in satellite network," *Proceedings of the 25th Annual IEEE Conference on Local Computer Networks, 2000 (LCN 2000)*, Tampa, FL, 2000.
- [LoL04] Loreti, P., M. Luglio, R. Kapoor, J. Stepanek, M. Gerla, F. Vatalaro, and M. A. Vazquez-Castro, "Mobile internet access using satellite networks," *International Journal of Satellite Communications and Networking*, vol. 22, no. 6, pp. 587-610, 2004.
- [MaG04] Macq, Jean-François and Michel X. Goemans, "Trade-offs on the location of the core node in a network," *Networks*, vol. 44, no. 3, pp. 179-186, 2004.
- [MAT07] The MathWorks, Inc.[®], MatLab, Natick, Massachusetts, <http://www.mathworks.com>, Accessed: July 30, 2007.

- [Mit97] Mittra, Suvo, "Iolus: a framework for scalable secure multicasting," *Proceedings of the ACM SIGCOMM '97*, Cannes, France, 1997.
- [MoS02] Mohorcic, Mihael, Ales Svigelj, Gorazd Kandus, and Markus Werner, "Performance evaluation of adaptive routing algorithms in packet-switched intersatellite link networks," *International Journal of Satellite Communications*, vol. 20, no. 2, pp. 97-120, 2002.
- [Moy94] Multicast Extensions to OSPF, <http://tools.ietf.org/html/1584>, Accessed: May 15, 2006.
- [NaK04] Narenthiran, K., M. Karaliopoulos, B. G. Evans, W. De-Win, M. Dieudonne, P. Henrio, M. Mazzella, E. Angelou, I. Andrikopoulos, P. I. Philippopoulos, D. I. Axiotis, N. Dimitriou, A. Polydoros, G. E. Corazza, and A. Vanelli-Coralli, "S-UMTS access network for broadcast and multicast service delivery: the SATIN approach," *International Journal of Satellite Communications and Networking*, vol. 22, no. 1, pp. 87-111, 2004.
- [NgZ05] Ng, W. H. D. and Sun Zhili, "Multi-layers balanced LKH," *Proceedings of the IEEE International Conference on Communications*, 2005.
- [NOR05] http://www.nortel.com/corporate/pressroom/feature_article/2005a/03_07_05_realtime.html, Accessed: 2005.
- [OPN06] OPNET Technologies, Inc.®, OPNET®, Bethesda, MD, <http://www.opnet.com>, Accessed: May 17, 2006.
- [PaO06] Park, Mirang, Naonobu Okazaki, and Shoichiro Seno, "A proposal and its evaluations of a re-keying system for dynamic secure group communications," *Systems and Computers in Japan*, vol. 37, no. 2, pp. 11-24, 2006.
- [PrR99] Pratt, Stephen R., Richard A. Raines, Carl E. Fossa Jr., and Michael A. Temple, "An operational and performance overview of the IRIDIUM low earth orbit satellite system," in *IEEE Communications Surveys & Tutorials*, vol. 2, 1999, pp. 2-10.
- [Pus04] Distance Vector Multicast Routing Protocol Internet Draft, <http://tools.ietf.org/wg/idmr/draft-ietf-idmr-dvmrp-v3/draft-ietf-idmr-dvmrp-v3-11.txt>, Accessed: May 15, 2006.
- [RaD99] Raines, Richard A. and Nathaniel J. Davis I. V., "The simulation modelling and performance analysis of low earth orbit satellite communication networks for personal communications," *International Journal of Communication Systems*, vol. 12, no. 3, pp. 197-215, 1999.

- [RaH03] Rafaeli, Sandro and David Hutchison, "A survey of key management for secure group communication," *ACM Computing Surveys*, vol. 35, no. 3, pp. 309-329, 2003.
- [RaJ97] Raines, R. A., R. F. Janoso, D. M. Gallagher, and D. L. Coulliette, "Simulation of two routing protocols operating in a low Earth orbit satellite network environment," *Proceedings of the IEEE MILCOM*, Monterey, California, 1997.
- [RoB01] Rodeh, Ohad, Kenneth P. Birman, and Danny Dolev, "The Architecture and Performance of Security Protocols in the Ensemble Group Communication System: Using Diamonds to Guard the Castle," *ACM Transactions on Information and System Security (TISSEC)*, vol. 4, no. 3, pp. 289-319, 2001.
- [Rod01] Roddy, Dennis, *Satellite Communications*, Third ed. New York, NY: McGraw-Hill, 2001.
- [RoP00] Multicast Ad hoc On-Demand Distance Vector (MAODV) Routing Internet Draft, <http://tools.ietf.org/wg/manet/draft-ietf-manet-maodv/draft-ietf-manet-maodv-00.txt>, Accessed: May 15, 2006.
- [Sae03] Saeger, Mark D., "Performance Analysis of Protocol Independent Multicasting - Dense Mode in Low Earth Orbit Satellite Networks," Master's thesis, Air Force Institute of Technology, 2003, AFIT/GCE/ENG/03-03.
- [SaM00] Sahasrabuddhe, L. H. and B. Mukherjee, "Multicast routing algorithms and protocols: a tutorial," *IEEE Network*, vol. 14, no. 1, pp. 90-102, 2000.
- [Sav06] Internet Engineering Task Force, Overview of the Internet Multicast Routing Architecture (draft-ietf-mboned-routingarch-03.txt), Accessed: May 26, 2006.
- [ScL02] Scheikl, O., J. Lane, R. Boyer, and M. Eltoweissy, "Multi-level secure multicast: the rethinking of secure locks," *Proceedings of the IPPW*, 2002.
- [ShG99] Shields, Clay and J. J. Garcia-Luna-Aceves, "KHIP—a scalable protocol for secure multicast routing," *Proceedings of the Conference on Applications, technologies, architectures, and protocols for computer communication*, Cambridge, Massachusetts, United States, 1999.
- [SMC06a] MILSATCOM Joint Program Office, <http://www.losangeles.af.mil/SMC/MC/>, Los Angeles Air Force Base, CA, Accessed: April 17, 2006.
- [SMC06b] Space and Missile Systems Center, http://www.losangeles.af.mil/SMC/PA/Fact_Sheets/, Los Angeles Air Force Base, CA, Accessed: April 17, 2006.

- [SPA06] Space & Naval Warfare Systems Command,
http://enterprise.spawar.navy.mil/UploadedFiles/next_gen_muos.pdf, San Diego, CA, Accessed: April 17, 2006.
- [Ste03] John P. Stenbit, *DoD Net-Centric Data Strategy*, (Washington, DC: May 9, 2003).
- [Sti95] Stinson, Douglas R., *Cryptography: Theory and Practice*. Boca Raton, Florida: CRC Press, Inc., 1995.
- [SuE02] Sumanasena, M. A. K., B. G. Evans, A. Vanelli-Coralli, and G. E. Corazza, "SATIN approach in W-CDMA adaptation for broadcast and multicast based S-UMTS," *Proceedings of the Vehicular Technology Conference*, 2002.
- [SuH03] Sun, Z., M. P. Howarth, H. Cruickshank, S. Iyengar, and L. Claverotte, "Networking issues in IP multicast over satellite," *International Journal of Satellite Communications and Networking*, vol. 21, no. 4-5, pp. 489-507, 2003.
- [Tho01] Thomas, Ryan W., "Multicast Algorithms for Mobile Satellite Communication Networks," Master's thesis, Air Force Institute of Technology, 2001, AFIT/GCE/ENG/01M-04.
- [ThR01] Thomas, R. W., R. A. Raines, R. O. Baldwin, and M. A. Temple, "Simulation, modeling, and evaluation of satellite-based multicasting protocols," *Proceedings of the Fall 2001 IEEE Vehicular Technology Conference*, Atlantic City, NJ, 2001.
- [ThR02] Thomas, Ryan W., Richard A. Raines, Rusty O. Baldwin, and Michael A. Temple, "Performance analysis of multicast algorithms for mobile satellite communication networks," *Computer Communications Journal, Special Issue on Advances in Performance Evaluation of Computer and Telecommunications Networking*, vol. 25, no. 11-12, pp. 1085-1093, 2002.
- [Tom05] Tomme, Edward B., "The Paradigm Shift to Effects-Based Space: Near-Space as a Combat Space Effects Enabler," Airpower Research Institute, Maxwell AFB, AL, 2005.
- [ViC04] IETF, RFC 3810: Multicast Listener Discovery Version 2 (MLDv2) for IPv6, <http://tools.ietf.org/html/3810>, Accessed: May 22, 2006.
- [Wal70] Walker, J.G., "Circular Orbit Patterns Providing Whole Earth Coverage," *Technical Report 70211*, November 1970, 1970.
- [Wal71] Walker, J.G., "Some circular orbit patterns providing continuous whole earth coverage," *Journal of the British Interplanetary Society*, vol. 24, pp. 369-384, 1971.

- [WeF01] Werner, Markus, Jochen Frings, Frédéric Wauquiez, and Gérard Maral, "Topological design, routing and capacity dimensioning for ISL networks in broadband LEO satellite systems," *International Journal of Satellite Communications*, vol. 19, no. 6, pp. 499-527, 2001.
- [WeS03] Wei-Chi, Ku and Chen Shuai-Min, "An improved key management scheme for large dynamic groups using one-way function trees," *Proceedings of the International Conference on Parallel Processing Workshops*, 2003.
- [WoC01] Wood, L., A. Clerget, I. Andrikopoulos, G. Pavlou, and W. Dabbous, "IP routing issues in satellite constellation networks," *International Journal of Satellite Communications*, vol. 19, no. 1, pp. 69-92, 2001.
- [WuS05] Wu, Feng-Ge, Fu-Chun Sun, Ke Yu, and Chang-Wen Zheng, "Performance evaluation on a double-layered satellite network," *International Journal of Satellite Communications and Networking*, vol. 23, no. 6, pp. 359-371, 2005.
- [XiP05] Xin, Li, Zhang Peng, and Ye Chengqing, "GAC/GKM: a group access control architecture for secure multicast," *Proceedings of the International Conference on Communications, Circuits and Systems*, China, 2005.
- [Yam97] Yamashita, Tomoyoshi, "The low-/medium-earth orbit constellations for global satellite systems," *Electronics and Communications in Japan (Part I: Communications)*, vol. 80, no. 4, pp. 106-114, 1997.
- [YaS01] Yang, Wen-Her and Shiuh-Pyng Shieh, "Secure key agreement for group communications," *International Journal of Network Management*, vol. 11, no. 6, pp. 365-374, 2001.
- [YiS03] On-Demand Multicast Routing Protocol (ODMRP) for Ad Hoc Networks Internet Draft, <http://tools.ietf.org/wg/manet/draft-ietf-manet-odmrp/draft-ietf-manet-odmrp-04.txt>, Accessed: May 15, 2006.
- [YuE02] Yue, Gaofeng, E. Ekici, and I. F. Akyildiz, "A new multicast routing algorithm in hierarchical satellite networks," *Proceedings of the IEEE Global Telecommunications Conference 2002 (GLOBECOM '02)*, 2002.
- [Yuh03] Yuh-Min, Tseng, "A scalable key-management scheme with minimizing key storage for secure group communications," *International Journal of Network Management*, vol. 13, no. 6, pp. 419-425, 2003.

VIII. Vita

Major Victor P. Hubenko, Jr. graduated Valedictorian from Brentwood High School in Brentwood, New York. He entered undergraduate studies at Cornell University in Ithaca, New York where he graduated with a Bachelors of Science degree in Electrical Engineering and was commissioned a Second Lieutenant, United States Air Force, in December 1996.

His first assignment was at Maxwell Air Force Base (Gunter Annex), Alabama, where he was a network engineer for Air Force Systems Networking. He designed, installed, configured, and maintained classified networks for Air Force, Air Force Reserve, and Air National Guard units throughout the continental United States and Alaska. He also managed the classified network connectivity deployment for the Air Force Defense Messaging System. In December 1999, he was assigned to the tri-agency National Polar-orbiting Operational Environmental Satellite System (NPOESS) Integrated Program Office, Silver Spring, Maryland. There he served as the Command, Control, and Communications Segment Integrated Product Team lead, managing all aspects of communications for NPOESS to include terrestrial and satellite telecommunications, network security, network operations, antenna and ground station development, Mission Management Center development, and software development. While assigned to NPOESS, he completed his Master of Science degree in Electrical Engineering at Johns Hopkins University, Baltimore, Maryland. In August 2004, he entered the Graduate School of Engineering and Management, Air Force Institute of Technology, Wright-Patterson Air Force Base, Ohio.

REPORT DOCUMENTATION PAGE				Form Approved OMB No. 074-0188	
<p>The public reporting burden for this collection of information is estimated to average 1 hour per response, including the time for reviewing instructions, searching existing data sources, gathering and maintaining the data needed, and completing and reviewing the collection of information. Send comments regarding this burden estimate or any other aspect of the collection of information, including suggestions for reducing this burden to Department of Defense, Washington Headquarters Services, Directorate for Information Operations and Reports (0704-0188), 1215 Jefferson Davis Highway, Suite 1204, Arlington, VA 22202-4302. Respondents should be aware that notwithstanding any other provision of law, no person shall be subject to a penalty for failing to comply with a collection of information if it does not display a currently valid OMB control number.</p> <p>PLEASE DO NOT RETURN YOUR FORM TO THE ABOVE ADDRESS.</p>					
1. REPORT DATE (DD-MM-YYYY) 19-06-2008		2. REPORT TYPE Doctoral Dissertation		3. DATES COVERED (From – To) August 2004 – June 2008	
4. TITLE AND SUBTITLE A Secure and Efficient Communications Architecture For Global Information Grid Users Via Cooperating Space Assets				5a. CONTRACT NUMBER	
				5b. GRANT NUMBER	
				5c. PROGRAM ELEMENT NUMBER	
				5d. PROJECT NUMBER	
6. AUTHOR(S) Hubenko, Victor, P. Jr., Major, USAF				5e. TASK NUMBER	
				5f. WORK UNIT NUMBER	
7. PERFORMING ORGANIZATION NAMES(S) AND ADDRESS(S) Air Force Institute of Technology Graduate School of Engineering and Management (AFIT/EN) 2950 Hobson Way, Building 640 WPAFB OH 45433-7765				8. PERFORMING ORGANIZATION REPORT NUMBER AFIT/DCE/ENG/08-02	
9. SPONSORING/MONITORING AGENCY NAME(S) AND ADDRESS(ES)				10. SPONSOR/MONITOR'S ACRONYM(S)	
				11. SPONSOR/MONITOR'S REPORT NUMBER(S)	
12. DISTRIBUTION/AVAILABILITY STATEMENT APPROVED FOR PUBLIC RELEASE; DISTRIBUTION UNLIMITED.					
13. SUPPLEMENTARY NOTES					
14. ABSTRACT <p>With the Information Age in full and rapid development, users expect to have global, seamless, ubiquitous, secure, and efficient communications capable of providing access to real-time applications and collaboration. The United States Department of Defense's (DoD) Network-Centric Enterprise Services initiative, along with the notion of pushing the "power to the edge," aims to provide end-users with maximum situational awareness, a comprehensive view of the battlespace, all within a secure networking environment. Building from previous AFIT research efforts, this research developed a novel security framework architecture to address the lack of efficient and scalable secure multicasting in the low earth orbit satellite network environment. This security framework architecture combines several key aspects of different secure group communications architectures in a new way that increases efficiency and scalability, while maintaining the overall system security level. By implementing this security architecture in a deployed environment with heterogeneous communications users, reduced re-keying frequency will result. Less frequent re-keying means more resources are available for throughput as compared to security overhead. This translates to more transparency to the end user; it will seem as if they have a "larger pipe" for their network links.</p> <p>As a proof of concept, this research developed and analyzed multiple mobile communication environment scenarios to demonstrate the superior re-keying advantage offered by the novel "Hubenko Security Framework Architecture" over traditional and clustered multicast security architectures. For example, in the scenario containing a heterogeneous mix of user types (Stationary, Ground, Sea, and Air), the Hubenko Architecture achieved a minimum ten-fold reduction in total keys distributed as compared to other known architectures. Another experiment demonstrated the Hubenko Architecture operated at 6% capacity while the other architectures operated at 98% capacity. In the 80% overall mobility experiment with 40% Air users, the other architectures re-keying increased 900% over the Stationary case, whereas the Hubenko Architecture only increased 65%.</p> <p>This new architecture is extensible to numerous secure group communications environments beyond the low earth orbit satellite network environment, including unmanned aerial vehicle swarms, wireless sensor networks, and mobile ad hoc networks.</p>					
15. SUBJECT TERMS Secure Multicast Architecture, Low Earth Orbit Satellite, Satellite Communications					
16. SECURITY CLASSIFICATION OF:			17. LIMITATION OF ABSTRACT	18. NUMBER OF PAGES	19a. NAME OF RESPONSIBLE PERSON
a. REPORT	b. ABSTRACT	c. THIS PAGE			Dr. Richard A. Raines (ENG)
U	U	U	UU	226	19b. TELEPHONE NUMBER (Include area code) (937) 255-6565, ext 4278 e-mail: Richard.Raines@afit.edu